This electronic thesis or dissertation has been downloaded from the King's Research Portal at https://kclpure.kcl.ac.uk/portal/

Investigating the mechanisms of p38 activation

Arabacilar, Pelin

Awarding institution:
King's College London

The copyright of this thesis rests with the author and no quotation from it or information derived from it may be published without proper acknowledgement.

END USER LICENCE AGREEMENT

Unless another licence is stated on the immediately following page this work is licensed

under a Creative Commons Attribution-NonCommercial-NoDerivatives 4.0 International

licence. https://creativecommons.org/licenses/by-nc-nd/4.0/

You are free to copy, distribute and transmit the work

Under the following conditions:

- Attribution: You must attribute the work in the manner specified by the author (but not in any way that suggests that they endorse you or your use of the work).
- Non Commercial: You may not use this work for commercial purposes.
- No Derivative Works - You may not alter, transform, or build upon this work.

Any of these conditions can be waived if you receive permission from the author. Your fair dealings and other rights are in no way affected by the above.

Take down policy

If you believe that this document breaches copyright please contact librarypure@kcl.ac.uk providing details, and we will remove access to the work immediately and investigate your claim.

Download date: 08. Jan. 2025

Investigating the mechanisms of p38 activation

Pelin Arabacilar

Thesis submitted for the degree of Doctor of Philosophy

2015

Department of Cardiology
Cardiovascular Division
Rayne Institute, BHF Centre
4th Floor Lambeth Wing
St Thomas' Hospital
London, SE1 7EH

ABSTRACT

BACKGROUND: p38 mitogen activated protein kinases (p38 MAPKs) respond to stress stimuli and play a role in cell differentiation and apoptosis. Four isoforms of p38 MAPKs have been found; p38-α/β/γ/δ and this project focuses on the role of p38α. There are three pathways leading to p38α activation, the canonical pathway, the ZAP70-mediated pathway and the TAB1-mediated pathway. The latter has been found to occur during myocardial ischaemia. Therefore, if this direct effect of TAB1 on p38α can be controlled and prevented, there might be a potential way to stop or minimise myocardial ischaemic injury. The aim of this project is to investigate the effect of TAB1 on p38α autophosphorylation, as well as assessing competition between this pathway and the canonical cascade of activation. Another signalling pathway, which involves p38α, with a potential role in heart failure, is the amino acid response pathway (AAR). Halofuginone, a compound which activates the AAR pathway, has been implicated in improved cardiac function. Exploring this system by using halofuginone as a tool would provide further insight into whether the activation of this pathway could lead to improvements in several aspects of heart failure, such as hypertrophy, autophagy and inflammation. RESULTS: Using HEK293 cells, co-expression of TAB1 and p38α results in increased phosphorylation of p38α. This phosphorylation is reduced by the p38 inhibitors SB203580 and BIRB796. Mutations in TAB1, preventing p38 binding, diminish TAB1-mediated p38α phosphorylation. Despite spatial overlap in docking domains on p38α, TAB1 does not compete with MKK3b in a mammalian overexpression model. TAB1 and MKK3b induce phosphorylation of p38 independently and this is probably due to their differential in-cell locations, with p38 predominantly localising with MKK3b.

p38 appears to be activated in response to halofuginone, and the simultaneous activation of the AAR pathway leads to increased autophagy, changes in the mRNA levels of inflammatory genes, as well as a potential p38-mediated negative feedback mechanism on the AAR pathway.

CONCLUSIONS: There is a TAB1-mediated, SB203580-sensitive p38α phosphorylation mechanism which involves direct binding of TAB1 to p38α and induction of p38α autophosphorylation. p38 is activated in response to halofuginone and the associated AAR pathway leads to changes in autophagy and inflammation.

Acknowledgements

Firstly, I would like to express my sincere gratitude to my first supervisor Professor Mike Marber for the continuous support throughout my PhD, for his patience, motivation, and immense knowledge. His encouragement has helped me conduct my research and write this thesis in an enjoyable manner. “People are creators of their own destiny,” a wise man once said and I thank him for helping me create mine with his advice and guidance. I could not have imagined having a better advisor and mentor for my PhD; I am eternally in debt.

Besides my first supervisor, I would like to thank my advisors; Dr Rekha Bassi, Dr Denise Martin and Dr Asvi Francois for their constant inspiration and enthusiasm, which propelled me forward. Thank you for all the laughter, stories and tears of joy we shared throughout these four years. Without their precious support, insight, smiles and humour it would not be possible to conduct this research.

My sincere thanks also goes to my supervisors at the Heart Failure DPU, GSK; Dr Bob Willette, Dr Gregory Gatto and Dr Pu Qin, who provided me with the invaluable opportunity to join their team as an intern, and gave access to the laboratory and research facilities in an industrial setting. Besides their insightful comments and inspiration, many thanks also for the challenging questions which motivated me to widen my research from various perspectives.

I thank my fellow labmates for the stimulating discussions, amusing conversations, the sleepless nights before deadlines, and for all the fun we have had in the last four years. A special thanks to my partner in crime, Aminah Loonat, for sharing this path with me with all the joys we have celebrated with the high-fives and the stress of answering the question ‘What are we doing with our life?’ together. Thank you for all the *science-*

related amusement, giggles, gossip, sneaky smiles, eye rolling, holidays and memories I will treasure forever. She was the γ isoform of the α me.

I would also like to thank all my friends and acquaintances at the Rayne Institute and Heart Failure DPU as well as outside of work. Their input and support has helped me to keep going and made it an enjoyable experience.

A special thanks to my guardian angel and husband, Behzad Golforoush, for never letting me give up and pushing me to always be the best I can be, even when I didn't believe I could.

Finally and most importantly, I would like to thank my family for celebrating my successes and tolerating me through my struggles, not just during my PhD but in life in general. My father for believing in me, my mother for all the positivity, my sister for all the motivation and my brother for all the admiration to which I aim to live up to. I would not be where I am without their love and support and it is to them that I dedicate this work.

Table of Contents

List of Figures

List of Tables

List of Common Abbreviations

$^{\circ}$C	Degree Celcius
µg	Microgram
µl	Microlitre
µM	Micromolar
AAR	Amino acid response
ATP	Adenosine triphosphate
bp	base pairs
BSA	Bovine serum albumin
CMV	Cytomegalovirus
C-terminal	Carboxy terminal
ddH_2O	deionised distilled water
DMEM	Dulbecco's modified Eagle's medium
DMSO	Dimethyl sulfoxide
DNA	Deoxyribonucleic acid
DR	Drug resistant
E.coli	Escherichia coli
ECL	Enhanced chemiluminescence
EDTA	Ethylenediaminetetraacetic acid
EGTA	Ethylene glycol tetraacetic acid
ERK	Extracellular signal-regulated kinase
FBS	Foetal bovine serum
g	Gram
hr	Hour

HSP	Heat shock protein
IPTG	Isopropyl beta-D-1-thiogalactopyranoside
ITC	Isothermal titration calorimetry
JNK	c-Jun N-terminal kinases
kb	Kilo base
kDa	Kilo Daltons
LB	Lysogeny
LPS	Lipopolysaccharide
M	Molar
MAPK	Mitogen activated protein kinase
MAPKKK	Mitogen activated protein kinase kinase kinase
mg	Milligram
mins	Minutes
ml	Millilitre
mM	Millimolar
MW	Molecular weight
ng	Nanogram
nM	Nanomolar
NMR	Nuclear magnetic resonance
NRVM	Neonatal Rat Ventricular Myocyte
N-terminal	Amino terminal
p38α	MAPK p38 alpha
PAGE	Polyacrylamide gel electrophoresis
PBS	Phosphate buffered saline
PCR	Polymerase chain reaction

RT	Room temperature
SDS	Sodium dodecyl sulfate
TAB1	TGF-β-activated kinase 1-binding protein 1
TAK1	Transforming growth factor beta–activated kinase 1
TBS	Tris-buffered saline
TBST	TBS-Tween
TEMED	Tetramethylethylenediamine
TGF-β	Transforming growth factor beta
TNF-α	Tumor necrosis factor alpha
V	Volts
WT	Wild-type

1 INTRODUCTION

1.1 Mitogen activated protein kinases (MAPKs)

Mitogen activated protein kinases (MAPKs) are widely conserved Ser/Thr kinases that play a major role in cells by regulating, activating and inhibiting other pathways. There are three families of MAPKs consisting of c-Jun N-terminal kinase (JNK), extracellular signal regulated kinase (ERK) and p38. All three families have similar activating stimuli ranging from cytokines to bacterial or viral infection. They are involved in cell growth, proliferation, differentiation, apoptosis, gene expression and respond to stress conditions depending on stimuli and cell-type (1). There are diverse stimuli activating these MAPKs and their pathways are intricately linked (see Figure 1.1). Transforming growth factor beta–activated kinase 1 (TAK1) is activated by many stimuli and goes onto activate several members of the MAPK kinases (MKKs) family including MKK3, MKK6, MKK4 and MKK7, which in turn activate p38α and/or JNK (2). TAK1 also plays an indirect role in the activation of the ERK1/2 signalling pathway (3).

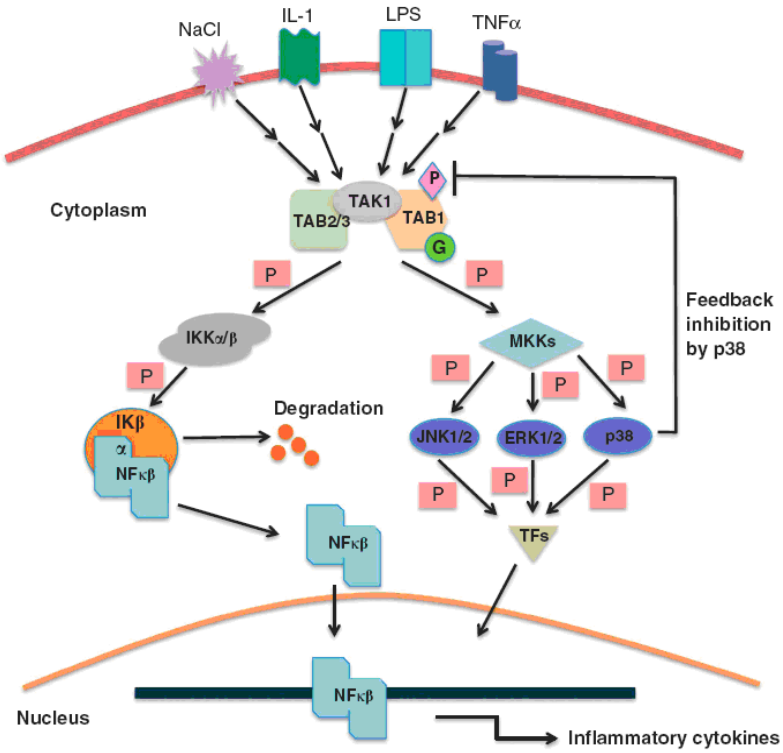

Figure 1.1 Diagram illustrating the intricate links between cell signaling pathways. Osmotic stress, inflammatory cytokines and bacterial factors trigger a stress-response system in the cell. These signals diverge at TAK1, which plays a role in several pathways including nuclear factor kappa B (NFκB), JNK, ERK1/2 and the p38 system to adequately generate responses depending on cell-type and stimulus. (4)

1.2 p38α

1.2.1 Isoforms and expression

p38α is a 38kDa MAPK which was identified in 1994 as becoming phosphorylated on Tyr residue in macrophages following bacterial endotoxin lipopolysaccharide (LPS) exposure (5) and as being activated by interleukin 1 (IL-1) and subsequently activating MAPK activated protein kinase 2 (MAPKAP-K2) (6, 7). It is also referred to as MAPK14 and stress activated protein kinase 2a (SAPK2a), and p38α is the homologue of the Hog1 protein in S.cerevisiae (8). It is 60% identical in sequence to the other p38 isoforms; β/γ/δ and ERK6 (9). The different p38 isoforms are encoded by different genes and have different tissue expression patterns. p38α and p38β are ubiquitously expressed, p38γ is abundant in skeletal and cardiac muscle and p38δ is expressed in the

lung, gut, pancreas, testes and kidney (10, 11). p38α also has alternatively spliced versions; Mxi2 has reduced binding to substrates and plays a role in ERK1/2 regulation (12) and Exip is not phosphorylated by the usual activating treatments of p38α and has been shown to regulate the nuclear factor κB (NFκB) pathway (13).

1.2.2 Activation and structure

During immune and stress responses involving p38α, there is a complex interaction of different kinases, scaffold proteins and receptor associated factor proteins. p38α pathway consists of a cascade of kinases, ultimately resulting in MKK3/6 phosphorylating p38α at its activation lip. One of the key players of the canonical p38α pathway is TAK1, a central effector that crosslinks different pathways involved in the stress response. TAK1 is activated by phosphorylation and protein-protein interactions. TAK1-binding proteins (TAB) 1/2/3 play a role in the tight control of TAK1 activation (4). TAK1 is known to be involved in the c-Jun N-terminal kinase (JNK), p38α and nuclear factor κB (NF- κB) pathways and intracellular signals diverge at TAK1-TAB1 association (2-4, 14). TAK1 is part of a complex with TAB1 and either TAB2 or TAB3. TAB2 and TAB3 are homologous proteins with C-terminal zinc-finger motifs acting as docking domains for Lys^{63}–linked polyubiquitination by the E3-ligases such as TNF receptor associated factors (TRAF) 6 and 2 which induce autophosphorylation of TAK1 (15, 16). TAK1 appears to form a complex with its specific activator TAK1 binding protein 1 (TAB1) which facilitates activation of TAK1 (17). TAB1 does not recruit TAK1 to receptors of the immune response, but instead it is able to bind directly and activate TAK1. Recently, it has been reported that TAB1 is modified with N-acetylglucosamine (O-GlcNAc) on a single site, Ser395, which is required for full TAK1 activation upon stimulation with IL-1 or osmotic stress (4).

p38α has 2 distinct lobes with a catalytic groove in between and has a larger ATP-binding pocket than p38β (18). Its N-terminal lobe is predominated by β-pleated sheets and has a larger C-terminal lobe made up mostly of α-helices (19) (see Figure 1.5 and Figure 1.6) with a hinge linking these two lobes. p38α is activated by phosphorylation on Thr180 and Tyr182 in a Thr-Gly-Tyr motif in a surface loop close to the active site, also known as the activation lip. Activation of p38α can result from the canonical kinase cascade or autophosphorylation (20, 21). The canonical pathway of p38α activation involves TAK1 being activated by extracellular stimuli such as transforming growth factor-β (TGF-β), bone morphological protein (BMP) and tumour necrosis factor-α (TNF-α) (22-24). TAK1 goes onto phosphorylate MKK3/6, which can then go onto phosphorylate the TGY motif on p38α. Activated p38α then relocates to the nucleus or cytoplasm depending on the stimulus, cell-type and its specific function (25). Unstimulated p38α is found in the both the cytoplasm and the nucleus and upon stimulation it relocates depending on the stimulus. For example it will be retained in the nucleus if there is damage to DNA, but when bound, TAB1 will locate p38α in the cytoplasm (26).

1.2.3 Alternative activation mechanisms

Nonetheless, the MKK-mediated cascade is not the sole activation mechanism of p38α (see Figure 1.2).

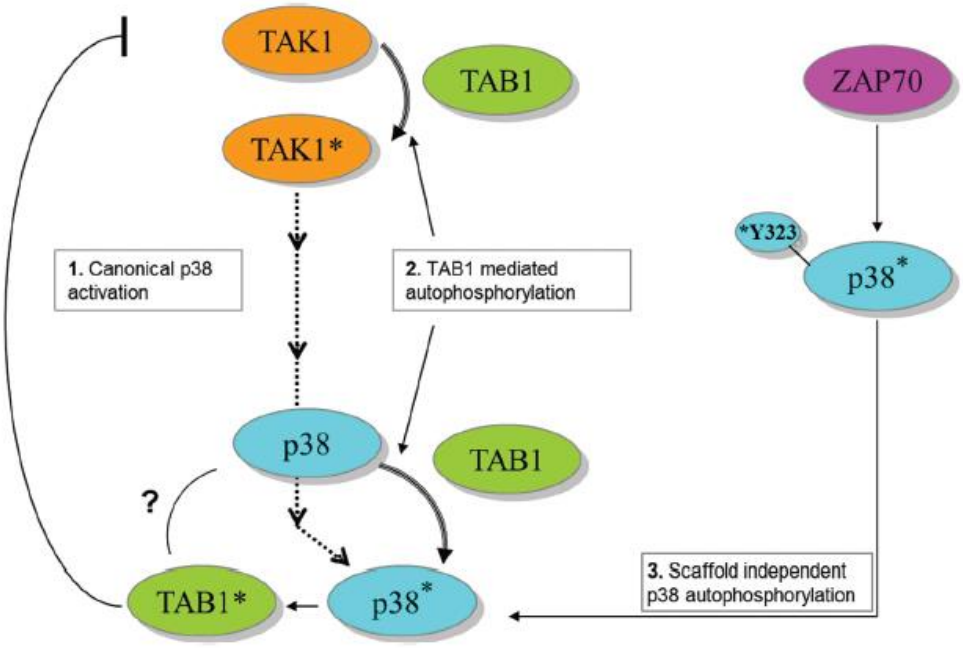

Figure 1.2 Schematic representation of the p38α activation pathways.
p38α is usually activated by environmental stress, inflammatory cytokines and virus infection. Main pathway of activation is via TAK1 in the canonical MKK system involving MKKs 3/6, which are in turn activated by MEKKs, MLKs and ASK1. A second activation mechanism is via direct interaction by the scaffold protein TAB1 inducing autophosphorylation of Thr180 and Tyr182 in the activation lip. A third mechanism also exists by ZAP70 tyrosine kinase which phosphorylates p38α on Tyr323 inducing its autophosphorylation of the TGY motif. (19)

There is a zeta-chain-associated protein kinase (ZAP70) mediated autophosphorylation mechanism which has so far not been identified to be involved in cardiac pathophysiology. ZAP70 is the tyrosine kinase subunit of the T-cell receptor (TCR) and once activated ZAP70 phosphorylates p38α on Tyr323 leading to p38α autophosphorylation (27).

Another mechanism of p38α activation involves direct binding between TAB1 and p38α. TAB1 is a scaffold protein, which plays a role in the canonical p38α activation pathway as already mentioned. However, it has also been found to interact with p38α directly and this mechanism is best described in ischaemia (28, 29). In ischaemia-reperfusion studies of MKK3-/- and MKK3+/+ mice hearts, infarction volume was similar despite undetectable activation of MKK3/6 in MKK3-/- hearts (29). Using mutated forms of p38α, it has been reported that phosphorylation of the activation lip is

not a prerequisite for the binding of TAB1 to p38α and the amount of p38α phosphorylation mediated by TAB1 is comparable to that mediated by the dominant active MKK6 (30). Recently, novel phosphorylation sites in the TAK1-binding domain of TAB1 have been discovered which appear to affect TAB1-dependent p38 phosphorylation and p38-bound TAB1 localisation (31). In cultured neonatal cardiomyocytes, TAB1 binds to p38, disrupts p38 interaction with MKK3 and leads to the relocalisation of p38 in the cytosol (32). Therefore it is possible that TAB1 competes with MKK3 in binding to p38 and altering its downstream effects depending on the stimuli.

There are indirect regulatory processes that also influence p38α activation. One such process reported in recent studies is the action of the E3 ubiquitin ligase, Itch. Itch binds directly and ubiquitinates TAB1, inhibiting p38α signaling and skin inflammation (33). In addition, through chemical-genetic approaches and coexpression in mammalian, bacterial and cell-free systems, it has been reported that p38 autophosphorylation occurs in cis by direct interaction with TAB1 (34). Crystallography revealed that TAB1 docks onto p38α C-terminal in a bipartite manner, stabilises active p38α and induces conformational changes leading to the extension of the activation lip allowing autophosphorylation (34). This study has reported that TAB1 residues 371-416 are sufficient to induce phosphorylation of p38α, and our genetic modifications in TAB1 are based on this set of in-house data.

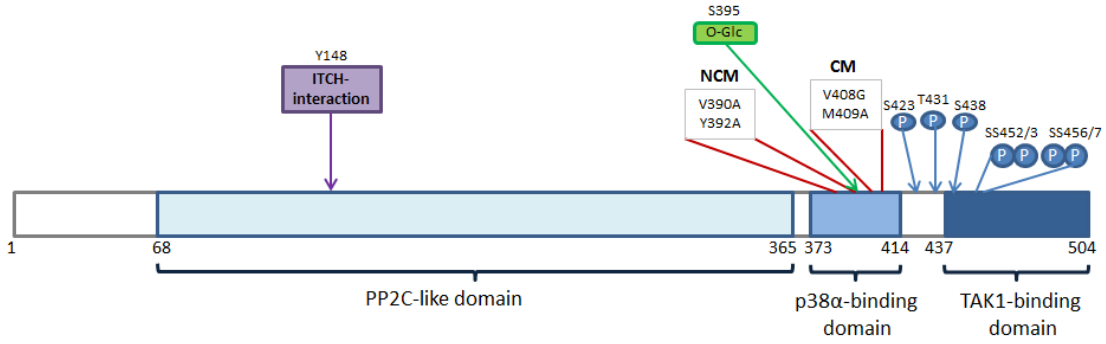

Figure 1.3 Schematic showing the different domains of TAB1 (amino acids 1-504). Amino acids 25-365 constitute the PP2C-like pseudophosphatase domain, amino acids 373-418 are involved in p38α-binding and the TAK1-binding domain is made up of amino acids 437-504. p38α phosphorylates TAB1 at S423 and T431, whereas both ERK1/2 and JNK1/2 phosphorylate at S438 (4). ITCH protein interacts at the Y148 (33) and O-GlcNAcylation takes place at S395 (4).

TAB1 has three domains; PP2C-like pseudophosphatase domain, p38α-binding domain and TAK1-binding domain (see Figure 1.3). Although the fold in protein phosphatase 2C is conserved in TAB1, through structural analyses and mutagenesis it was observed that TAB1 lacks the key residues required for dual metal-binding and catalysis (3). There is a splice variant, TAB1β, which lacks exons 10 and 11, which correspond to the TAK1-binding domain and has a different exon, β, instead (see Figure 1.4). TAB1β differs from TAB1, as it cannot bind or activate TAK1, but maintains the ability to induce p38α activation (35).

Figure 1.4 Sequence and structure of TAB1β, the splice variant of TAB1.

(A) amino acid sequences of TAB1β and TAB1. (B) structure of exon and intron in TAB1β and TAB1. (35)

TAB1 is involved in crosslinking/integrating several pathways within a cell and has several phosphorylation sites which are acted upon by different kinases. p38α has been found to phosphorylate TAB1 at Ser423 and Thr431, whereas ERK1/2 phosphorylates Thr431 and JNK1/2 acts on Ser438. Nevertheless, TAB1 has not yet been widely studied so its function and relation to other proteins within a cell is not completely understood.

It is not yet clear exactly how TAB1 binding to p38α induces p38α autophosphorylation on the TGY motif. It is of interest to investigate this interaction further as it has the potential to have an important role in ischaemic injury and could reveal targets for treatment of cardiovascular diseases.

1.2.4 Substrates

It is evident that in order to be efficient and specific, an important aspect of a signalling pathway is the presence of specialised interaction and docking domains in scaffold proteins and substrates. p38α is a Ser/Thr kinase associated with phosphorylation of Ser-Pro and Thr-Pro motifs. However, there are several other domains on downstream substrates necessary for interaction with, and subsequent phosphorylation by p38α. Docking domains (D-domains) are positively charged regions surrounded by hydrophobic residues and are involved in p38α binding besides the enzyme-substrate interaction at the active site of the kinase (36). A C-terminal docking (CD) motif is a region of acidic and hydrophobic residues outside the catalytic region of p38α, which is necessary for hydrophobic and electrostatic interactions with D-domain residues (37, 38). Different substrates utilise different motifs to facilitate p38α binding, but these conserved features are heavily exploited for specificity and efficiency of p38α function.

Some of p38α substrates are other protein kinases such MAPKAPK2 (or MK2) and MK3 which were found to phosphorylate heat shock protein 27 (Hsp27), activating transcription factor 1 (ATF1) and cAMP responsive element-binding protein (CREB). Other protein kinases activated by p38α include mitogen- and stress-activated protein kinase 1 (MSK1), MSK2 and MAPK-interacting serine/threonine-protein kinase 1 (MNK1). Transcription factors are another major group of substrates for p38α and these include ATF1, ATF2 and ATF6, CCAAT-enhancer-binding protein homologous protein (CHOP), p53 and myocyte enhancer factor 2C (MEF2C). p38α substrates identified to date are listed (see Table 1.1).

Table 1.1 Identified substrates of p38α and their corresponding phosphorylation sites
(adapted from *http://www.kinasource.co.uk/Database/S%20Substrates/SAPK2a%20substrates.html)*

Substrates	Sites	Reference
ATF-2	Thr 69 and Thr 71	van Dam et al., 1995 EMBO J. 14:1798-811
Cdc25B		Bulavin et al., 2001 Nature 411:102-107
Cdc25C		Bulavin et al., 2001 Nature 411:102-107
CHOP-1, GADD153	Ser78, Ser81	Wang et al., 1996 Science 272:1347-9
Cyclin D3	Thr283	Casanovas et al., 2004 Oncogene 23:7537-44
MAPKAP K2	Thr222, Ser272, Thr334	Rouse et al., 1994 Cell 78, 1024-1034 Ben Levy et al., 1995 EMBO J. 14, 5920-5930 Xu et al., 2006 Oncogene. 25:2987-98. Kumar et al., 2010 Cancer Res. 70:832-41
MAPKAP K3	Thr201, Ser251, Thr313	McLaughlin et al., 1996, JBC 271, 8488-8492
MAPKAP K5, PRAK	Thr182	New et al., 1998, EMBO J. 17, 3372-3384
MSK1	Ser 360, Thr 581	Deak et al., 1998 EMBO J. 17;:4426-41 McCoy et al., 2005 Biochem J. 387:507-17
MITF	Ser 307	Mansky et al., 2002, JBC 277, 11077-11083
MNK1	Thr221	Waskiewicz et al., 1997 EMBO J. 16:1909-20
MNK2	Thr 197, Thr 202 and Thr 332	Waskiewicz et al., 1997 EMBO J. 16:1909-20
C/EBP beta	Thr45	Horie et al., 2007, Microbes Infect. 9:721-8
Cyclin D1	Thr 286	Casanovas et al., 2000 JBC 275:35091–7
MEF2A	Thr312, Thr319	Zhao et al., 1999 Mol Cell Biol. 19:21-30
MEF2C	Thr293, Thr300, Ser 387?	Han et al., 1997 Nature 386:296-9 Zhao et al., 1999 Mol Cell Biol. 19:21-30 Khiem et al., 2008 Proc Natl Acad Sci. 105:17067-72
PLA2 (Ca 21 -sensitive 85-kDa cytosolic phospholipase A2)	Ser 505	Kramer et al., 1996 JBC 271:27723–9 Schmidlin et al., 2000 Naunyn Schmiedebergs Arch Pharmacol. 361:247-54
PPARa (peroxisome proliferator-activated receptor)	Ser6, Ser12, Ser21	Barger et al., 2001 JBC 276:44495–501

p47phox	Ser345, Ser348	Manke et al., 2005 Mol Cell 17:37-48
p53	Ser 33	Sanchez-Prieto et al., 2000 Cancer Res. 60:2464-72
RSK-B	Ser 343, Thr 568 and Thr 687	Pierrat et al., 1998 JBC 273:29661-71 Tomas-Zuber et al., 2001 J Biol Chem. 276:5892-9
Sap-1a	Ser381, Ser387	Jahnknecht & Hunter, 1997 EMBO J.16:1620-7
STAT1	Ser727	Kovarik et al., 1999 Proc Natl Acad Sci U S A. 96:13956-61
TAB1 (TAK1 binding protein) also isoforms 2 & 3	Ser 423 and Thr 431	Cheung et al., 2003 EMBO J. 22:5793-805 De Nicola et al., 2013 Nat Struct Mol Biol. 20:1182-90
Tau	Thr 181, Ser 202, Thr 205, Ser 396 and Ser 422	Reynolds et al., 1997 J Neurochem. 69:191-8 Hartzler et al., Neurobiology of Aging, 23:855–859

1.2.5 In-cell localisation

As a signalling molecule, the localisation of the p38 in the cell is not fixed and highly dependent on the stimulus and cell type. It shuttles between the nucleus and cytoplasm depending on the response required to the particular prevalent stimuli.

In a study in 293T cells, basally p38 is distributed throughout the cell with the exposure to UV irradiation or X-radiation triggering accumulation of it in the nucleus (26). Basal phosphorylation of p38 was low, and increased, specifically in the nucleus, in response to these stimuli. Other activators of p38 MAPK; TNFα and Fas ligand induced p38 phosphorylation but did not result in its nuclear-relocation.

One of p38 substrates MK2, has been reported to form a complex with p38 and facilitate its nuclear-export upon the phosphorylation of MK2 (25). The p38 activators MKK3 and MKK6 are present in both the nucleus and the cytoplasm, consistent with their role in the induction of p38 activity leading to the activation of a wide range of substrates and effectors.

A recent study has reported that the autophosphorylation of ERK1/2 on its Thr188 residue leads to its relocalisation to the nucleus to induce the phosphorylation of its nuclear targets known to cause cardiac hypertrophy (39). A corresponding residue is found on p38α (Thr185), and it is possible that the phosphorylation state of this residue plays a role in determining the localisation of p38 in the cell, which is an aspect that will be investigated in this thesis.

1.2.6 Inhibitors

p38α utilises ATP to phosphorylate its substrates and is therefore a target of pyridinylimidazole drugs as competitive inhibitors. SB203580 being an example of these ATP-mimetic molecules, competes with ATP and binds specifically to the ATP-binding site of p38α and p38β and inhibits phosphorylation of downstream substrates

such as MAPKAP kinase 2 and heat shock protein 27 (20, 40). SB203580 only inhibits isoforms p38α and p38β and its selectivity is due to a gatekeeper residue, Thr106, guarding a hydrophobic pocket at the margin of the ATP-binding pocket (41, 42) (see Figure 1.5). A bulkier Met residue is substituted in p38γ and p38δ rendering these isoforms resistant to inhibition (41). Another ATP-mimetic p38 inhibitor is SB236093 which displays more than 220-fold selectivity over ERK, JNK1 and other kinases and is ~3-fold more selective than SB203580.

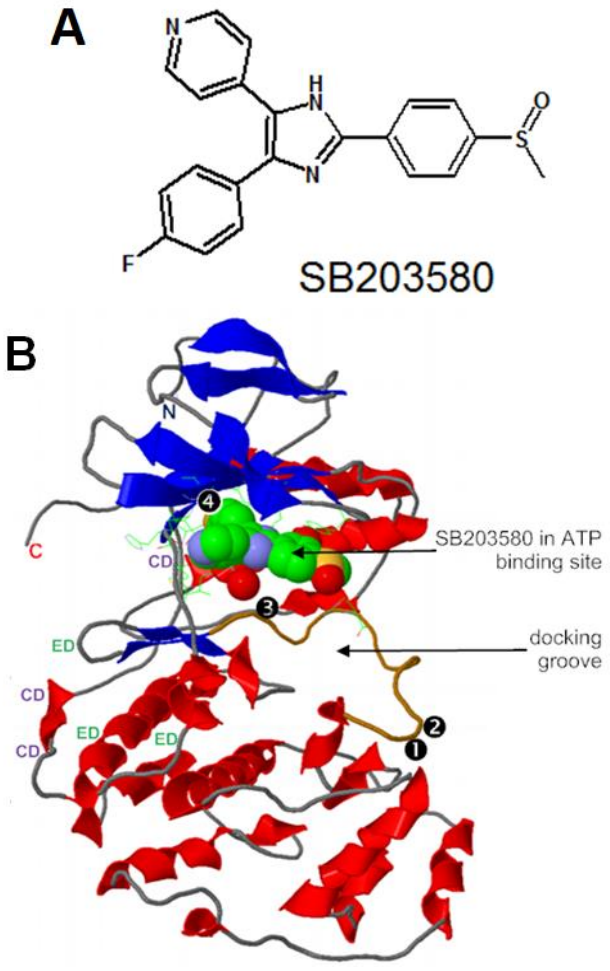

Figure 1.5 Structure of the Type I p38α inhibitor SB203580.
(A) chemical structure, (B) spacefill structure bound to ribbon structure of p38α. Black circle numbers 1 and 2 are the Thr180 and Tyr182 on the activation lip where p38α is phosphorylated, 3 is Tyr323 where ZAP70 induces autophosphorylation and 4 is the Thr106 important in SB203580 binding. *Image A - Pubchem Compound, NCBI; image B*- (43)

Another series of p38α inhibitors are diaryl urea compounds, which are structurally different to pyridinylimidazoles. BIRB796 is one of the most potent examples of this class of inhibitors and inhibits p38α activity by indirectly hindering ATP-binding. p38α has a DFG motif as part of its activation loop and this motif is believed to enable flexibility for conformational rearrangement upon activation (44). BIRB796 binds to the Phe residue of the DFG motif in a hydrophobic pocket between the two lobes of p38α (see Figure 1.6) leading to reorganisation of the activation loop resulting in a conformation unable to bind ATP (45). As well as p38α, all isoforms of the p38 family are also inhibited by BIRB796 (46). However, BIRB796 more potently inhibits p38α and p38β compared to p38γ and p38δ potentially due to the fact that this inhibitor exploits the hydrophobic pocket surrounding Thr106 residue not present in p38γ and p38δ (46).

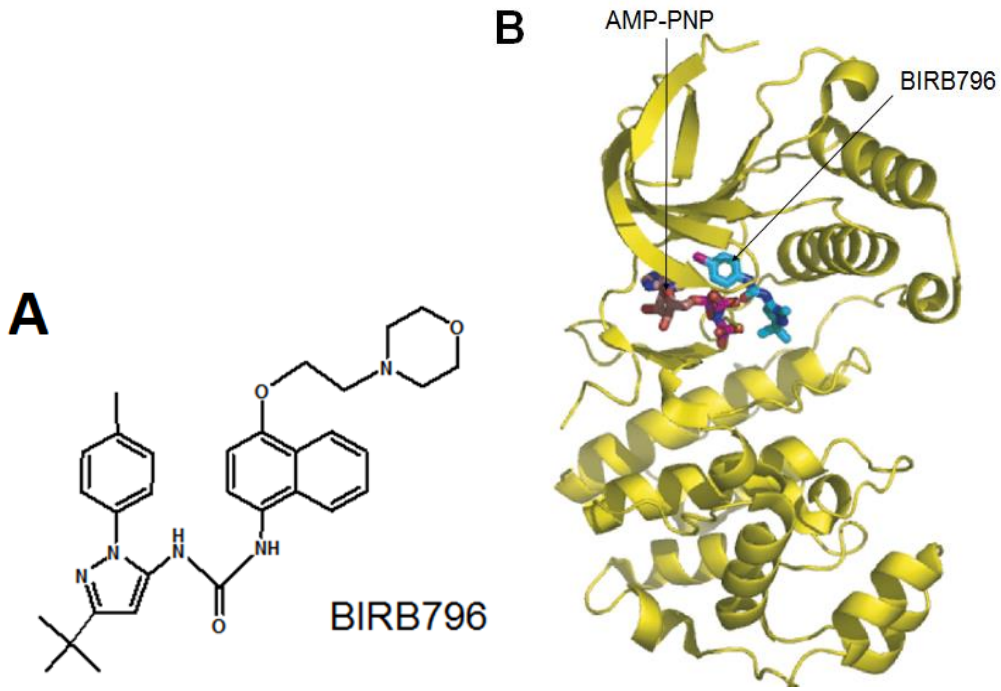

Figure 1.6 Structure of the Type II p38α inhibitor BIRB796.
(A) chemical structure, (B) ball and stick structure bound to ribbon structure of p38α. *Image A - Pubchem Compound, NCBI; image B-* (47)

1.2.7 In physiology

p38α has been implicated in many aspects of cell biology including inflammation, gene expression, the cell cycle, cell differentiation and apoptosis. Some of the stimuli which activate p38α are inflammatory cytokines, environmental stress, ischaemia, UV irradiation, oxidative stress, hypoxia, TGF-β and lipopolysaccharide (LPS) (7, 48). There is a strong link between p38α and inflammation and it has been found to play a role in inflammatory diseases such as rheumatoid arthritis and inflammatory bowel disease (49).

Some of the main functions of p38α are to induce enzymes involved in inflammation such as cyclooxygenase-2 and inducible NO synthase, regulate cell adhesion proteins and promote the secretion of inflammatory cytokines such as interleukin-1 (IL-1) and tumour necrosis factor-α (TNFα). The role of p38α in apoptosis has been found to depend on cell type and stimulus (50, 51). In some cells it induces cell death through the apoptotic pathway involving caspases (52), while in other cell types it promotes cell differentiation (53).

In addition, p38α activity has been reported to be decreased in tumours and dysfunction of the p38α pathway caused an increase in cell proliferation and tumorigenesis suggesting that p38α has tumour suppressive qualities (54-56). Moreover, p38α plays a role in development as loss of p38α causes embryonic death in mice due to placental defects (57-59). This also infers the lack of compensation for p38α in development by its other isoforms. Nonetheless upon loss of the other isoforms, p38α can compensate for them and development is not perturbed.

p38α plays a role in myocardial ischaemia, its activation induces lethal injury (60-62) and inhibition is cardioprotective (62-65). Nonetheless, p38α has also been found to play a role in ischaemic preconditioning (IPC) associating p38α activation with protection of the cardiac tissue (66-69). IPC is a mechanism where a short duration of

ischaemia during which p38α has been found to be activated, protects against subsequent periods of prolonged ischaemia.

The main activation pathway of p38α is through MKKs in the canonical mechanism as already mentioned. However this pathway was not found to be involved in the activation of p38α during ischaemia. Instead, TAB1 was found to mediate autophosphorylation of p38α observed during myocardial ischaemia (29).

1.3 Cardiovascular disease and myocardial ischaemia

Cardiovascular disease is a general term used to refer to numerous diseases of the heart and the circulatory system. It includes stroke, coronary heart disease, angina and heart attack and was the most common cause of death in the world in 2008 (74). The common factor of these conditions is their association with atheromas, which are the deposit of fatty plaques in blood vessels, making it more difficult to carry blood along the arteries. These atherosclerotics plaques can rupture leading to platelet activation and thrombus formation. The consequent cessation of blood flow down the conduit artery restricts the perfusion of the distal tissue. This results in the tissue being deprived of nutrients (oxygen and substrates for metabolism) and a means to washout metabolites (carbon dioxide and lactic acid), a condition referred to as ischaemia (72). During ischaemia many processes within a cell are activated causing injury. These include but are not limited to a switch to anaerobic metabolism producing lactic acid, failure of ATP-dependent ion transport pumps, induction of excess calcium entry into cells causing excitotoxicity, stimulation of caspase-dependent apoptosis and an inflammatory response (70). Many protein pathways are involved in this ischaemic response including the recently identified TAB1 -mediated p38α activation pathway (71).

1.4 Heart failure

Chronic heart failure, also referred to as congestive heart failure, is a progressive condition that occurs when the heart at a normal filling pressure is unable to pump sufficient blood to meet the body's requirements. The syndrome is multifaceted including abnormalities in heart muscle, valves and/or pericardium as well as systemic disturbances in neuro-humoral, cytokine and/or vascular function (72-75). The changes can include but are not limited to deterioration in the force of contraction and vascular tone and alterations in hypertrophy, apoptosis, fibrosis, autophagy and inflammatory cytokines as will be discussed further.

1.5 Evidence for p38 activation in heart failure

The mitogen-activated protein kinase p38 is a key Ser/Thr kinase that responds to a variety of the multifaceted abnormalities contributing to heart failure (see Figure 1.7). There have been extensive studies on the role of p38 in different disease states, primarily ischaemic heart disease in the cardiac setting. Though not as thoroughly explored as ischaemia, the role of p38 has been investigated in heart failure. Activation of p38 has been observed in animal models of heart failure and studies on myocardial biopsies from heart failure patients show increased p38 activity in comparison to "healthy" hearts (76-78). In cultured cardiomyocytes, p38 activation augments hypertrophy and pharmacologic inhibition attenuates hypertrophy occurring in response to stimuli such as endothelin-1 and phenylephrine (79). Whilst inhibiting p38 activity using SB203580 in adult rat cardiomyocytes, increases contractility (80).Variations in patient populations and genetic differences between animal models make it challenging to determine the precise role of p38 in heart failure. Collectively, it appears that p38 plays an important role in the progression of heart failure. The structure and function of p38 has been recently reviewed in the cardioprotective context (81). The mechanisms

and consequences of p38 activity in heart failure with the aim of highlighting areas for further research required to clarify future potential therapeutic benefit is discussed in this thesis.

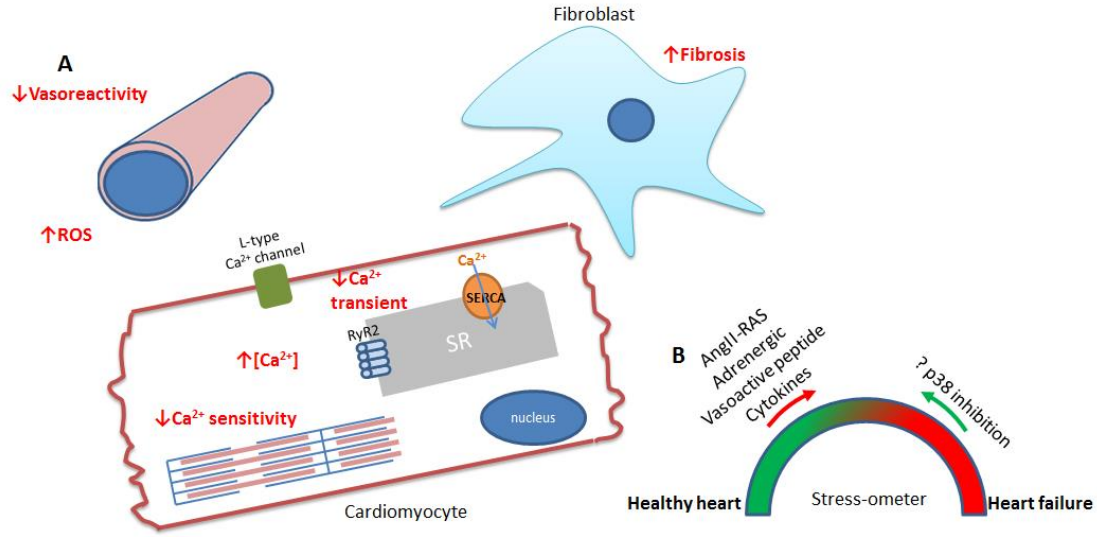

Figure 1.7 The downstream effects of p38 in cardiomyocytes, fibroblasts and vasculature during heart failure.
A) Emphasised in red are the effects of p38 which are associated with the progression of heart failure. p38 activity has been linked to increased interstitial fibrosis, reduced vasoreactivity and increased ROS production. The effects on the force of cardiomyocyte contraction are mediated by the effect of p38 on the Ca2+ transient and the sensitivity of the sarcomeres. B) Schematic showing balance between stresses on the heart that lead to healthy adaptation and the pathological increases in cytokines and neurohormones that lead to, or aggravate, heart failure. The question is whether these pathological signals can be reversed by inhibiting p38?

1.6 Pathological features of heart failure that may lie downstream of p38

1.6.1 The force of contraction

An intricate protein signalling cascade exists to control the contraction of cardiomyocytes. The increase in cytosolic Ca^{2+} ions in the cell leads to actin interacting with myosin and the power stroke that shortens the sarcomere. Most heart failure is characterised by decreased contractility and reduced ejection fraction and the most common underlying process is pressure overload due to hypertension or cavity dilatation after myocardial infarction acting through the Law of LaPlace. Pressure

overload in turn leads to hypertrophy and loss of contractile function (82, 83). It appears that activation of the p38 pathway depresses contractility and enhances matrix remodelling (84). In studies involving the activation of this pathway through gene transfer of the activated upstream kinases of p38 (mitogen-activated protein kinase kinase 3/6 (MKK3/6)) or blocking the pathway through dominant negative p38 mutants and pharmacologic inhibition, it is evident that p38 activity leads to negative inotropic effects (80, 85). More than one mechanism has been proposed through which p38 decreases contractility. Such mechanisms include prolongation of the decay phase of the cardiac calcium transient increasing diastolic Ca^{2+} concentration and relaxation. This is thought to be mediated through downregulation of sarcoplasmic/endoplasmic reticulum calcium ATPase (SERCA2), responsible for the translocation of Ca^{2+} from the cytosol to the sarcoplasmic reticulum (86, 87). In support of this, tumour necrosis factor α (TNFα)-induced contractile dysfunction in isolated hearts is attenuated in MKK3 knock out mice and by pharmacologic inhibition (77). Furthermore other studies suggest that there may be an additional contribution through p38 activity diminishing the Ca^{2+} sensitivity of the sarcomere (80, 85, 88).

1.6.2 Vascular tone

p38 is activated in the vessel wall in response to pressure overload, hypoxia and heart failure (89, 90) and also by neurohormonal stimuli such as angiotensin II or endothelin-1; both associated with vasoconstriction and ventricular remodelling (91, 92). Vasoreactivity is improved, and survival is increased, by pharmacologic inhibition of p38 in several different models involving these stressors (90, 93, 94). In a rat model of heart failure, inhibition of p38 with SB239063 normalises vascular p38 activity and endothelial dysfunction is prevented (95). Current literature mainly focuses on the activation mechanisms of p38 during heart failure and less on the downstream

mechanisms which may lead to the pathological features of the syndrome. Though further investigation is required, it appears that SB239063 leads to a decrease in vascular superoxide anion formation, suggesting that p38 plays a role in generation of reactive oxygen species (ROS) during heart failure (95). Furthermore, one of the main subsets of p38 substrates are transcription factors, such as myocyte enhancer factor 2A (MEF2A) and myocyte enhancer factor 2C (MEF2C), that are implicated in the regulation of vascular tone (96-98), as well as ROS generation. In summary, the dysfunction mediated in part by p38 appears to be via ROS generation and possibly an effect on downstream transcription factors (93, 99, 100).

1.6.3 Hypertrophy

The data concerning the role of p38 in hypertrophy are difficult to reconcile; there is evidence both for and against its involvement (101-103). Perhaps due to differences in models and experimental detail, substantial variability of p38 activity in heart failure and/or hypertrophy has been observed.

In an adenoviral-mediated overexpression system in cardiomyocytes expressing upstream activators for p38; MKK3 and MKK6, leads to a pro-hypertrophic response including increase in cell size and atrial natriuretic factor expression, suggesting a causative role (104). However, in an in vivo model with transgenic mice expressing the dominant-negative mutants of MKK3, MKK6 and p38α, cardiac hypertrophy following aortic banding is enhanced, potentially through the regulation of nuclear factor of activated T cells (NFAT) (105). In vivo studies, and data acquired from heart failure patients, suggest that p38 contributes to the progression of heart failure but that this is not through the aggravation of hypertrophy (76, 94, 102, 106). For example, p38 does not appear to be activated in hypertrophied hearts, but in failing hearts a two-fold increase in p38 phosphorylation is observed (101).

Overall, in isolated cardiomyocytes p38 activation appears to increase hypertrophy and its inhibition, using pharmacological compounds or genetic methods, attenuates the development of hypertrophy in response to hypertrophic stimuli (79, 104, 107). However, the picture is more complex in in vivo models and it is not clear that hypertrophy in the absence of heart failure causes p38 activation in patients.

1.6.4 Apoptosis

Cardiomyocyte death is an integral component of decompensated cardiac hypertrophy and the dysfunction leading to heart failure (108). Three systems of cell death exist, namely, necrosis, apoptosis and autophagy. Cardiac apoptosis is regulated by an elaborate array of stress-activated signalling pathways. p38 has been associated with both anti- and pro-apoptotic downstream effects depending on the upstream stimulus and cell type (109-112). However, in the cardiac setting, the role of p38 in regulating apoptosis is still under investigation. The apoptotic effects of anisomycin and overexpressing activated mitogen-activated protein kinase kinase kinase 1(MEKK1) are reversed by overexpressing constitutively active MKK6 (113) and a similar result is observed with the augmentation of norepinephrine-induced apoptosis by a p38 inhibitor in cardiac myocytes (114). It appears that the protective role of MKK6 overexpression is, in part, mediated through NFκB activation, interleukin 6 (IL-6) induction and αB-crystallin phosphorylation (113, 115-117).

Nonetheless, there are a few reports contradicting these findings, suggesting that p38 activation is, in fact, pro-apoptotic in cardiomyocytes. In transgenic mice with cardiac-specific expression of a dominant-negative mutant form of p38α after experimental diabetes; myocardial apoptosis, the number of caspase-3-positive cells, and the downregulation of antiapoptotic protein B-cell lymphoma-extra large (Bcl-X_L) are all

attenuated, suggesting a pro-apoptotic role for p38 (118). In addition, it has been previously reported that apoptosis is reduced by p38 inhibitors; SB203580, SB239063 or FR167653 in cardiac cells in response to several stimuli (63, 119-123). In isolated perfused hearts, p38 inhibitors are also cardioprotective (62, 64, 124). In bovine aorta endothelial cells, p38 involvement on β_2AR-mediated caspase-3 cleavage is suggested via negative regulation by the p38 inhibitor SB203580 (125). In Raf-1-knockout mice which demonstrated left ventricular systolic dysfunction, heart dilatation and an increase in apoptosis was associated with an increase in p38 kinase activity (126). Furthermore, overexpression of p38α or activated MKK3b in cultured neonatal cardiomyocytes (104) and expression of transforming growth factor-β-activated kinase-1 (TAK1) in the mouse heart by transgenesis, are associated with increased cardiac apoptosis (127).

The opposing findings on the role of p38 in apoptosis could be attributed to variation among genetic models and nonspecific effects of pharmacologic compounds. Nonetheless, the literature in models utilising more specific methods which are less prone to off-target effects, such as overexpression of wild-type or dominant-negative mutants, indicates that its activation plays a pro-apoptotic role in the cardiac setting.

1.6.5 Fibrosis

As already discussed, in cultured cardiomyocytes p38 activity is associated with myocyte hypertrophy and apoptosis. It also appears that p38 activity in cardiomyocytes contributes to remodelling in the adult heart. In intact mouse hearts although p38 overexpression/activation does not lead to hypertrophy, it increases remodelling of the extracellular matrix and diminishes contractile function (80, 128, 129). In a p38α knock out mouse model exposed to pressure overload, increased interstitial fibrosis is observed (102) whilst a mouse model expressing dominant-negative p38α displays resistance to

fibrosis in response to pressure overload (130). Furthermore, p38 activation using cre/loxP-based gene switch to create transgenic animals expressing the activated upstream kinases of p38, MKK3b and MKK6, leads to the induction of interstitial fibrosis, depresses contractility and compromises diastolic function (128).

In a recent study, overexpression of myostatin, a member of the TGF-β superfamily that is up-regulated under disease conditions, is shown to cause interstitial fibrosis via activation of the TAK1-MKK3/6-p38 pathway suggesting that upstream effectors also play a role in p38 activation leading to fibrosis. In addition, mitogen activated protein kinase-activated protein kinase 2 (MK2) is an important substrate of p38 that is associated with heart failure; since cardiac fibrosis and dysfunction are diminished in MK2 knockout mice (131, 132) potentially through an involvement of SERCA2 regulation. Treatment of hamster hearts with SB203580 reduces the area of fibrosis and heart /body weight ratio, increases LV ejection fraction and contractility (119). These findings provide evidence that p38 activation can contribute to fibrosis in the failing heart.

1.6.6 Autophagy

Autophagy serves as a double-edged sword with both anti and pro-apoptotic functions. In patients with heart failure, an increase in autophagy is observed and is associated with left ventricular systolic dysfunction (133, 134). There are studies suggesting that autophagy is a maladaptive process during the progression of heart failure and others which propose a protective role. In vivo studies blunting autophagy using 3-methyladenine, an inhibitor of class III phosphoinositide-3-kinase (PI3K), show heart failure progression is accelerated with an increase in interstitial fibrosis, worsening ventricular function and early mortality (135). In addition, a decrease in autophagy has been implicated in cardiac hypertrophy whilst an increase in autophagy in transgenic

mouse models has been linked to cardio-protection (136). However, excessive autophagy has been associated with the progression of cardiac remodeling and heart failure in response to pressure overload (137). Molecular studies of biopsy samples of left ventricular myocardium from patients with idiopathic dilated cardiomyopathy before the implantation, and after the removal, of a left ventricular assist device suggest that mechanical unloading of the heart leads to a decrease in markers of autophagy (138). In this study, it is suggested that autophagy may serve an adaptive purpose during the progression of heart failure.

Autophagy-related genes are upregulated in response to H_2O_2 treatment in myotubes, with a positive correlation to p38 activity. Inhibition of p38 using SB202190 decreases H_2O_2-induced expression of Atg7 (139). However in senescent human $CD8^+$ T cells, p38 inhibition using BIRB796 inhibits autophagy (140). In addition, in cultured neonatal rat cardiomyocytes exposed to 48 hours of mechanical stretch and in mice following transverse aortic constriction, p38 inhibition causes a decrease in the autophagy marker microtubule associated protein 1 light chain 3 β II (LC3b-II) (141). As the impact of autophagy in heart failure itself is controversial, it is difficult to assess whether the effect of p38 activation is protective or detrimental in heart failure. Nonetheless, it is apparent that p38 plays a role in the mechanism of autophagy.

1.6.7 Inflammation and cytokine signalling

Increasing evidence indicates that inflammatory cytokines, including TNF-α, interleukin 1β (IL-1β) and IL-6, are elevated in, and may contribute to, heart failure. TNF-α levels increase in patients with advanced heart failure and correlate with prognosis (142-145). TNF-α is not expressed in the non-failing heart, but is significantly increased in the end stage failing human hearts (146). This has been associated with negative inotropic effects, with the IL-1β-mediated expression of SERCA and phospholamban prolonging

the Ca^{2+} transient (143, 147). In addition, TNF-α induction in failing hearts leads to a further loss of contractility and worsening of extracellular matrix remodelling (148, 149). Interestingly, a similar array of pathological alterations is observed in response to p38 activation (128). Due to more than one inflammatory cytokine being associated with the progression of heart failure, studies involving manipulation of only one factor might not be the most effective way to investigate their summative effect on heart failure. Thus p38, by regulating varied inflammatory cytokines, becomes a more attractive therapeutic target and consequently has been explored in a number of studies (150, 151). In SB239063-treated spontaneously hypertensive stroke-prone rats, pro-inflammatory gene expression is attenuated and survival is increased (152). In transgenic mice expressing active MKK6, TNF-α and IL-6 induction and extracellular remodelling is increased (153). Administration of SB239068 in the same transgenic model reduces plasma levels of these cytokines, interstitial fibrosis and cardiac remodelling. In a MKK3 knock out model, similar results to pharmacologic inhibition of p38 are observed with a reduction in TNF-α-induced contractile dysfunction (77). Furthermore, knocking out MK2 in mice prevents the TNF-α-induced negative inotropic response (77). Other than the direct induction of inflammatory cytokine production, p38 is implicated in the amplification of ROS generation; a principal feature of vascular inflammation (154-157). These studies suggest that p38 inhibition in the stressed heart will be beneficial, at least in part through the suppression of inflammatory cytokines and consequent improvement in myocardial remodelling.

1.7 Clinical trials

With detrimental effects observed in *in vivo* and *in vitro* studies, clinical trials were performed using the agents, etanercept, a decoy approach to block TNF-α interaction with its receptor, and infliximab, a monoclonal antibody to neutralise TNF-α.

Unfortunately, results of either no benefit or harm were observed (158). A clinical trial for semapimod, an anti-inflammatory agent which inhibits p38 activity, was started for heart failure patients, but was apparently terminated upon the disclosure of the discouraging results of the TNF-α-targeted clinical trials (84).

Currently, there is an ongoing phase 3 clinical trial running with losmapimod (LATITUDE-TIMI 60, NCT02145468), which could potentially benefit acute coronary syndrome (ACS) patients. Losmapimod is an anti-inflammatory medication which inhibits p38 and may improve vascular function and reduce subsequent cardiac events following ACS.

Though further research is required on the mechanisms and consequences of p38 activation in heart failure, the substantial evidence for an important role of p38 in the development of heart failure and its potential as a therapeutic target has been discussed.

1.8 Amino acid response pathway and GCN2

Mammals have adaptive mechanisms to detect and regulate amino acid homeostasis in response to deficiencies in the diet. As multicellular organisms cannot make all amino acids and due to a lack of an amino acid store within cells, certain signalling pathways must be activated in order to adapt to the stress induced by imbalanced diet and starvation. During starvation, there is an amino acid response (AAR) pathway which is activated as an adaptive response (159) conserved from yeast to mammals. The key protein responsible to sense amino acid deficiency is the Ser/Thr kinase general control nonderepressible 2 (GCN2).

1.8.1 Aminoacyl tRNA synthetases

The structure and function of proteins are dependent on the accuracy of their amino acid sequence determining primary structure and errors can have severe consequences.

Aminoacyl tRNA synthetases play a major role in translation to ensure the specificity required to prevent errors in protein synthesis. Aminoacyl tRNA synthetases are the enzymes responsible for catalysing the linkage of tRNAs and their respective amino acids in order to produce amino-acyl tRNAs which can then be incorporated into proteins by the ribosome. The selectivity in this process of both the amino acid and the cognate tRNA is essential to maintaining the fidelity of the genetic code. To initiate this process, a particular aminoacyl tRNA synthetase binds a specific amino acid and a molecule of ATP at the active site of the aminoacyl tRNA synthetase, forming a covalent bond between the AMP and the carboxyl terminal of the amino acid and releasing a pyrophosphate. There is a specific anticodon on the tRNA that corresponds to the particular amino acid facilitating the binding of the correct tRNA to the aminoacyl tRNA synthetase. Once the tRNA is bound, the bond between the AMP and the amino acid is broken, releasing the AMP. A covalent bond is formed between the 3' end of the tRNA and the amino acid, and the tRNA is now referred to as being 'charged'. Following release from the aminoacyl tRNA synthetase, the charged tRNA is used to form proteins in the process of translation on a ribosome.

1.8.1.1 Prolyl-tRNA synthetase

There are two classes of aminoacyl-tRNA synthetases based on their sequence motifs and structure. Class I enzymes possess the Rossmann fold, whilst the class II enzymes contain a different fold around a six-stranded antiparallel beta-sheet (160). In addition, though both classes of enzymes catalyse the same reaction of charging tRNAs with their corresponding amino acid, they differ in the positioning of the amino acid on the tRNA, with class I causing attachment at the 2' hydroxyl whereas the class II act on the 3' hydroxyl group.

In higher eukaryotes, glutamyl- (class I) and prolyl- (class II) tRNA synthetases have been observed in a single peptide chain. The N-terminal of this glutamyl-prolyl tRNA-synthetase (EPRS) comprises the glutamyl-tRNA synthetase and the C-terminal specifies the prolyl-tRNA synthetase. It has been proposed that the association of these two enzymes is due to a gene fusion event to form a bifunctional synthetase with the two subunits acting independently as the two enzymes do not share functional domains and their separate expression has previously been observed (161, 162).

1.8.2 Role of eIF2 in protein translation

Protein translation is the step following the transcription of genes, in order to create functional proteins, which can perform their role within the cell. In simple terms, transcription is the transfer of the information contained in the DNA to a messenger RNA (mRNA) molecule using DNA as a template for complementary base pairing with an enzyme called RNA polymerase II playing a major role. Consequently, this mRNA copy of the gene is used for protein translation.

Eukaryotic translation of mRNA is an intricate process involving at least 12 proteins which cooperate to bring the mRNA, initiator Met-tRNA and the two ribosomal subunits together to form the 80S complex that can perform peptide chain elongation (163, 164). The assembly of the translation initiation machinery on the mRNA involves eukaryotic initiation factors (eIFs). eIF2 is a major component of the ternary complex required for the initiation of translation. eIF2 binds GTP and the initiator Met-tRNA forming a complex which consequently contributes to the 43S preinitiation complex (PIC) with the 40S ribosomal subunit. eIF4s facilitate the unwinding of the secondary structure in the 5’ untranslated region of the mRNA, which enables the binding of the PIC and subsequent scanning of the mRNA for the initiator AUG codon (165). Once the AUG codon binds to the complementary Met-tRNA, eIF5 induces the hydrolysis of the

GTP on eIF2, leading to the release of eIF2-GDP. The 60S ribosomal subunit is then recruited to form the 80S initiation complex and translation can begin. The guanine exchange factor eIF2B catalyses the exchange of GDP to GTP on eIF2 in a regulated manner, to initiate a new round of translation (166).

1.8.3 Activation of General Control Nonderepressible (GCN2)

Limitation of amino acids within the cell causes an increase in uncharged tRNA which bind to GCN2 and induce its autophosphorylation. Uncharged tRNA binds to a region homologous to histidyl-tRNA synthetase (HisRS) at the C-terminal of the kinase domain, which is essential for tRNA binding to GCN2 (167-169). It has been reported that GCN2 binds different uncharged tRNAs with similar affinities though as expected, it can distinguish between charged and uncharged forms of tRNA (170). The kinase domain of GCN2 is basally inert and requires interactions with four other domains to achieve activation (171). A rigid hinge between the N- and C- lobes of the kinase domain aids the occlusion of the ATP-binding site and promotes the closed state of the active site (172). Binding of uncharged tRNA to the HisRS-like domain leads to a conformational change facilitating autophosphorylation of the kinase at the activation loop. This can in turn promote the required alignment of residues involved in substrate binding and phosphoryl transfer (173, 174).

1.8.4 eIF2alpha phosphorylation and downstream of the AAR pathway

eIF2 is a heterotrimer consisting of an alpha, a beta and a gamma subunit. Once activated GCN2, phosphorylates the alpha subunit of eIF2 (eIF2alpha), thereby halting global translation while paradoxically increasing the translation of selected mRNA species. As previously mentioned, to initiate translation GDP on eIF2 must be exchanged for GTP by eIF2B. The phosphorylation of eIF2alpha prevents this GDP-

GTP exchange by stabilizing the eIF2-GDP-eIF2B complex, therefore halting global translation (175).

This consequently induces the translation of a subset of proteins that enable the cell to cope with starvation. Amongst these proteins are activating transcription factor 4 (ATF4), activating transcription factor 5 (ATF5) and growth arrest and DNA damage-inducible 34 (GADD34). GADD34 is involved in recruiting protein phosphatase 1 (PP1) to phosphorylated eIF2alpha, which is then dephosphorylated and general translation can resume along with the upregulated stress-responsive genes in response to starvation (176-178). Among the upregulated genes are;

DDIT3 (gene name for C/EBP homologous protein (CHOP-1)) known for its role in apoptosis, inflammation and regulation of transcription (179-182);

TRIB3 (gene name for tribbles pseudokinase 3) reported to regulate apoptosis, cell survival and stress-induced transcription (183, 184);

and *ASNS* (gene name for asparagine synthetase) catalysing the synthesis of asparagine to aid the cell to survive through starvation-induced stress (185).

1.8.4.1 Mechanism of induction of gene upregulation via amino acid response elements (AARE)

In response to starvation, gene upregulation is facilitated by amino acid response elements (AARE) in the promoter sequences of the targets genes. AARE act as enhancer elements to increase transcription (185, 186) and are made up of 9 base pair core elements (5′-A/GTTG/TCATCA-3′). It is widely recognised that protein complexes bind to AARE elements in order to regulate transcription including a combination of ATF4, ATF2, ATF3 and/or CHOP. Importantly, all of the known AAREs have been reported to bind to ATF4, the key player in the regulation of AAR genes. Nonetheless, the combination of transcription factors and the effect of positive or negative regulation

of transcription are determined by the AARE sequence and chromatin structure. For example, both ATF4 and ATF2 are required to bind to the AARE of the *DDIT3* (CHOP) gene for its induction (186, 187). In addition, CHOP interaction with ATF4 leads to the negative regulation of the *ASNS* gene through interaction with its promoter (188).

1.8.4.2 *DDIT3* (CHOP)

The CCAAT-enhancer binding proteins (C/EBP) are a group of transcription factors that bind to CCAAT motifs in DNA and play an important role in cell differentiation (189-191). The prototype of a C/EBP protein contains a transcriptional activation/repression domain and a bZIP region with a basic DNA binding domain and a leucine zipper motif required for dimerisation. Proline and glycine substitutions exist in CHOP at the sites of conserved residues essential for C/EBP to interact with DNA (192, 193). It has been proposed that the reason why CHOP lacking the DNA binding activity exists, is to form nonfunctional dimers and sequester the activity of bZIP proteins. Despite studies showing evidence for this negative regulation by CHOP (192), other studies have provided a platform where CHOP could induce the transcription of other genes, depending on its binding partner and the target gene (194, 195).

1.8.4.3 TRIB3

TRIB3 is a pseudokinase associated with roles in the stress response, apoptosis and metabolic processes induced by its interaction with several transcription factors, kinases and other proteins (195-197). Within the starvation response, it has been reported to perform negative feedback on the ATF4-mediated control of stress-regulated genes (198), as well as a role in cardiovascular disease (199). TRIB3 has been reported to bind to ATF4 at AARE sequences, potentially performing its negative feedback through this

interaction to inhibit the induction of other genes, two of which are CHOP and ASNS (183).

1.8.4.4 ASNS

As already mentioned ASNS is the enzyme required for the synthesis of asparagine and metabolically the increase in this gene in response to stress is associated with cells lacking adequate ASNS activity reaching cell cycle arrest and apoptosis (200, 201).

1.8.5 Other upstream kinases of eIF2alpha

Phosphorylation of eIF2alpha has previously been found to be a common mechanism to downregulate global protein synthesis under certain stress conditions (159). In addition to GCN2, three other kinases upstream of eIF2alpha share sequence and structural similarities but differ in their regulatory domains. These kinases are the interferon-induced double-stranded RNA (dsRNA)-dependent protein kinase R (PKR), protein kinase RNA-like endoplasmic reticulum kinase (PERK) in the unfolded protein response and haem regulated inhibitor kinase (HRI) in response to haem deficiency. There is a high extent of similarity in the catalytic domains of these proteins and they all phosphorylate Ser51 of eIF2alpha (202). Nonetheless, the regulation of each upstream kinase of eIF2alpha and their downstream responses are different and circumstance-specific.

1.9 Halofuginone

Plant bioactives have been used extensively as a source of new drugs and many current commonly prescribed drugs are derived from plants. Febrifugine is a piperidine quinazolinone alkaloid isolated from the Chinese herb chang shan, *Dichroa febrifuga* (203) used in Chinese medicine for over 2,000 years to treat malaria-induced fever. Febrifugine has been important for its therapeutic activity despite lack of information on

its exact molecular target in part related to side effects impeding relevant studies. Halofuginone is a racemic halogenated derivative of this plant bioactive, designed to overcome the toxic effects of febrifugine whilst still providing the protective characteristics (204). Halofuginone has recently progressed to phase 2 clinical trials for its potential therapeutic applications in cancer and fibrotic disease (205-208).

1.9.1.1 Mechanism of action

Halofuginone plays a role in inhibiting T_H17 cell differentiation by inducing the amino acid response pathway (209). The mechanism of action of halofuginone is through the inhibition of prolyl-transfer RNA synthetase (ProRS) leading to an accumulation of uncharged tRNAs within the cell (159, 204). It has been recently reported that unhydrolysed ATP is required for halofuginone-mediated inhibition of the ProRS. ATP is involved in directly binding to halofuginone via hydrogen bonds and orienting it onto the ProRS in a conformation that will allow halofuginone to mimic proline and 3' end of tRNA simultaneously (210) inhibiting ProRS in a bipartite manner (see Figure 1.8).

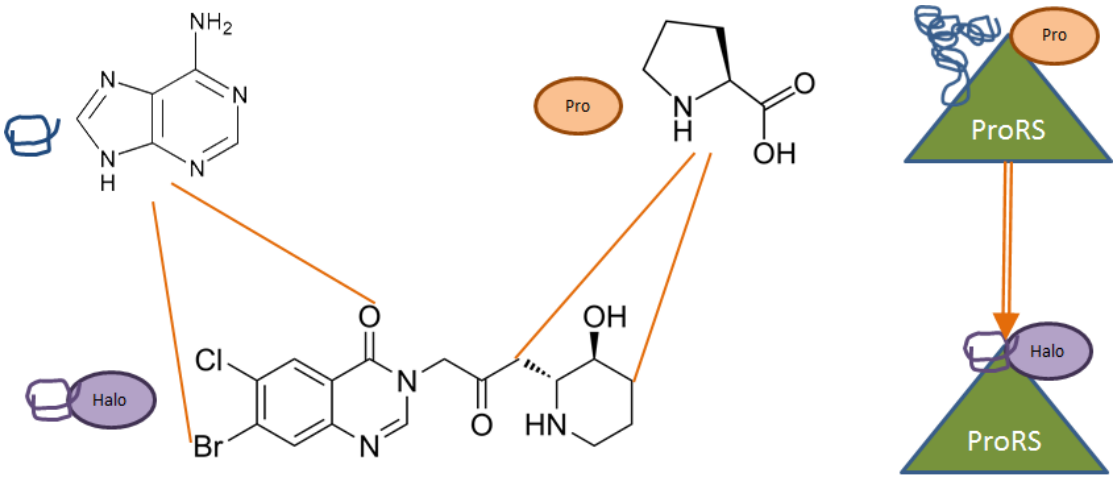

Figure 1.8 Chemical structure of halofuginone and its similarities to proline and 3' end of tRNA.
Halofuginone is composed of a hydroxypiperidine ring joined by bridging atoms to a double-ring halogenated 4-quinazolinone. The piperidine ring mimics the pyrrolidine ring of proline, whereas the halogenated quinazolinone has a similar structure to the conserved adenine at the 3' end of tRNA. These similarities of halofuginone to the two substrates of ProRS, enable its mechanism of blocking their binding to the ProRS, leading to an accumulation of uncharged tRNA.

1.9.1.2 Role in fibrotic diseases

Collagen and other matrix proteins are important in the development and repair systems of organs. However, excessive accumulation of these proteins leads to fibrosis resulting in an overload of extracellular matrix (ECM) deposition with collagen type I being the key player. Excessive production of connective tissues regardless of the organ involved leads to the tissue damage, loss of structure and function, consequently resulting in organ failure (211). The mechanism of fibrosis typically involves the continual activation of the transcription of the ECM genes, increased deposition as well as inefficient degradation and removal of the ECM, a function of the matrix metalloproteinases (212).

Several studies have reported an antifibrotic role for halofuginone through inhibition of TGF-β-mediated collagen synthesis in a variety of conditions (205, 206, 213, 214). The increase in collagen synthesis due to chronic graft versus host disease and scleroderma is abrogated with halofuginone treatment in mice (205, 215). In addition, halofuginone results in a reduction in pulmonary and liver fibrosis (213, 216), peritoneal adhesions (217) and colitis in rats (218). Overall, halofuginone plays an antifibrotic role in a wide range of organs in acute and chronic conditions.

Duchenne muscular dystrophy (DMD) is a recessive X-linked disease caused by a mutation in the dystrophin gene (219) leading to a deficiency of this protein, which is an essential component of muscle tissue. In addition to skeletal muscle, dystrophin plays a fundamental role in stabilising the cardiac cytoskeleton. DMD has been associated with dilated cardiomyopathy and left ventricular dysfunction with an increased correlation in the later stages of the disease (220, 221). The mdx mouse is an extensively studied model of DMD, as it has a point mutation in its dystrophin gene resulting in the absence of the functional dystrophin in its striated muscles mimicking the phenotype observed in DMD patients. In a study on mdx mice, halofuginone decreased fibrosis, collagen I and

III gene expression and collagen protein levels, as well as improving cardiac and respiratory function (222).

The activation of phosphoinositide 3'-kinase/Akt (PI3K/Akt), ERK and p38 are crucial for myotube fusion. In a C2 muscle cell line and in primary myoblasts from wild-type and mdx mice diaphragms, halofuginone lead to a reduction in Smad3 phosphorylation levels mediated by the activation of these kinases (223). Therefore, besides its antifibrotic activity halofuginone also has muscle regenerative effects.

1.9.1.3 Clinical trials

In addition to the evidence in animal models, antifibrotic effect of halofuginone in early clinical studies of topical administration (NCT00064142) and anti-angiogenic effects in progressive advanced solid tumours (NCT00027677) were reported in patients treated with halofuginone. Recently, a phase 2 clinical trial has been proposed to evaluate the safety, tolerability and pharmacokinetics of halofuginone in patients with DMD (HT-100, NCT01847573).

1.9.1.4 Halofuginone and p38

There are only a few studies implicating a role for halofuginone in regulating p38 activity. Halofuginone appears to have anti-inflammatory properties in rats with experimental colitis, involving suppression of neutrophil accumulation and inhibition of reactive oxidant generation (218). With this observation and given the role p38 plays in inflammation (224), it is logical to expect halofuginone to inhibit p38. Indeed, halofuginone treatment inhibits activated peripheral blood T cell functions as well as proinflammatory cytokine production by inhibiting NF-kappaB activation and p38 MAPK phosphorylation (225).

Nonetheless, this halofuginone-mediated inhibition of p38 is not the case in all cells of the body and it appears that halofuginone has a cell-type specific effect. The anti-

fibrotic effects of halofuginone have been associated with its regulation of matrix metalloproteinases (MMPs); enzymes capable of degrading extracellular matrix proteins. In rat hepatic stellate cells, halofuginone up-regulates MMP-3 and MMP-13 expression between 10- and 50-fold, and accordingly increases interstitial collagenase activity mediated by p38. This increase in mRNA expression of MMP-3 and MMP-13 was also present at 1.5- and 2-fold, respectively in the in vivo setting in rats with established liver fibrosis. A causal role for p38 in this setting was established using the p38 inhibitor, SB203580 (226).

Perhaps more related to this thesis is the observation that halofuginone enhances p38 phosphorylation and inhibited Smad3 phosphorylation in myotubes (223). This would explain the improvements observed in cardiac and skeletal muscle in the DMD setting. Nonetheless, the effects of halofuginone have not yet been investigated in the context of cardiomyocytes. Given the importance of p38 in a wide range of processes and established role in heart failure, besides the observed improvements in cardiac function in mdx models of mice by halofuginone, I decided to investigate the effects of halofuginone treatment on p38 activity in cardiomyocytes.

1.10 Endothelin-1

Endothelin (ET) is a 21 amino acid peptide secreted by vascular endothelial cells (227). It is produced from a 39 amino acid precursor, big ET, by proteolytic processing activity of an enzyme called endothelin converting enzyme (ECE) found on the endothelial cell membrane. Once released, ET binds receptors on target cells in order to trigger downstream events. Three isoforms of the ET family exist; ET-1, ET-2 and ET-3 and different responses can be evoked depending on the receptors they bind (228). There are two types of ET receptors found in mammals; ET_A and ET_B, of which both are G-protein coupled seven transmembrane receptors. ET_A receptors are localised on

smooth muscle cells and ET_B receptors are found on endothelial cells, smooth muscle cells and macrophages (229, 230). ET_A receptors bind to ET-1 and ET-2 with a 100 times higher affinity than ET-3, while ET_B receptors have similar affinity for all three ET isoforms (231). Both receptors are coupled to a phospholipase C (PLC)-coupled Gq-protein involved in the formation of inositol 1,4,5-trisphosphate (IP_3) from phosphatidylinositol biphosphate (PIP2) through the activity of phospholipase C (PLC). Increased levels of IP_3 within the cell induce calcium release from the sarcoplasmic reticulum and causes smooth muscle contraction. Under normal conditions, ET_A plays a dominant role in determining the tone of blood vessels. However, ET_B receptors are also present on the endothelium and upon binding of ET-1 to these receptors, intracellular calcium levels increase, resulting in the activation of the enzyme, nitric oxide synthase producing nitric oxide (NO). NO then diffuses to the vascular smooth muscle cells leading to the activation of soluble guanylate cyclase to form cyclic GMP (cGMP) which initiates vasodilatation.

The initial vasodilatation followed by prolonged vasoconstriction in response to systemic administration of ET-1 can be explained by the distribution of the endothelial and smooth muscle cell receptors (232, 233). Baroreceptor reflexes regulate the response of the heart by altering arterial pressure upon treatment with ET-1. Other effects of ET-1 include aldosterone secretion, renal blood flow regulation and release of atrial natriuretic peptide (ANP) (234-236).

Regulation of signalling pathways is important in maintaining control of processes within a cell and stimulating downstream changes in a stimulus dependent manner. Negative feedback systems must exist to enable the cessation of action when it is no longer necessary or needs to be diminished to basal levels. Receptor internalisation is one of the essential processes required to control the effects of ligands. Receptor-bound ligands are internalised by endocytosis and the ligand is recycled or degraded by the

lysosome. It has previously been reported that ET does not dissociate easily from its receptors (237) and induces long-lasting vasoconstriction. Receptor internalisation is one system that has been proposed as a negative feedback on the ET-mediated changes as it appears that ET-1 triggers ET_A internalisation in a time-dependent manner (238) possibly via β-arrestin binding(239). In addition to this distal regulatory process; receptor down-regulation (240), and desensitisation through phosphorylation of the ETA receptor by G-protein coupled receptor kinase 2 (GRK2) are other negative feedback mechanisms proposed.

In previous studies, ET-1 has been implicated in the development of cardiovascular diseases including hypertension, vascular remodelling, myocardial infarction and heart failure (241-244). Increased ET-1 production has been reported in heart failure patients (241) and animal models (245, 246) and circulating ET-1 correlates with symptoms (247, 248).

1.11 Summary of introduction

p38α is involved in innumerable cellular processes and is exquisitely controlled through at least 3 different mechanisms of activation. During myocardial ischaemia the mechanism of activation is unusual, differing from the usual MKK-dependent canonical pathway, and is instead reliant on an association with TAB1. The purpose of this thesis was to examine this association with the ultimate aim of understanding and preventing it. If this could be achieved it is possible it would be of benefit to patients with ischaemic myocardium where the association between TAB1 and p38α has been shown to aggravate injury.

Another signalling pathway involving p38α, with a potential role in heart failure, is the AAR pathway. Halofuginone, a compound which activates the AAR pathway, has been implicated in improved cardiac function in mdx models of mice. Exploring this system

by using halofuginone as a tool compound could provide further insight as to whether the activation of this pathway can influence hypertrophy, autophagy and inflammation, processes relevant to heart failure. The main purpose of the research presented within this thesis is to understand and manipulate the activation of p38α in myocardial ischaemia and heart failure.

1.12 Aims

The specific aims of the thesis are;

1. To confirm whether TAB1 overexpression causes a pattern of p38α phosphorylation consistent with autophosphorylation
2. To understand the residues and regions of TAB1 responsible for p38α activation and whether these affect p38α phosphorylation and TAB1 substrate presentation
3. To determine whether TAB1 phosphorylation state affects the canonical activation pathway
4. To examine whether there is competition between TAB1 and MKK3b in binding to p38α
5. To investigate the role of Thr185 in p38α in-cell localisation
6. To investigate the activation of the AAR pathway with halofuginone in cardiomyocytes
7. To observe the effects of AAR pathway activation on autophagy and inflammation
8. To observe the effect of halofuginone on p38α activity and the relation of this to the AAR pathway

2 MATERIALS and METHODS

2.1 Recombinant protein expression

2.1.1 The principle

Recombinant DNA methods describe the processes of combining DNA from two or more sources in order to create a unique protein. In our case, a recombinant plasmid was constructed using a pET vector in order to express the mammalian gene of interest in Escherichia coli (E.coli) cells. The pET vector contains the antibiotic resistance gene, lac repressor gene (lac I) and the T7 promoter. The gene of interest is inserted just after the ribosome binding site, which is downstream of the T7 promoter and lac operator DNA sequences. As the target gene is controlled by the T7 promoter, T7 polymerase must be present for its transcription. In order to manipulate this system for the induction of the gene of interest, the T7 polymerase gene has been inserted downstream of the lac promoter in the E.coli genome.

In the absence of lactose (a combined galactose-glucose disaccharide), the lac repressor binds to the lac operator and prevents the T7 polymerase gene being expressed. However, when lactose is present, it binds to the lac repressor and changes its conformation rendering it unable to bind to the lac operator. The galactose analog isopropyl β-D-1-thiogalactopyranoside (IPTG) also induces this conformational change in the lac repressor and cannot be metabolised by E.coli, making it possible to keep IPTG concentrations constant. IPTG enables the transcription of the T7 polymerase, which in turn induces the transcription of the gene of interest. Therefore, the transcription of the gene of interest is indirectly inducible by IPTG.

The induction of this system by IPTG is performed at the mid-log phase of growth when the OD600nm is between 0.3 and 0.8, in order to maximize the yield of the transcribed protein.

2.1.2 The protocol

E.coli Rosetta (DE3) strain *(Bioline)* was used to express the recombinant protein encoded by the pETDuet-1 vectors. 50 µl of E.coli was transformed with the vectors as in section 2.5.2 and 100 µl of the final culture was spread onto lysogeny broth (LB) plates (containing 1% (w/v) NaCl, 1% (w/v) Tryptone, 0.5% (w/v) yeast extract and 1.5% (w/v) agar) with Ampicillin (100 µg/ml) *(Sigma)* and incubated at 37ºC overnight. 5 ml of previously autoclaved LB broth (containing 1%(w/v) NaCl, 1% (w/v) Tryptone, 0.5% (w/v) yeast extract with Ampicillin (100 µg/ml) was inoculated with a single colony from each plate and incubated at 37ºC under gentle agitation and optical density at 600 nm (OD600) was measured at 20 minute intervals until it reached 0.3-0.4. Then, 1 ml of the culture was aliquoted to induce the protein expression by 1 mM IPTG *(Sigma)* for 5 hours and another 1 ml aliquot was kept without IPTG induction as a negative control, and the rest of the culture was kept as a stock. Pellets were obtained by centrifuging at 16,400 rpm for 1 minute at 4ºC. The supernatant was removed and the pellet was resuspended in 1 ml cold lysis buffer (containing 1 mM EDTA, 1 mM EGTA, 20 mM HEPES, 150 mM NaCl, 50 mM NaF, 1 Mm Na_3VO_4 and 1 tablet (per 50 ml of lysis buffer) of protease inhibitor cocktail *(Roche Diagnostics)*). Equal amounts of the lysate and 2X sample buffer (containing 20% glycerol, 6% SDS in 0.12 M Tris, pH 6.8 with 10% 2-mercaptoethanol (BME) *(Aldrich)*) were boiled for 10 minutes and then loaded onto a polyacrylamide gel for western blotting.

2.2 In vitro kinase assay

2.2.1 The principle

The role of protein kinases is to phosphorylate their substrate by transferring the γ-phosphate group of an ATP molecule to an acceptor site on their substrate (249). An vitro kinase (IVK) assay is a commonly used method to measure the activity of a protein kinase by observing the phosphorylation level of the substrate. The method is based on combining the kinase, substrate, and ATP in the presence of $MgCl_2$ in a tube and incubating it at an optimal temperature for the kinase to undertake its function and phosphorylate its substrate. The samples can then be analysed by Western blotting using phospho-specific antibodies to detect changes in the level of phosphorylation of the substrate under different conditions.

2.2.2 The protocols

2.2.2.1 Different TAB1 peptides to mediate p38 phosphorylation

Three TAB1 peptides were ordered from *Activotec* and diluted in peptide dilution buffer (20 mM Tris-HCl pH 7.5). These peptides were:

- 46mer peptide including both p38 binding regions (common docking domain and unique hydrophobic domain):

[NH_2-EMSQPTPTPAPGGRVYPVSVPYSSAQSTSKTSVTLSLVMPSQGQMV-COOH]

- 13mer peptide binding to the common docking domain of p38α: [NH_2-KTSVTLSLVMPSQ-COOH]
- 13mer peptide binding to the unique hydrophobic groove of p38α [NH_2-RVYPVSVPYSSAQ-COOH]

8.5 µl 10X kinase buffer (KB) (containing 250 mM Tris-HCl (pH 7.5), 50 mM beta-glycerophosphate, 1 mM Na_3VO_4, 100 mM $MgCl_2$ and 20 mM dithiothreitol (DTT)), 600 µM ATP, 3 µM p38α (non-active, unless a control), 15 µM substrate (TAB1 peptides – only one in their respective samples) and peptide dilution buffer up to 85 µl were mixed in a tube and the kinase reaction was performed at 37°C for differing lengths of time for comparison of phosphorylation. 15 µl aliquots were taken at each time point. 3.75 µl of 5X sample buffer were added and samples were boiled at 100°C for 10 minutes and stored at -20°C until analysis by Western blotting.

2.2.2.2 Competition between TAB1 peptide and MKK3b to mediate p38 phosphorylation

In IVK experiments examining the competition between TAB1 and MKK3b, p38 was incubated with TAB1 before the addition of MKK3b. In addition, due to the different efficiencies of phosphorylation of p38 mediated by MKK3b and TAB1, a lower concentration of MKK3b protein than TAB1 peptide was used. This was to allow TAB1 a chance to compete with MKK3b and minimise phosphorylation bias based on efficiencies, as we were purely interested in the binding site competition between MKK3b and TAB1. 8.5 µl 10X KB, 600 µM ATP, 3 µM p38α (non-active) were mixed in a tube and for treatments involving p38 inhibition, samples were pretreated with 10 uM SB203580 for 10 minutes at 37°C, before the addition of the 29mer TAB1 peptide, [NH_2-RVYPVSVPYSSAQSTSKTSVTLSLVMPSQ-COOH]. Upon TAB1 addition, the samples were incubated at 37°C for 4 hours. Then, 0.00847 µM (determined by titration of MKK3b concentration to a low enough concentration where p38 begins to be phosphorylated) of constitutively active form of MKK3b (MKK3bEE S218E/T222E), recombinant protein previously made by Dr Denise Martin, and activation buffer (containing 50 mM Tris-HCl pH 7.5, 0.1 mM EGTA, 0.1% BME, 10 mM MgAc and

0.1 mM ATP) was added to the samples. After a further 30 minute (unless otherwise stated) incubation at 37^{o}C, 2X sample buffer was added to samples and boiled at 100^{o}C for 10 minutes and then loaded onto a polyacrylamide gel for Western blotting.

2.3 Subcloning inserts from a bacterial vector (pETDuet-1) to a mammalian vector (pcDNA3)

In scientific research, simple models are utilised to gain a better understanding of certain mechanisms. In vitro assays, bacterial protein expression systems, tissue culture and working with animals are a few of the methods used for this purpose. However, depending on the different methods employed, specific tools must be used. IVK assays require purified proteins whereas bacterial transformation and cell transfection systems will only express the protein of interest if the specific promoter is present in the plasmid before the gene of interest. Therefore, in our case the plasmids containing the mutant versions of TAB1 used to transform bacteria cannot be used to transfect mammalian cells, as they lack the mammalian promoter and the bacterial promoter cannot induce expression in the mammalian system. To confirm the effect of the TAB1 mutations observed in section 3.4, the effect of the mutations in TAB1 must be investigated in a mammalian cell line; e.g. Human Embryonic Kidney (HEK) 293 cells. Nonetheless, as already mentioned the bacterial plasmid does not have the features to be expressed in the mammalian cell line, and the TAB1 mutant genes must be cloned into a mammalian vector (see Figure 2.1).

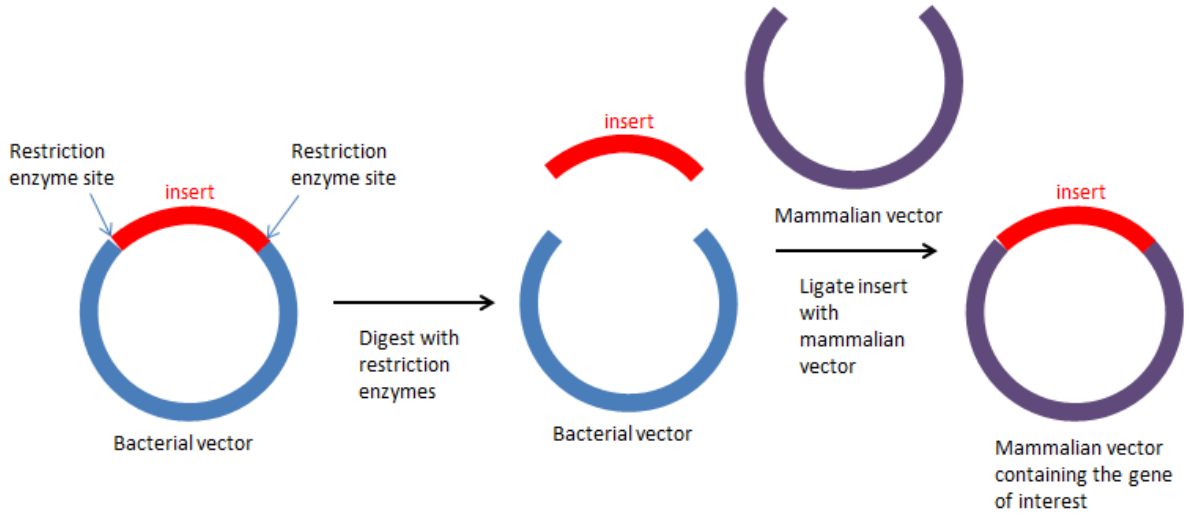

Figure 2.1 Schematic showing subcloning of an insert from a bacterial vector into a mammalian vector

The bacterial vector pETDuet-1 (see Figure 2.2), has two multiple cloning sites (MCS) making it possible to have two inserts in the same vector, in our case these genes are p38α and wild-type (WT) or mutants of TAB1. Being given pETDuet-1 containing p38α and the WT or mutated versions of TAB1 by Dr Gian Felice de Nicola, it was known that p38α was inserted between the BamHI and PstI restriction enzyme sites and the TAB1 genes were inserted between NdeI and XhoI sites.

2.3.1 Introducing new restriction enzyme sites by Polymerase Chain Reaction

2.3.1.1 The principle of PCR

Polymerase chain reaction (PCR) was developed in the 1980s by Kary Mullis and is a widely used technology in biological research (250). PCR exploits the enzyme, DNA polymerase, in order to synthesise DNA fragments by replicating genetic material. A primer, an oligonucleotide specific to the target gene, is used to target the polymerase to the site chosen on one of the original DNA strands to start the synthesis. Primers enable the replication of only the chosen sequences and the result is vast number of copies of the target DNA sequence (251). A thermal cycler is used for PCR reactions and there are four main steps in the process. The initialization step is usually required to activate

DNA polymerases and consists of increasing the temperature to around 94ºC. After holding, the cycles are started with the denaturation step to separate the DNA template into single-stranded DNA molecules by disrupting the hydrogen bonds for 20-30 seconds. The following annealing step consists of lowering the temperature to allow the annealing of the primers to the single-stranded DNA template. Hydrogen bonds between the primer and template DNA are formed when the primer sequence closely matches the template. Then, the DNA polymerase binds to this hybrid and begins copying the template DNA. The next step is for the elongation of the sequence by the DNA polymerase and is performed at the optimal temperature for the specific polymerase being used. The enzyme works by adding deoxynucleotide triphosphates (dNTPs) that are complementary to the template in a 5'→ 3' fashion, joining the 5' phosphate group of the free dNTPs with the 3' hydroxyl group of the nucleotide on the existing DNA strand. Under optimum conditions, after each extension step DNA is doubled leading to an exponential amplification of the template DNA. A final elongation step is often performed to ensure that any remaining single-stranded DNA is fully extended.

2.3.1.2 The protocol

Observing the destination mammalian vector map (see Figure 2.3), it is clear that NdeI enzyme cleaves at middle of the cytomegalovirus (CMV) promoter. Removing a section of this promoter would prevent the cells transfected with this vector expressing the gene of interest as the function of a promoter is driving gene expression. Therefore, the insert needs to be inserted elsewhere in the pcDNA3 MCS and the NdeI restriction enzyme must be substituted by the new chosen restriction enzyme site. BamHI was chosen for this purpose. The second restriction enzyme was kept as XhoI, which is at the carboxyl

terminal of the TAB1 insert in the pETDuet-1 vector. Two different restriction enzyme sites were used to prevent religation of the vector onto itself.

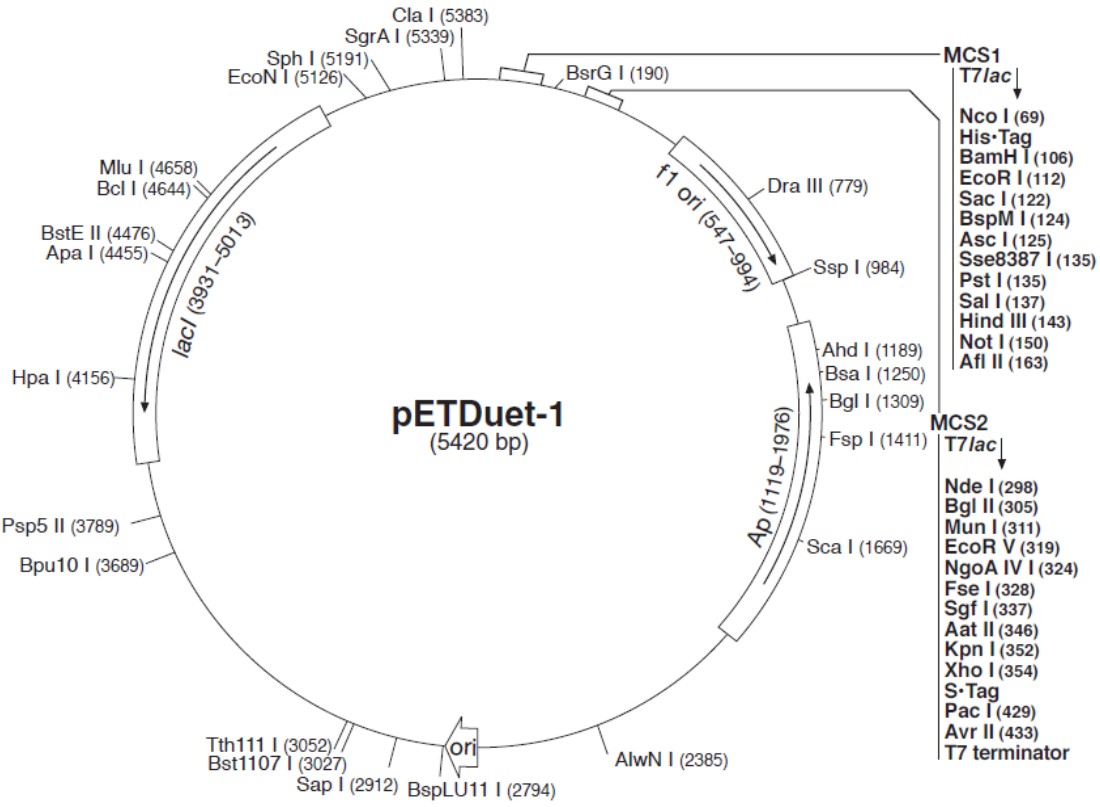

Figure 2.2 Map of the bacterial expression vector pETDuet-1. ***Novagen***

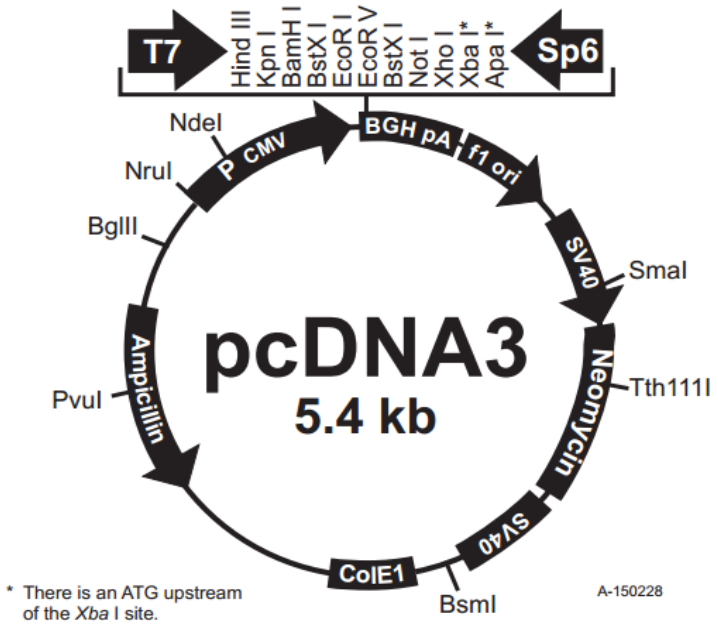

Figure 2.3 Map of the mammalian expression vector pcDNA3. ***Invitrogen***

The TAB1 inserts were amplified by PCR using the pETDuet-1 plasmids as template. 10 µl of 5X RANGER reaction buffer *(Bioline)*, 20 µM of forward primer, 20 µM of reverse primer, 5 ng DNA, 1 µl of Ranger DNA polymerase *(Bioline)* were combined in a PCR tube and made upto a final volume of 50 µl with ddH_2O. The PCR cycling conditions are shown in Table 2.1.

Table 2.1 PCR cycling conditions

Step	Temperature	Time	Cycles
Initial denaturation	95°C	1 min	1
Denaturation	98°C	10 sec	30
Annealing	77°C	30 sec	
Extension	68°C	7 min	
Final Extension	68°C	10 min	1

The templates and primers were provided by Dr Gian Felice de Nicola and have the following sequences:

Forward primer introducing the BamHI site highlighted in pink and the '^' symbol indicates point of cleavage:

ATATATG^GATCCGCCATGGCAGCACAACGTCGTTCTCTGC

Reverse primer with the XhoI site highlighted in blue and the '^' symbol indicates point of cleavage:

TATATC^TCGAGTTATTACGGGGCGGTCATCACAG

Following PCR, the products were run on a 0.7% agarose gel *(AGTC Bioproducts Ltd)* (see Figure 2.4) to ensure they were the correct size, excised and purified using High Pure PCR Product Purification Kit *(Roche)*.

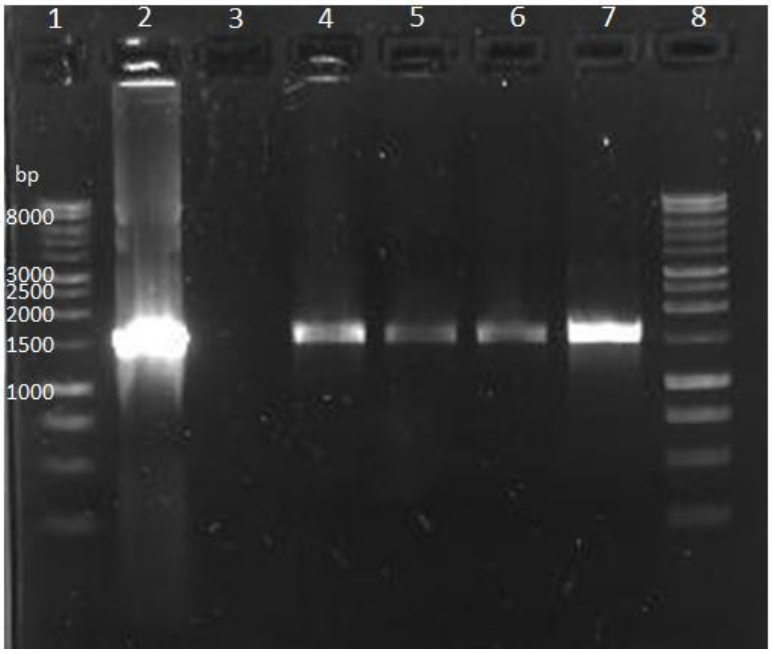

Figure 2.4 PCR products.
20 µl of PCR products were ran on a 0.7% agarose gel. Lane 1: 1 kb ladder *(Promega)*, lane 2: positive control – PCR product from a previous positive clone, lane 3: empty, lane 4: WT TAB1 PCR product, lane 5: CM mutant TAB1 PCR product, lane 6: NCM mutant TAB1 PCR product, lane 7: CM/NCM mutant TAB1 PCR product, lane 8: 1 kb ladder.

2.3.2 Gel extraction of DNA

Once the band of interest was excised, High Pure PCR Product Purification Kit *(Roche)* was employed to purify the DNA. The excised gel was placed in a 1.5 ml tube and gel mass was determined by first pre-weighing the tube and the reweighing the tube with the gel slice. 300 µl Binding Buffer for every 100 mg agarose gel slice was added to the tube. The agarose gel slice was dissolved to release the DNA by vortexing the tube 15-30 seconds first then once every 2-3 minutes during the incubation of the tube at 56^{o}C for 10 minutes. Once the agarose gel slice was completely dissolved, 150 µl isopropanol for every 100 mg agarose gel slice was added to the tube and vortexed thoroughly. The entire contents of the tube were pipetted into a High Pure Filter tube placed in a collection tube. The tubes were centrifuged at maximum speed for 30-60 seconds at room temperature (RT) and the flowthrough solution was discarded. 500 µl of wash buffer was added to the tube and centrifuged for 1 minute at maximum speed, as above.

The flowthrough solution was discarded and this step was repeated once again with 200 µl of wash buffer. The filter tube was combined with a clean 1.5 ml tube. 50-100 µl of elution buffer was added and the tube was centrifuged at maximum speed for 1 minute at RT and the resulting DNA was either stored at -20^{o}C or used as required.

2.3.3 Restriction enzyme digestion

Following purification, 1 µg of each PCR product and the pcDNA3 vector was double digested independently using 1 µl of each of the restriction enzymes BamHI *(New England Biolabs)* and XhoI *(New England Biolabs)* with 4 µl of 10X Buffer 4 *(New England Biolabs)* and 4 µl of bovine serum albumin (BSA) *(New England Biolabs)* made upto 40 µl with ddH_2O and incubated at 37^{o}C for 3 hours. The restriction enzymes were then heat inactivated for 20 minutes at 80^{o}C.

2.3.4 Ligation

Digested vector and each of the inserts (PCR products) were combined at a 1:3 ratio respectively, to a total of 100 ng DNA in a 1.5 ml tube with 5 µl 5X Quick-Stick ligase buffer *(Bioline)*, 1 µl Quick-Stick ligase *(Bioline)* and ddH_2O upto 20 µl. The mixtures were incubated at RT for 5 minutes and the whole mixture was used to transform E.coli cells as described in section 2.5.2. Several clones for each insert were picked to inoculate LB with 100 µg/ml Ampicillin in the 37^{o}C shaking incubator overnight. DNA was extracted from this bacterial culture using the Plasmid DNA Purification kit *(Macherey-Nagel)* and digested by restriction enzymes as described in section 2.3.3 and ran on a 0.7% agarose gel to reveal which clones had successfully incorporated the insert (see Figure 2.5). As can be seen, some clones only have a higher band which indicates the vector alone, and these are false positives. Whereas, other clones have the insert at a size of 1500 base pairs (bp) as well as the vector.

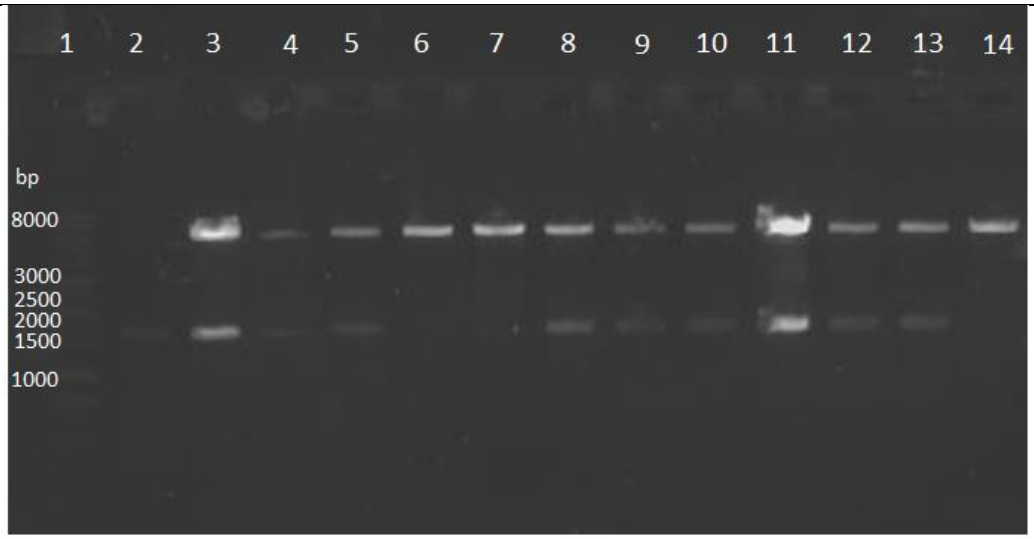

Figure 2.5 Ligation products double digested to check presence of insert.
Lane 1: 1 kb ladder (Promega), lane 2: positive control – PCR product from a previous positive clone, lane 3-5: WT TAB1 clones, lane 6-8: CM mutant TAB1 clones, lane 9-11: NCM mutant TAB1 clones, lane 12-14: CM/NCM mutant TAB1 clones. Lanes 3-5, 8-13 contain the positive clones whereas lanes 6, 7 and 14 contain false positives.

These positive clones were sent for DNA sequencing to ensure they have the correct TAB1 insert and the only changes in amino acid sequence are the ones designed.

Once sequencing was correct, the DNA was used for transfection of HEK293 cells.

2.4 DNA sequencing

DNA sequencing was performed using the 'value read' service of Eurofins MWG Biotech (Germany). Tubes containing 50-100 ng/µl of DNA in a total volume of 15 µl were prepared per sequencing reaction and sent off. The sequencing results were analysed by a comparison to their WT counterpart. DNA was sequenced using the primers T7 and Sp6 from the Eurofins MWG Biotech for forward and reverse orientations respectively.

2.4.1 TAB1 sequences

Below is the sequence of mouse WT TAB1 and highlighted in yellow is the region previously identified to interact with p38 (34). Highlighted in pink is the region which

binds to the unique hydrophobic groove in p38 and in turquoise is the region which interacts with the common docking domain of p38.

```
  1  MAAQRRSLLQSEQQPSWTDDLPLCHLSGVGSASNRSYSADGKGTESHPPEDNWLKFRSEN
 61  NCFLYGVFNGYDGNRVTNFVAQRLSAELLLGQLNTEHTEADVRRVLLQAFDVVERSFLES
121  IDDALAEKASLQSQLPEGVPQHQLPPQYQKILERLKALEREISGGAMAVVAVLLNSKLYV
181  ANVGTNRALLCKSTVDGLQVTQLNMDHTTENEDELFRLSQLGLDAGKIKQMGVICGQEST
241  RRIGDYKVKYGYTDIDLLSAAKSKPIIAEPEIHGAQPLDGVTGFLVLMSEGLYKALEAAH
301  GPGQANQEIAAMIDTEFAKQTSLDAVAQAVVDRVKRIHSDTFASGGERAKFCPRHEDMTL
361  LVRNFGYPLGEMSQPTPTPAPGGRVYPVSVPYSSAQSTSKTSVTLSLVMPSQGQMVNGSH
421  SASTLDEATPTLTNQSPTLTLQSTNTHTQSSSSSSDGGLFRSRPAHSLPPGEDGRVEPYV
481  DFAEFYRLWSVDHGEQSVMTAP
```

The p38 interacting region and the mutations in TAB1 are presented below and the mutations to generate the canonical mutant (CM), noncanonical mutant (NCM) and the mutant with both set of mutations (CM/NCM) are underlined. These mutants were used to perform transformations and transfections which will be discussed in detail in section 3.

```
WT:      EMSQPTPTPAPGGRVYPVSVPYSSAQSTSKTSVTLSLVMPSQGQMV

NCM:     EMSQPTPTPAPGGRVYPVSAPASSAQSTSKTSVTLSLVMPSQGQMV

CM:      EMSQPTPTPAPGGRVYPVSVPYSSAQSTSKTSVTLSLGAPSQGQMV

CM/NCM: EMSQPTPTPAPGGRVYPVSAPASSAQSTSKTSVTLSLGAPSQGQMV
```

2.5 DNA amplification and purification using bacteria

2.5.1 The principle

Through attachment to the bacterial membrane, divalent cations facilitate the uptake of plasmid DNA into a competent strain of E.coli that can absorb foreign DNA (252). Instant heating of E.coli permeabilises the membrane, enabling the entry of the DNA into the cell. Then, bacteria are grown in LB media containing the antibiotic against which the plasmid provides resistance so selectively amplifying those which have acquired the gene of interest. Once exponential growth of bacteria has occurred, meanwhile amplifying the DNA, a modified alkaline lysis procedure followed by

binding of DNA to a resin under appropriate low-salt and pH conditions is employed in order to purify the DNA. RNA, proteins, dyes, impurities and chromosomal DNA are removed by series of washes and plasmid DNA is eluted at the end in high-salt buffer and concentrated and desalted by isopropanol precipitation.

2.5.2 Transformation

E.coli DH5α strain *(Invitrogen)* was used to amplify DNA. 100 ng of DNA was added to 50µl of E.coli and left on ice for 30 minutes. Heat shock was performed at 42^{o}C for 45 seconds and tubes were returned to ice for another 2 minutes. 1ml LB without antibiotics was added to cells and left at 37^{o}C for 45 minutes on a shaker. 100µl of the mixture was spread on agar plates containing 100 µg/ml Ampicillin and kept at 37^{o}C overnight.

2.5.3 DNA amplification and purification by a Maxi Prep

A single colony was picked from the agar plate and 5 ml of LB (with Ampicillin) was inoculated using aseptic technique and incubated overnight at 37^{o}C in an orbital incubator, at 220 rpm. The plasmid DNA was then amplified in a large scale preparation. 4 ml of the previous culture was added to 200 ml LB (with Ampicillin) and incubated overnight at 37^{o}C in an orbital incubator, shaking at 220 rpm. The next day, plasmid DNA was purified using the HiSpeed Plasmid Purification Maxi Kit *(Qiagen).* Bacterial cells were harvested by centrifugation at 600 x g for 15 minutes at 4^{o}C. The bacterial pellet was resuspended in 10 ml resuspension buffer P1. 10 ml lysis buffer P2 was added and the mixture was inverted 4-6 times and incubated at RT for 5 minutes. During this incubation the QIAfilter cartridge was prepared by screwing the cap onto the outlet nozzle. 10 ml of chilled neutralisation buffer P3 was added and the mixture was mixed thoroughly by inverting 4-6 times and the contents were immediately placed into the QIAfilter cartridge. The mixture was incubated at RT for 10 minutes, during

which time the HiSpeed maxitip was equilibrated with 10 ml equilibration buffer QBT. The supernatant of the mixture was applied to the Maxitip and allowed to enter the resin by gravity flow. The Maxitip was washed in 30 ml wash buffer QC, and this was repeated. The DNA was then eluted with 15 ml elution buffer QF and precipitated with 10.5 ml isopropanol by incubating at RT for 5 minutes. During this incubation, QIAprecipitator Maxi module was attached to a 30 ml syringe. The eluate/isopropanol mixture was filtered through the module using constant pressure. 2 ml 70% ethanol was added to the syringe and the DNA was washed by pressing the ethanol through the module using constant pressure. The membrane was air-dried by pressing air through it quickly and forcefully. This step was repeated. The module was attached to a 5 ml syringe and 1 ml elution buffer TE was added to elute the DNA into a clean 1.5 ml tube. The yield of DNA was determined using a spectrophotometer with TE buffer as blank.

2.5.4 DNA purification by a Mini Prep

In experiments where only a small yield of DNA was sufficient such as for sequencing or cloning, a mini prep instead of the above maxi prep method was used. NucleoSpin Plamid kit *(Macherey-Nagel)* was used for this procedure. 1 ml of bacterial culture was centrifuged at 11000 x g for 30 seconds to pellet cells. The supernatant was removed and the pellet was resuspended in 250 µl of buffer A1 in order to lyse the cells. Then, 250 µl of buffer A2 was added to the tube and inverted several times to ensure thorough mixing. Samples were incubated at RT for 5 minutes and 300 µl of buffer A3 was added, mixing thoroughly by inversion. Cell lysates were clarified by centrifugation at 11000 x g for 5 minutes, and supernatants transferred to NucleoSpin® Plasmid Columns. Columns were centrifuged at 11000 x g for 1 minute and flow through was discarded. Samples were washed with 600 µl of buffer A4 and centrifuged at 11000 x g for 1 minute. The flowthrough was discarded and the membrane was dried by

centrifugation at 11000 x g for 2 minutes. 50 µl of buffer AE was added to each tube and after an incubation of 1 minute DNA was eluted into a clean tube by centrifugation at 11000 x g for 1 minute.

2.6 Tissue culture

2.6.1 Human embryonic kidney cells

2.6.1.1 Origins of cell line

Human embryonic kidney 293 (HEK293) cells were generated and established in 1977 by transformation of cultures of normal human embryonic kidney cells with sheared DNA of adenovirus 5 (253). The transformation led to the incorporation of approximately 4.5 kilobases from the viral genome into the human chromosome 19 of the HEK293 cells (254). For many years, it was assumed that HEK293 cells had epithelial, endothelial or fibroblastic origin as these cells are abundant in the kidney. Nonetheless, the group which originally transformed the cells provided evidence that these cells might have originated from neurons as the cells share many properties with immature neurons, suggesting that the adenovirus has transformed a neuronal cell in the original kidney culture (255).

HEK293 cells are popular in biological research for their ease of growth and maintenance, as well as their biochemical machinery that can perform most of the post-translational modifications and correct folding of both mammalian and non-mammalian proteins (256). As well as studying intracellular signaling, HEK293 cells are commonly used to produce exogenous proteins or viruses for biomedical research purposes.

2.6.1.2 Culture conditions

HEK293 cells were grown in Dulbecco's Modified Eagle Medium (DMEM) *(PAA)* containing L-glutamine (584 mg/l) with 10% (v/v) foetal bovine serum (FBS) *(PAA)*

and antibiotics (1% v/v streptomycin/penicillin) *(PAA)*. When the cells reached approximately 80% confluency, cells are transferred to a new flask with fresh media. In order to split HEK293 cells, first they were washed twice in phosphate buffered saline (PBS) (*Gibco*). Following the PBS wash, cells were then trypsinised with 1 ml of prewarmed Trypsin/EDTA *(PAA)* and incubated at 37ºC in a 5% CO_2 incubator for 5-10 minutes. Following incubation, cells were checked under the microscope to confirm loss of adhesion to the surface of the flask. 9 ml of prewarmed DMEM was used to resuspend the trypsinised cells, separate adherent cells and to dilute the trypsin/EDTA. Different dilutions of cells were seeded as required. Cells were incubated at 37ºC in a 5% CO_2 incubator.

When required cells were trypsinised, centrifuged at 1000rpm for 5 minutes, media aspirated to remove cell debris and dead cells and were resuspended in fresh DMEM. According to requirements cells were aliquoted in different plates.

2.6.2 H9c2 rat cardiomyoblast cells

2.6.2.1 Origins of cell line

H9c2 myoblast cell line was derived from the embryonic rat heart tissue in 1976 (257) and is widely used in cardiac and skeletal muscle-based research (258, 259) as they exhibit many of the properties observed in these type of cells.

2.6.2.2 Culture conditions

H9c2 were cultured in DMEM supplemented with 10% FBS and antibiotics (1% v/v streptomycin/penicillin) at 37ºC in a 5% CO_2 incubator. H9c2 cells were cultured in 6-well or 12-well plate formats depending on the requirements.

2.6.3 iPS cardiomyocytes from Cell Dynamics International

2.6.3.1 Origins of cell line

Induced pluripotent stem (iPS) cardiomyocytes are highly purified, human cardiomyocytes derived from iPS cells *(Cellular Dynamics International's (CDI)).* These cells have been obtained by CDI's proprietary differentiation and purification protocols. iPS cardiomyocyte-like cells are a mixture of atrial, nodal, and ventricular-like myocytes which are spontaneously electrically active and possess biochemical, electrophysiological, and mechanical characteristics similar to those expected of a cardiomyocyte. Depending on the stimulus, they display the expected responses and provide a platform which can be used as a surrogate for cardiac cells. Therefore, these cells are widely used as a reliable source of human cardiomyocytes suitable for use in cardiac-based research.

2.6.3.2 Culture conditions

In order to facilitate optimal cell viability and performance, the CDI instructions for thawing and plating iPS-cardiomyocytes were followed. The frozen iPS cardiomyocyte vial was placed in a 37^{o}C water bath for 4 minutes and held stationary. The contents of the vial were gently transferred to a 50 ml tube using a 1 ml pipette. The empty vial was rinsed using 1 ml of RT plating medium to recover residual cells from the vial. The rinse from the vial was transferred to the 50 ml tube in a drop-wise manner over 90 seconds, gently swirling the tube after each drop. 8 ml of RT plating medium was added to the 50 ml tube in a drop-wise manner with the first 1 ml being added over 60 seconds and the rest of the media over the next 30 seconds. The contents of the tube were gently mixed and inverted slowly. The cells were counted and seeded on gelatin-coated plates as required.

48 hours after plating, the cells were washed twice with maintenance media and fresh 37^{o}C maintenance media was added to wells. The iPS-cardiomyocytes were maintained in culture for two weeks at 37^{o}C in a 7% CO_2 incubator, replacing the maintenance media every other day.

2.7 Neonatal rat ventricular myocyte isolation

2.7.1 Harvesting neonatal rat heart ventricles

Neonatal rat ventricular myocytes (NRVM) were isolated from Sprague Dawley neonatal rat pups, which were 0–3 days of age. Sterilized surgical instruments, a beaker containing 70% ethanol, a 90 mm culture dish containing ADS buffer (containing 0.68% NaCl (w/v), 0.476% HEPES (w/v), 0.012% NaH_2PO_4 (w/v), 0.1% glucose (w/v), 0.04% KCl (w/v), 0.01% $MgSO_4$ (w/v), pH 7.35) and a 150 mm sterile culture dish were placed on the bench. Following euthanasia, the chest of the animal was opened with the surgical scissors and the forceps were used to remove the heart. The heart was transferred into the dish containing the ADS buffer after the scissors were used to remove the atria, as well as slice the heart into 1 mm pieces. This procedure was repeated for all the pups. Throughout the procedure, surgical equipment not being used was kept in 70% ethanol.

In a tissue culture hood, curved and sharp scissors were used to slice the hearts into very fine pieces. The heart-ADS solution was transferred to a 50 ml tube and allowed to settle.

2.7.2 Enzymatic dissociation of cardiac tissue

The ADS was carefully aspirated and 7 ml of the enzyme solution was added to the heart pieces. This mixture was placed in the 37^{o}C water bath for 7 minutes, swirling the tube from time to time. After the heart pieces had settled, the solution was aspirated and

7 ml of the enzyme solution was added, repeating the 7 minute incubation step. After this step, the true digestions were started. The supernatant was aspirated and 7 ml of the enzyme solution was added to the heart pieces. The tube was incubated at 37^{o}C for 15 minutes, swirling the tube from time to time. After the hearts settled, the supernatant was transferred to a 15 ml tube containing 2 ml filtered FBS, this was the first digest. 7 ml of enzyme solution was added to the tube containing the heart pieces and incubated at 37^{o}C for a further 15 minutes. The 15 ml tube containing the supernatant and FBS, was centrifuged at 1000 rpm for 6 minutes at RT and the supernatant was discarded. The cell pellet was resuspended in 6 ml pre-plating media and transferred to a 50 ml tube. The above steps were repeated until 8 digestions were completed and all the digests were pooled in the 50 ml tube.

2.7.3 Separation of fibroblasts and NRVMs

The pooled digest was centrifuged at 1000 rpm for 6 minutes at RT and the supernatant was aspirated. The pellet was resuspended in a 50 ml solution of equal volumes of plating media and pre-plating media. The cells were resuspended gently and transferred to a 90 mm culture dish in order for non-myocyte cells to attach. Dishes were incubated at 37^{o}C for 60-90 minutes. After the incubation, the media containing the myocytes was transferred to a 50 ml tube.

2.7.4 Determination of cell yield and seeding

Cell viability was determined using Trypan Blue *(Sigma)* and cells were counted using a hemocytometer. Cells were seeded on gelatin-coated plates depending on requirements. The plating media was replaced with maintenance media 24 hours after plating and experiments were performed 48 hours after the isolation procedure.

2.8 Cell counting and seeding

Cells were counted by preparing a 1 in 10 dilution of cells in media. An equal volume of this dilution and Trypan Blue (*Sigma)* was added to a 1.5 ml tube. 20 µl of this was then mounted on a hemocytomter *(VWR)* and observed under a light microscope. Viable cells have a round shape and white outline, whereas dead cells appear blue and usually have lost their round shape. Only the viable cells within the grid were counted.

2.9 Cation-mediated DNA Transfection

2.9.1 The principle

TurboFect Transfection Reagent (*Thermo Scientific)* is a polymer of cations in water. The DNA forms stable, positively charged complexes with the cationic polymer, which protect it from degradation by nucleases and increase the internalization of the DNA into eukaryotic cells.

2.9.2 The protocol

Cells were placed in serum-free medium (SFM) *(PAA)* with antibiotics (1% v/v streptomycin/penicillin) and were at 50-80% confluency prior to transfection. 100 µl Optimem *(Gibco)*, 1 µg of DNA and 2 µl Turbofect were added to a 1.5 ml tube and mixed. The mixture was incubated at RT for 20 minutes. The solution was made upto 1 ml per reaction with Optimem. SFM was aspirated from wells and the cells were washed with warm PBS. The Optimem/DNA mixture was added to cells in a drop-wise manner. Cells were incubated at 37^{o}C in a 5% CO_2 incubator for 24 hours. The transfection mixture was removed and replaced with SFM. If required cells were exposed to p38 inhibitors (10 µM SB203580 *(Sigma)* or 20 µM BIRB796 *(Prof P. Cohen, Dundee University)*) and incubated for the required amount of time (see Table

2.6). 24 hours after transfection cells were ready to be collected for Western blot analysis.

These were the conditions to transfect 1 μg DNA into 1 well of 6-well plate, if more than 1 μg DNA was used the reaction components were scaled as required.

2.10 Cell lysis

To run a Western blot, cell lysates must be obtained with the cell proteins in solution. Cells were washed with cold PBS and 200 μl 2x concentrated sample buffer was added to each well. The cells were harvested using a scraper *(Fisher Scientific)* and collected into 1.5 ml tubes. The samples were boiled at 100^{o}C for 10 minutes and shaken on the vortex for 10 seconds. The tubes were frozen at -20^{o}C until used for Western blot analysis.

2.11 BCA assay

2.11.1 The principle

Total protein in cell lysate was determined using the BCA Protein Assay *(Thermo Scientific Pierce).*This assay is based on bicinchoninic acid (BCA) for the colorimetric detection of total protein and works by combining the biuret reaction of the reduction of Cu^{2+} to Cu^{+} by protein in an alkaline medium, with the selective and sensitive detection of the Cu^{+} cation. Chelation of two molecules of BCA with one Cu^{+} cation leads to the purple reaction product, which displays a strong absorbance at 562 nm that appears to be linearly related to protein concentrations in the range 20-2000 μg/ml.

The protein concentrations are determined with a reference to standards of bovine serum albumin (BSA) *(Thermo Scientific Pierce)*. A series of dilutions of BSA are measured besides the samples of interest and unknowns are calculated from the standard curve.

2.11.2 The protocol

Reagents A and reagent B were mixed in a tube to a ratio of 50:1 to prepare the working reagent. Replicates of 20 µl of each standard and unknown sample were pipetted into a 96-well plate. 200 µl of the working reagent was added to each well and the contents of the wells were mixed briefly on a shaker for 30 seconds. The plate was covered with the lid and incubated at 37^{o}C for 30 minutes. The absorbance at 562 nm was measured using a plate reader. The average 562 nm reading for standards and the unknown samples was subtracted from the blank measurement. A standard curve was plotted and was used to determine concentrations of the unknown samples.

2.12 Sodium dodecyl sulphate polyacrylamide gel electrophoresis

2.12.1 The principle

Polyacrylamide Gel Electrophoresis (PAGE) is a commonly used technique for the separation of proteins based on their size. Electrophoresis enables charged molecules to migrate in an electric field towards the electrode with the opposite charge and this forms the basis of PAGE. The mobility of a protein depends on both its charge and size. Sodium dodecyl sulfate (SDS) is an anionic detergent, which is used to treat the samples in order to denature the proteins and coat them with a negative charge. This overcomes the issue of differential charge of proteins within a sample and allows them to go through electrophoresis in a comparable manner. The electrophoresis is carried out by applying the denatured samples through a porous matrix such as polyacrylamide. Under the influence of applied voltage, different proteins move through the polyacrylamide gel towards the anode due to their negative charge, at different speeds depending on their size. A known set of standards is loaded beside the samples as a reference molecular

weight ladder, which facilitates the identification of proteins of interest by comparison to the standards.

2.12.2 The protocol

Samples were run on a pre-cast polyacrylamide gel. The polyacrylamide gel was prepared using glass plates at the desired thickness with the recipe shown in Table 2.2 depending on the percentage of gel.

Table 2.2 Recipe for different percentage polyacrylamide gels

Reagent	**5% gel**	**10% gel**	**12.5% gel**	**15% gel**	**Stack (4%)**
MW range (kDa)			10-100	5-70	
ddH_2O (ml)	7	5	4	3	7
30% acrylamide (ml) *(National Diagnostics)*	2	4	5	6	2
1.5M Tris-HCl -pH 8.8 (ml) *(Sigma)*	3	3	3	3	-
1.0M Tris-HCl -pH 6.8 (ml) *(Sigma)*	-	-	-	-	3
10 % Ammonium Persulphate (µl) *(Sigma)*	60	60	50	50	100
TEMED (µl) *(Fisher Scientific)*	15	15	15	15	10

15 µl of each sample was loaded in the wells and 5 µl of pre-stained PageRuler prestained protein ladder (Thermo Scientific) was used as a marker of molecular weight. The gel was electrophoresed in 1X running buffer containing 25 mM Tris, 0.192 M glycine, 0.1% (w/v) SDS, pH 8.3 at 90 V until the samples reached the stacking and resolving gel interface and then 120 V for 1 hour and 30 minutes.

2.13 Western blotting

2.13.1.1 The principle

Following SDS-PAGE, the proteins are transferred onto a membrane, such as polyvinyledene fluoride (PVDF) or nitrocellulose. This transfer process is based on a

similar method to SDS-PAGE, with an electric current being applied across the gel towards the membrane, moving the proteins across. The membrane with the immobilized proteins is blocked with blocking buffer to minimize nonspecific binding of the antibody to proteins other than the targeted one. The antibody is then applied allowing it to bind specifically to its target under optimal conditions. After this step, the membrane is washed to remove residual antibody and the membrane is incubated with a secondary antibody which is specific to the species used to raise the primary antibody and will therefore bind the primary antibody. The secondary antibody is usually conjugated to the enzyme horseradish peroxidase, which will catalyze the oxidation of substrates by hydrogen peroxide, which will yield a signal as a byproduct which can be detected.

2.13.1.2 The protocol

The gel from SDS-PAGE was used to transfer the proteins onto a polyvinylidene fluoride (PVDF) membrane *(GE Healthcare)* through semi-dry transfer with the Semi-dry transfer system *(Bio-Rad).* Filter papers and the gel were soaked in 1X transfer buffer containing 25 mM Tris, 192 mM glycine, and 20% methanol per litre dH_2O. The PVDF membrane was activated in methanol, and soaked in buffer. Electrophoresis was undertaken at 24 V for 1 hour.

Following transfer of proteins onto the membrane, the membrane was blocked in 4% milk *(Marvel)* and 1% bovine serum albumin (BSA) *(PAA)* in 1X Tris-Buffered Saline containing 20 mM Tris Base, 140 mM NaCl pH 7.4 and 0.1% Tween 20 *(Sigma-Aldrich)* ($TBST_{0.1\%}$) for 1 hour at RT with gentle agitation. The membrane was then incubated at 4^{o}C, with gentle agitation overnight with the primary antibodies at correct concentrations (see Table 2.5).

The following day, the membrane was washed with $TBST_{0.1\%}$ for 10 minutes three times under gentle agitation. This was followed by incubating the membrane with secondary antibodies with their complementary dilutions (see Table 2.5) under gentle agitation for 1 hour**.** The washing step was repeated following secondary antibody incubation again with $TBST_{0.1\%}$ for 10 minutes three times under gentle agitation. Enhanced chemiluminescence reagent *(GE Healthcare)* was used to develop the membrane via exposure to X-ray film *(GE Healthcare).* Differing time durations were used to develop films in order to find the best signal with little background.

2.14 Immunofluorescence

Cells were seeded and grown on glass cover slips until they were 40-50% confluent. After treatments, cells were washed with cold PBS and fixed in cold 4% paraformaldehyde in PBS for 10 minutes. Care was taken not to move the cells during this incubation. The cells were washed two more times with PBS for 5 minutes each time. Permeabilisation was achieved with 0.2% v/v Triton X100 for 20 minutes at RT. Cells were washed two times in cold PBS for 5 minutes each. Blocking was performed by a 2 hour incubation in blocking buffer (PBS, 0.2% Triton X100, 2% w/v BSA) at RT. Cells were probed with the primary antibody at the appropriate dilution (see Table 2.5) in 2% w/v BSA overnight at 4^{o}C.

The next day, cells were washed with cold PBS three times for 5 minutes each time. The following steps were all performed in the dark unless otherwise stated. Cells were incubated with the suitable secondary antibody at the required dilution (see Table 2.5) in PBS with 2% w/v BSA at RT. Three washes in cold PBS were performed. The cover slip was taken out and air-dried. 3 drops of Vectashield + DAPI solution was placed on the cover slip and it was mounted on a microscope slide, fixing the corners with nail

varnish. After the nail varnish had set, the slides were stored in the dark at 4^{o}C until images were taken.

2.15 RNA extraction

2.15.1 The principle

The RNeasy procedure represents a widely used method for RNA purification. Using selective binding properties of a silica-based membrane and a high-salt buffer system enables the extraction of up to 100 μg of RNA longer than 200 bases. Samples are first lysed and homogenised in a highly denaturing guanidine-thiocyanate-containing buffer, rendering RNAses inactive to enable purification of undamaged RNA. After addition of ethanol to enable binding, the sample is transferred to an RNeasy Mini spin column to which total RNA binds and the waste is removed. RNA is then eluted in water.

2.15.2 The protocol

The QIAvac 96 vacuum manifold was prepared by placing the waste tray inside the base and the top plate was placed over the base tightly. The QIAvac 96 manifold was attached to the vacuum source. The media in the sample wells were aspirated and 150 μl of Buffer RLT with 10% 2-mercaptoethanol (BME) was added to each sample well. The plate was shaken vigorously for 20 seconds. 150 μl 70% ethanol was added to each well and mixed by pipetting up and down 3 times. The samples were transferred onto the columns in the RNeasy 96 plate and the vacuum source was switched on until the sample had passed through the column. 80 μl DNase I incubation mix was applied onto the column and the plate was sealed with an AirPore tape sheet and incubated at RT for 15 minutes. The tape sheet was removed and 1 ml of Buffer RW1 was added to each column. The plate was incubated at RT for 5 minutes before the vacuum source was switched on until transfer was complete. 1 ml of Buffer RPE was added to each column

and the vacuum source was switched on until the transfer was complete. Another 1 ml Buffer RPE was added to each column and the plate was sealed with an AirPore tape sheet. The plate was centrifuged at 6000 rpm for 10 minutes to dry the membranes. The RNeasy plate was placed on top of an elution microtube rack and the RNA was eluted with 30 µl RNase-free water by centrifugation at 6000 rpm for 4 minutes at RT. The elution step was repeated with a second volume of 30 µl RNase-free water. The RNA was stored at -20^{o}C until required.

2.16 Real time reverse transcription-PCR analysis

2.16.1 The principle

2.16.1.1 Reverse transcription

Reverse transcriptases are a group of enzymes which generate complementary DNA from a RNA template and are mainly associated with retroviruses. This activity is used by retroviruses to convert their single stranded RNA into double-stranded cDNA which can then integrate into the host genome, enabling viral replication using the host transcription and translation machinery (260). This system is exploited by researchers for use in molecular cloning and RNA sequencing as well as genome analysis.

2.16.1.2 Reverse transcription PCR

PCR has previously been described in section 2.3.1.2. Reverse transcription PCR (RT-PCR) is a commonly used technique to measure RNA expression (261). RT-PCR results in the formation of cDNA from RNA by a reverse transcriptase and the DNA then amplified by PCR for analysis. This technique is often used to determine gene expression in an organism or cell-type under control or treatment conditions.

2.16.1.3 Quantitative real-time PCR

Quantitative real-time PCR (qPCR) is used to quantitatively measure the amplification of DNA with fluorescent probes. The TaqMan solutions contain a primer, specific to the gene of interest to target the Taq polymerase, and a probe, to bind to the gene of interest downstream of the primer. TaqMan probes, which are sequence-specific oligonucleotides with a fluorophore and a quencher moiety attached, are utilised to determine the amount of DNA in the sample. The signal from the fluorophore fluorescein (FAM) at the 5' end of the probe is quenched by the nonfluorescent quencher (NFQ) when the gene is not amplified and therefore no signal is detected. However during the extension phase of PCR, Taq polymerase cleaves the probe due to its exonuclease activity and this results in the separation of the fluorophore and the quencher leading to a signal proportional to the amount of PCR product from the DNA of that specific gene. Relative quantification of the DNA of the gene of interest is determined with an internal reference house-keeper gene to determine fold-differences in expression of the target gene.

2.16.1.4 Reverse transcription quantitative PCR

RT-PCR and qPCR can be combined to measure the relative RNA amounts within a sample and this method is termed RT-qPCR. QuantiTect Probe RT-PCR kit *(Qiagen)* allows both reverse transcription and qPCR to be performed in the same tube. All the components required for both methods are added at the beginning of the experiment and several precautions are taken to ensure the correct order of events. For reverse transcription to occur at the beginning, one cycle of 50^{o}C for 30 minutes is added to the PCR cycling conditions. The polymerase used is HotStarTaq polymerase, and does not interfere with the reverse transcription as it has been modified to be activated after the reverse transcription step, at the 95^{o}C for 15 minutes part of the PCR cycle. This high

temperature step also inactivates the reverse transcriptase ensuring temporal separation of the two steps.

2.16.2 The protocol

QuantiTect 2 x Probe RT-PCR Master Mix, RT Enzyme Mix, template RNA, Taqman probe & primer solution and RNase free water were thawed and reaction mixture was set up as in Table 2.3. The reaction was mixed thoroughly and appropriate volumes were dispensed into PCR plates. The real-time cycler Taqman 7900HT console *(Applied Biosystems)* was set up as in Table 2.4 and the cycling program was started.

Table 2.3 RT-qPCR reaction setup

	Stock	Final	Volume per reaction (µl)
QuantiTect 2x Master Mix	2x	1x	5
RT Enzyme Mix			0.1
Taqman Prime & Probe mix	20x	1x	0.5
RNA (10 ng/µl)			1.25
H_2O			3.15
Final			10

Beta-2-microglobulin (B2M) readout was used as a housekeeper control and relative RNA amplification of genes of interest were plotted.

Table 2.4 qPCR cycling conditions

Step	Temperature	Time	Cycles
Reverse transcription	50ºC	30min	1
Initial denaturation	94ºC	15min	1
Denaturation	94ºC	15sec	40
Annealing/Extension	60ºC	60sec	
Final Extension	60ºC	10min	1

2.17 Adenylate kinase assay of cytotoxicity

2.17.1 The principle

Cytotoxicity of NRVMs and iPS cardiomyocytes was observed using the ToxiLight™ non-destructive bioassay *(Lonza)*. Adenylate kinase (AK) is an enzyme present in all cells and the bioluminescent measurement of it is the basis of this assay. Upon cytotoxicity, cell integrity is lost and the plasma membrane dissociates, leading to the leakage of certain components of the cell into the surrounding environment, in this case; into the media in the wells. Therefore the measurement of AK release enables us to determine cytotoxicity accurately.

There are two steps to this system. Firstly, ADP, which is a substrate of AK, is added, which is then converted to ATP by the enzyme AK.

$$Mg^{2+}ADP + ADP \xleftrightarrow{\text{Adenylate kinase}} Mg^{2+}ATP + AMP$$

The bioluminescent part of this assay uses the enzyme luciferase in order to create light from ATP and luciferin as below:

$$ATP + Luciferin + O_2 \xrightarrow{\text{Luciferase}} Oxyluciferin + AMP + PP_i + CO_2 + LIGHT$$

Mg^{2+}

As a result of these two reactions, the light emitted is linearly correlated to the release of AK. The resulting light is measured using a luminometer.

2.17.2 The protocol

All the reagents were brought to RT. The AK detection reagent (AKDR) was reconstituted in the assay buffer and left at RT for 15 minutes to ensure complete rehydration. The culture plate was removed from the incubator and allowed to cool to RT for at least 5 minutes. The luminometer was programmed to take an immediate 1 second integrated reading of the appropriate wells. 20 µl of cell supernatant was transferred to a compatible 96 well plate and 100 µl of the AKDR was added to each well. The plate was incubated at RT for 5 minutes and the readings were taken using the luminometer.

2.18 Caspase assay of cytotoxicity

2.18.1 The principle

Caspase-Glo 3/7 Assay *(Promega)* is a luminescent assay measuring cytotoxicity through observing the activities of cysteine aspartic acid-specific protease (caspase) 3 and 7. Caspases are a family of proteases with an essential role in apoptosis and necrosis in mammalian cells (262, 263). The assay contains a luminogenic substrate of caspases-3/7 with the sequence DEVD. After adding the reagent, cells are lysed and the contents are released, enabling the active caspases-3/7 within the cells to cleave the substrate and generate a luciferase-mediated signal. The luminescent signal is proportional to the caspase activity.

2.18.2 The protocol

In order to support observations from the AK assay described in section 2.17.2, another cytotoxicity assay, Caspase-Glo 3/7 Assay *(Promega)* was employed. Before starting the assay, Caspase-Glo reagent was prepared by allowing it to equilibrate to RT and mixing well. 96-well plates containing cells were removed from the incubator and allowed to equilibrate to RT. 100 µl of the reagent was added to each well of a white-walled 96-well plate containing 100 µl of blank, negative control cells or treated cells in culture medium. The plate was covered with a lid. To avoid cross-contamination, care was taken to ensure that the pipette tips did not touch the wells. The contents of the wells were gently mixed at 300-500 rpm for 30 seconds using a plate shaker. Plates were incubated at RT for 30 minutes. Luminescence of each sample was measured in a plate-reading luminometer.

2.19 Lentivirus production

2.19.1 The principle

There are several features of lentiviral vectors that make them attractive tools for biological research. They can transduce both dividing and non-dividing cells due to the ability of their pre-integration complex to efficiently pass from the cytoplasm into the nucleus through the nuclear pores and integrate into the genome of the target cell (264). In addition, they provide a research platform with low toxicity, the ability to accommodate large inserts (up to 8kb) and they achieve stable expression of transgenes in a broad range of host cell types (265-268).

Lentivirus generation systems rely on transfecting multiple plasmids harbouring different infectious yet replication-incompetent components of the lentivirus. HEK293T cells are a variant of the HEK293 cells, which constitutively express the Simian Virus

40 (SV40) large T antigen enhancing transfection of these cells. HEK293T cells are widely used for lentiviral production due to their increased transfection efficiency, high propagation of viral particles from plasmids harbouring the SV40 episomal replication origin and ability to grow rapidly in basic cell culture medium containing 5-10% serum (269, 270).

2.19.2 The protocol

MISSION Lentiviral Packaging Mix *(Sigma Aldrich)* was used to produce lentiviruses in HEK293T cells. On day one, HEK293T cells were plated in complete DME medium supplemented with 10% fetal bovine serum and 4 mM L-glutamine, 24 hours prior to transfection. Cells were at 50-70% confluency the day of transfection.

On day two, the vial of Lentiviral Packaging Mix was thawed at RT and added to a sterile polypropylene tube for each transfection. Transfer vector was added to the lentiviral packaging mix and FuGENE 6 transfection reagent, previously prepared in serum-free media, was added to the tube. The contents of the tubes were mixed gently by pipetting up and down. The transfection cocktail was incubated at RT for 15 minutes. The transfection cocktail was added to flasks containing HEK293T cells.

On day three, 16 hours post-transfection, the media was removed without disturbing the cells and replaced with an equal volume of pre-warmed DME complete media. Cells were incubated at 37°C in a 5% CO_2 incubator for an additional 24 hours.

On day four, between 36-48 hours post-transfection, viral particles were collected by carefully removing the media and placing it in a collection tube. An equal volume of fresh pre-warmed complete media was added to the cells and the flasks were incubated for a further 24 hours. Between 60-72 hours post-transfection, viral particles were collected by carefully removing the media and pooled with the first harvest. The viral particles were titrated by performing the HIV p24 Antigen ELISA assay after pooling.

2.20 Lentiviral transduction

96-well plates were coated with 0.1% gelatin at 37ºC for 1 hour and iPS cardiomyocytes were seeded in CDI plating media. After culturing for two weeks, the cells were ready for treatment. Transduction mixtures were prepared by combining a predetermined ratio of the lentiviruses and CDI maintenance media. To this mix, polybrene was added at a final concentration of 5 µg/ml. 48 hours after transduction; media was removed and replaced with an equal volume of fresh maintenance media. Cells were cultured for a further 24 hours and then treated as required.

2.21 Isothermal titration calorimetry

2.21.1 The principle

Isothermal titration calorimetry (ITC) is a method to observe the change in enthalpy as a result of an interaction between two molecules. Through this thermodynamic characterization protein-protein interactions can be determined revealing intermolecular changes that occur during the modification of unbound to bound forms of the molecules in the assay (271). The number and type of bonds formed between the two components are determined and it is the thermodynamic effect of changes in hydrogen bonds, van der Waals and hydrophobic interactions which is measured in ITC (272). In a typical ITC experiment, using a syringe, one of the molecules is titrated into a calorimetric cell containing the other molecule. This is done in a stepwise manner in order to elicit the binding process and a cycle of binding to equilibrium occurs in the system determined by the association constant. The consequence of this titration is heat being absorbed or emitted in direct proportion to the amount of binding that occurs. When the protein in the calorimetric cell is saturated by the titrated molecule, the heat signal diminishes until a point when only the background heat of dilution is detected (273). Measurement

of the heat of the reaction enables the calculation of equilibrium association constant, stoichiometry based on the known concentration of the molecules and an appropriate model to fit the binding isotherm, as well as the change in entropy and free energy. ITC can be used to infer structural alterations upon binding and examine regions of the interacting molecules relevant to the interaction. ITC was used to determine the ability of TAB1 to compete with MKK3 in binding to p38 and all the ITC experiments were performed by Dr de Nicola, King's College London.

2.21.2 The protocol

All ITC experiments were performed using an ITC-200 microcalorimeter from Microgal *(GE Healthcare).* At the beginning of the experiment, the pH of both the protein sample and the peptide was observed and adjusted for any discrepancy and the reference cell was filled with ddH_2O. In order to remove air bubbles, the protein solutions were degassed for 2-5 minutes prior to loading into the appropriate sample chamber. Baseline stability was confirmed before the first addition of the peptide and analysis did not include the first injection in order to ensure artefacts due the diffusion through the injection port did not affect protein concentration near the tip of the needle. Before the titration was initiated, the sample cell was allowed to equilibrate to the temperature of the reference cell.

In order to investigate the interaction between p38 and TAB1, a computer-controlled 40 µl microsyringe was used to inject 150 µM p38α which was titrated into an identical buffer with 18 µM TAB1 (1-438) and 20 µM TAB1 (371-416). 400 seconds interspersed between each injection to allow the system to reach equilibrium before the next injection. A control experiment, titrating into buffer alone, under the same conditions was performed to verify that the heat produced by titrant dilution was negligible. Integrated heat data were corrected for heats of dilution and fitted using a

nonlinear least-squares minimisation algorithm to a theoretical titration curve using the MicroCal Origin 7.0 software package. The fitting parameters were ΔH° (reaction enthalpy change in kcal·mol^{-1}), K_b (equilibrium binding constant in M^{-1}), and n (molar ratio between the two species in the syringe and calorimetric cell respectively). The entropy of the reaction was calculated using $\Delta G = -RT \cdot \ln K_b$ (R 1.987 cal·mol^{-1}*K^{-1}, T 298 K) and $\Delta G = \Delta H - T\Delta S$.

Gibb's free energy is a thermodynamic potential used to predict how favourable a process is at constant pressure and temperature, as well as the chemical potential that is minimized when a system reaches equilibrium. It is defined as:

G (free energy) = H (enthalpy) – T (temperature) S (entropy).

2.22 Nuclear magnetic resonance

2.22.1 The principle

Nuclear magnetic resonance (NMR) was first observed in 1945 and it has become an eminent technique for determining structural and chemical properties of organic compounds. NMR is based on the ability of nuclei of many elements to absorb and re-emit electromagnetic radiation when subjected to a magnetic field and makes use of atoms with an odd number of protons (^{1}H, ^{13}C, ^{15}N and ^{31}P) and their characteristic absorption frequencies depending on their environment (274). For example, hydrogens in different locations within a protein will give different peaks according to the chemical environment generated by surrounding atoms. In the case of this environment having high electron density, an 'upfield' peak will be observed and in the case of an environment with low density, the peak will be 'downfield'. As the hydrogen atom has two spin states, the spectrum measures the ease of alteration between the different spins of the atom, with one spin being aligned with the magnetic field and the other being against the field. The higher spin is the one against the magnetic field and when

electromagnetic radiation is applied to atoms, the magnetic field can be changed to the higher spin by the atoms ability to absorb radiation, which is measured by NMR. If the atom in question is in an environment with a high density of electrons, it is shielded from the effect of the magnetic field and therefore can absorb less radiation than at a location with a low density of electrons (275). This measurement enables the determination of structural properties of different atoms within a protein. Combining a series of these measurements, interactions between atoms and protein-protein interactions can be determined.

The chemical shift is the resonant frequency of a nucleus compared to a standard and is often used to determine the structure of molecules. Due to the dependence of the absorption and re-emission of the atoms on their environment, upon a change in this environment and the electron distribution, the characteristic frequencies observed are altered reflecting their newly acquired surroundings, binding partners, bond types and bond lengths and angles, and this is referred to as the chemical shift.

2.22.2 The protocol

Spectra of free p38α and of p38α:TAB1(371-416) complex were acquired in buffer containing 50 mM NaCl, 20 mM Tris (pH 7.5) and 2 mM DTT, while those of TAB1(371-416) were acquired in buffer containing 20 mM Tris (pH 7.5) and 2 mM DTT. Concentrations of free p38α and free TAB1(371-416) were 0.5 mM. Samples of p38α:TAB1(371-416) where p38α was [^{2}H/^{15}N/^{13}C]-labeled and TAB1 unlabeled were prepared by mixing the components in a molar ratio of 1:2 at low micromolar concentrations and the complex was concentrated to a final concentration of 0.5 mM. An inverted stoichiometric ratio in the same procedure was employed for the complex of unlabeled p38α and selectively [^{15}N/^{13}C]-labeled TAB1 (371-416).

NMR spectra were recorded at 298 K (24.85ºC) on Varian Inova spectrophotometers at 800 MHz (^{1}H frequency) and Bruker Avance spectrophotomer operating at 700 and 500 MHz, all equipped with triple resonance cryoprobes. The spectra were processed using the manufacturers' software or using NMRpipe, NMRViewJ, and XEASY. A Gaussian or sine –bell window function were applied to the spectra and prior to Fourier transformation they were zero-filled to double the size of the data. ^{15}N-TROSY and ^{13}C-HSQC spectra were acquired in a standard manner. ^{15}N-TROSY spectrum of free p38α with that of p38α:TAB1(371-416) were compared in order to obtain the chemical shift variations. The weighted average chemical shift variation ($\Delta\delta_{AV}$) was calculated using the formula $([(\Delta_{HN})^2 + (\Delta_N)^2/5]/2)^{½}$ where Δ_{HN} and Δ_N are the chemical shift variations in the two dimensions. Chemical shift variations were classified as being weak ($\Delta\delta_A \leq 0.5$), strong ($\Delta\delta_{AV} > 0.5$), undefined (where signals are lost upon interaction) or unclear (unassigned peaks and where spectra overlapped prevented the unambiguous analysis). The classes were mapped onto the structure of p38α (PDB ID: 1P38).

2.23 Antibodies

Table 2.5 Primary and secondary antibodies with their corresponding conditions and details

Antigen (clone)	**Species**	**Application**	**Dilution**	**Source**
p38	Rabbit	Western blot	1:1000 in 1% BSA in $TBST_{0.1\%}$	Cell Signalling #9212
phospho Thr180/Tyr182 p38	Rabbit	Western blot	1:1000 in 1% BSA in $TBST_{0.1\%}$	Cell Signalling #9211
true dual phospho Thr180 and Tyr182 p38	Mouse	Western blot	1:1000 in 1% BSA in $TBST_{0.1\%}$	Sigma #M8177
TAK1	Rabbit	Western blot	1:500 in 1% BSA in $TBST_{0.1\%}$	Cell Signalling #4505
phospho Thr184/Thr187 TAK1	Rabbit	Western blot	1:500 in 1% BSA in $TBST_{0.1\%}$	Cell Signalling #4531
TAB1	Sheep	Western blot	1:1000 in 1% BSA in $TBST_{0.1\%}$	Santa Cruz
phospho Ser423 TAB1	Sheep	Western blot	1:1000 in 1% BSA in $TBST_{0.1\%}$	Prof P. Cohen, Dundee University, UK
phospho Thr431 TAB1	Sheep	Western blot	1:1000 in 1% BSA in $TBST_{0.1\%}$	Prof P. Cohen, Dundee University, UK
MKK3	Rabbit	Western blot	1:500 in 1% BSA in $TBST_{0.1\%}$	Santa Cruz #sc-13069
phospho Ser189 MKK3	Rabbit	Western blot	1:1000 in 1% BSA in $TBST_{0.1\%}$	Cell Signalling #9231
phospho Ser82 Hsp27	Rabbit	Western blot	1:1000 in 1% BSA in $TBST_{0.1\%}$	Cell Signalling #2401
phospho Thr334 MK2	Rabbit	Western blot	1:1000 in 1% BSA in $TBST_{0.1\%}$	Cell Signalling #3007
GAPDH	Rabbit	Western blot	1:1000 in 1% BSA in $TBST_{0.1\%}$	Cell Signalling #2118
GCN2	Rabbit	Western blot	1:1000 in 1% BSA in $TBST_{0.1\%}$	Cell Signalling #3302
phospho Thr899 GCN2	Rabbit	Western blot	1:1000 in 1% BSA in $TBST_{0.1\%}$	Abcam #ab75836
eIF2alpha	Rabbit	Western blot	1:1000 in 1% BSA in $TBST_{0.1\%}$	Cell Signalling #9722
phospho Ser51 eIF2alpha	Rabbit	Western blot	1:1000 in 1% BSA in $TBST_{0.1\%}$	Cell Signalling #9721
p62	Guinea pig	Western blot	1:1000 in 1% BSA in $TBST_{0.1\%}$	American Research Products #03-GP62-C
B-actin	Rabbit	Western blot	1:1000 in 1% BSA in $TBST_{0.1\%}$	Cell Signalling #4967
LC3A/B (Alexa Fluor 555-	Rabbit	Immunofluorescence	1:50 in 1% BSA in PBS, 0.3% Triton x-100	Cell Signalling #13173

conjugated)				
Rabbit Isotype Control (Alexa Fluor 555-conjugated)	Rabbit	Immunofluorescence	1:50 in 1% BSA in PBS, 0.3% Triton x-100	Cell Signalling #3969
HA tag	Mouse	Immunofluorescence	1:100 in 2% BSA in PBS	Cell Signalling #2367
FLAG tag	Rabbit	Immunofluorescence	1:250 in 2% BSA in PBS	Cell Signalling #2368
Sheep (Horseradish peroxidise-conjugated)	Rabbit	Western blot	1:4000 in $TBST_{0.1\%}$	Thermo Scientific #31240
Rabbit (Horseradish peroxidise-conjugated)	Donkey	Western blot	1:2000 in $TBST_{0.1\%}$	GE Healthcare #NA934-1ML
Mouse (Horseradish peroxidise-conjugated)	Sheep	Western blot	1:4000 in $TBST_{0.1\%}$	GE Healthcare #NA931-1ML
Mouse (Cy3-conjugated)	Goat	Immunofluorescence	1:200 in 2% BSA in PBS	Jackson Laboratories #115-165-205
Rabbit (Cy5-conjugated)	Goat	Immunofluorescence	1:200 in 2% BSA in PBS	Jackson Laboratories #111-605-003

2.24 Inhibitors and compounds

Table 2.6 Compounds used in treatment of cells and their details

Inhibitor/Compound	**Function**	**Treatment**	**Source**
SB203580	p38 inhibitor – ATP mimetic	30 mins	Sigma #S8307
SB239063	p38 inhibitor – ATP mimetic	30 mins	Sigma #S0569
BIRB796	p38 inhibitor	2 hr	Prof P. Cohen, Dundee University
Halofuginone	Prolyl tRNA synthetatse inhibitor	24 hr	Sigma #32481
Borrelidin	Threonyl tRNA synthetase inhibitor	24 hr	Sigma #B3061

2.25 Vectors

Table 2.7 Vectors used in transformation and transfection of cells and their details

Vector name	Backbone	Insert	Tag	Organism	Expected molecular weight (kDa)	Source
WTp38	pcDNA3	p38	HA	Mammalian	40	Dr Y Wang, UCLA, Los Angeles, CA, USA
	pcDNA3	p38	FLAG	Mammalian	40	Dr G de Nicola, KCL
	pETDuet-1	p38	no tag	Bacterial	38	Dr G de Nicola, KCL
DRp38	pACCMVpLpA-SR	p38 (T106M/H107P/L108F)	no tag	Mammalian	38	Dr J Martin. Loyola University, Chicago, IL, USA
KDp38	pAdTrackCMV	p38 (D168A)	FLAG	Mammalian	40	Dr B Foxwell, The Kennedy Institute of Rheumatology. Imperial College, London, UK
WT-TAB1	pETDuet-1	TAB1	no tag	Bacterial	56	Dr G de Nicola, KCL
	pcDNA3	TAB1	CFP	Mammalian	83	Cloned from pETDuet-1 version
CM-TAB1	pETDuet-1	TAB1 (V408G/M409A)	no tag	Bacterial	56	Dr G de Nicola, KCL
	pcDNA3		CFP	Mammalian	83	Cloned from pETDuet-1 version
NCM-TAB1	pETDuet-1	TAB1 (V390A/Y392A)	no tag	Bacterial	56	Dr G de Nicola, KCL
	pcDNA3		CFP	Mammalian	83	Cloned from pETDuet-1 version

CM/NCM-TAB1	pETDuet-1	TAB1 (V390A/Y392A/V408G/M409A)	no tag	Bacterial	56	Dr G de Nicola, KCL
	pcDNA3		CFP	Mammalian	83	Cloned from pETDuet-1 version
MKK3	pcDNA3	MKK3b	HA	Mammalian	40	Dr R Bassi, KCL
TAK1	pCMV	TAK1	HA	Mammalian	80	Dr J Ninomiya-Tsuji, North Carolina State University, USA
T185G-p38	pcDNA3	p38 (T185G)	HA	Mammalian	38	Dr G de Nicola, KCL
T185D-p38	pcDNA3	p38 (T185D)	HA	Mammalian	38	Dr G de Nicola, KCL

3 RESULTS – TAB1-mediated p38 activation

In several studies, employing pharmacologic compounds and transgenic animals, a role for p38 has been implicated in myocardial infarction. It has been shown that p38 interacts with TAB1 directly in ischaemic hearts, but not in normal hearts (28). In addition, MKK3 knockout mice do not differ from wild-type mice in infarct size upon myocardial infarction, induced through a ligation of the left anterior descending (LAD) coronary artery (29). SB203580 treatment lead to a MKK3- independent reduction in infarct size in retrogradely perfused mouse hearts subjected to 30 minutes global ischaemia and 120 minutes of reperfusion (29). The direct interaction between p38 and TAB1 is further confirmed by crystal structures and characterisation in solution, revealing a bipartite docking mechanism (34). In order to confirm this interaction and TAB1-mediated p38 autophosphorylation, HEK293 cells were transfected and the phosphorylation state of p38 and TAB1 were explored in this chapter. In addition, the interaction points in TAB1 have been mutated and transfected to explore the effects of these mutations on p38 phosphorylation and presentation of TAB1 as a substrate, as it is downstream of p38 besides its role in inducing autophosphorylation.

MAPK binding partners share conserved docking site sequences which enable interactions between their respective MAPKs (276) and these contain a basic region and a hydrophobic region (277). One of the consensus motifs shared by some of these proteins is R/K-X4-φA-X-φB (where φA and φB are hydrophobic residues [Leu, Ile, or Val]), which is present in two of the binding partners of p38; MKK3b and MEF2A (278). Despite the similarity in docking sites, different conformation of the active site could lead to the differential downstream effects dependent on the binding partner. One of the p38 binding sites identified in TAB1 appears to share a region on p38 with these other binding partners. In order to answer the question of whether TAB1 and MKK3b

compete in binding to p38, we have transfected HEK293 cells and analysed the level of phosphorylation of p38. Pharmacologic inhibition and genetic mutations in p38 were utilised to explore this further enabling the differentiation between MKK3b-mediated transphosphorylation from autophosphorylation induced by TAB1.

3.1 Optimisation of transfection

Firstly to establish consistent transfection efficiency, a series of experiments were conducted in HEK293 cells with mammalian vectors encoding WTp38 (all 'p38' mentioned from here on is p38α, unless otherwise stated), WT-TAB1, a drug-resistant version of p38 mutated at residues at the ATP-binding site (DRp38 (T106M-H107P-L108F)) and co-transfections of TAB1 with both versions of p38. The protein expression of ectopic WTp38 which runs at a higher molecular weight than the endogenous p38 due to a FLAG-tag was lower than expected (see Figure 3.1). Successful overexpression from a high-copy plasmid such as the pcDNA3 vector used here, usually results in greater protein accumulation than achieved by the endogenous gene. In addition, there were inconsistencies in loading in my initial experiments, which required optimisation and confounded the interpretation of transfection efficiency.

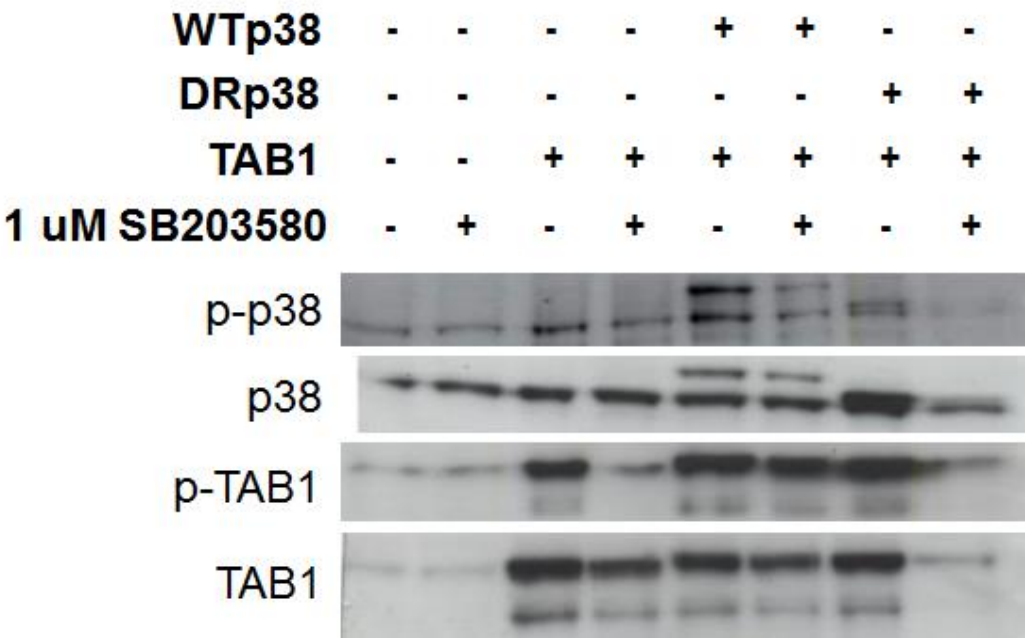

Figure 3.1 Optimisation of transfection efficiency of p38α and TAB1 in mammalian cells.
HEK293 cells were transfected as described in the Materials and Methods section 2.9. 24 hours after transfection, 10 µM SB203580 was added as indicated (+) with an equivalent volume of DMSO added to the control wells. Cells were incubated for 30 minutes, after which cell lysates were obtained and phospho-Thr180/Tyr182 p38, total p38, phospho-Ser423 TAB1 and total TAB1 levels were determined using appropriate antibodies described in the Materials and Methods section 2.23. WTp38 is FLAG-tagged and therefore runs at 40kDa, higher than the expected 38 kDa for native p38, DRp38 and TAB1 are untagged.

In order to reduce variation, it was decided to use a mastermix of transfection reagents to achieve consistent efficiencies throughout the samples. The method was further improved by adding reagents in a dropwise manner to the cells throughout the transfection protocol. Transfection efficiency was more consistent after optimisation (see Figure 3.2).

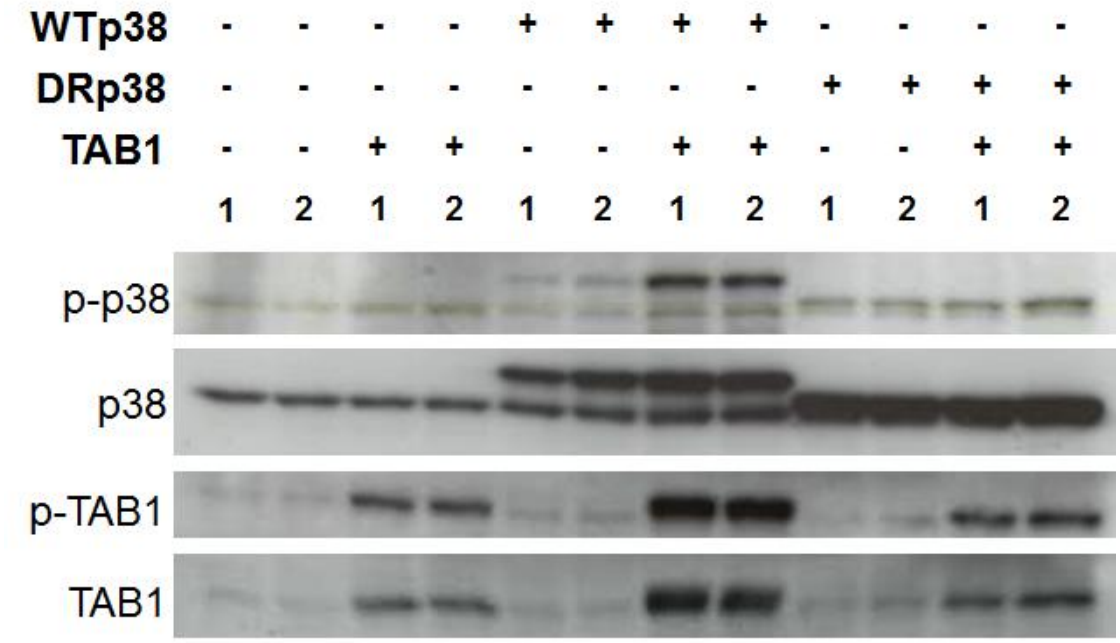

Figure 3.2 Optimisation of tranfection efficiency of p38α and TAB1 – improved transfection efficiency in mammalian cells.
HEK293 cells were transfected as described in the Materials and Methods section 2.9. 24 hours after transfection, cell lysates were obtained and phospho-Thr180/Tyr182 p38, total p38, phospho-Ser423 TAB1 and total TAB1 levels were determined using appropriate antibodies shown in the Materials and Methods section 2.23.

3.2 SB203580 reduces TAB1-mediated WTp38 phosphorylation

To investigate the effect of TAB1 on p38 phosphorylation, HEK293 cells were co-transfected with TAB1 and p38. In addition, to verify whether this effect of TAB1 on p38 phosphorylation is autophosphorylation, the sensitivity of this mechanism to the ATP-mimetic p38 inhibitor, SB203580 was examined. Cells were treated with 10μM SB203580 half an hour before collection. Addition of SB203580 should block p38 kinase activity and therefore TAB1-mediated autophosphorylation. TAB1-mediated p38 phosphorylation increases when p38 is co-transfected with TAB1 (see Figure 3.3). Moreover when SB203580 is added TAB1-mediated p38 phosphorylation decreases but as expected this is not the case with the drug-resistant p38 (DRp38) as it is mutated at the site where SB203580 binds. SB203580 cannot bind drug-resistant p38 therefore p38 phosphorylation does not decrease when this version of p38 is co-transfected and

exposed to SB203580. As discussed in section 1.2.2, TAB1 is also involved in the canonical activation pathway of p38. Therefore SB203580 is a logical way to dissect transphosphorylation from autophosphorylation in this set of experiments.

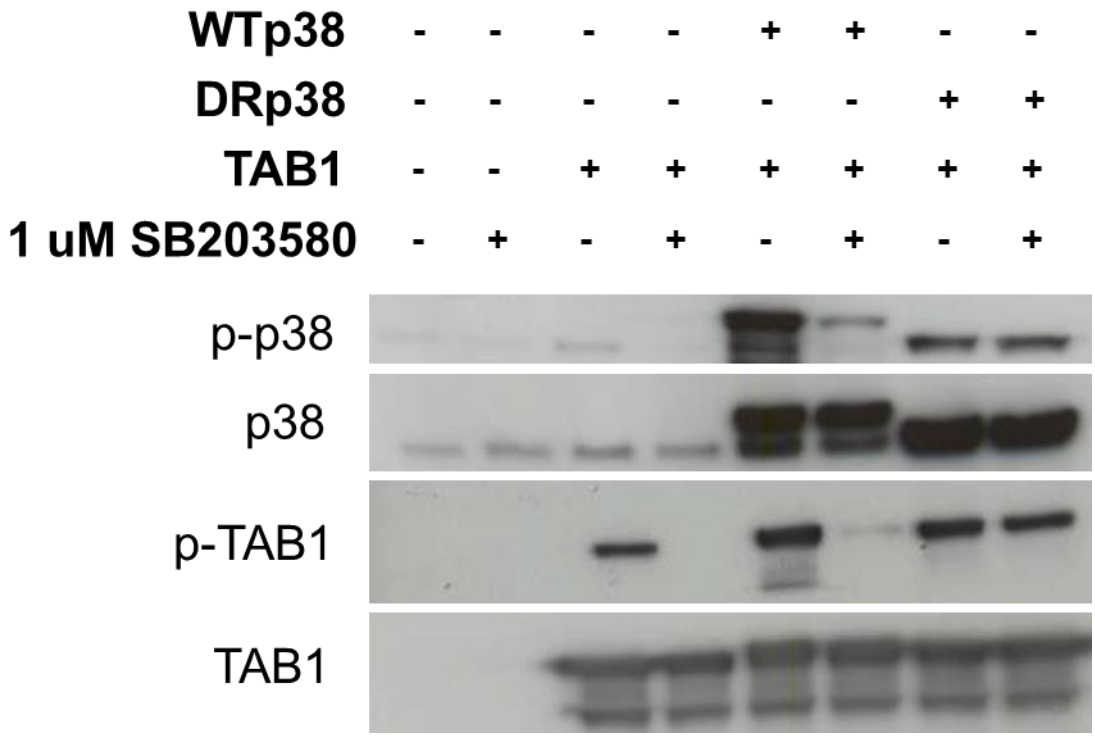

Figure 3.3 Western blot analysis of the effect of SB203580 on TAB1-mediated WTp38α and DRp38α phosphorylation.
HEK293 cells were transfected as described in the Materials and Methods section 2.9. 24 hours after transfection, 10 μM SB203580 was added as indicated (+) with an equivalent volume of DMSO added to the control wells. Cells were incubated for 30 minutes, after which cell lysates were obtained and phospho-Thr180/Tyr182 p38, total p38, phospho-Ser423 TAB1 and total TAB1 levels were determined using appropriate antibodies as described in the Materials and Methods section 2.23. The blot shown is a representative of three experiments.

3.3 BIRB796 reduces TAB1-mediated WTp38α and DRp38α phosphorylation

With the aim to confirm that SB203580 does actually act on the ATP-binding site and DRp38 can also be inhibited in an allosteric manner by an unrelated inhibitor of p38, an allosteric inhibitor of p38, BIRB796, was employed. When 20μM BIRB796 is added to HEK293 cells co-transfected with TAB1 and WT p38, p38 phosphorylation decreases

(see Figure 3.4). As expected, this is also the case with DRp38 as BIRB796 binds to a different site than the ATP-binding site which is mutated in this version of p38.

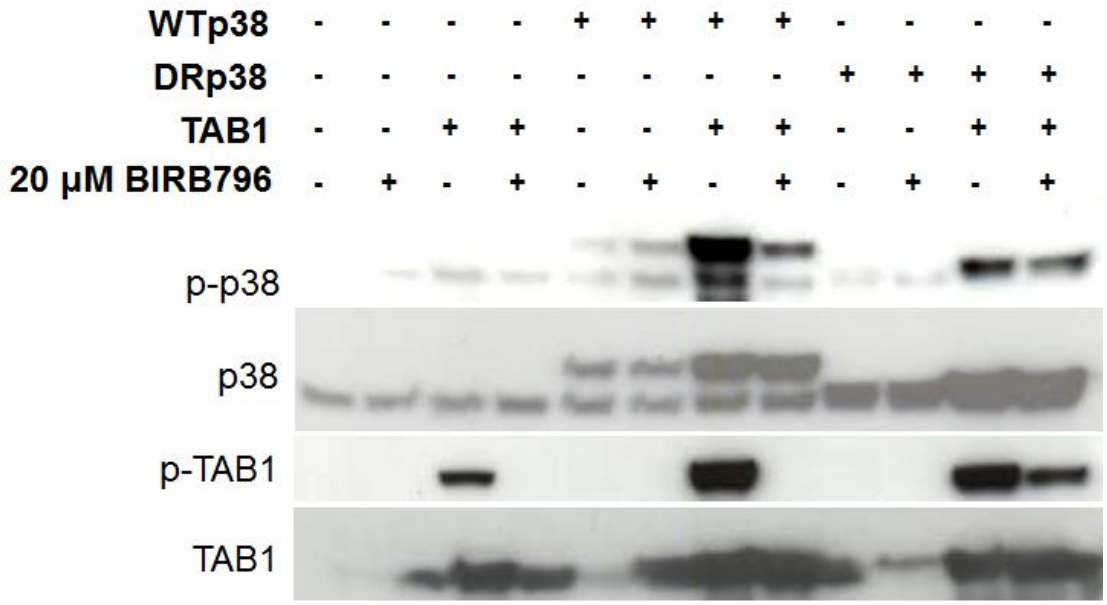

Figure 3.4 Western blot analysis of the effect of BIRB796 on TAB1-mediated WTp38α and DRp38α phosphorylation.
HEK293 cells were transfected as described in the Materials and Methods section 2.9. 24 hours after transfection, 20 µM BIRB796 was added as indicated (+) with an equivalent volume of DMSO added to the control wells. Cells were incubated for 2 hours, after which cell lysates were obtained and phospho-Thr180/Tyr182 p38, total p38, phospho-Ser423 TAB1 and total TAB1 levels were determined using appropriate antibodies as described in the Materials and Methods section 2.23.

3.4 Different regions of TAB1 induce p38 phosphorylation at different efficiencies

Through experiments performed in our research group by Dr Gian Felice DeNicola we have identified the regions of TAB1 that interact with p38. This identification was performed by nuclear magnetic resonance (NMR) and X-ray crystallography and then confirmed by isothermal titration calorimetry (ITC). It was found that residues 385-394 and 404-412 of TAB1 are involved in binding to p38 on the unique hydrophobic groove and the common docking domain of p38 respectively.

An IVK assay was used to assess TAB1 and p38 interaction points without the limitation of other proteins within the cell interfering with their binding or in data

interpretation by occult activation of TAK1. Full length TAB1 protein was unstable and therefore shorter versions of TAB1 were used, as described previously (34). A 46 amino acid residue TAB1 peptide (371-416) with the amino acid sequence [EMSQPTPTPAPGGRVYPVSVPYSSAQSTSKTSVTLSLVMPSQGQMV] including both interaction points, a canonical (C) domain binding 13 amino acid long peptide with the amino acid sequence [NH_2-KTSVTLSLVMPSQ-COOH] and a noncanonical (NC) domain binding 13 amino acid residue peptide with the amino acid sequence [NH_2-RVYPVSVPYSSAQ-COOH] that binds to the aforementioned unique hydrophobic groove were ordered *(Activotec)*. The IVK assay products of p38 and these peptides of TAB1 were analysed by Western blotting. At earlier time points most p38 phosphorylation is observed with the 46mer peptide, followed by the C peptide and then by the NC peptide compared to basal levels (see Figure 3.5). Nonetheless, after 4 hours C peptide seems to have caught up and exceeded the p38 phosphorylation that the 46mer has induced. The NC peptide does not appear to have a major effect on p38 phosphorylation even after 4 hours. Nevertheless, a combination of the C and NC peptide showed similar results to the canonical peptide alone. The effect of the combination of C and NC peptides was variable through several experiments, but it consistently aided p38α autophosphorylation more than the NC peptide alone.

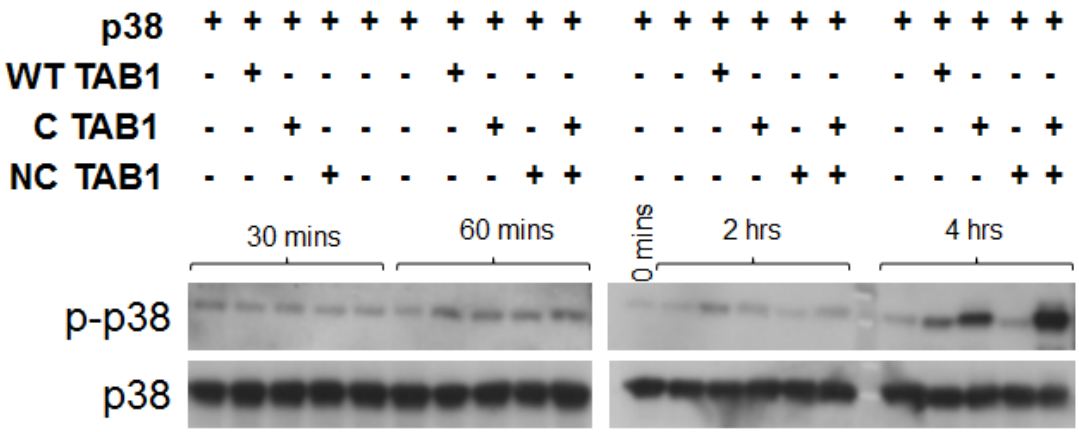

Figure 3.5 Western blot analysis of an IVK assay assessing the effect of TAB1 mutations on p38α phosphorylation.
IVK assay was performed at 37ºC for 0, 30, 60, 120 and 240 minutes for p38α and each TAB1 peptide either the (WT TAB1 in the figure above) 46mer consisting of both canonical (C) region and noncanonical (NC) region docking peptides or the canonical region docking 13mer peptide or the noncanonical region docking 13mer peptide or both canonical and noncanonical peptides at the same time. Samples were boiled with sample buffer and Western blotting was carried out to determine the phospho-Thr180/Tyr182 p38, total p38 levels using appropriate antibodies described in the Materials and Methods section 2.23. The blot shown is a representative of three experiments.

3.5 TAB1 mutations alter its ability to induce p38 phosphorylation in the bacterial system

Mutant versions of TAB1 were made with 2 amino acid substitutions in each of the two regions that are involved in p38 binding; the V408G/M409A mutant is referred to below as the canonical mutant (CM) and the V390A/Y392A mutant is referred to as the noncanonical mutant (NCM), as well as a mutant with both sets of mutations V390A/Y392A/V408G/M409A (CM/NCM).

Escherichia coli (E.coli) lack most of the eukaryotic post-translational machinery such as protein kinases and the absence of p38 was verified in the strain Rosetta™ (DE3) by antibody recognition before IPTG induction (see Figure 3.6). Following IPTG induction and recombinant expression of p38 and WT and mutant TAB1 proteins in the transformed E.coli, phosphorylation of p38 and TAB1 were analysed by Western

blotting. It appears that the strong p38 phosphorylation by WT TAB1 is reduced with all CM, NCM and CM/NCM mutations of TAB1 (see Figure 3.6). Most of the decrease is by the CM/NCM mutant; CM/NCM and CM appears to reduce p38 phosphorylation slightly more than NCM. This is reflected on TAB1 phosphorylation, with virtually no phosphorylation when p38 is co-expressed with the CM/NCM mutant. Due to the variability of the bacterial system, the changes of p38 phosphorylation with TAB1 mutations differed in repeats of this experiment. Nonetheless it is evident that p38 phosphorylation is reduced by all three of the mutants compared to the co-transformation with WT TAB1. The effect on TAB1 phosphorylation was similar in three independent experiments.

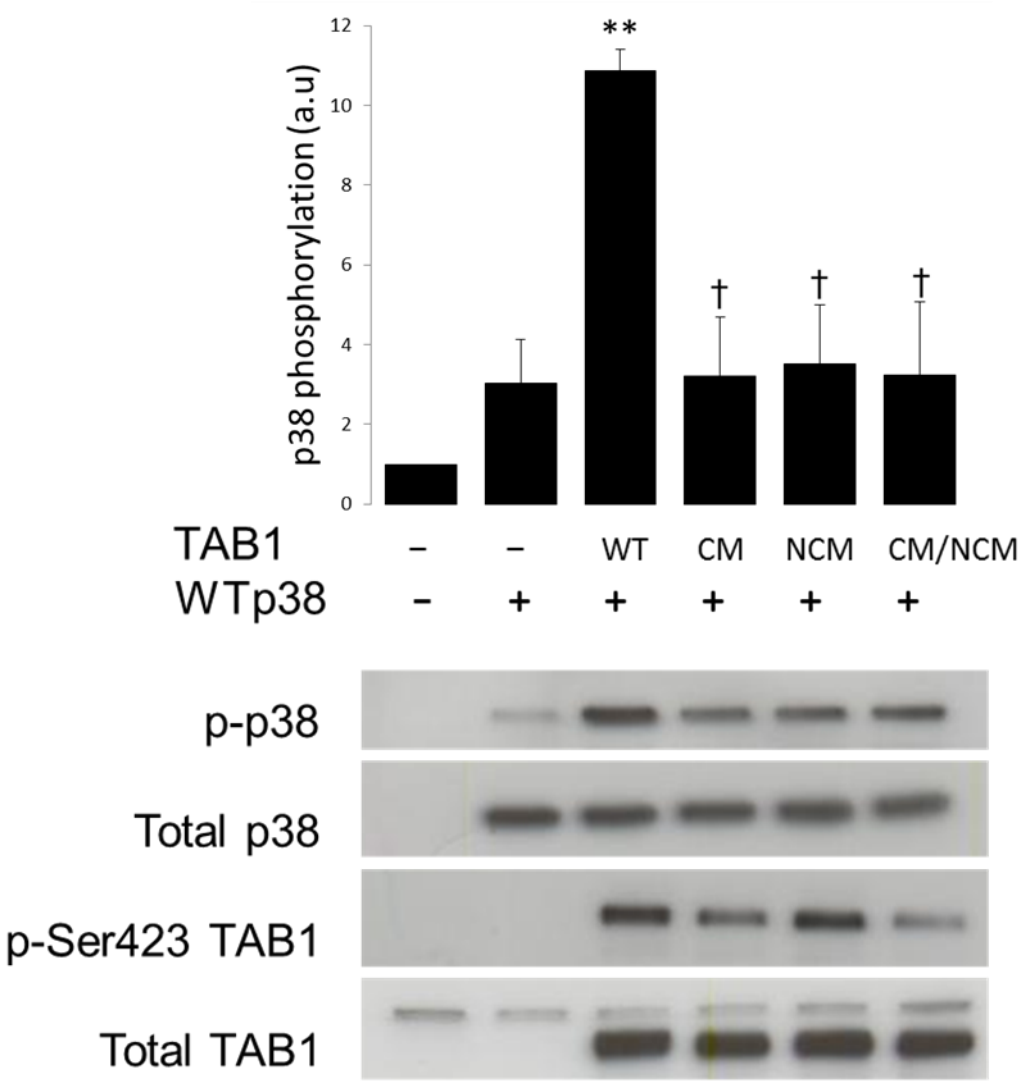

Figure 3.6 Recombinant protein expression in E.coli assessing the effect of TAB1 mutations on p38α phosphorylation.
Rosetta strain of E.coli were transformed with p38α and with either WT or one of the mutant versions of TAB1. Following 5 hour IPTG induction of protein expression, cell lysates were obtained and phospho-Thr180/Tyr182 p38, total p38, phospho-Ser423 TAB1 and total TAB1 levels were determined using appropriate antibodies described in the Materials and Methods section 2.23. The blot shown is a representative of three experiments. Shown in the upper panel is the quantification of three independent repetitions of this experiment. *, $p<0.05$; ANOVA compared to control. †, $p<0.05$; ANOVA compared to WT TAB1.

3.6 TAB1 mutations alter its ability to induce p38 phosphorylation in the mammalian system

To support the results regarding TAB1 mutants observed in the bacterial system, a similar investigation was performed in a mammalian cell line. It appears that as in the

bacterial system, the strong p38 phosphorylation by WT TAB1 is reduced with all CM, NCM and CM/NCM versions of TAB1 in the mammalian system too (see Figure 3.7). Most of the decrease is by the CM/NCM mutant; CM and NCM reduce p38 phosphorylation to similar levels. This is reflected on TAB1 phosphorylation, with virtually no phosphorylation when p38 is co-expressed with the CM/NCM mutant.

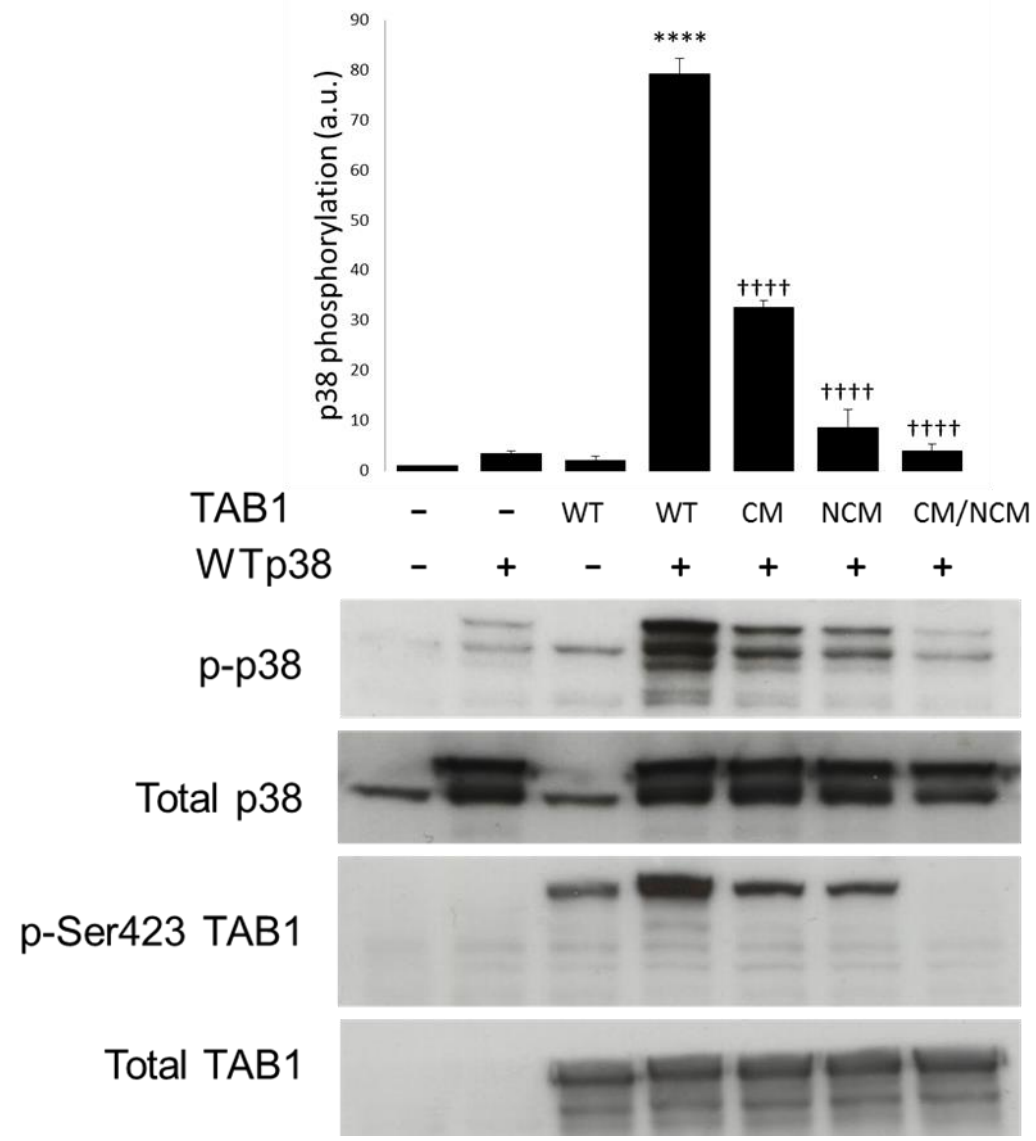

Figure 3.7 Western blot analysis of the effect of TAB1 mutations on p38α phosphorylation in mammalian cells.
HEK293 cells were transfected as described in the Materials and Methods section 2.9. 24 hours after transfection, cell lysates were obtained and phospho-Thr180/Tyr182 p38, total p38, phospho-Ser423 TAB1 and total TAB1 levels were determined using appropriate antibodies decribed in the Materials and Methods section 2.23. The blot shown is a representative of three experiments. Shown in the upper panel is the quantification of three independent repetitions of this experiment. ****, $p<0.0001$; ANOVA compared to control. ††††, $p<0.0001$; ANOVA compared to WT TAB1.

3.7 TAB1 mutations affect TAB1 substrate presentation in the mammalian system

As TAB1 is a substrate of p38 as well as an activating binding partner, it was assessed whether the reduction in TAB1 phosphorylation was due to reduced p38 autophosphorylation by the mutated versions of TAB1 or whether it was because the mutations were diminishing TAB1 substrate presentation to p38. MKK3b and TAB1 both bind to the common docking domain of p38. However, the exact contact positions are not yet identified, so it is not known whether they compete for interaction points on p38. As well as testing whether TAB1 substrate presentation is affected by the mutations by using MKK3b to constitutively activate p38 at similar levels throughout samples, the experiment below tested whether MKK3b and TAB1 compete for the same binding site on p38.

p38 phosphorylation does not differ upon co-transfection of the different versions of TAB1 along with p38 and MKK3b except only a slight decrease with the CM/NCM mutant TAB1. Though TAB1 phosphorylation is diminished with the CM/NCM mutant TAB1, the other TAB1 mutations do not appear to affect TAB1 phosphorylation (see Figure 3.8).

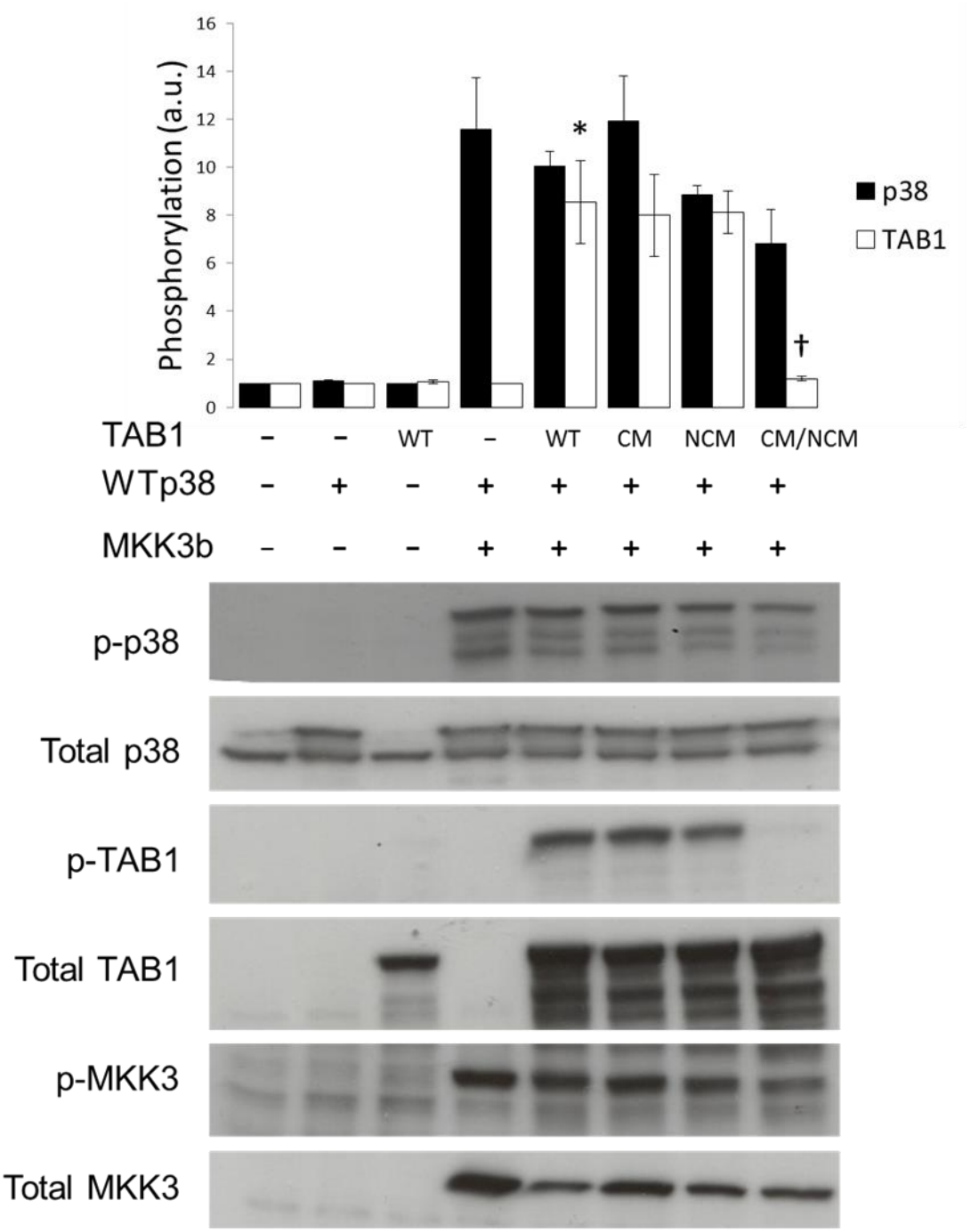

Figure 3.8 Western blot analysis of the effect of TAB1 mutations on TAB1 substrate presentation in mammalian cells.
HEK293 cells were transfected as described in the Materials and Methods section 2.9. 24 hours after transfection, cell lysates were obtained and phospho-Thr180/Tyr182 p38, total p38, phospho-Ser423 TAB1, total TAB1, phospho-Ser189 MKK3 and total MKK3 levels were determined using appropriate antibodies described in the Materials and Methods section 2.23. The blot shown is a representative of three experiments. Shown in the upper panel is the quantification of three independent repetitions of this experiment. *, $p<0.05$; ANOVA compared to control. †, $p<0.05$; ANOVA compared to WT TAB1.

3.8 The mutations and phosphorylation state of TAB1 have no effect on TAK1 activity and phosphorylation

As discussed previously, TAB1 has a TAK1-binding domain that is separate from the p38-binding region and TAB1β lacks the TAK1 binding region (see Figure 1.4) and does not activate TAK1 (35). It has previously been shown that the phosphorylation state of TAB1 plays a role in its effect on the activity of TAK1; the phosphorylated state of TAB1 having a negative impact (279). Surprisingly, in HEK293 cells overexpressing TAK1 and TAB1, we did not see this result. The phosphorylation of TAB1 at the p38-mediated phosphorylation site Ser423 was reduced with SB203580 treatment but this had no effect on the TAB1-mediated TAK1 phosphorylation (see Figure 3.9). As expected, TAB1β did not induce TAK1 phosphorylation, therefore it is the presence of the TAK1-binding domain of TAB1 rather than its phosphorylation state which determines TAK1 phosphorylation.

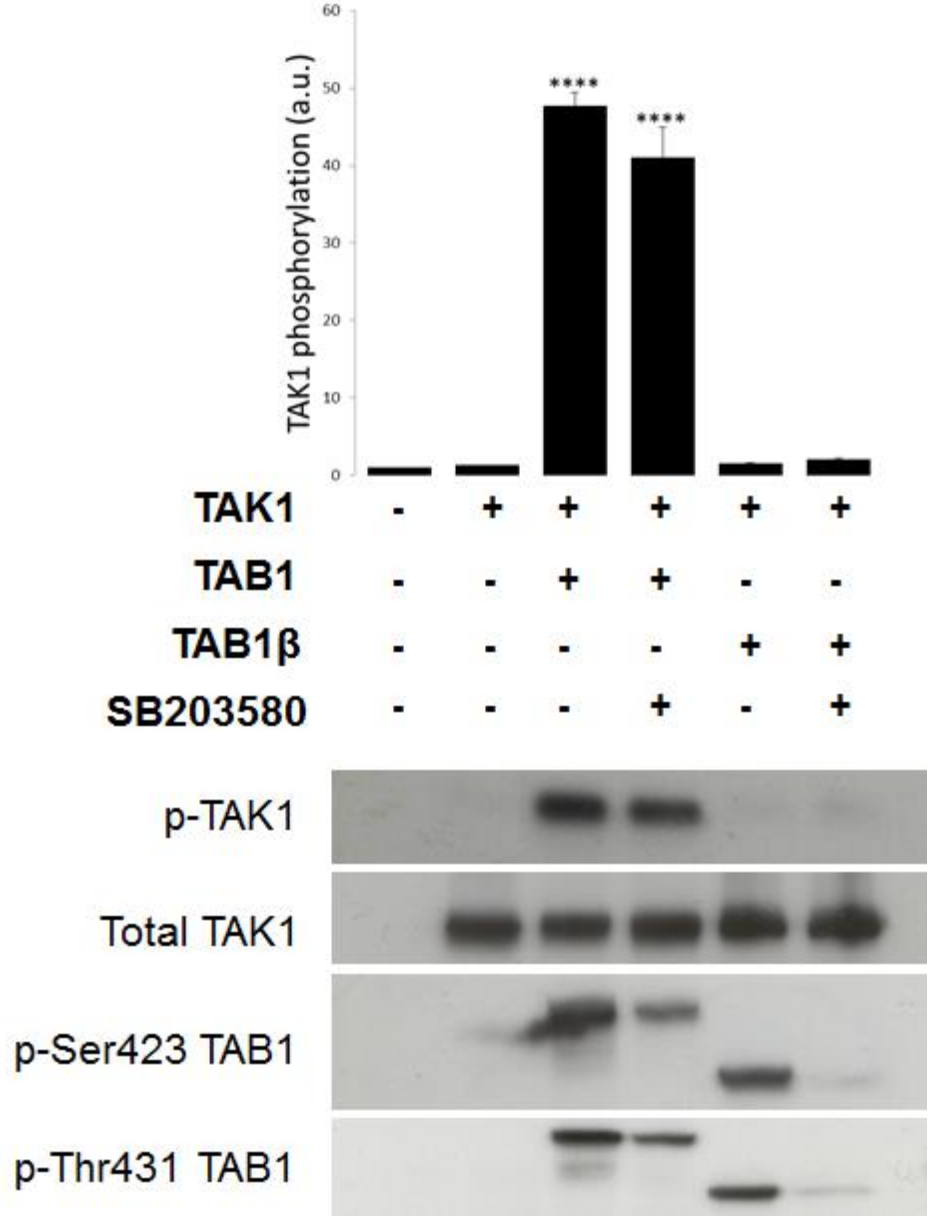

Figure 3.9 Western blot analysis of TAK1 phosphorylation by TAB1 or TAB1β in mammalian cells.
HEK293 cells were transfected as described in the Materials and Methods section 2.9. 24 hours after transfection, cell lysates were obtained and phospho-Thr184/Thr187 TAK1, total TAK1 and phospho-Ser423 and phospho-Thr431 TAB1 levels were determined using appropriate antibodies described in the Materials and Methods section 2.23. The blot shown is a representative of three experiments. Shown in the upper panel is the quantification of three independent repetitions of this experiment. ****, $p<0.0001$; ANOVA compared to control.

In addition, in order to investigate whether the mutations in TAB1 explored earlier have an effect on its ability to induce TAK1 phosphorylation, TAK1 and TAB1 were co-transfected in HEK293 cells, and TAK1 and TAB1 phosphorylation were evaluated (see

Figure 3.10). It appears that, despite the CM/NCM TAB1 mutant being phosphorylated to a much lower level than WT TAB1; TAK1 phosphorylation does not appear to be affected by this reduction in phosphorylation of TAB1 or by the mutations that are present. Similar levels of TAK1 phosphorylation are also seen in presence of the CM and NCM mutants, suggesting that these mutations in p38-binding domain of TAB1 do not affect its ability to induce TAK1 phosphorylation.

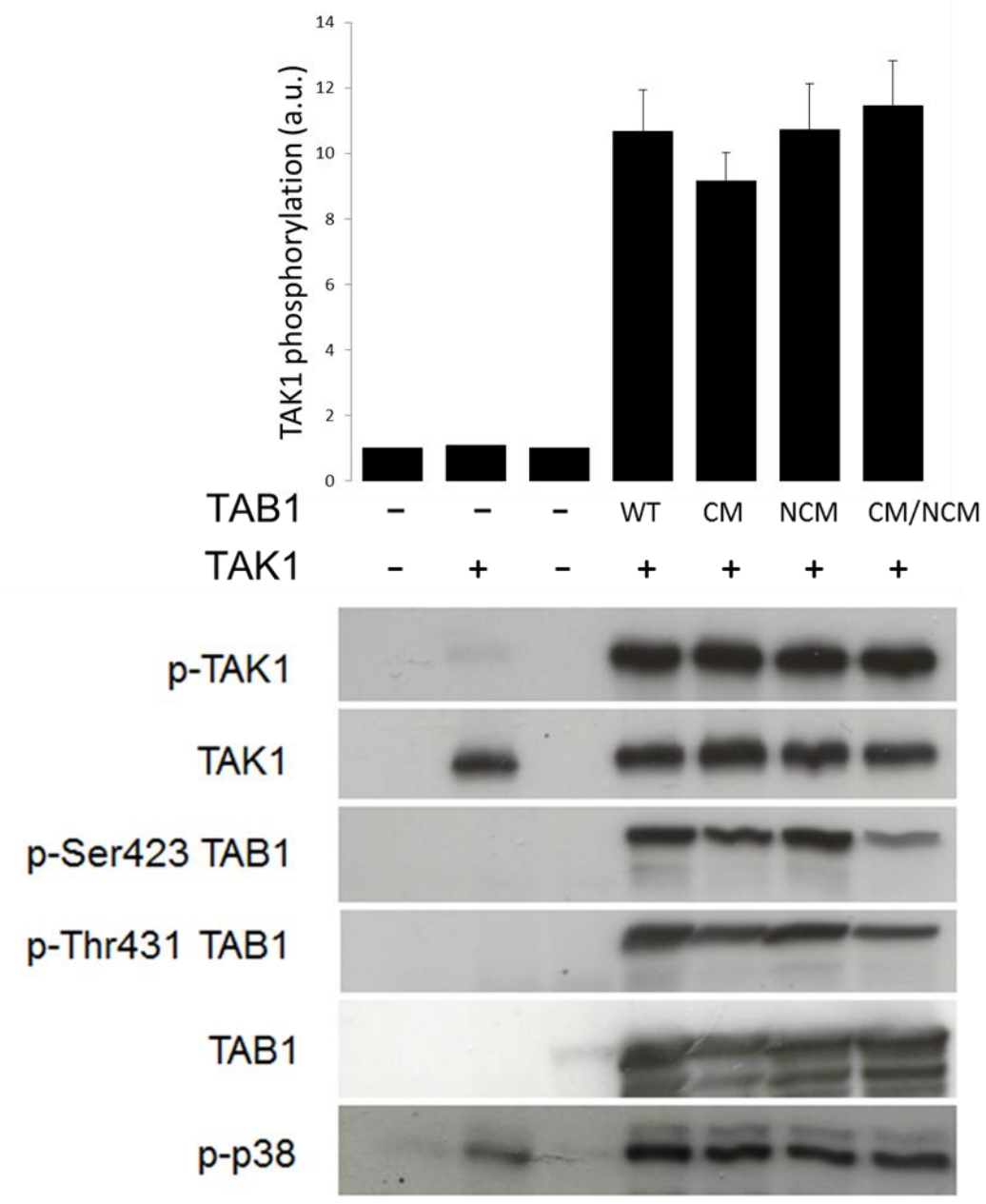

Figure 3.10 Western blot analysis of the effect of TAB1 mutations on TAK1 phosphorylation in mammalian cells.

HEK293 cells were transfected as described in the Materials and Methods section 2.9. 24 hours after transfection, cell lysates were obtained and phospho-Thr184/Thr187 TAK1, total TAK1 and phospho-Ser423 and phospho-Thr431 TAB1, total TAB1 and phospho-Thr180/Tyr182 p38 levels were determined using appropriate antibodies described in the Materials and Methods section 2.23. The blot shown is a representative of three experiments. Shown in the upper panel is the quantification of three independent repetitions of this experiment. *, $p<0.05$; ANOVA compared to control

3.9 TAB1 displaces MKK3b from its binding partner p38α

ITC experiments were performed to determine whether TAB1 affects MKK3b binding to p38. The results confirmed a direct interaction between MKK3b and p38, revealing in the experimental conditions used, a monophasic 1:1 binding isotherm and a binding affinity in the low micromolar range (see Figure 3.11 and Table 3.1). Presence of TAB1 peptide [NH_2-RVYPVSVPYSSAQSTSKTSVTLSLVMPSQ-COOH] led to a change in the interaction between MKK3b peptide [NH_2-SKGKSKRKKDLRISCNSK-COOH] and p38 observed as a change in enthalpy of interaction. Based on these data and the fact that the peptide is necessary and sufficient for TAB1-mediated activation of p38 as seen in our previous studies (34), we hypothesise that this short polypeptide contains the residues required for TAB1 recognition and is sufficient to affect the interaction between MKK3b and p38.

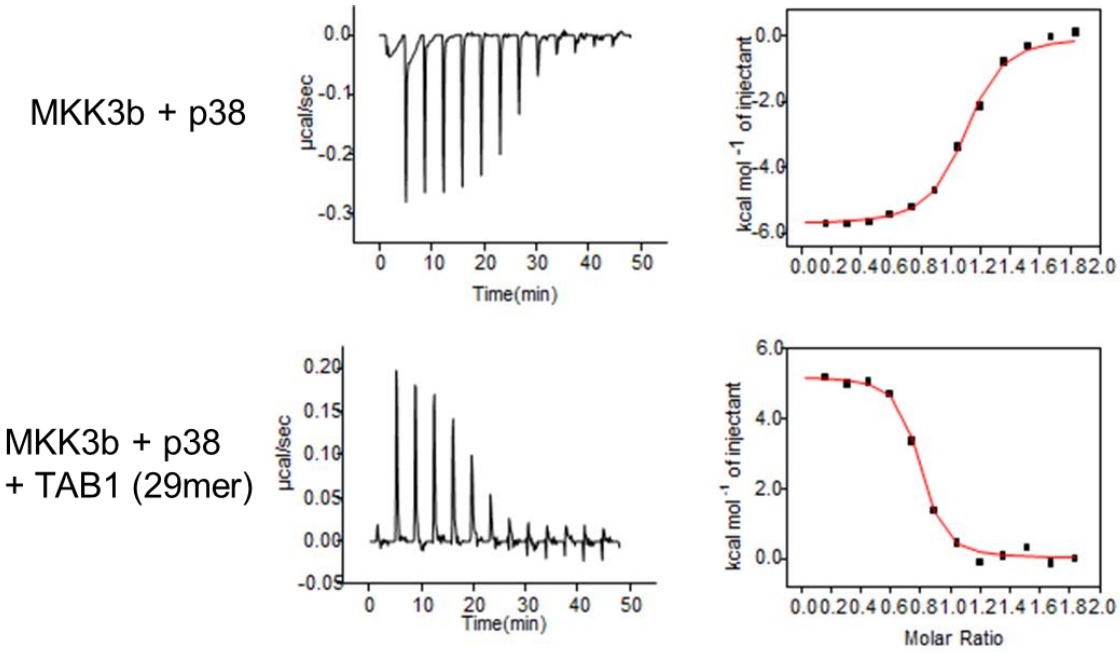

Figure 3.11 Thermodynamic characterisation of p38:MKK3b complex formation and competition by TAB1 (29mer).
ITC analysis of the interaction between p38 and MKK3b. A solution of MKK3b was titrated into p38 in the presence (bottom graphs) or absence (top graphs) of TAB1(29mer). The values reported are averaged over three experiments, and the errors were found to be less than 5%. All the measurements were performed at 25°C. All but the first point were used for curve fitting and derived thermodynamic parameters are shown in Table 3.1.

Table 3.1 Thermodynamic parameters determined by ITC of the association of p38 with TAB1 and MKK3

	n	**Kd (µM)**	**ΔG (kcal/mol)**	**ΔH (kcal/mol)**	**−TΔS (kcal/mol)**
p38α/ MKK3b	1.0	0.27	-8.9	−5.7	3.2
p38α/ MKK3b/TAB1(29mer)	0.7	0.24	-8.9	5.5	14.4

3.10 TAB1 and MKK3b compete to phosphorylate p38 in an IVK system

In order to further assess the competition between the two binding partners of p38; MKK3b and TAB1, IVK assays were performed using recombinant proteins. A constitutively active mutant of MKK3b (S218E/T222E – MKK3bEE) was used in these

experiments. The concentration of MKK3bEE low enough to induce phosphorylation of p38 without overloading the phospho signal and to enable observation of differences between trans and autophosphorylation in TAB1 and MKK3bEE co-expression system, was determined from previous experiments in our laboratory. To verify the accuracy of this concentration in these experiments, KDp38 (D168A) and several concentrations of MKK3bEE were used in an IVK assay observing p38 phosphorylation (see Figure 3.12). It is evident that 8.47 nM is the optimal concentration to see a clear difference in phosphorylation of p38 in comparison to control, as lower concentrations do not appear to induce phosphorylation. This concentration of MKK3bEE was used in IVKs with TAB1 and p38 to investigate the competition between MKK3bEE and TAB1 in binding to p38 and inducing its phosphorylation.

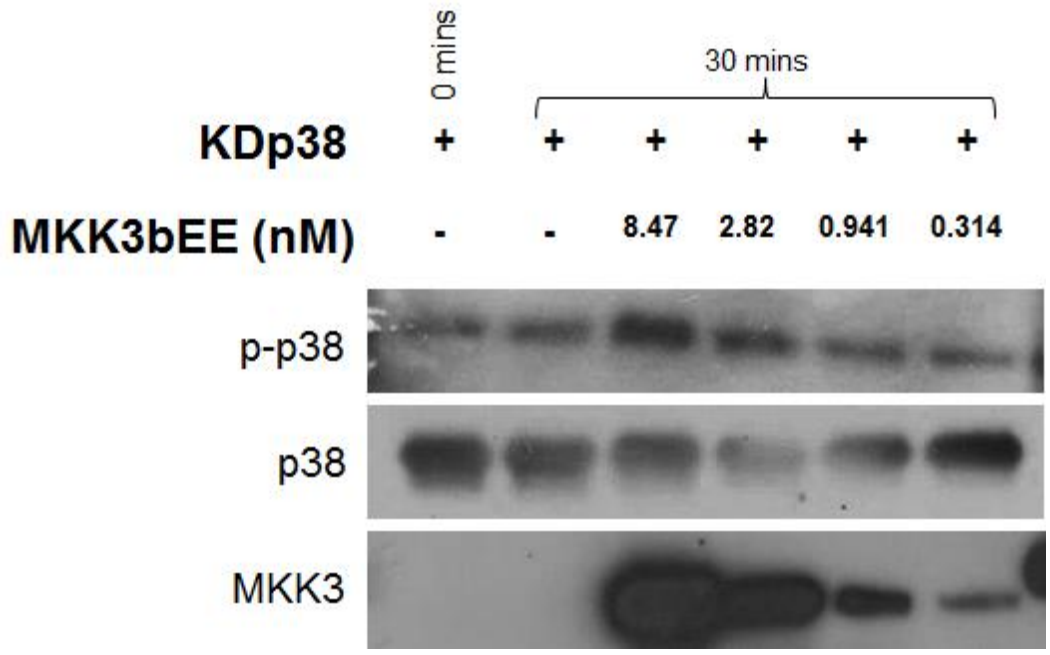

Figure 3.12 Western blot analysis of an IVK assay determining the optimum MKK3bEE concentration to induce p38 phosphorylation.
IVK assay was performed at 37ºC for 30 minutes for MKK3bEE and KDp38 recombinant proteins. Samples were boiled with sample buffer and Western blotting was carried out to determine the phospho-Thr180/Tyr182 p38, total p38, and total MKK3 levels using appropriate antibodies described in the Materials and Methods section 2.23.

30 minutes is a commonly used incubation time for IVK assays, and the suitability of this was verified by testing a set of incubation times for the induction of p38 by MKK3bEE and TAB1. It appears that there is an adequate signal at 30 minutes for both TAB1 and MKK3bEE mediated phosphorylation of p38 (see Figure 3.13). Therefore, this incubation time was used to induce the MKK3bEE-mediated transphosphorylation. Nonetheless, for TAB1-mediated autophosphorylation, the TAB1 and p38 proteins have been incubated for 4 hours to allow p38 to accommodate TAB1 and aid the process of any potential competition between TAB1 and MKK3bEE, before the addition of MKK3bEE which appears to be much more efficient at inducing p38 phosphorylation and possibly at binding to p38 as well.

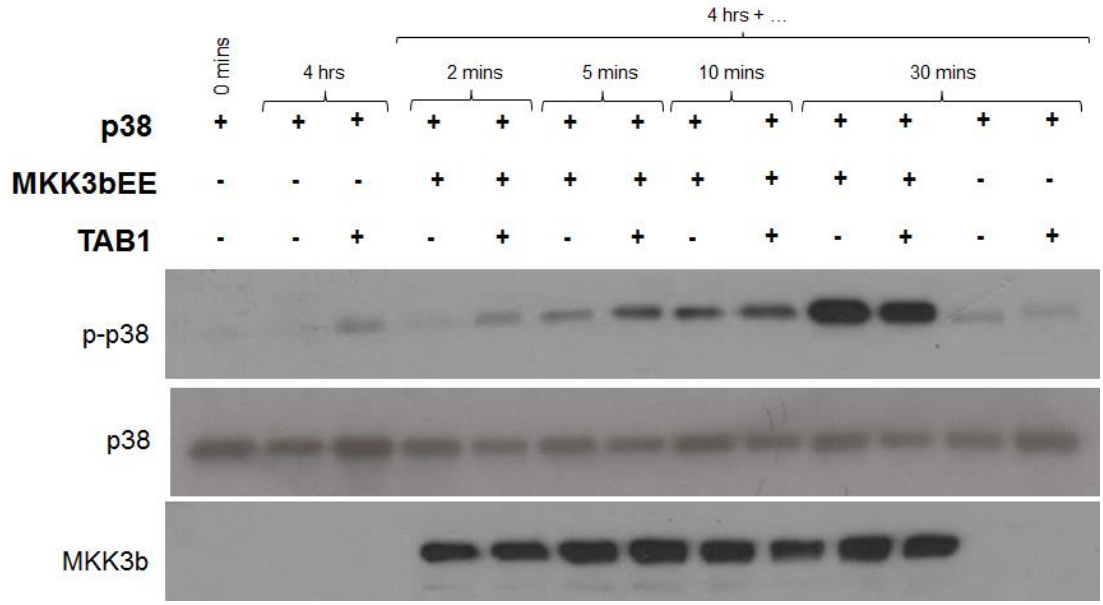

Figure 3.13 Western blot analysis of an IVK assay determining induction time to induce substantial p38 phosphorylation by MKK3bEE and TAB1.
IVK assay was performed at 37ºC for 4 hours for p38α alone and in the presence of 29mer TAB1 peptide. MKK3bEE was added to these samples and they were incubated for a further 2, 5, 10 and 30 minutes. Samples were boiled with sample buffer and Western blotting was carried out to determine the phospho-Thr180/Tyr182 p38, total p38, and total MKK3 levels using appropriate antibodies described in the Materials and Methods section 2.23.

IVK assays show that TAB1 and MKK3bEE both phosphorylate p38, with MKK3bEE being more efficient at doing so. Upon addition of MKK3bEE to an assay of TAB1 and

p38, the phosphorylation level of p38 appears to be at similar levels with that of the MKK3bEE and p38 sample (see Figure 3.14). When SB203580 is added to block the TAB1-mediated autophosphorylation, there is a reduction in p38 phosphorylation with TAB1 alone to basal levels. A reduction is observed in the TAB1, MKK3bEE and p38 sample, which is theoretically showing the phosphorylation of p38 mediated by MKK3bEE alone. Comparing p38 phosphorylation levels in the samples of MKK3b co-expressed with p38 and the sample expressing MKK3b, TAB1 and p38, we can deduce the difference in phosphorylation as that which is mediated by TAB1, suggesting that in this system TAB1 does compete with MKK3b in inducing p38 phosphorylation.

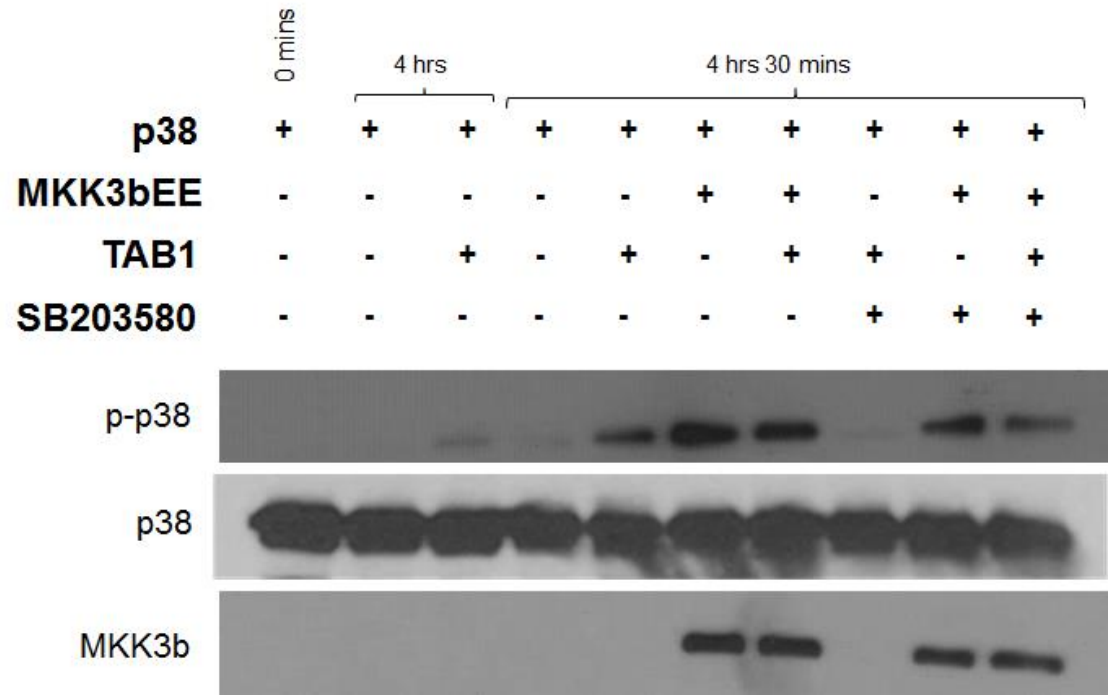

Figure 3.14 Western blot analysis of an IVK assay assessing the competition between MKK3b and TAB1 to induce p38 phosphorylation.
IVK assay was performed at 37ºC for 4 hours for p38α alone and in the presence of 29mer TAB1 peptide. MKK3bEE was added to these samples and they were incubated for a further 30 minutes. Samples were boiled with sample buffer and Western blotting was carried out to determine the phospho-Thr180/Tyr182 p38, total p38, and total MKK3 levels using appropriate antibodies described in the Materials and Methods section 2.23. The blot shown is a representative of three experiments.

3.11 TAB1 and MKK3b do not compete in phosphorylating p38 in the mammalian system

It has been attempted to create a constitutively active version of p38 by overexpressing p38 and its activator MKK3b in the experiment in Figure 3.8 to investigate whether TAB1 mutations alter TAB1 substrate presentation. Following the results of the ITC and IVK experiments investigating competition between TAB1 and MKK3b to bind to p38, we wanted to verify the results in the in-cell setting. In order to verify that the p38 phosphorylation in cells co-transfected with MKK3b and TAB1 is via the canonical pathway and not autophosphorylation due to TAB1, the TAB1-mediated pathway must be blocked to see if the p38 phosphorylation induced by MKK3b is reduced when TAB1 is present. For this the p38 inhibitor SB203580 and a kinase-dead (KD) version of p38 (D168A mutant) have been used. SB203580 is known to bind p38 and inhibit its autophosphorylation mediated by TAB1, yet it does not inhibit the MKK-mediated pathway (see Figure 3.15). Therefore using SB203580 blocks the TAB1 mediated p38 activation whilst keeping the canonical pathway intact, providing results which can be interpreted to observe the effect, if any, of TAB1 on p38 phosphorylation when transfected along with p38 and MKK3b.

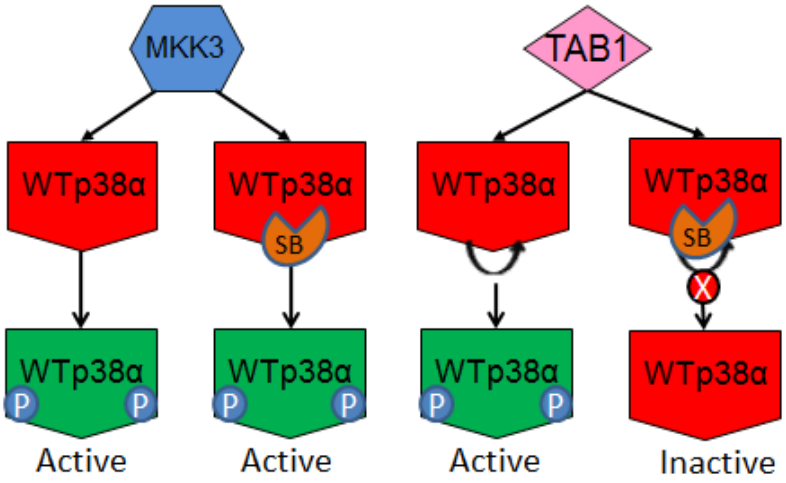

Figure 3.15 Schematic showing whether MKK3 and TAB1 can activate WTp38α upon addition of SB203580.

SB203580 prevents binding of ATP to p38. p38 must bind ATP in order to autophosphorylate whereas this is not required for MKK3-mediated phosphorylation. MKK3 is able to phosphorylate p38 in presence of SB203580, whereas TAB1-mediated autophosphorylation does not occur, permitting observation of MKK3 activated p38 alone.

p38 phosphorylation is increased when co-transfected with MKK3b, and this does not appear to decrease upon 10μM SB203580 addition (see Figure 3.16). On the contrary, in cells co-transfected with p38 and TAB1, the augmented p38 phosphorylation is reduced to basal levels upon addition of SB203580. Whereas when both TAB1 and MKK3b, as well as p38 are transfected into cells, there is hardly any reduction in p38 phosphorylation with addition of SB203580. This shows that most of the p38 phosphorylation we observe is due to the canonical activation pathway and addition of TAB1 does not interfere with MKK3b binding and activation of p38.

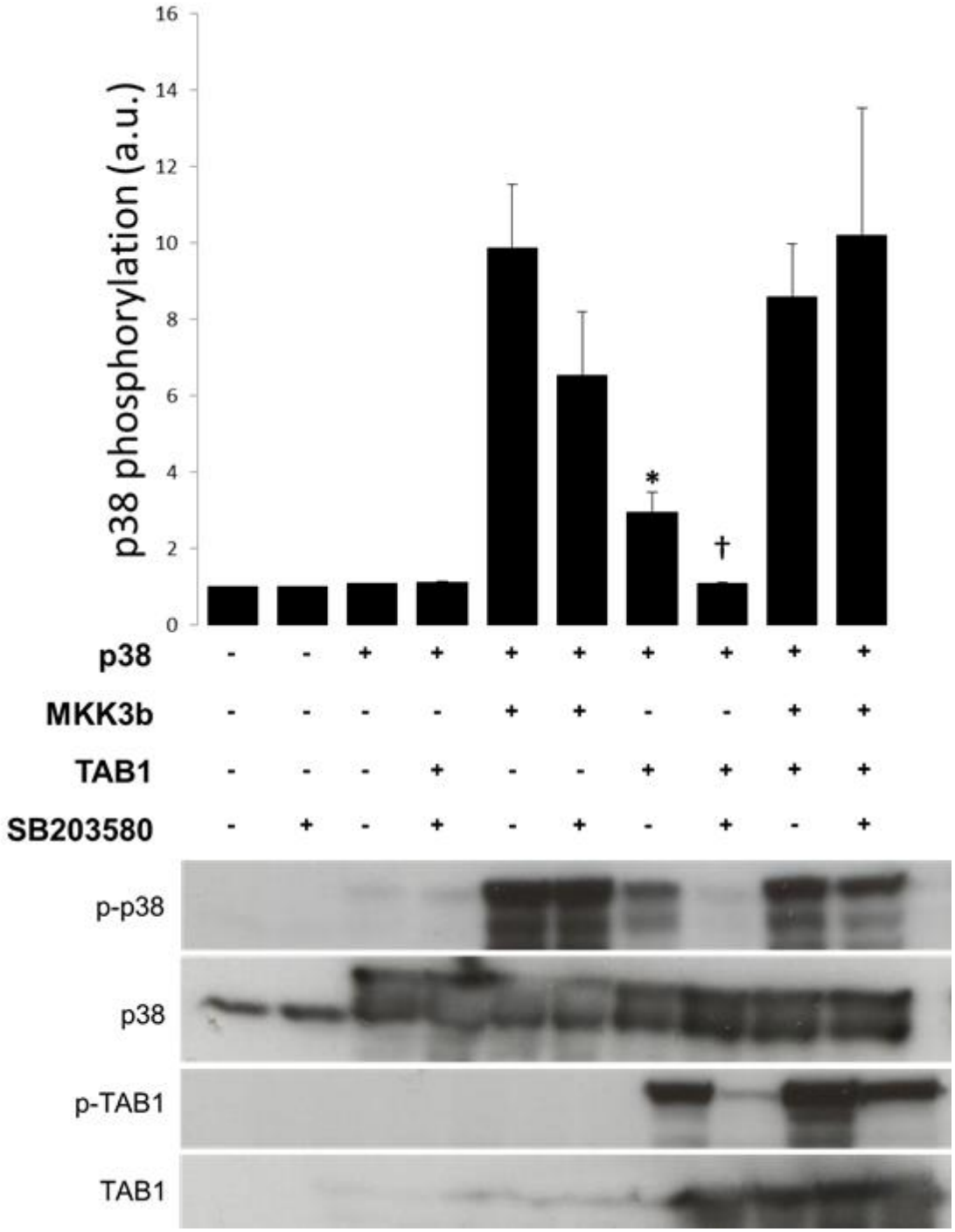

Figure 3.16 Western blot analysis of the effect of SB203580 on MKK3-mediated and/or TAB1-mediated p38α phosphorylation in mammalian cells.
HEK293 cells were transfected as described in the Materials and Methods section 2.9. 24 hours after transfection, 10 μM SB203580 was added as indicated (+) with an equivalent volume of DMSO added to the control wells. Cells were incubated for 30 minutes, after which cell lysates were obtained and phospho-Thr180/Tyr182 p38, total p38, phospho-Ser423 TAB1 and total TAB1 levels were determined using appropriate antibodies described in the Materials and Methods section 2.23. The blot shown is a representative of three experiments. Shown in the upper panel is the quantification of three independent repetitions of this experiment. *, $p<0.05$; ANOVA compared to control, †, $p<0.05$; ANOVA compared to with TAB1-mediated activation.

In addition, KDp38 is a mutated form of p38 that cannot autophosphorylate but is still able to be transphosphorylated by upstream kinases such as MKK3b. This, just like the SB203580 inhibited WTp38, and will be able to reveal phosphorylation caused by the canonical pathway and not by the TAB1-mediated mechanism (see Figure 3.17).

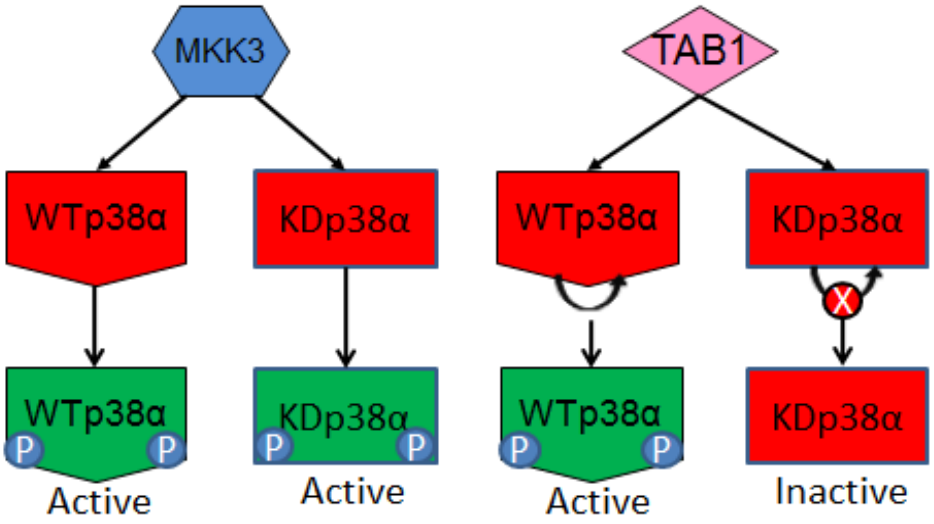

Figure 3.17 Schematic showing whether MKK3 and TAB1 can activate WTp38 and KDp38.
MKK3 is able to activate both versions of p38, whereas as TAB1 induces autophosphorylation and KDp38 is unable to autophosphorylate, only MKK3 can activate this p38 version, permitting observation of MKK3 activated p38 alone.

WTp38 and KDp38 phosphorylation increases when co-transfected with MKK3b and though not to a similar level WTp38 phosphorylation also increases when co-transfected with TAB1 (see Figure 3.18). However, KDp38 phosphorylation levels with TAB1 are similar to that of KDp38 alone. Whereas triple transfection with KDp38, TAB1 and MKK3b causes an increase in KDp38 phosphorylation, suggesting that the main pathway of phosphorylation is via MKK3b and TAB1 does not interfere with MKK3b activating p38 in cells.

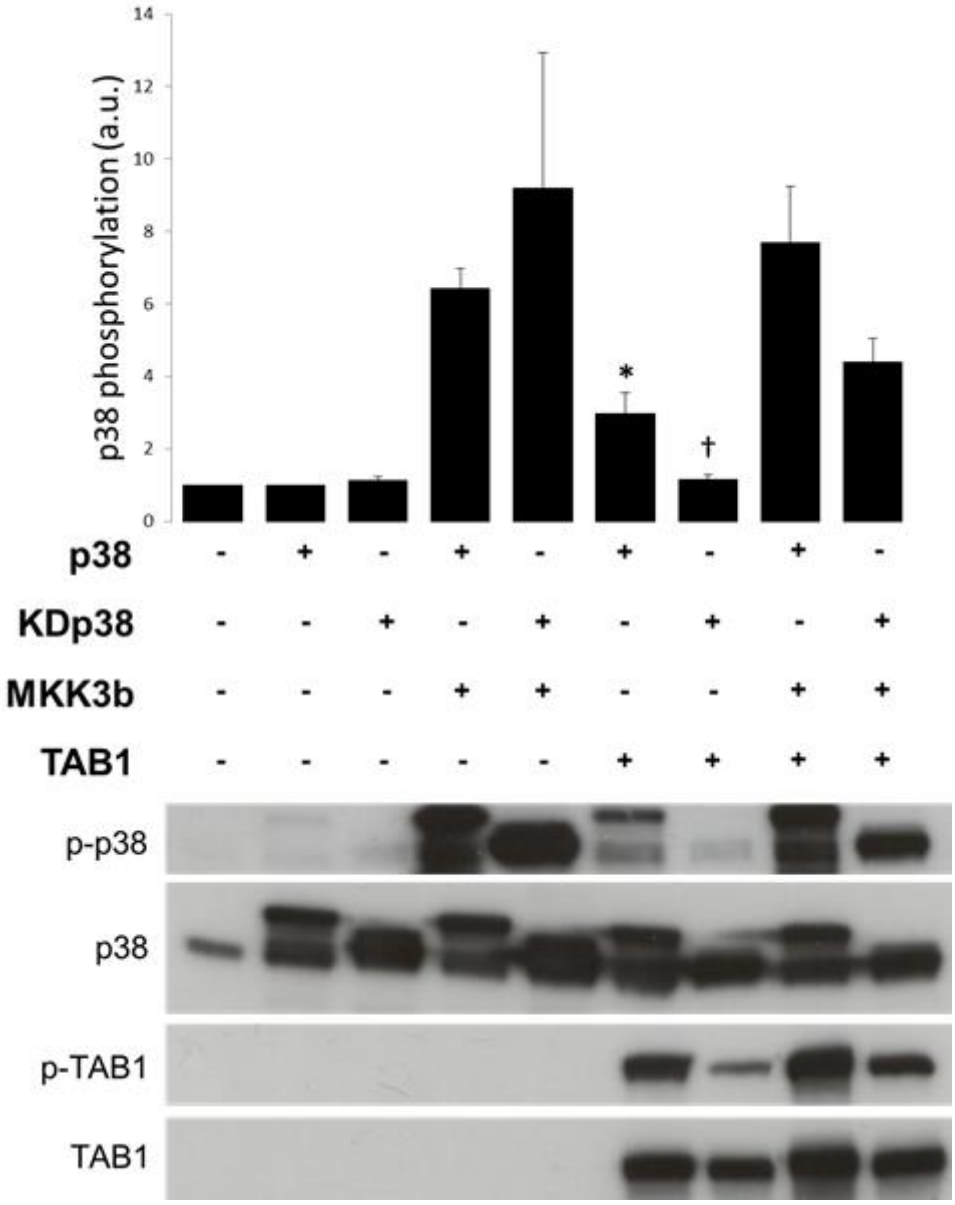

Figure 3.18 Western blot analysis of WTp38α and KDp38α phosphorylation by MKK3 and/or TAB1 in mammalian cells.
HEK293 cells were transfected as described in the Materials and Methods section 2.9. 24 hours after transfection, cell lysates were obtained and phospho-Thr180/Tyr182 p38, total p38, phospho-Ser423 TAB1 and total TAB1 levels were determined using appropriate antibodies described in the Materials and Methods section 2.23. The blot shown is a representative of three experiments. Shown in the upper panel is the quantification of three independent repetitions of this experiment. *, $p<0.05$; Student's T-test compared to control, †, $p<0.05$; Student's t-test compared to with TAB1-mediated activation.

3.12 The localisation of p38 is dependent on its binding partner

The results obtained *in vitro* suggest TAB1 and MKK3b (see Figure 3.14) compete for p38 access/activation whilst those obtained in cells (see Figure 3.16 and Figure 3.18)

suggest they are independent. We hypothesised that this dichotomy maybe the result of spatial constraints in the cell-based assays preventing competition between TAB1 and MKK3b (Figure 3.16 and Figure 3.18). In order to investigate this, the localisation of p38 in response to expression of MKK3b and/or TAB1 was observed.

In Figure 3.19, MKK3b appears to be localised in the cytoplasm residing close to the plasma membrane, whilst TAB1 is located in the nuclear/perinuclear area. It is clear that p38 is preferentially co-localised according to which binding partner is co-expressed. While MKK3b and TAB1 co-localise with p38 in their respective in-cell locations when they are overexpressed with p38 on their own; the majority of p38 appears to co-localise with MKK3b when both MKK3b and TAB1 are co-expressed in HEK293 cells (see Figure 3.19). This preferential colocation with MKK3b may be the result of the dominant effect it has on the activation of p38 in Figure 3.16 and Figure 3.18.

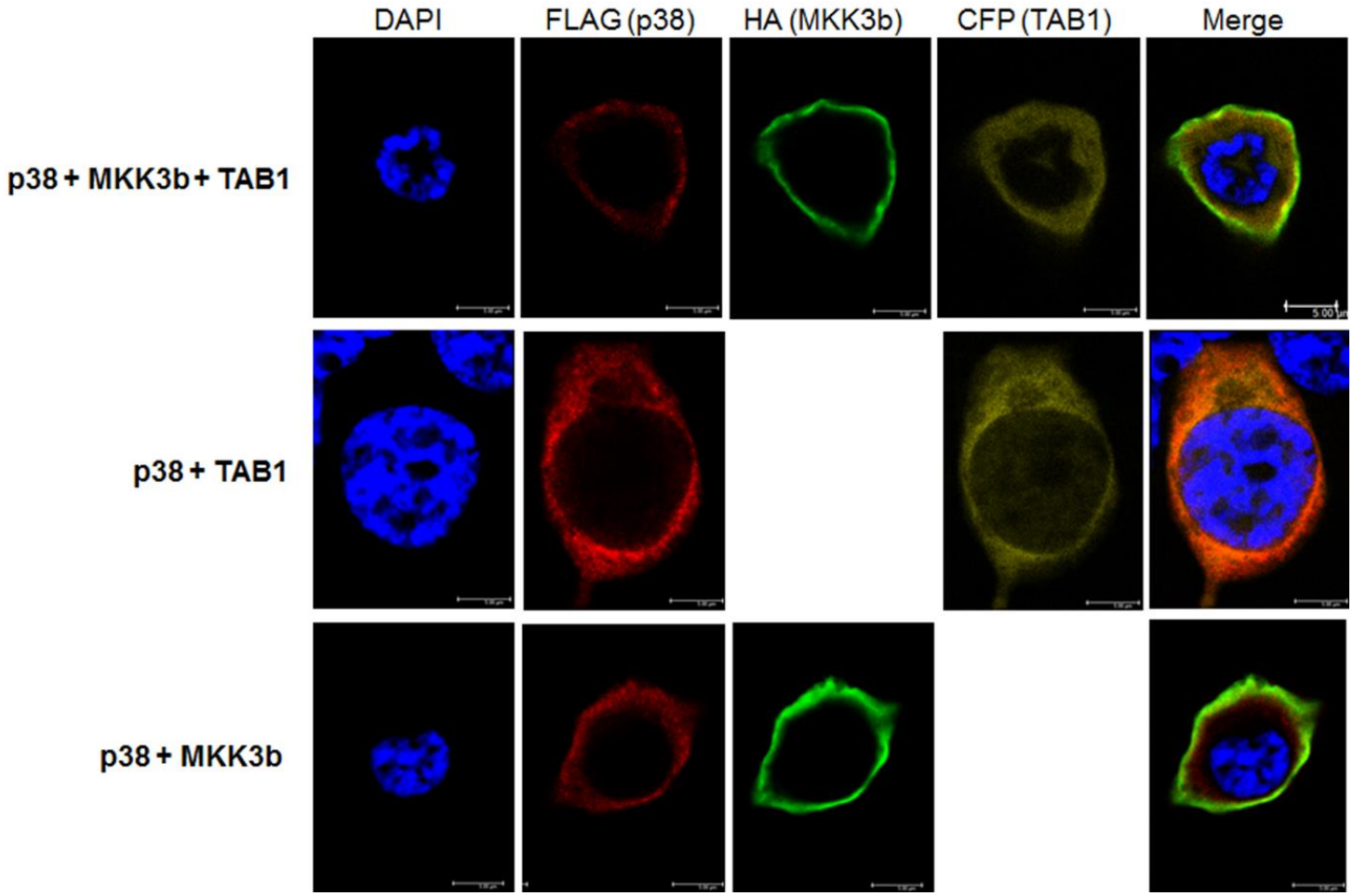

Figure 3.19 Immunofluorescence determining the localisation of p38 in HEK293 cells depending on its co-expressed binding partner.
HEK293 cells were transfected with FLAG-p38, HA-MKK3 and CFP-TAB1 as described in the Materials and Methods section 2.9. 24 hours after transfection, cells were fixed and permeabilised as in the Materials and Methods section 2.14. DAPI, FLAG-p38, HA-MKK3 and CFP-TAB1 were detected using appropriate antibodies described in the Materials and Methods section 2.23.

3.13 The importance of Thr185 in the localization of p38

The localisation of a protein within a cell determines its ability to perform its function due to its proximity to its binding partners, downstream substrates and the in-cell location of the other members of the particular signalling pathway. The importance of the phosphorylation of the Thr188 residue in ERK1/2 and its role in its localisation has been previously discussed in section 1.2.5. This residue is conserved in p38 at the 185 site and based on the ERK1/2 study and previous mass spectrometry data generated in our laboratory regarding this residue, we have hypothesized that it potentially plays a role in the localisation of p38. Having determined that the localisation of p38 with MKK3b and TAB1 are distinct from each other (see Figure 3.19), and based on our findings that the phosphorylation of this residue is associated with TAB1 presence, the localisation of p38 was examined using phosphomimetic (T185D) and phosphorylation-deficient (T185G) mutants of p38 at this residue.

Inspecting the quantification of the immunofluorescence data and observing the images (see Figure 3.20); p38 resides throughout the cell with similar levels in the cytoplasm and the nucleus. There does not appear to be an effect of the T185G mutant, except possibly a slight increase in the levels of p38 in the nucleus. However, the T185D mutation results in a significant relocation into the cytoplasm.

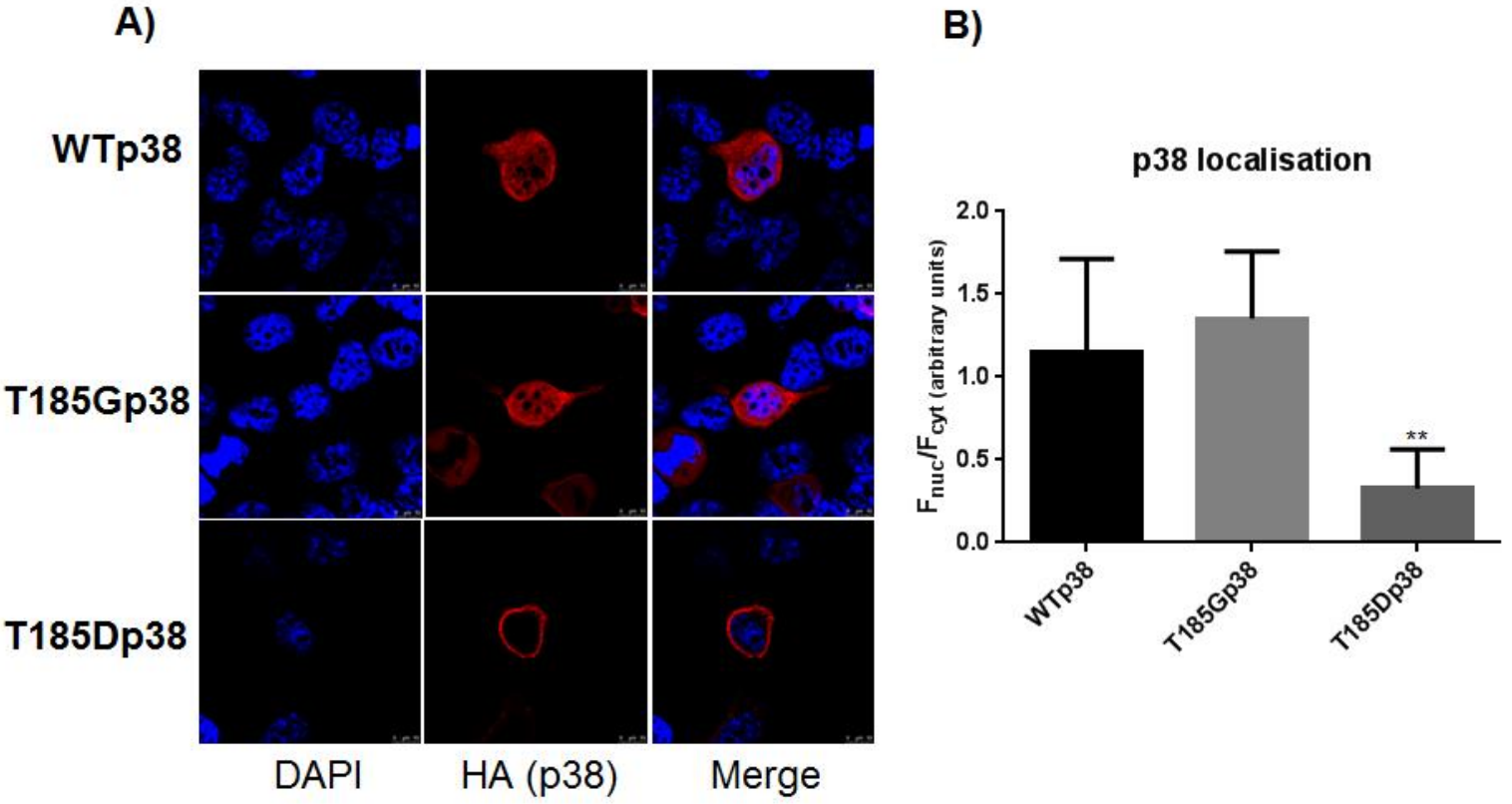

Figure 3.20 Immunofluorescence determining the localisation of p38 and its T185 mutants.
HEK293 cells were transfected with HA-p38, HA-T185G-p38 and HA-T185D-p38 as described in the Materials and Methods section 2.9. 24 hours after transfection, cells were fixed and permeabilised as in the Materials and Methods section 2.14. **A)** DAPI, and HA-p38, HA-T185G-p38 and HA-T185D-p38 were detected using appropriate antibodies described in the Materials and Methods section 2.23. **B)** Quantification of immunofluorescence images using ImageJ program. **, $p<0.01$ ANOVA.

4 RESULTS – Role of the amino acid response pathway in cardiomyocytes

Amino acid response pathway is one of the basic mechanisms that enables organisms to survive starvation by limiting the usage of their resources for the most essential processes within cells. Furthermore, as discussed earlier in this thesis, the mechanism of halofuginone-mediated activation of the amino acid response pathway is through its competition with proline for the EPRS. This leads to an accumulation of uncharged tRNAs activating GCN2 which in turn leads to a halt in global translation and the induction of the translation of a subset of mRNAs to aid the cell deal with the starvation, which is mimicked through halofuginone treatment. In addition, halofuginone treatment has previously been associated with improvement in mdx models of mice with decreased fibrosis and decreased collagen I and III gene expression and collagen protein levels, as well as improving cardiac and respiratory function (222). There are several features of heart failure, on which we were interested in testing the effect of halofuginone treatment in cardiomyocytes and our hypothesis was that if halofuginone is capable of improving cardiac function and decreasing fibrosis in other experimental models, amino acid response pathway might be a potential target in cardiomyocytes. Therefore, we conducted experiments in iPS cardiomyocytes and NRVMs observing hypertrophic markers, autophagy markers, inflammation markers and p38 activation, as these are associated with heart failure. Before these experiments, several characterisation studies were conducted including the identification of the active yet non-toxic concentration of halofuginone in these cells and the activation of downstream effectors of the amino acid response pathway, as well as the response of these cells to the stressor we have used; ET-1.

4.1 Determining the optimal concentrations of halofuginone to induce the amino acid response in cardiomyocytes

In order to use halofuginone as a tool effectively in the in-cell setting, toxicity and activation of the AAR pathway were observed simultaneously. We have found that different cell lines have different sensitivities to halofuginone. Toxicity was measured by adenylate kinase (AK) release for both iPS cardiomyocytes and NRVMs. The optimal concentration of halofuginone to activate the AAR in iPS cardiomyocytes and NRVM cells without inducing toxicity is 30 nM (see Figure 4.1).

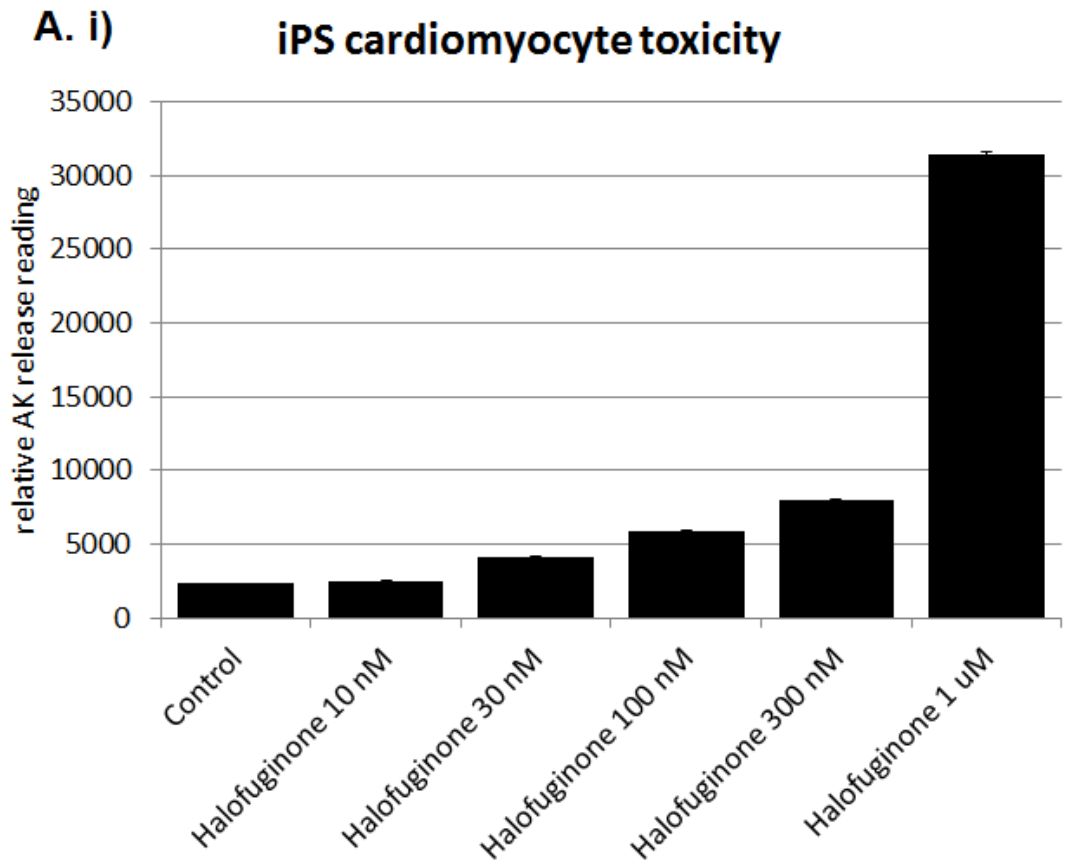

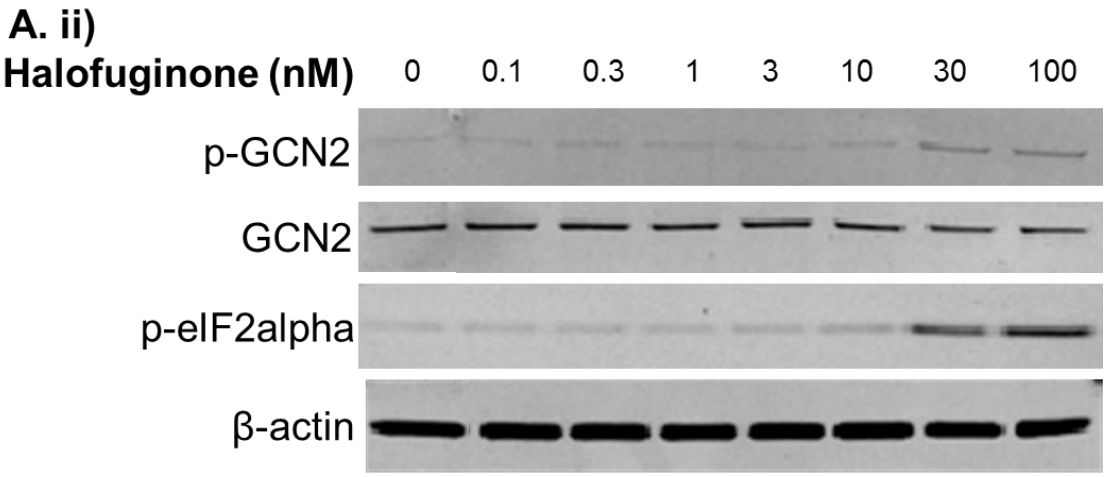
A. ii)
Halofuginone (nM)
0
0.1
0.3
1
3
10
30
100
p-GCN2
GCN2
p-eIF2alpha
β-actin

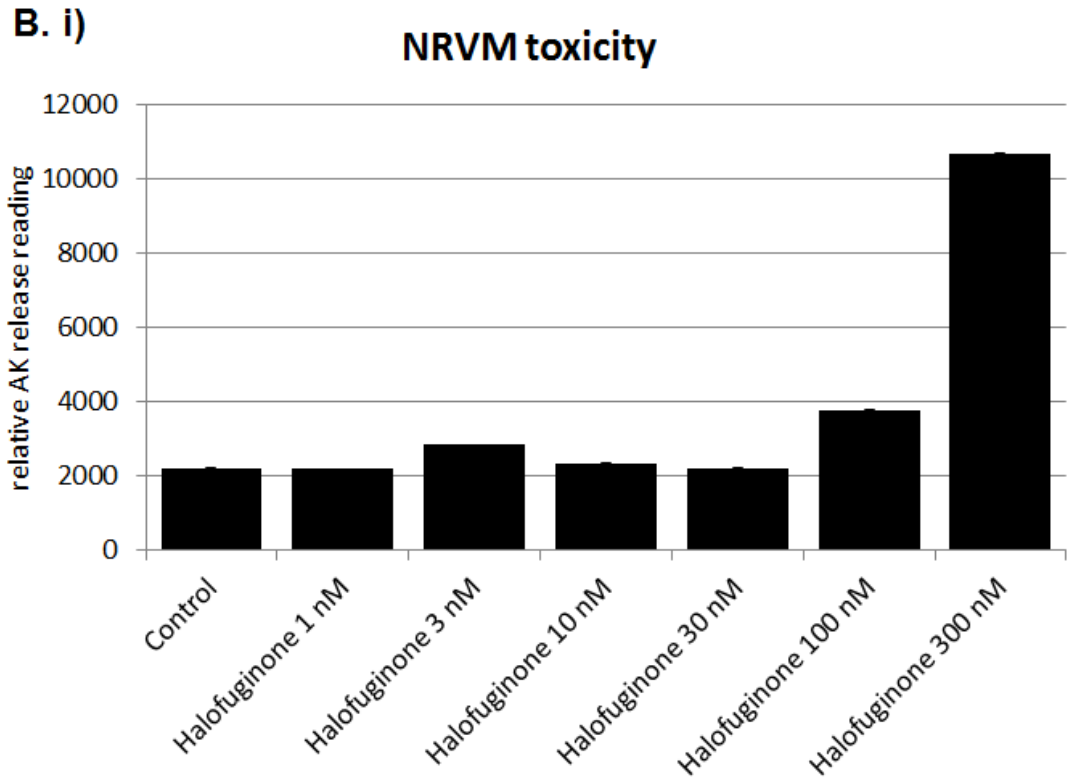
B. i)
NRVM toxicity
relative AK release reading
12000
10000
8000
6000
4000
2000
0
Control
Halofuginone 1 nM
Halofuginone 3 nM
Halofuginone 10 nM
Halofuginone 30 nM
Halofuginone 100 nM
Halofuginone 300 nM

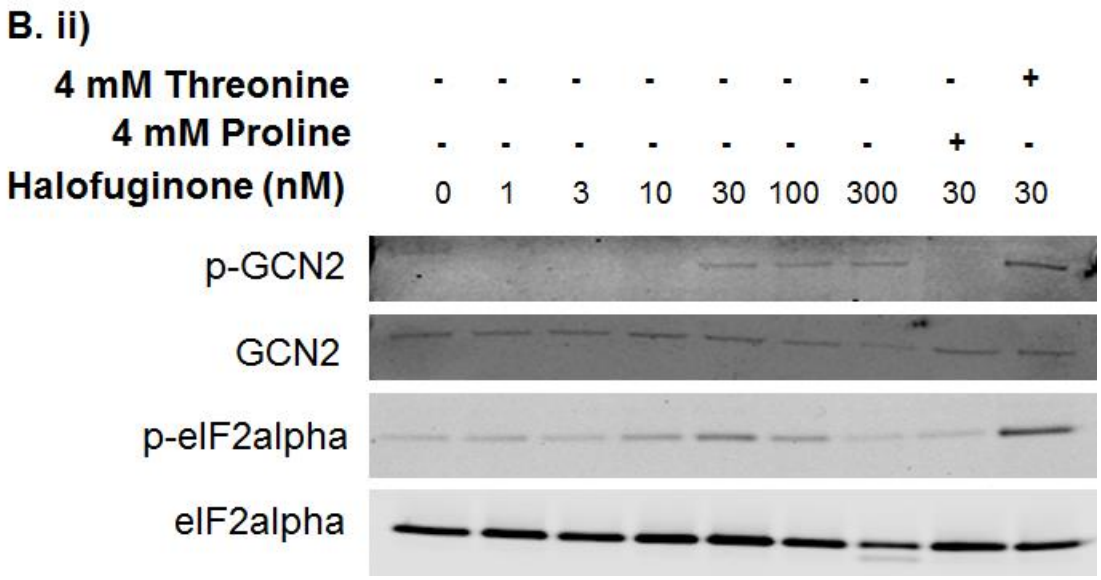

Figure 4.1 A-B. Activation of the AAR pathway and toxicity in response to halofuginone treatment in two different cardiomyocyte types.
Adenylate kinase release assay was performed on iPS cardiomyocytes (A.i) and NRVM (B.i) cells treated with increasing concentrations of halofuginone for 24 hours. The phosphorylation of GCN2 and eIF2alpha were used as readouts of the activation of the AAR pathway by halofuginone in iPS cardiomyocytes (A.ii) and NRVMs (B.ii). Samples were boiled with sample buffer and Western blotting was carried out to determine the phospho-Thr899 GCN2, total GCN2, phospho-Ser51 eIF2alpha and total eIF2alpha levels using appropriate antibodies described in the Materials and Methods section 2.23. In the case of NRVMs, proline was added to revert the activation and threonine to show actions are specific to proline tRNA synthetase.

The induction of the AAR pathway by halofuginone is confirmed by the phosphorylation of GCN2 and eIF2alpha (see Figure 4.1 A.ii and B.ii). In iPS cardiomyocytes, protein phosphorylation and gene expression of proteins involved in the AAR pathway are observed at a nontoxic dose (see Figure 4.1 and Figure 4.2), which is why we have continued our studies in this cell line. I used NRVMs to support my observations in iPS cardiomyocytes and gene expression of proteins of interest were observed at a nontoxic dose as well. There was an increase in the gene expression of the downstream components of the AAR pathway; *DDIT3, TRIB3* and *ASNS* at the optimal dose of halofuginone (30 nM) based on the toxicity and AAR pathway induction. These changes revert to basal levels upon the addition of proline but not threonine, as expected (see Figure 4.3).

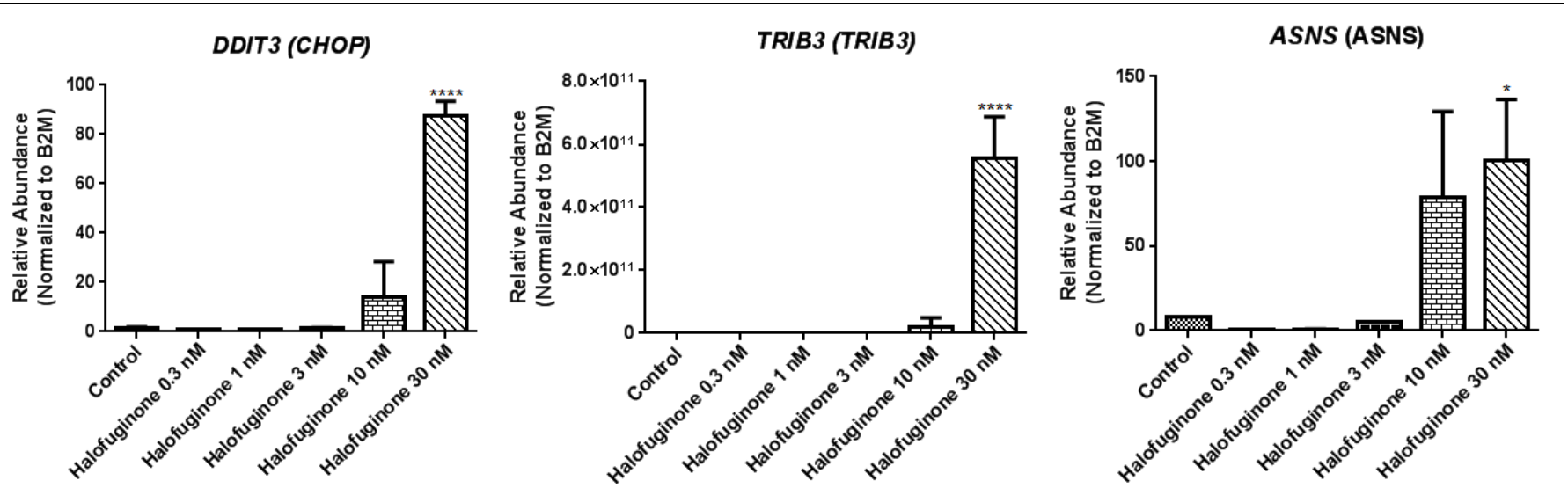

Figure 4.2 Gene expression of downstream components of the AAR pathway in response to halofuginone treatment in iPS cardiomyocytes.
Cells were treated with increasing concentrations of halofuginone for 24 hours and real time reverse transcription-PCR analysis of downstream genes *DDIT3*, *TRIB3* and *ASNS* was performed. *, $p<0.05$; ****, $p<0.0001$ ANOVA compared to control.

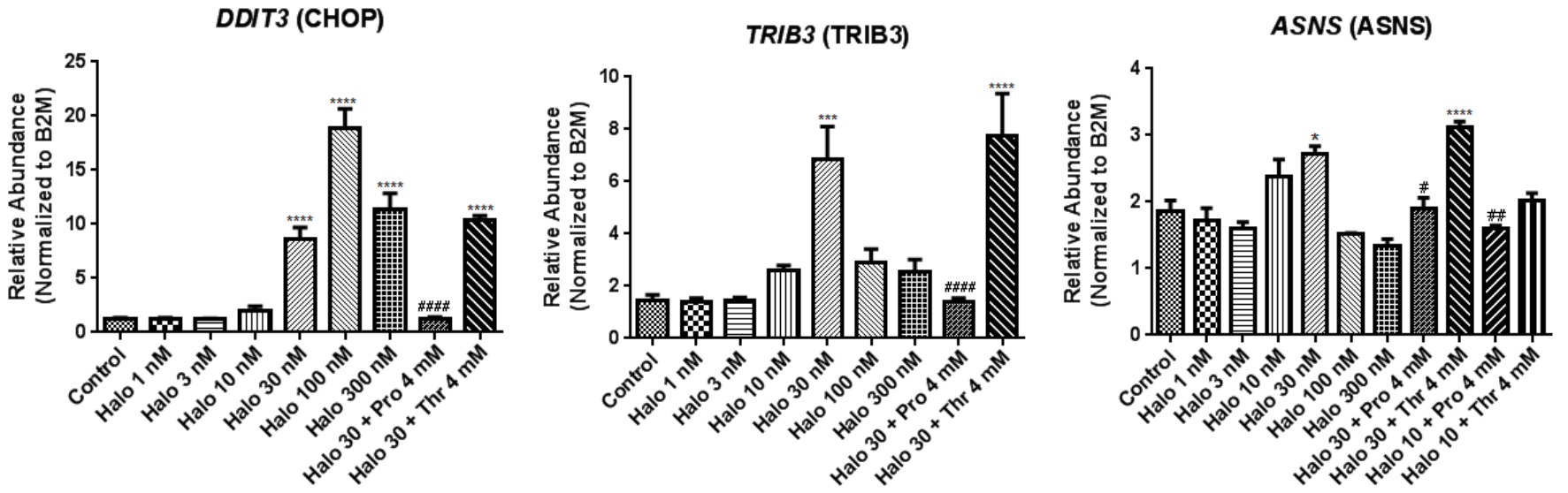

Figure 4.3 Gene expression of downstream substrates of the AAR pathway in response to halofuginone treatment in NRVMs. Cells were treated with increasing concentrations of halofuginone for 24 hours, proline was added to revert the activation and threonine to show actions are specific to proline tRNA synthetase. Real time reverse transcription-PCR analysis of downstream genes *DDIT3*, *TRIB3* and *ASNS* was performed. *, $p<0.05$; ****, $p<0.0001$ ANOVA compared to control. #, $p<0.05$; ##, $p<0.01$, ####, $p<0.0001$ ANOVA compared to without Pro/Thr.

4.2 Use of ET-1 as a stressor in cardiomyocytes

As discussed previously, ET-1 is increased in heart failure patients and this appears to correlate with an increase in hypertrophic marker levels in plasma (248). In addition, iPS cardiomyocytes are a powerful tool for scientific research, albeit they do not respond to several hypertrophic agents such as phenylephrine and angiotensin-II (unpublished in-house data at GSK), possibly due to the lack of receptors for these hormones. Fortunately, they produce the expected response to ET-1 and therefore this was used to induce hypertrophic pathways in order to determine whether halofuginone has a protective effect in cardiomyocytes. Firstly, the gene expression of several hypertrophy marker genes such as *ANP*, *BNP*, *ATP2A2*, and the ratio of *MYH7* to *MYH6* in response to 4 hour ET-1 treatment was measured.

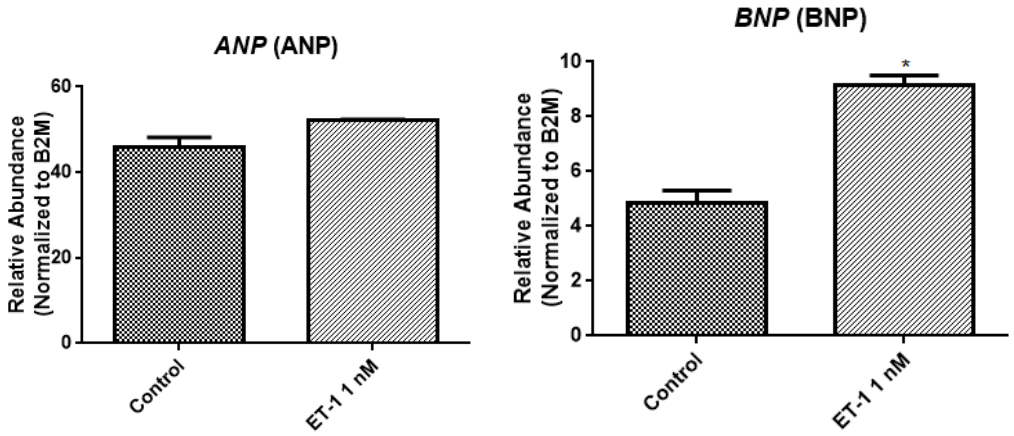

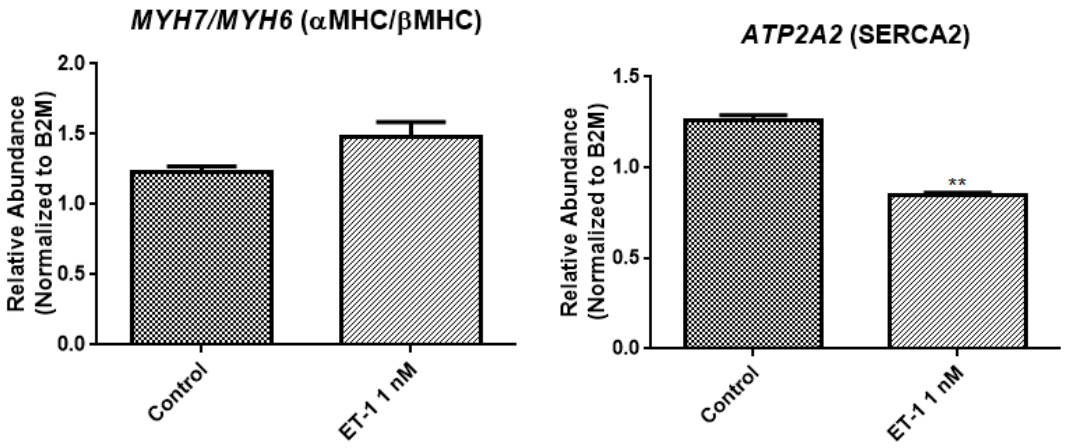

Figure 4.4 Gene expression of hypertrophic marker genes in ET-1-treated iPS cardiomyocytes.
Cells were treated with ET-1 for 4 hours and real time reverse transcription-PCR analysis of hypertrophy markers *ANP*, *BNP*, *MYH7/MYH6* and *ATP2A2* was performed. *, $p<0.05$; **, $p<0.01$ ANOVA compared to control.

The gene expression of *ANP*, *BNP* and the ratio of *MYH7* to *MYH6* increase with ET-1 treatment together with a decrease in *ATP2A2* gene expression (see Figure 4.4). However, these changes are not of the magnitudes we were hoping to observe based on past experience. This could be due to the 4 hour incubation being too short for the ET-1 treatment to have maximal effect. Therefore, the exposure time was increased from 4 hours to 24 hours. In addition, several concentrations of ET-1 were used to determine the optimal dose to trigger substantial changes in the expression of the classical marker genes. More substantial changes are needed to observe any potential influence of halofuginone exposure and to increase the statistical power of follow-on experiments.

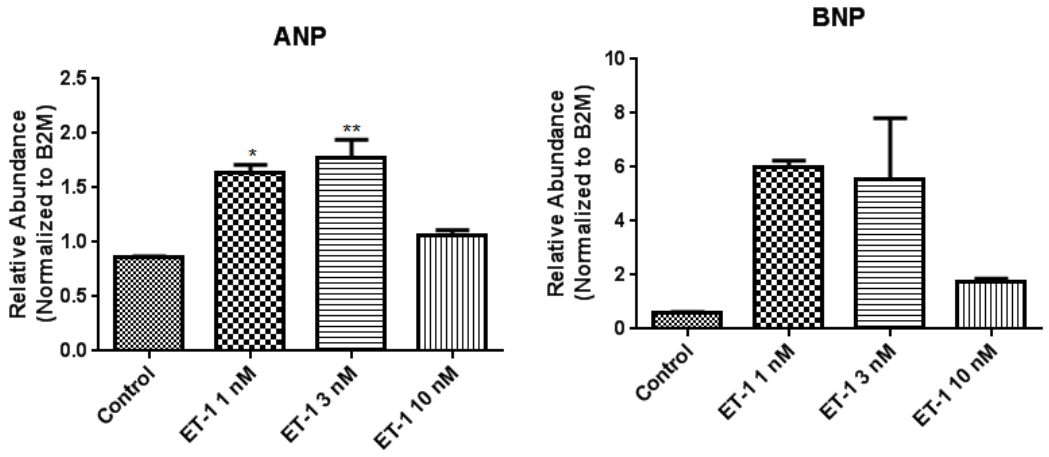

Figure 4.5 Gene expression of hypertrophic marker genes with different doses of ET-1 in iPS cardiomyocytes.
Cells treated with different ET-1 concentrations for 24 hours and real time reverse transcription-PCR analysis of hypertrophy markers *ANP, BNP, MYH7/MYH6* and *ATP2A2* was performed. *, $p<0.05$; **, $p<0.01$ ANOVA compared to control.

As discussed previously, upon an increase in ET-1 binding, ET-1 receptors are internalised with time in order to provide a negative feedback system to reduce the long-lasting effects of ET-1, which could otherwise be detrimental (238). *ANP* and *BNP* genes are increased with 1 nM ET-1 treatment in iPS cardiomyocytes, but decrease when the dose of ET-1 reaches 10 nM (see Figure 4.5), possibly due to the internalisation of receptors. Therefore, 1 nM ET-1 treatment for 24 hours appears to be the most optimal dose and incubation time to induce hypertrophic effects in iPS cardiomyocytes.

4.3 The effect of halofuginone on hypertrophy in cardiomyocytes

Having determined the optimal concentration and incubation time to induce the effects of ET-1 in cardiomyocytes as a model of hypertrophy, we have examined whether halofuginone plays a role in reducing these effects. The gene expression of hypertrophy markers *ANP*, *BNP,* and *MYH7 to MYH6* ratio were examined upon halofuginone treatment. Using ET-1 as a stressor to increase *ANP* and *BNP* levels, halofuginone

exposure decreases the gene expression of these hypertrophy markers, significantly in the case of *ANP* (see Figure 4.6).

Expression of alpha and beta myosin heavy chain (MHC-α/β – gene names *MYH6/7*) are dependent on the stage of development of the organism as well as being controlled through hormones (280, 281). Cardiac disease states affect the ratio of the two isoforms and in adult mouse heart models of heart failure, an increase in MHC-β expression is observed (282). Though MHC-β is the predominant isoform in normal adult human hearts, even a small shift in the expression patterns can affect cardiomyocyte function (283). MHC-β has been reported to have lower ATPase activity and lower filament sliding velocity and can induce cross-bridge force with lower energy use than MHC-α. It is possible that the shift in isoforms is an adaptive mechanism to maintain levels of energy (284), though this is associated with cardiac pathophysiology progression (285). Therefore, the ratio compared to basal levels is a marker of hypertrophy and was measured in this experiment. Halofuginone exposure does not alter the ratio of *MYH7/MYH6* (Figure 4.6), which is a well-established marker of hypertrophy (286).

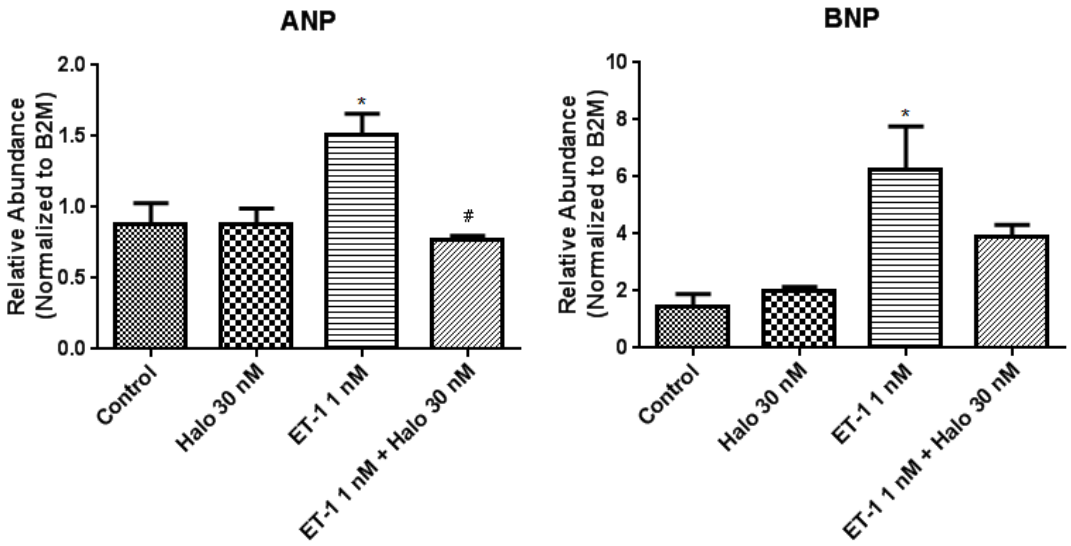

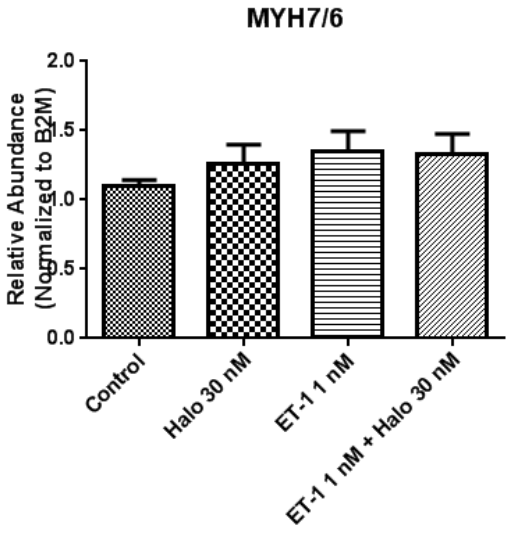

Figure 4.6 Halofuginone decreases gene expression of some hypertropy markers in cardiomyocytes.
Cells were treated with ET-1 in the presence and absence of halofuginone for 24 hours and real time reverse transcription-PCR analysis of hypertrophy markers *ANP*, *BNP* and *MYH7/MYH6* ratio was performed. *, $p<0.05$; ANOVA compared to control, #, $p<0.05$; ANOVA compared to with ET-1.

4.4 The effect of halofuginone on autophagy in cardiomyocytes

Autophagy is an essential intracellular degradation system for balancing sources of energy during development and in response to amino acid starvation. Maladaptive autophagy has been implicated in cardiac hypertrophy and an increase in autophagy has previously been linked to cardio-protection in the heart (287, 288). The eIF2alpha kinase, GCN2, is the ‘starvation-sensor‘ of the cell and is important in initiating the amino acid response (AAR) pathway to modulate amino acid metabolism for adaptation when one or more amino acids become limiting. I have investigated whether mimicking this system would improve autophagy.

In previous studies, we have observed halofuginone to inhibit fibrosis in cardiac fibroblasts and improve several aspects of pressure-induced cardiac hypertrophy in mice (unpublished data). As autophagy plays a major role in pathogenesis of cardiomyopathies, I have investigated whether halofuginone has an effect on autophagy.

4.4.1 Gene expression of the autophagy related genes *ULK1, ULK2, GABARAPL1,* and *MAP1LC3B* after halofuginone exposure

In order to investigate whether the GCN2 pathway plays a role in autophagy, iPS cardiomyocytes were treated with ET-1 in presence and absence of halofuginone. Halofuginone treatment significantly increases the gene expression of autophagy markers, *ULK1, ULK2, GABARAPL1* and *MAP1LC3B* (see Figure 4.7). *BECN1* gene expression is not altered significantly, though there appears to be a trend with halofuginone addition to ET-1 increasing *BECN1* mRNA compared to ET-1 alone.

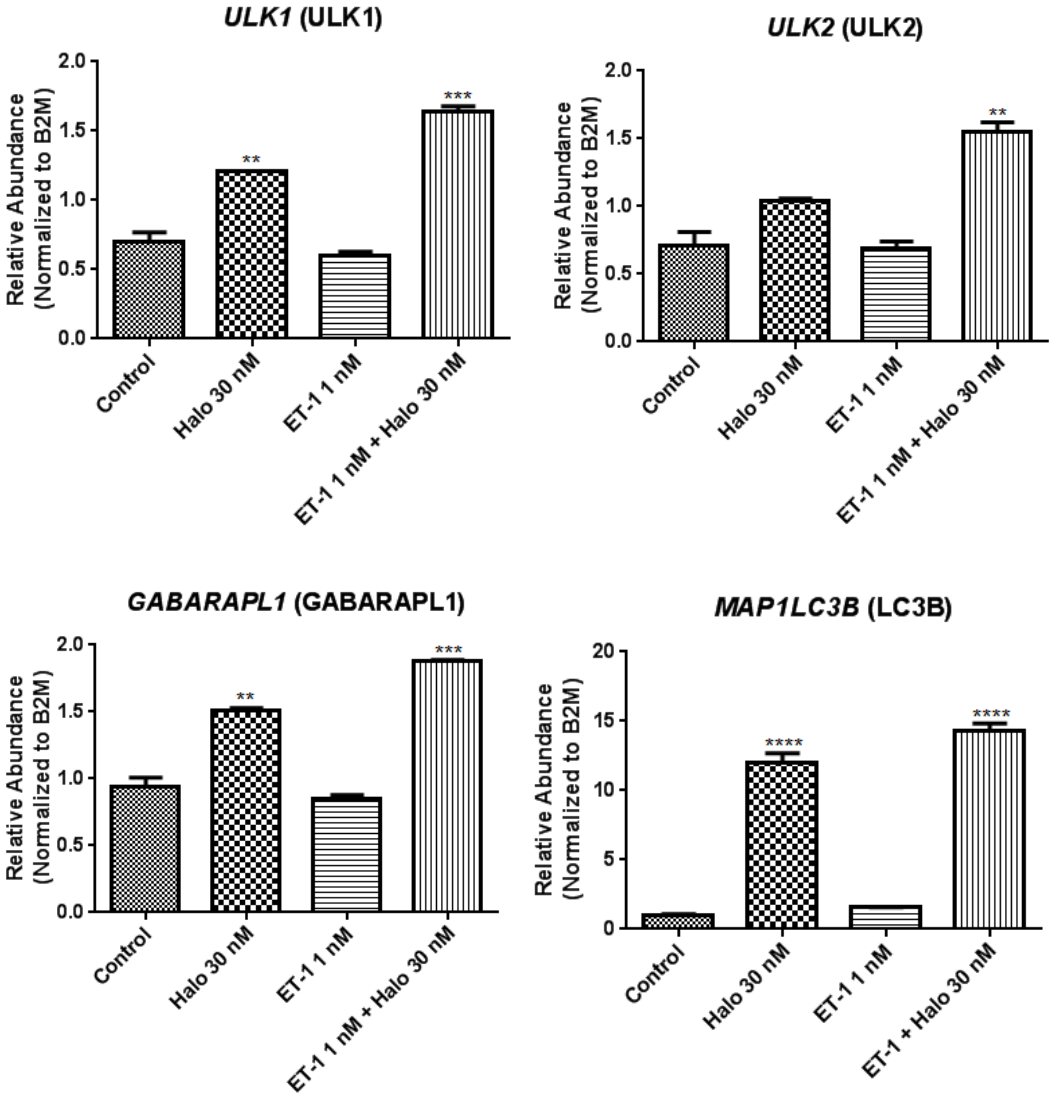

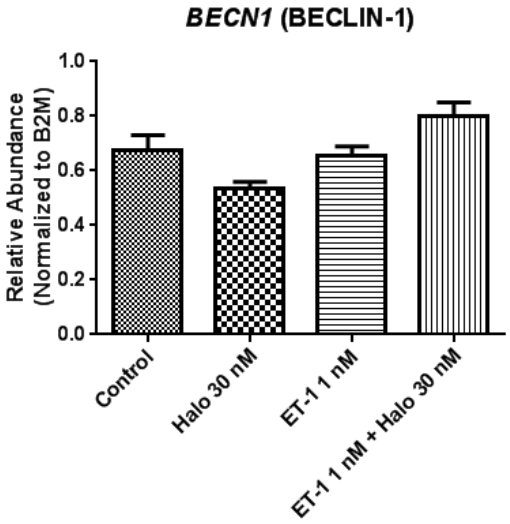

Figure 4.7 Halofuginone increases gene expression of autophagy markers in cardiomyocytes.
Cells were treated with ET-1 in the presence and absence of halofuginone for 24 hours and real time reverse transcription-PCR analysis of autophagy markers *ULK1*, *ULK2*, *GABARAPL1*, *MAP1LC3B* and *BECN1* was performed. **, $p<0.01$; ***, $p<0.001$ ANOVA.

4.4.2 Protein levels of p62 decrease with halofuginone

p62 protein, also referred to as sequestosome 1 (SQSTM1) is a ubiquitin-binding scaffold protein, which recruits ubiquitinated proteins to the autophagosomes in the cell for degradation (see Figure 4.8). p62 binds directly to Atg8 family members, LC3 and GABARAPL1 that are involved in autophagosome formation, and p62 itself is degraded through autophagy. Therefore, p62 can be used to measure the level of autophagy within cells, with levels of p62 negatively correlating with autophagy, i.e. less p62 protein means more autophagy (289, 290).

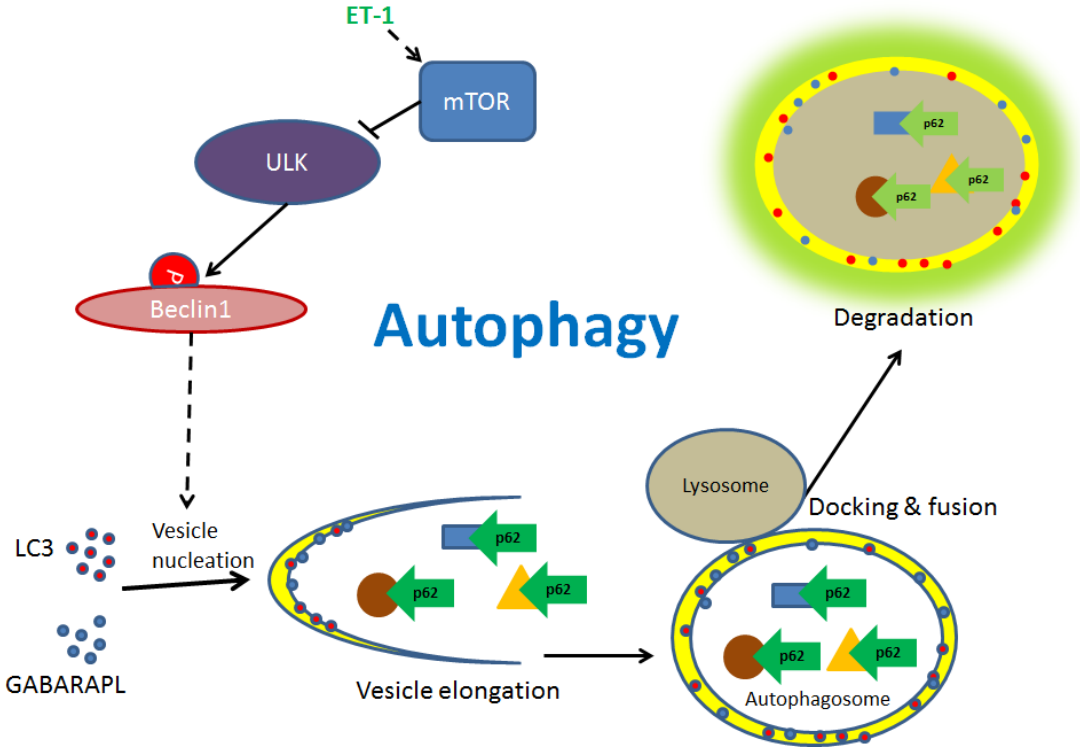

Figure 4.8 Schematic showing the process of autophagy within cells.
ET-1 is known to activate mTOR which in turn is known to phosphorylate ULK1/2 and inhibit autophagy when there is sufficient supply of energy and nutrients within the cell. Otherwise, ULK1/2 is involved in inducing autophagy by phosphorylating its substrate Beclin1, which leads to the formation of autophagosomes by inducing vesicle nucleation by LC3 and GABARAPL proteins. p62 recruits proteins to be degraded into the autophagosome and upon docking and fusion of lysosomes, it is degraded in the process.

Changes in p62 protein levels suggest that, ET-1 treatment decreases autophagy and this is reversed back to basal levels upon addition of halofuginone (see Figure 4.9).

Therefore, in support of gene expression data, halofuginone increases autophagy in iPS cardiomyocytes.

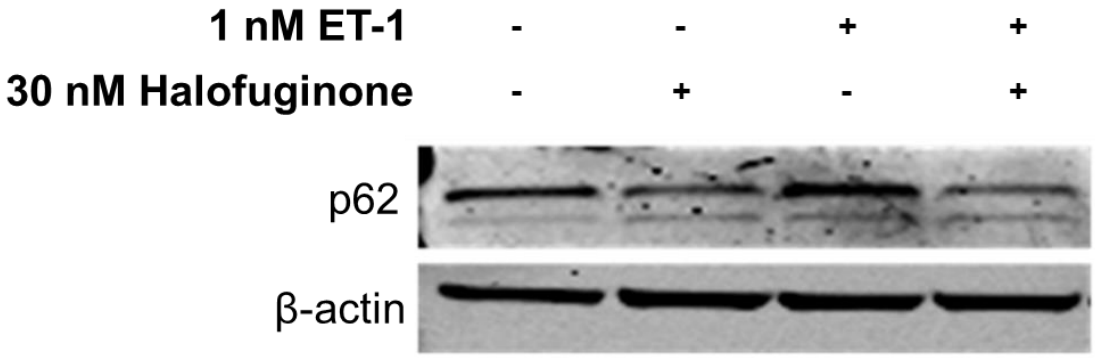

Figure 4.9 Halofuginone reverses ET-1 induced increase in p62 protein levels in cardiomyocytes.
Cells were treated with ET-1 in the presence and absence of halofuginone for 24 hours and protein levels of p62 were observed by Western blot analysis.

4.4.3 Punctate localisation of LC3A/B is induced by halofuginone

LC3 is a major component of autophagosomes and critical to the process of autophagy. There are three isoforms A, B and C and all are post-translationally modified during autophagy. LC3 is cleaved at its carboxy terminus leading to the formation of LC3-I, which is in turn conjugated to phosphatidylethnolamine by a ubiquitin-like system involving Atg7 and Atg3. Following this conjugation, the LC3-II, autophagic vesicles are formed, acquiring a punctate localisation within the cell. Following our data on gene expression and protein expression of autophagy markers inferring that halofuginone may enhance autophagy, I have attempted to verify this further by investigating immunofluorescence of LC3 assessing the presence of autophagosomes.

It appears that upon addition of halofuginone to ET-1 treated cardiomyocytes, the amount of LC3A/B staining is increased in comparison to control (see Figure 4.10) verifying our data that halofuginone does increase autophagy. Chloroquine raises the lysosomal pH and is therefore an inhibitor of the lysosomal enzymes, which require an acidic pH, preventing the fusion of lysosomes with the autophagosomes leading to build-up of autophagosomes along with their contents within the cell. Chloroquine was

used as a positive control in our LC3A/B staining experiment to give us an insight into what to expect in the presence of autophagosomes.

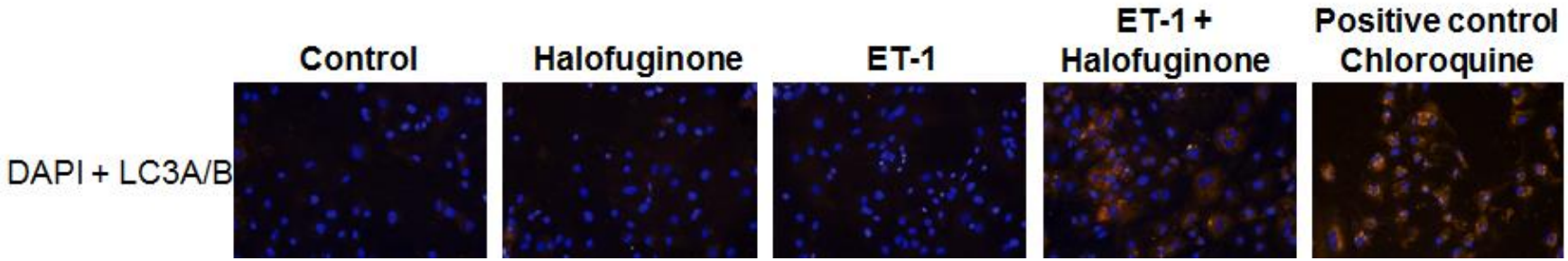

Figure 4.10 Immunofluorescence of LC3A/B protein upon halofuginone treatment.
iPS cardiomyocytes have been treated with 1 nM ET-1 and 30 nM halofuginone for 24 hours and stained for LC3A/B (red). 25 µM chloroquine has been used as a positive control. Cells were fixed and permeabilised as described in the Materials and Methods section 2.14. LC3A/B was detected using appropriate antibodies shown in the Materials and Methods section 2.23

4.5 p38 activation by halofuginone and its downstream effects

4.5.1 Halofuginone-mediated p38 activation mechanism in cardiomyocytes

The effect of halofuginone on p38 activity in cardiac cells has not been previously investigated. Therefore, I was interested to explore activity of p38 in the halofuginone-treated iPS cardiomyocytes. Surprisingly, halofuginone induces p38 phosphorylation and activity and this is reversed with addition of proline but not threonine suggesting that the effects of halofuginone on p38 are specific (see Figure 4.11).

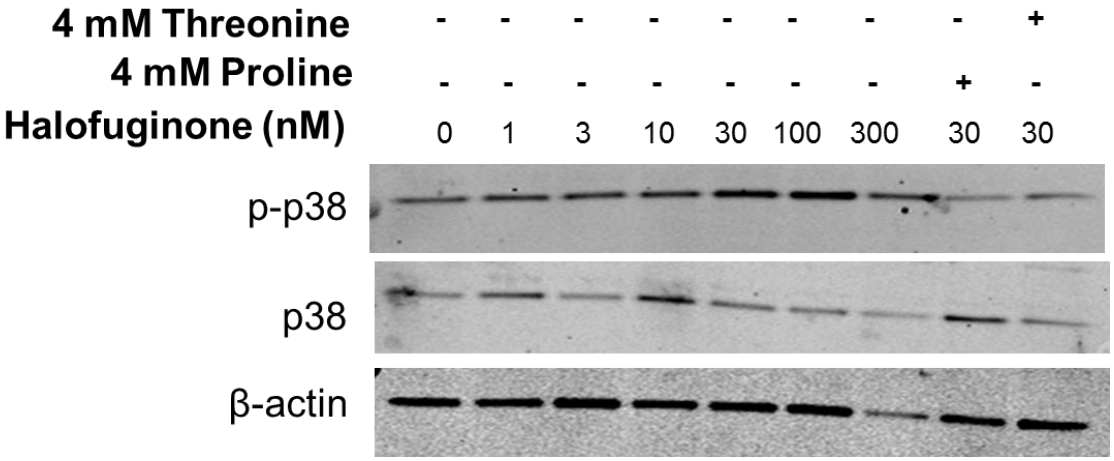

Figure 4.11 Western blot anaysis of p38 phosphorylation as a dose-response in halofuginone-treated NRVMs.
Cells were treated with increasing concentrations of halofuginone for 24 hours and samples were boiled with sample buffer and Western blotting was carried out to determine the phospho- Thr180/Tyr182 p38 and total p38 levels using appropriate antibodies described in the Materials and Methods section 2.23

p38 can be phosphorylated by its upstream kinases MKK3/6 or by autophosphorylation depending on the stimulus. In order to find out which pathway is involved in halofuginone-induced p38 activation, I have used SB239063 to block the kinase activity of p38 and therefore its autophosphorylation. Surprisingly, SB239063 increases the phosphorylation of p38 further (see Figure 4.12). The paradoxical enhancement of phospho-kinase signal when the kinase itself is inhibited has been previously shown with several kinases. The underlying hypothesis is linked to the ATP-binding region

being occupied by the inhibitors leading to intramolecular interactions that restrict phosphatase access and sustaining the phosphorylation rather than enhancement of upstream activators to compensate for kinase inhibition through a feedback loop (291, 292).

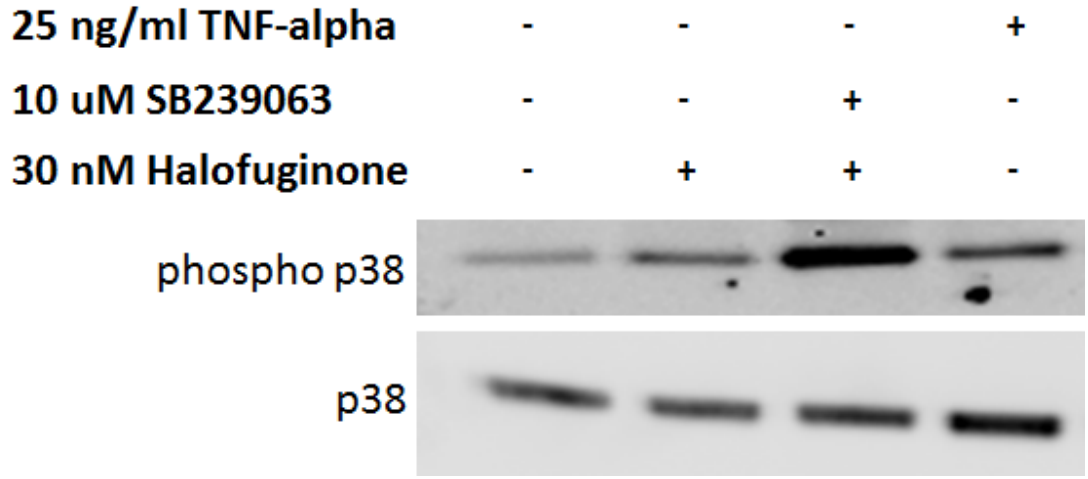

Figure 4.12 Halofuginone increases p38 phosphorylation and halofuginone-induced p38 activity is SB-sensitive.
iPS cardiomyocytes were treated with halofuginone in the presence and absence of SB239063, and TNF-alpha as positive control for 24 hours. Samples were boiled with sample buffer and Western blotting was carried out to determine the phospho-Thr180/Tyr182 p38 and total p38 levels using appropriate antibodies described in the Materials and Methods section 2.23.

4.5.2 Halofuginone-mediated p38 activation in HEK293 cells overexpressing TAK1

Since I was unable to determine whether p38 activation by halofuginone was through the canonical pathway or via TAB1, due to the inhibitor-related phenomenon mentioned previously, I decided to have a look at the activity of the members of the canonical p38 activation pathway, such as TAK1 and MKK3. However, due to a combination of very low abundance of these proteins and antibody challenges, I was not able to detect analysable signals in this case. Therefore, subsequent studies were performed in HEK293 cells, which can easily be transfected with vectors for these proteins to yield

an adequate signal to analyse the phosphorylation states. First, I determined the lowest concentration of halofuginone to induce the AAR pathway using phospho-GCN2 levels as the readout (see Figure 4.13).

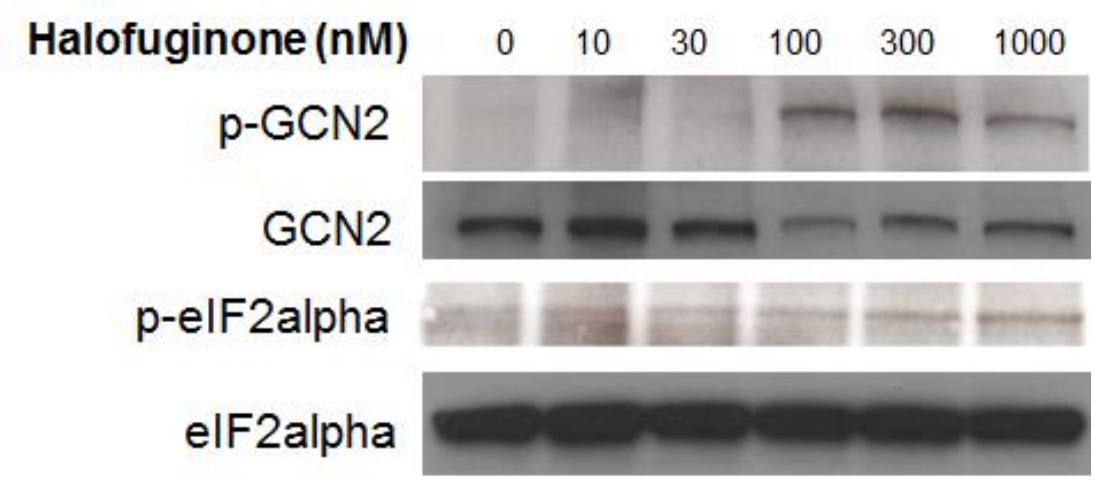

Figure 4.13 Activation of the AAR pathway in response to halofuginone treatment in HEK293 cells.
Cells were treated with increasing concentrations of halofuginone for 24 hours. The phosphorylation of GCN2 and eIF2alpha were used as readouts of the activation of the AAR pathway by halofuginone. Samples were boiled with sample buffer and Western blotting was carried out to determine the phospho-Thr899 GCN2 and phospho-Ser51 eIF2alpha levels using appropriate antibodies described in the Materials and Methods section 2.23.

Following this, TAK1 overexpression and a TAK1 inhibitor, 5Z-7-oxozeaenol, were used to examine whether p38 activation mediated by halofuginone is via the canonical pathway. As expected halofuginone and borrelidin increase p38 phosphorylation (see Figure 4.14). This increase in p38 phosphorylation is augmented in TAK1-transfected cells, possibly due to a synergistic effect of TAK1 and halofuginone on p38 activation. Nonetheless, in these transfected cells, proline is unable to block the halofuginone-mediated increase in phosphorylation, potentially due to the presence of TAK1 maintaining p38 phosphorylation in the absence of halofuginone. p38 phosphorylation increases in response to the other AAR activator, Thr-tRNA synthetase inhibitor; borrelidin. As observed with halofuginone, there is a further increase in TAK1-transfected cells after borrelidin treatment inferring a synergistic effect.

Besides their role in p38 phosphorylation, both halofuginone and borrelidin increase phosphorylation of TAK1. 5Z-7-oxozeaenol treatment blocks halofuginone and borrelidin-mediated TAK1 and p38 phosphorylation.

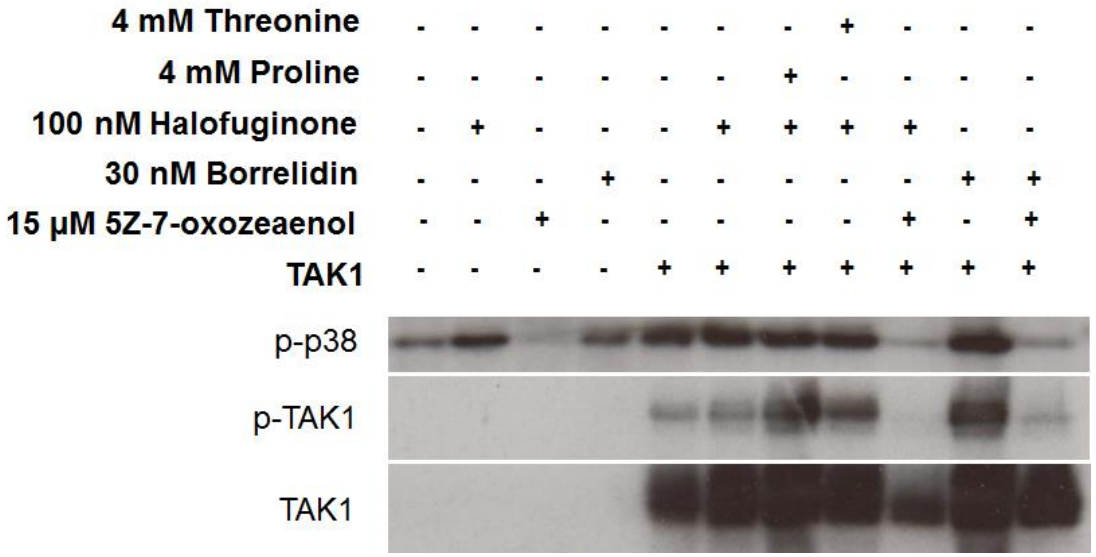

Figure 4.14 TAK1 overexpression in HEK293 cells to examine the canonical p38 activation pathway by halofuginone.
Cells were transfected as described in the Materials and Methods section 2.9. 24 hours after transfection, cells were treated with halofuginone, borrelidin, 5Z-7-oxozeaenol and proline/threonine as above. Cells were incubated for 24 hours, after which cell lysates were obtained, samples were boiled with sample buffer and Western blotting was carried out to determine phospho-Thr180/Tyr182 p38, phospho-Thr184/Thr187 TAK1 and total TAK1 levels were determined using appropriate antibodies described in the Materials and Methods section 2.23.

4.5.3 Downstream activity of p38 activated by halofuginone treatment

Furthermore, I wanted to investigate whether the halofuginone-induced phosphorylation of p38 correlates with increased activity. MAPKAPK-2 (MK2) is a well-known substrate of p38 and its phosphorylation was used as a measure of p38 activity. Halofuginone induces MK2 phosphorylation in an SB-dependent manner suggesting that this induction is through p38 activity (see Figure 4.15).

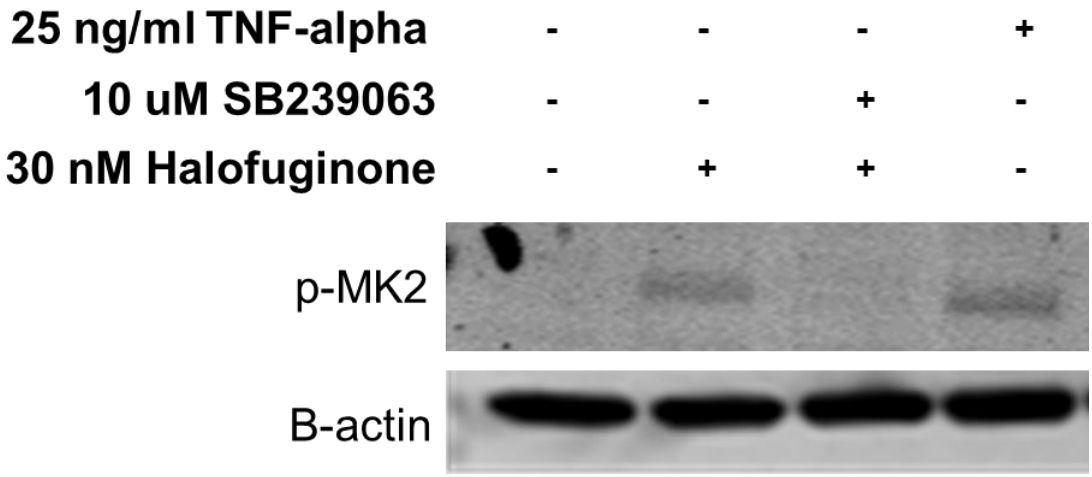

Figure 4.15 Halofuginone increases p38 activity in an SB-sensitive manner. iPS cardiomyocytes were treated with halofuginone in the presence and absence of SB239063, and TNF-alpha as positive control for 24 hours. Samples were boiled with sample buffer and Western blotting was carried out to determine the phospho-Thr334 MK2 and B-actin levels using appropriate antibodies described in the Materials and Methods section 2.23.

4.5.4 Negative regulation of the AAR pathway through p38 activity

AAR pathway has been previously shown to induce the expression of CHOP (182, 293) in support of the observations in our studies in halofuginone-induced cardiomyocytes. p38 augments the activity of CHOP as a transcription factor by phosphorylating it on two adjacent serine residues (78 and 81) (294). However, it has not yet been demonstrated whether p38 regulates CHOP at a transcriptional level. As halofuginone increases CHOP transcription and activates p38, I tested the hypothesis that p38 plays a role in the induction of CHOP transcription by halofuginone. Halofuginone-induced CHOP gene expression does not appear to be SB-sensitive, therefore does not occur through p38 activity (see Figure 4.16 and p. 155).

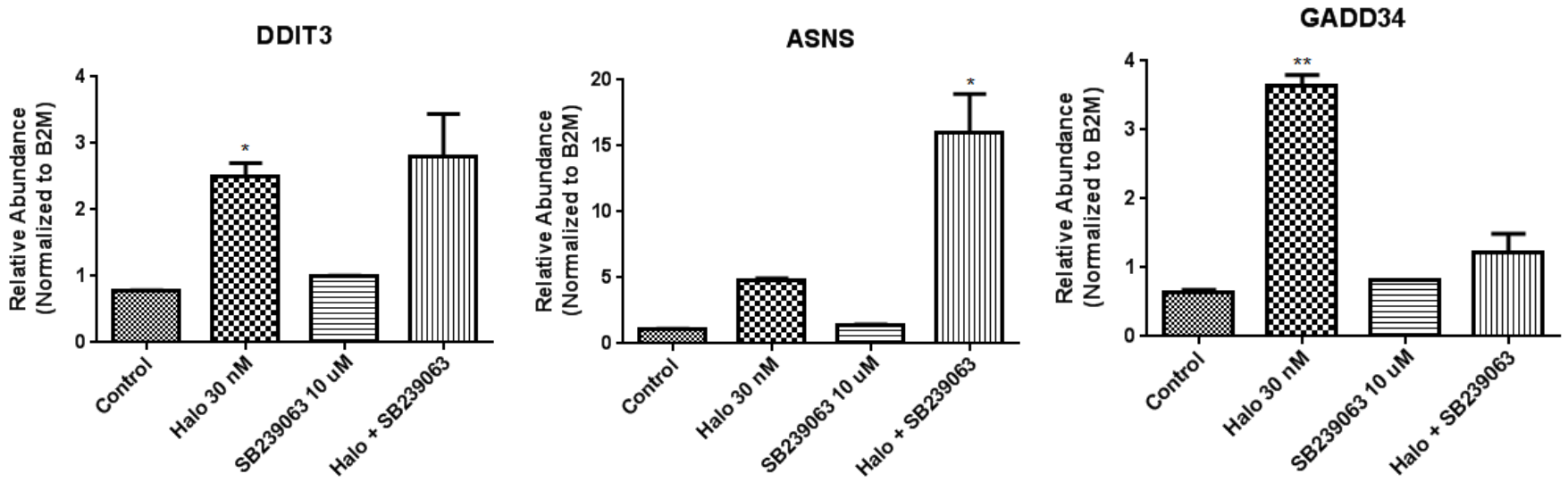

Figure 4.16 The effect of SB239063 on the gene expression of *Ddit3, Asns* and *Gadd34* in halofuginone-treated iPS cardiomyocytes. Cells were treated with halofuginone in the presence and absence of SB239063 for 24 hours and real time reverse transcription-PCR analysis of *Ddit3, Asns* and *Gadd34* was performed. *, $p<0.05$; **, $p<0.01$; ***, $p<0.001$ ANOVA compared to control.

It would have been interesting to examine the phosphorylation state of the CHOP residues regulated by p38 upon halofuginone and SB treatment. Unfortunately, as of yet there are no antibodies recognising these sites in CHOP. Therefore, downstream targets of CHOP-regulated transcription, growth arrest and DNA damage-inducible protein 34 (GADD34 - gene name *PPP1R15A)* and *ASNS* were observed as readouts of CHOP activity and to determine SB-sensitivity. *Asns* gene expression is known to increase in response to amino acid limitation (293), and interestingly CHOP has been shown to suppress *ASNS* gene expression (188). I have seen that both CHOP (*DDIT3*) and *ASNS* increase upon halofuginone treatment. Upon SB239063 addition to halofuginone-treated cardiomyocytes, the gene expression of *ASNS* induced by halofuginone increases further (see Figure 4.16). This suggests that the p38-induced enhancement of CHOP activity negatively regulates and dampens halofuginone-induced *ASNS* gene expression. GADD34 recruits the serine/threonine phosphatase, PP1, to dephosphorylate eIF2alpha in order to reverse the halt in protein translation caused by stress-induced kinases upstream of eIF2alpha such as GCN2. Previous studies have shown that GADD34 *(PPP1R15A)* gene expression is regulated by p38 and CHOP (295, 296) though in different contexts. I have used SB to test our hypothesis that the negative regulation of the amino acid response pathway is via p38-induced CHOP activity. The increase in *PPP1R15A* gene expression by halofuginone is SB-sensitive and thus via p38 activity, possibly through enhancing CHOP activity by phosphorylation (see Figure 4.16).

4.5.5 The effect of halofuginone on the inflammation response in cardiomyocytes

Halofuginone is known to be a potent anti-inflammatory agent and has previously been associated with inhibition of p38 in activated T-cells (225). As p38 has previously been associated with inflammation and interestingly halofuginone, an anti-inflammatory

agent, activates p38; I decided to look at some downstream substrates previously associated with p38 in inflammation. In iPS cardiomyocytes, these were cyclooxygenase-2 (gene *PTGS2*), IL-1 receptor (*IL1R1*), IL-6 (*IL6*), and IL-1 receptor antagonist (*IL1RN*). *PTGS2* and *IL6* gene expression increase significantly upon halofuginone treatment (see Figure 4.17). The results were variable for *IL1R1* and *IL1RN*, but halofuginone on its own appears to reduce both of these genes.

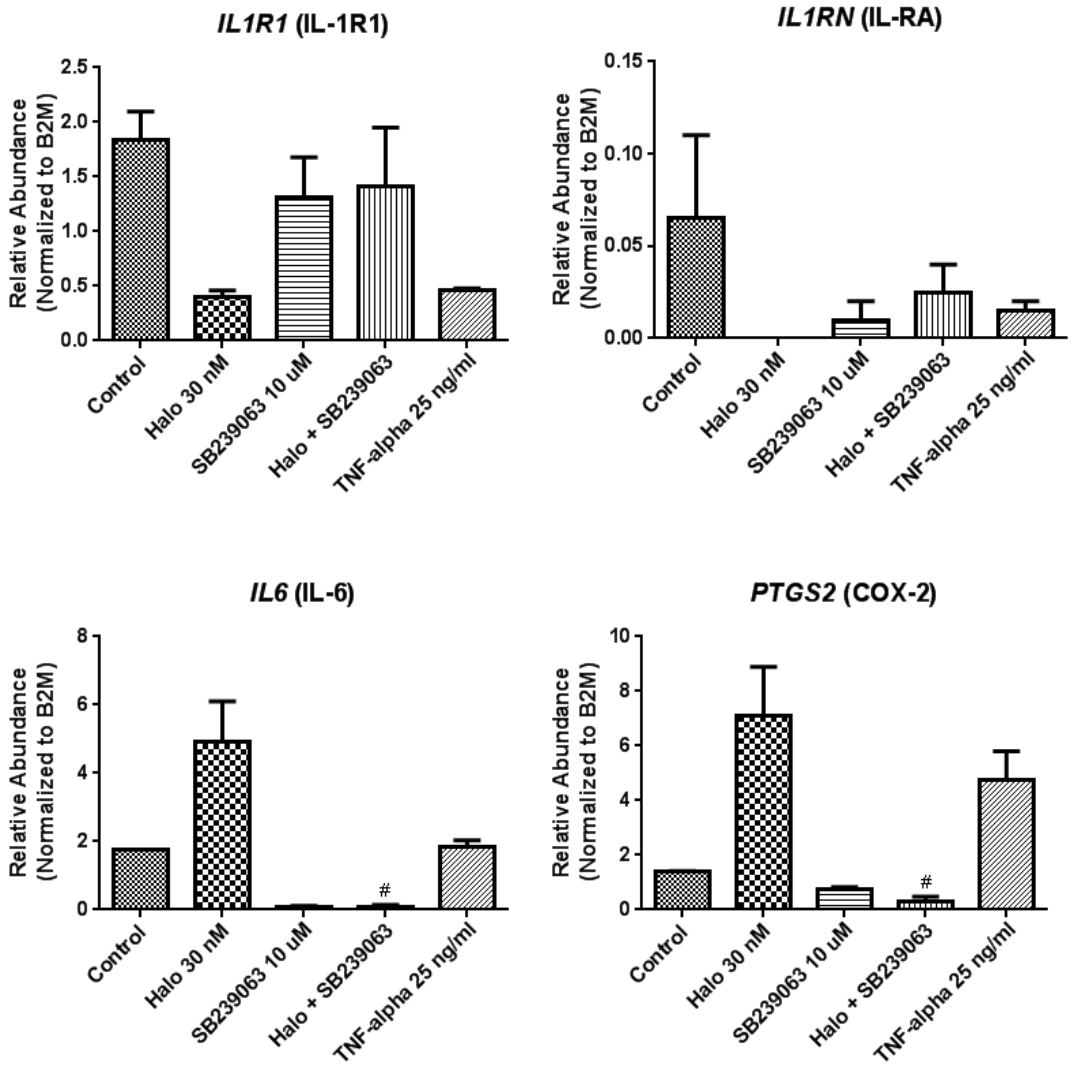

Figure 4.17 Gene expression of inflammation-related genes in halofuginone-treated iPS cardiomyocytes.
Cells were treated with ET-1 in the presence and absence of halofuginone for 24 hours and real time reverse transcription-PCR analysis of *IL1R1*, *IL1RN*, *IL6* and *PTGS2* was performed. *, $p<0.05$; **, $p<0.01$; ***, $p<0.001$ ANOVA compared to control.

4.6 Characterising lentiviral vectors for overexpression of constitutively active GCN2, WT GCN2 and shRNA against GCN2

The hypothesis of this project is that halofuginone activates several responses through GCN2. Nonetheless, from our previous studies I have seen that halofuginone has many off-target effects. Therefore, in order to ensure that the effects I see are through the AAR pathway, I have utilised lentiviral vectors in order to knock down and overexpress GCN2. Below is the list of lentiviral vectors that I have used:

Table 4.1 Lentiviral vectors used to transduce iPS cardiomyocytes for overexpression and knock down of GCN2

Sample ID	Sample	Comments
GCN2 2X	pLex GCN2	Overexpression vector for WT-GCN2
B.	SHC201 TRC2 pLKO.5-puro Empty Vector Control	Empty vector
pLex GFP	pLex GFP	GFP control vector for the overexpression vectors
#1	TRCN0000300850	shRNA #1
#2	TRCN0000300851	shRNA #2
#3	TRCN0000304216	shRNA #3 – problems cloning
#4	TRCN0000304149	shRNA #4
#5	TRCN0000304214	shRNA #5
GCN2 S808G	pLex GCN2 S808G	Overexpression vector for constitutively active GCN2 #1
GCN2 F855L	pLex GCN2 F855L	Overexpression vector for constitutively active GCN2 #2

Firstly, I have used four of the five shRNAs, as shRNA #3 had extremely low titre, the producer group did not recommend using it. In order to test the optimal virus:media ratio to transduce the cells with, without causing toxicity; I have designed an experiment using three different percentages of the virus and looking at GCN2 (gene name EIF2AK4) mRNA levels. 25% virus gave a good gene expression increase (with the overexpression vector)/knockdown (with the shRNA vectors) to virus percentage

ratio; therefore I went ahead with further experiments using this percentage of virus. From the four shRNA vectors, shRNAs 1 and 2 gave the best level of knockdown (see Figure 4.18), therefore I have used these two vectors in future experiments.

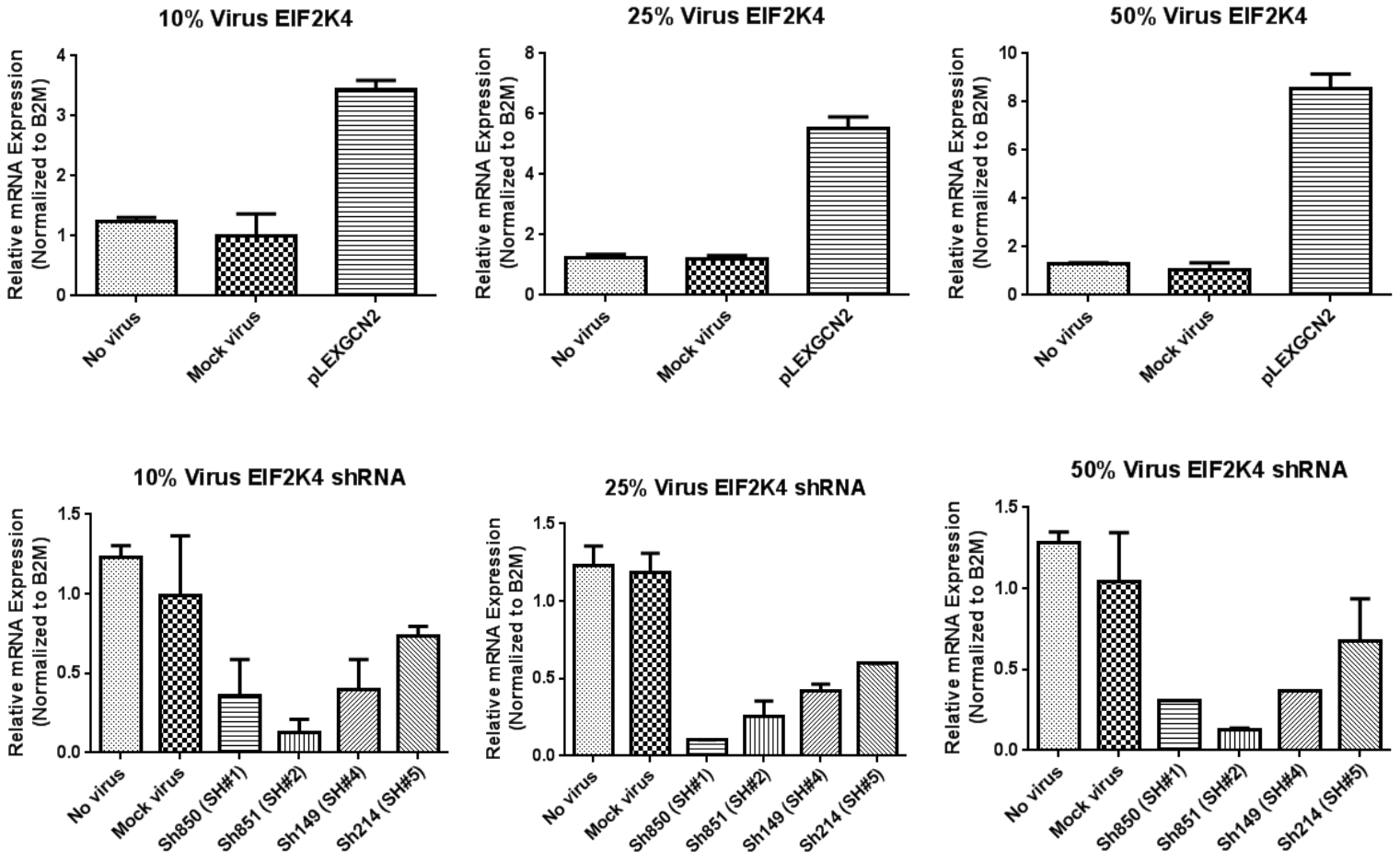

Figure 4.18 Characterising the lentiviral vectors and exploring different percentages of virus for optimal transduction of iPS cardiomyocytes.

Cells were transduced with lentiviral vectors; pLexGCN2, SHC201 TRC2 pLKO.5-puro empty vector control and the shRNA vectors TRCN0000300850, TRCN0000300851, TRCN0000304149 and TRCN0000304214 as described in Materials and Methods section 2.20. 10%, 25% and 50% of lentiviral vectors in maintenance media have been used to determine optimal transduction percentages. Real time

reverse transcription-PCR analysis of EIF2AK4 determined mRNA levels and the overexpression and knock down efficiencies of the vectors.

4.7 Using lentiviral vectors to explore the off-target effects of halofuginone

In order to ensure that GCN2 was successfully overexpressed and knocked down depending on the vector used, I checked the mRNA levels of GCN2. It appeared that mRNA levels of GCN2 increase with the overexpression vectors, pLEXGCN2 for WT GCN2, pLEXGCN2 F855L for constitutively active GCN2 and decrease with the shRNA vectors, Sh850 and Sh851, as expected. GCN2 mRNA levels increase further with halofuginone treatment when the vector pLEXGCN2 is used (see Figure 4.19). However, using the overexpression vector for constitutively active mutant GCN2; pLEXGCN2 S808G, transduction does not seem to have worked as there is no increase in the mRNA levels of GCN2.

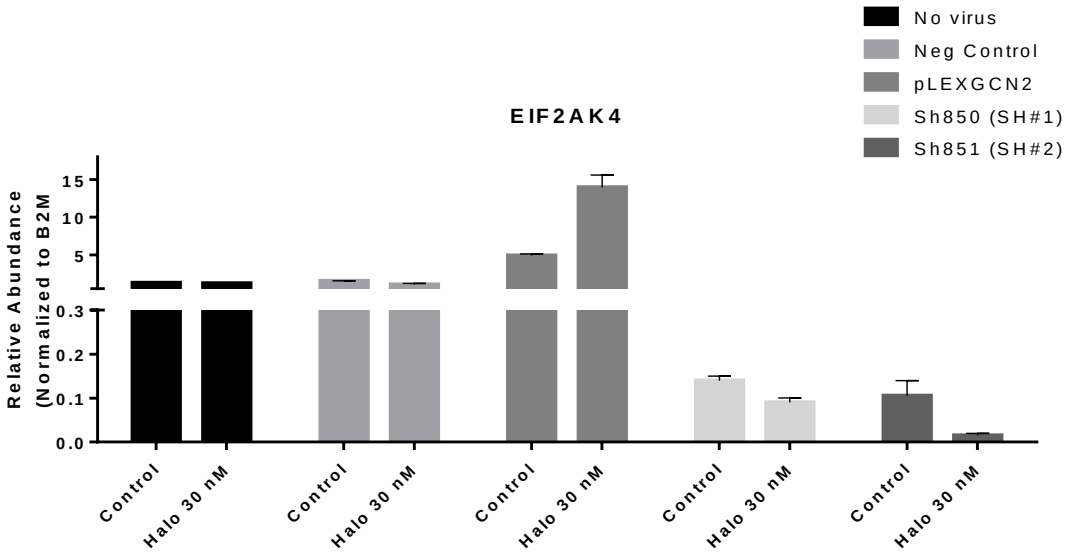

Figure 4.19 Confirming the overexpression and knock down of GCN2 mRNA using lentiviral vectors in halofuginone-treated iPS cardiomyocytes.
Cells were transduced with lentiviral vectors, pLexGCN2 and shRNA vectors TRCN0000300850 and TRCN0000300851, as described in Materials and Methods section 2.20. The cells were treated with halofuginone for 24 hours and real time reverse transcription-PCR analysis of EIF2AK4 was performed.

To confirm that the knockdown and overexpression were successful, protein levels of total GCN2 were evaluated. These results support the observations in mRNA levels,

with an increase in total GCN2 levels with the overexpression vectors, pLEXGCN2 and pLEXGCN2 F855L and a decrease with the shRNA vectors (see Figure 4.20). As with the mRNA levels, there is no increase in GCN2 protein with the pLEXGCN2 S808G mutant suggesting that transduction has not worked.

Once the overexpression and knockdown were successful, the effect on the downstream substrates in the AAR pathway were explored. Our hypothesis was that the effects of halofuginone would be amplified with overexpression, and diminished or reduced with shRNA. Observing the phosphorylation state of eIF2alpha, it is clear that the phosphorylation level of GCN2 is not reflected by eIF2alpha phosphorylation. Even after knocking down GCN2, eIF2alpha is phosphorylated upon halofuginone addition (see Figure 4.20). eIF2alpha is phosphorylated in the presence of the F855L mutant despite an absence of halofuginone, though adding halofuginone to these cells reveals an further increase in eIF2alpha phosphorylation, possibly due to the additive effect of endogenous GCN2 ativating eIF2alpha as well.

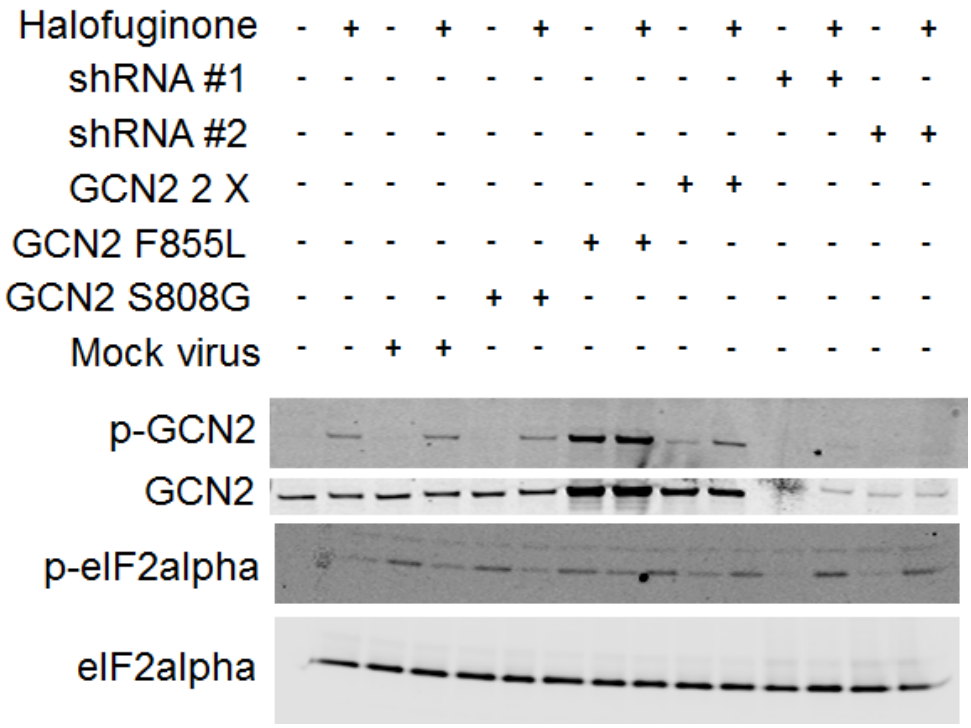

Figure 4.20 Halofuginone induces eIF2alpha phosphorylation regardless of GCN2 overexpression/knock down.

Cells were transduced with lentiviral vectors; pLexGCN2 and shRNA vectors TRCN0000300850 and TRCN0000300851, as described in Materials and Methods section 2.20. The cells were treated with halofuginone for 24 hours. Samples were boiled with sample buffer and Western blotting was carried out to determine the phospho-Thr899 GCN2, total GCN2, phospho-Ser51 eIF2alpha and total eIF2alpha levels using appropriate antibodies shown in the Materials and Methods section 2.23.

In addition, observing the mRNA levels of DDIT3, it appears that whether or not GCN2 is overexpressed or knocked down, the increase in DDIT3 mRNA levels stays the same (see Figure 4.21). In the case of knockdown, this could be due to the small amount of GCN2 present being sufficient to induce this response. Alternatively, it could be a compensation mechanism by the other kinases upstream of eIF2alpha. In the case of overexpression, it is possible that increasing GCN2 levels further does not have an effect, as the small amount of GCN2 is enough to elicit the response observed with basal levels of GCN2.

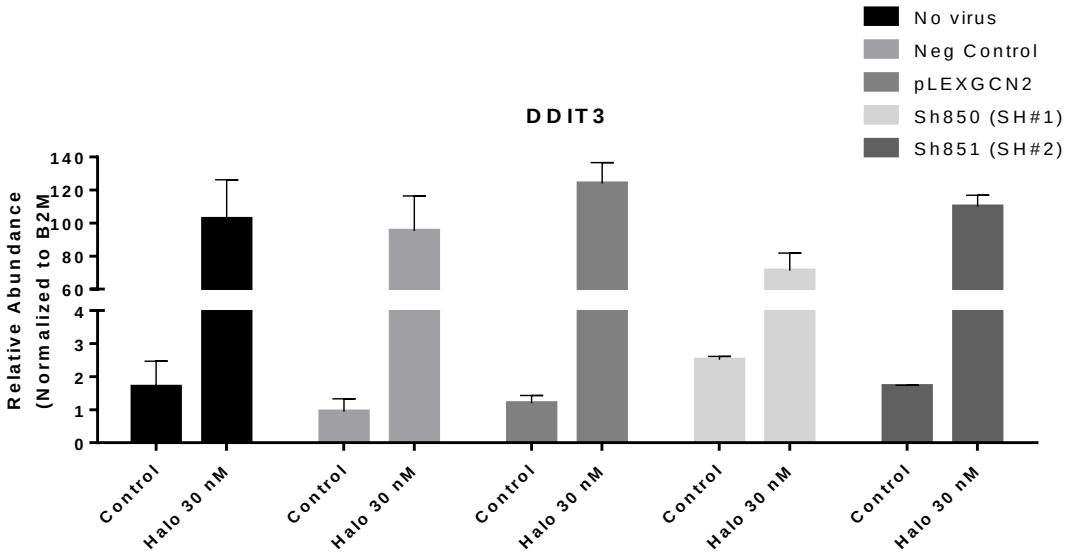

Figure 4.21 Halofuginone induces DDIT3 gene expression regardless of GCN2 overexpression/knock down.
iPS cardiomyocytes were transduced with lentiviral vectors; pLexGCN2 and shRNA vectors TRCN0000300850 and TRCN0000300851, as described in Materials and Methods section 2.20. The cells were treated with halofuginone for 24 hours and real time reverse transcription-PCR analysis of DDIT3 was performed.

As previously shown p38 is phosphorylated by halofuginone treatment and it would be interesting to explore the mechanism through which this happens. In order to investigate

whether this effect of halofuginone is GCN2-dependent, I have looked at cells transduced with the constitutively active mutant pLEXGCN2 F855L, and whether p38 was activated in these cells in the absence and presence of halofuginone. It appears that p38 is not active unless halofuginone is present, regardless of GCN2 phosphorylation state (see Figure 4.22). Therefore, it is possible that p38 is activated by a GCN2-independent mechanism.

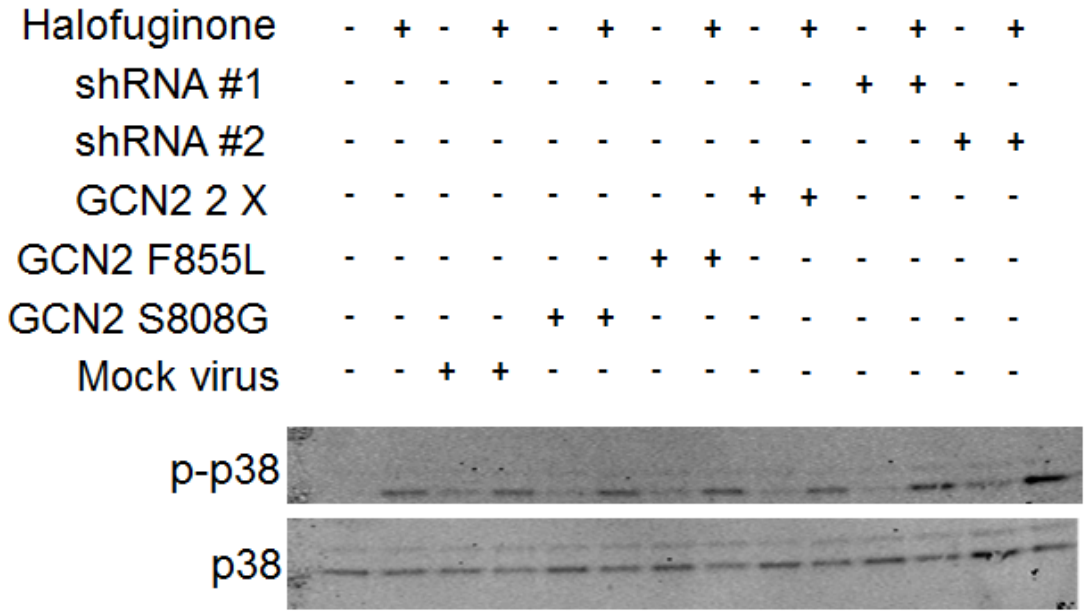

Figure 4.22 Halofuginone effects on p38 phosphorylation appears to be GCN2-independent.
iPS cardiomyocytes were transduced with lentiviral vectors; SHC003 pLKO.1-puro-CMV-TurboGFP, pLexGCN2 and shRNA vectors TRCN0000300850 and TRCN0000300851, as described in the materials and methods. The cells were treated with halofuginone for 24 hours and protein levels of phosphorylated and total GCN2 and p38 were measured by Western blot analysis.

5 DISCUSSION

There is a large body of literature relating to the function of p38α or TAB1. However, little is known concerning the mechanism of interaction between these two proteins and of the consequent activation of p38α. Even less is known about the substrates specifically phosphorylated by this unusual activation pathway. Some studies suggest that this TAB1-mediated activation pathway is specific to myocardial ischaemia and aggravates myocardial injury. However, this is not the only function of TAB1 as it also plays a role in the canonical pathway of p38α activation by binding to TAK1. Once p38α is activated, it phosphorylates TAB1. The phosphoform of TAB1 is meant to be less able to activate TAK1, closing a negative feedback loop. Nonetheless, if the direct effect of TAB1 on p38α activation is proven specific to ischaemia, discovering the mechanism of this pathway could provide new therapeutic targets for cardiovascular medicine.

5.1 There is a TAB1-mediated p38α autophosphorylation mechanism

p38α is involved in many cellular processes ranging from apoptosis to cell differentiation depending on cell types and stimuli. The main activation cascade of p38α is the MAPKKK pathway and this is involved in response to inflammatory cytokines and oxidative stress (71). Nonetheless, the other activation mechanism of p38α via autophosphorylation mediated by TAB1 has been described during ischaemia aggravating injury in the heart (29). In order to gain more insight into this mechanism I have shown that p38α autophosphorylation is increased by co-expression with TAB1 (see Figure 3.3). It has been shown in other studies that p38α phosphorylation and ischaemic injury is increased in mice lacking MKK3, inferring that the canonical pathway is not the main contributor to p38α activation during myocardial ischaemia (28,

29). Though still in need of further research and confirmation, if TAB1 effects on p38α are specific to ischaemia, as suggested by current studies, this mechanism could be taken advantage of to combat myocardial infarction by reducing the injury.

5.2 TAB1-mediated p38α autophosphorylation is SB203580-sensitive

Being an ATP-mimetic type I inhibitor of p38α, SB203580 blocks p38α activation by directly binding to the p38α ATP-binding site (297, 298). I have shown that TAB1-mediated p38α phosphorylation is diminished upon addition of SB203580 (see Figure 3.3). SB203580 prevents the binding of ATP and therefore p38α cannot phosphorylate itself or its substrates as it requires the gamma phosphate group of ATP. There are studies showing that SB203580 does not act on other members of the canonical MAPKKK pathway of p38α activation (299) so the inhibition is specific to p38α itself and not due to any off-target effects.

In the cardiac context, a study in MKK3$^{-/-}$ mice reported diminished p38 phosphorylation and reduced infarct volume with the use of SB203580, but TNF-α induced activation of p38 was not affected (29). In addition, p38 was associated with TAB1 in ischaemic hearts but not in hearts treated with TNF-α. Using SB203580 as a tool to block p38 kinase activity, the reduction in infarct size implies that p38 autophosphorylation plays at least a partial role in the induction of ischaemic injury and it is likely this is through an interaction with TAB1.

5.3 SB203580 binds to Thr106 of p38α and blocks ATP-binding

A particular region of p38α structure is important for the unique interaction of the fluorophenyl ring of SB203580. In our studies, mutating the key residue for SB-binding in this region, Thr106, to Met in the drug-resistant version of p38α, diminishes binding of SB203580 and therefore the TAB1-mediated phosphorylation is not affected upon

addition of SB203580 (see Figure 3.3). Nonetheless, when Thr106 is mutated to Ala, there is no effect on the activity of SB203580 (300). p38γ and p38δ lack the residues Thr106, His107 and Leu108 which are important for SB203580 binding so SB203580 is only inhibits p38α and p38β. When these residues are introduced into p38γ and p38δ, SB203580 is able to inhibit their phosphorylation (301). Therefore, Thr106 is important for SB203580 binding and is required for the inhibition of p38α activation.

5.4 Certain points of interaction are important for TAB1-p38α binding

Identifying interaction points and essential amino acids in protein sequences for substrate binding is important in cell biology. It enables the determination of the regions which may overlap with other binding partners or give an in-depth insight to the nature of the protein-protein interaction in question. There is not much information yet on which residues are important to the p38α and TAB1 interaction. Nonetheless, the effect of different mutations of TAB1 and p38α and truncated versions of these proteins on this interaction has been investigated. It appears that Pro412 in TAB1 and Ile116 and Gln120 in p38α are essential for TAB1-p38α recognition. However these residues are only important in the direct binding of TAB1 and p38α and their substitution does not appear to influence MKK6-mediated p38α activation (302). In addition, mutating the CD and ED domains of p38α did not have an effect on TAB1 interaction, suggesting a dissimilarity between TAB1 and most other p38α binding partners. Nonetheless, in common with other p38α substrates TAB1 also has a D-domain though this differs from the consensus motifs in other substrates.

As already mentioned, I have found through X-ray crystallography that TAB1 interacts with p38α on two regions; the common docking region (canonical), which is shared with other binding partners of p38α such as MEF2C and MKK3 and a unique

hydrophobic groove (non-canonical), which appears to be specific to TAB1 binding alone. Using peptides of TAB1 involved in binding to each of these regions I found that the canonical region of TAB1 is more important in inducing p38α autophosphorylation than the non-canonical region(see Figure 3.5), which is most obvious after 4 hr incubation.

5.5 TAB1 mutations at interaction points decrease p38α autophosphorylation

In order to support the data inferring that the canonical region of TAB1 is more important in inducing p38α autophosphorylation, TAB1 versions mutated at either or both the common docking binding region and the section binding to the unique hydrophobic groove of p38α were used to investigate the effect of mutations in these regions. Substituting bulkier residues found in WT TAB1 with smaller residues in order to diminish interaction with p38α, TAB1 mutants were tested in bacterial and mammalian cell lines. Supportive of our findings of the canonical peptide increasing phosphorylation of p38α, there was reduced p38α phosphorylation when the residues important in the TAB1-p38α interaction were mutated at the common docking domain binding region of TAB1 (see Figure 3.6 and Figure 3.7). However, there was also a reduction in p38α phosphorylation when the residues of TAB1 involved in binding to the unique hydrophobic groove were mutated. This suggests that both regions of TAB1 play an important role in p38α phosphorylation in the context of full-length protein.

5.6 TAB1 mutations affect TAB1 substrate presentation

Difficulty determining whether TAB1 phosphorylation decreases due to the decreased phosphorylation of p38α or due to TAB1 mutations causing a deficiency in TAB1 substrate presentation to p38α was overcome by mimicking a constitutively active p38α

by co-transfecting cells with MKK3b and p38α. It seems that there is no difference in p38α phosphorylation upon addition of different TAB1 mutants to this co-transfection, except only a slight decrease with the CM/NCM mutant version of TAB1 (see Figure 3.8). This suggests that p38α is active enough to give us an understanding of differences in TAB1 phosphorylation with different mutants. The phosphorylations of p38α caused by MKK3 and TAB1 were analysed separately and in combination to confirm that p38α phosphorylation was due to MKK3 and TAB1 addition did not alter p38α activation by MKK3. Unlike p38α phosphorylation, TAB1 phosphorylation is decreased to basal levels with the CM/NCM mutant of TAB1. Therefore, TAB1 substrate presentation is markedly reduced when both interaction points are mutated.

5.7 TAB1 phosphorylation does not affect TAK1 phosphorylation

As discussed earlier, TAK1 is the MAP3K upstream of MKK3/6 in the p38 canonical activation pathway and TAB1 plays a role in its activation. Through the yeast two-hybrid system, TAB1 and TAB2 have been identified to interact with TAK1 and TAB1 and TAK1 have been co-immunoprecipitated in mammalian cells (303). In addition, TGF-β signal transduction through TAK1 is increased with enhanced TAB1 levels (303). It has been reported that autophosphorylation of two Thr residues in the activation loop of TAK1 is required for its activation and this is facilitated through an association with TAB1 (304). The C-terminal of TAB1 consists of two functional subdomains and is essential for full TAK1 activation.

TAB1β is a splice variant of TAB1 in which the 69 C-terminal residues are replaced with an unrelated 27-amino acid sequence. Therefore, as expected, TAB1β does not bind or activate TAK1, yet is still able to stimulate p38 activation (35). Ge et al. have determined that TAB1β does not bind or activate TAK1 through immunoprecipitations and an activity assay using MKK4 as a substrate, respectively. I have verified the lack

of TAK1 phosphorylation upon co-expression of TAK1 and TAB1β in HEK293 cells using phospho-TAK1 specific antibodies (see Figure 3.9).

Furthermore, TAK1 activation is enhanced by SB203580 in macrophages stimulated by LPS and proinflammatory cytokines, as well as in TNF-α-treated embryonic fibroblasts from $p38\alpha^{-/-}$ mice (279). SB203580 had no effect in cells from $p38\alpha^{-/-}$ mice, suggesting that in some way, p38α provides a negative feedback system on TAK1 activity. TAB1 sites that are phosphorylated by p38α, lie around the regions of TAB1 that are involved in p38 and TAK1-binding, which are adjacent to each other. Cheung et al. suggest that since TAK1 is not a substrate for p38α, it is probably the phosphorylation of TAB1, which prevents TAK1 activation through a conformational change or via the stimulation of TAK1 deactivation. Another possibility is a negative feedback system on TAK1 through a different protein in the complex, such as TAB2, which is downregulated by p38α. To our surprise, I did not find the phosphorylation state of TAB1 to affect TAK1 phosphorylation (see Figure 3.9 and Figure 3.10). The reduction in TAB1 phosphorylation due to mutations preventing its substrate presentation to p38 or by pharmacologic inhibition of p38 by SB203580 did not have an effect on TAK1 phosphorylation. This, coupled with Cheung et al.'s data suggest that it is possible that p38 downregulates TAK1 activity via a different route than TAB1 phosphorylation.

5.8 The competition between TAB1 and MKK3 in binding to p38

It has been previously mentioned that p38 plays a role in a wide range of processes within a cell, with a main downstream effect being inflammation. The onset and progress of the pathophysiology of heart failure has been associated with an elevated inflammatory response (305, 306). p38 activation has been associated with several pathological features in the cardiac context such as neuro-hormonal and mechanical stimulation, as well as ischaemic injury (307, 308). As already mentioned TAB1 is

involved in the canonical activation pathway of p38, as well as an independent autophosphorylation mechanism. The evidence that TAB1 might also play a role in the negative feedback on the canonical activation mechanism, highlights the multifunctional potential of TAB1.

It has been reported that TAB1 prevents nuclear localisation of p38 and attenuates the MKK3-mediated induction of inflammatory gene expression by p38 (32). It appears from this study that TAB1 can mediate MKK3-independent activation, while simultaneously negatively regulating MKK-dependent effects on p38. In this study in rat neonatal ventricular cardiomyocytes (RNVC), p38 is localised throughout the cell cytoplasm and nucleus when co-expressed with MKK3, yet upon co-expression with TAB1, it is excluded from the nucleus. The authors conclude that intracellular localisation of p38 and its complex interactions determine downstream effects. Homologous docking sites exist in MAPK scaffold proteins (276) and all of the docking site sequences identified contain a basic region and a hydrophobic region (277). One of the consensus motifs shared by some of these proteins is R/K-X4-φA-X-φB (where φA and φB are hydrophobic residues [Leu, Ile, or Val]). A study on the crystal structure of p38 and peptides derived from two of its binding partners MKK3b and MEF2A revealed that these two proteins share a common docking groove that interacts with the hydrophobic φA-X-φB motif of docking peptides (278). The docking groove on p38 shared by these peptides contains residues Ile116 and Gln120, which are key to recognition of the φA-X-φB motif. Both MKK3b and MEF2A bind in the same groove and trigger similar changes in local conformation, but different conformational changes occur in the active site. As mentioned previously, two regions of interaction were identified for TAB1 and p38, the canonical upper domain and the unique hydrophobic groove i.e. the non-canonical domain. The canonical upper site of p38 referred to in De Nicola et al.'s study, as well as in our studies, overlaps with the region of p38 used for

interaction by its binding partners such as MKK3b and MEF2A (34). Therefore, due to the above evidence, I have hypothesised that there is potential for competition between TAB1 and MKK3b to compete in binding to p38.

Through ITC, I have observed that the interaction between MKK3b and p38 is altered by the addition of the TAB1 peptide (see Figure 3.11), which suggests that there is potential for competition in binding to p38 between these two proteins. This data is supported by IVK assays, in which the presence of TAB1 decreased MKK3b-mediated p38 phosphorylation. This is more obvious when TAB1-mediated phosphorylation of p38 is blocked by SB203580 whilst binding remains unaffected, however MKK3b-mediated p38 phosphorylation remains reduced (see Figure 3.14). Nonetheless, to our surprise, there appears to be no competition between TAB1 and MKK3b in p38 binding in HEK293 cells (see Figure 3.16 and Figure 3.18). One possible reason to explain these discrepant results is that in ITC and IVK assays the native in-cell localisation of proteins is irrelevant since close proximity is forced by purity and artificial nature of the assay. Therefore, the likelihood of an alteration in existing interactions by addition of another protein is possible through mere steric hindrance due to the presence of the newly added protein. However, in the in-cell system, proteins are located where they would be natively and the results obtained from these methods are more reliable regarding the biological function of proteins.

To confirm the differential localisation of p38 in the presence of TAB1 and MKK3b, immunofluorescence of these proteins when co-expressed with p38 on their own or both at the same time were observed. TAB1 appears to be localised more in a perinuclear fashion, whereas MKK3b is confined to sub-cell membrane region (see Figure 3.19). When p38 was co-expressed with each of these binding partners it appears to be co-localised with its binding partner. Nonetheless, when both MKK3b and TAB1 are overexpressed beside p38, p38 predominantly localises with MKK3b. This is different

from what is observed in Lu et al.'s study (32) in that TAB1 triggers the relocation of p38 towards the nucleus, instead of excluding it from there. In addition, another difference from Lu et al.'s study is that I have not observed a competition or difference in MKK3-mediated activity whereas they have. This could be due to the difference in cell type and transfection methods. Nonetheless, in both cases, TAB1 and MKK3b have differential locations and they alter the location of p38. This explains why the MKK3b-mediated phosphorylation of p38 is not altered by the presence of TAB1 as they are in different locations within the cell and MKK3b is more dominant at attracting p38 to it.

5.9 ET-1 release in stress and its effects in the cardiac context

As previously discussed, ET-1 is synthesised in and acts on the ET_A and ET_B receptors in cardiomyocytes, cardiac fibroblasts and heart endothelial cells. Plasma ET-1 concentrations are increased in various pathological conditions such as myocardial infarction (309), atherosclerosis (310) and chronic heart failure (CHF) (248, 311, 312) in humans as well as in experimental models. In chronic heart failure, the severity of symptoms and hemodynamic malfunction appear to correlate with plasma levels of ET-1, which can also be used as a prognostic guide in these patients (311, 313). ET-1 has a broad range of downstream effects, with a main feature being its role in the induction of neurohormones such as vasopressin, angiotensin II and norepinephrine, important in the progression of heart failure. ET-1 stimulates cardiac hypertrophy and plays a key role in ventricular remodelling (244, 314, 315). Aortic banding in rats leads to an increase in the mRNA levels of ET-1, BNP and β-myosin heavy chain (β-MHC – gene name *MYH7*) (315). ET-1 treatment in isolated rat aorta leads to an increase in BNP gene expression (316) and ET receptor antagonist improved the changes observed in various hypertrophy-related genes in failing hearts of CHF rats. ANP, β-MHC, ryanodine receptor, sarcoplasmic reticulum Ca2+-ATPase (SERCA2A), angiotensin-converting

enzyme (ACE), angiotensin II type 1 receptor, and prepro-ET-1mRNA levels were improved in these rats (317). The natriuretic peptides are active hormones involved in diuresis and the reduction of blood pressure and the plasma levels of these hormones can be used as a prognostic indicator of left ventricular ejection fraction and mortality in CHF patients. I have shown in our experiments that mRNA levels of ANP, BNP, ratio of β-MHC to α-MHC (gene name *MYH6*) and SERCA2A are altered in response to ET-1 treatment in cardiomycytes (see section 4.2). As discussed earlier, internalisation of ET receptors have been proposed as a negative feedback system (238) and using different concentrations of ET-1, I have found that above a certain concentration the responses to ET-1 are blunted, possibly due to an internalisation of receptors (see Figure 4.5).

In the case of chronic heart failure in patients and animal models, acute administration of bosentan, a competitive antagonist of ET-1 at the ET_A and ET_B receptors, decreases vascular resistance and improves left ventricular function (318-320). ET_A selective antagonism using BQ-123 in patients resulted in an increased cardiac index. Nonetheless, though it appears logical to target the ET-1 pathway in heart failure, clinical trials with compounds targeting this system have not been successful (321). In a recent clinical trial, Endothelin Antagonist Bosentan for Lowering Cardiac Events in Heart Failure (ENABLE), treatment with bosentan lead to worsening of heart failure and subsequent hospitalisation, as a result of fluid retention (322).

5.10 Hypertrophy in cardiomyocytes and the role of the AAR pathway

Left ventricular hypertrophy is one of the main risk factors for heart failure. Hypertrophy induces myocardial tissue remodelling and can lead to disturbances in myocardial blood flow and diastolic dysfunction.

The role of ET-1, its receptors and downstream effects in heart failure has been discussed previously. ET-1 plays an important role in the heart and regulates myocardial contractility, and increases in both experimental models of heart failure and in patients (248, 323). In order to maintain the circulatory homeostasis, several endogenous vasodilators and antagonists of ET-1 exist. Two of these are ANP and BNP, with increased levels in heart failure positively correlating with severity of the disease (324), suggesting an adaptive mechanism to balance the effects of vasoconstrictor hormones such as ET-1.

As ANP and BNP levels are indicators of the disease severity, a cardioprotective compound would reduce these levels. Upon exposure of ET-1-treated cardiomyocytes to halofuginone ANP and BNP levels are reduced (see Figure 4.6). This result, in combination with the other cardioprotective effects of halofuginone observed suggests the AAR pathway is a promising target with therapeutic potential in heart failure. Nonetheless, the efforts of several groups aiming to explore the potential benefits of increasing ANP and BNP levels must be considered (325-327). Authors have concluded that a prominent increase in natriuretic action improves ventricular dysfunction in patients with heart failure. Therefore, caution must be taken when analysing such decreases in ANP and BNP levels to ensure that these decreases do not block the protective mechanisms present in the cell as a response to the stress but indeed are a result of the cardioprotective effects of halofuginone.

MHC-β to MHC-α ratio was not altered by ET-1 treatment or by exposure to halofuginone (see Figure 4.6). This could be due to the induction time required for the changes to occur being different than the one applied in these experiments. It is possible that ANP and BNP act much faster than the transition of MHC isoforms in response to ET-1. In experiments in animal models to induce changes in MHC expression levels, much longer induction times were employed (328). Another possibility is that MHC

proteins are not a target of the AAR pathway, though this is a low possibility as the MHC-β is an energy-preserving protein, which would fit in well with the starvation response.

Furthermore, a recent study in GCN2 knockout mice that have undergone transverse aortic constriction (TAC) has reported a protected phenotype compared to the wild-type controls, which is surprisingly contrary to our hypothesis and data. The expression of the anti-apoptotic protein Bcl-2 was elevated in GCN2 knockout hearts and the authors concluded that GCN2 prevents ventricular adaptation to pressure overload through a reduction of Bcl-2 making cardiomyocytes more susceptible to apoptosis. Nonetheless, the explanation for this could be the fact that GCN2 is a stress-response kinase and can induce apoptosis depending on the level of stress. In terms of autophagy in this model, beclin-1 and LC3B levels are significantly attenuated in $GCN2^{-/-}$ hearts and increased in wild-type controls. This supports our data in that GCN2 is involved in increasing autophagy, which is a controversial mechanism in heart failure regarding its adaptive/maladaptive status. Taking into account the data in GCN2 knockout animals, further research is required to explore the role of the AAR pathway in heart failure.

5.11 Autophagy in cardiomyocytes and the role of the AAR pathway

Autophagy is the degradation process within a cell important to maintain cell function, remove damaged organelles and provide the building blocks for new protein synthesis. In heart failure, characteristics of autophagy can be observed in damaged cardiomyocytes and it appears to be a failed repair mechanism or a pathway to result in apoptosis. Evidence for autophagy was observed in tissue samples of dilated cardiomyopathy in end-stage heart failure patients (329). Upon adrenergic overload in cardiomyocytes, there was an increase in punctate staining of LC3 (330). In a TAC model of mice, autophagosome accumulation was observed as early as 24 hr after TAC

and remained at increased levels for 2 weeks (331). Another group reported that autophagy is suppressed 1 week following TAC, but upregulated simultaneously with left ventricular dysfunction after 4 weeks (137). As discussed in section 1.6.6, autophagy in the cardiac context is controversial and there is evidence for its occurrence in heart failure being both adaptive and maladaptive depending on the context.

Amino acid homeostasis is regulated by the integrated stress response and autophagy. Mechanistic target of rapamycin complex 1 (mTORC1) plays a key role in autophagy and it inhibits autophagy by phosphorylating the kinase involved in the induction of autophagy, ULK1 (332). Several studies have shown that ER stress leads to the induction of autophagy as a survival mechanism and it has been reported that the eIF2alpha/ATF4 pathway plays an important role in autophagy (333, 334). Induction of an increase in the gene expression of *Map1lc3b* in response to ER stress and hypoxia has been reported in recent studies (335). The upregulation of autophagy appeared to be essential to maintain autophagy and for cell survival. Upon amino acid starvation, it was reported that GCN2-mediated phosphorylation of eIF2alpha is crucial to induce autophagy (336, 337). The role of eIF2alpha in the initiation of the autophagy response is not yet clear, however one highly likely mechanism is through its effects on the physical formation of autophagosomes at the ER. Another possible mechanism is the ATF4-mediated stimulation of genes involved in autophagy. Though it appears that ATF4 is involved in the autophagy response through eIF2alpha (338), the target genes involved in this process remains to be elucidated. A third possibility is the interaction of eIF2alpha with core autophagy proteins, though the importance of these interactions is yet to be determined (339).

Using halofuginone to trigger the AAR pathway through eIF2alpha phosphorylation, several genes were identified to be upregulated in response to this pathway in cardiomyoyctes. *ULK1, ULK2, GABARAPL1* and *MAP1LC3B* gene expression were

increased significantly in response to halofuginone treatment alone and in the presence of ET-1 treated cells (see section 4.4.1) suggesting that the activation of the AAR pathway does increase autophagy, at least in part, at the gene expression level.

To date, a well-established method to identify the occurrence of autophagy is the detection of LC3 processing by Western blot analysis and the observation of immunofluorescence of autophagosome components. Observing immunofluorescence of LC3A/B, I have identified an increase in autophagosome formation in halofuginone treated cardiomyocytes (see Figure 4.10) which was in support of our gene expression data inferring that the activation of the AAR pathway does appear to induce autophagy. However, there is a caveat in this readout, which is the fact that autophagy is a dynamic and multi-step process. The accumulation of autophagosomes could suggest an increase in overall autophagy or it could be due to the malfunctioning of the proteins downstream of this process, such as a decrease in lysosomal fusion. A good example of this is chloroquine, a lysosomotropic agent which accumulated inside the acidic parts of the cell such as the lysosomes. Lysosomal enzymes require an acidic pH to function (340, 341) and chloroquine inhibits autophagy as it raises the lysosomal pH preventing the fusion of lysosomes with autophagosomes, leading to the accumulation of autophagosomes (342). Therefore, the mere detection of an increase in autophagosome formation is not a reliable measure of the overall autophagy within the cell. As already discussed in section 4.4.2, p62 protein levels correlate negatively with the level of autophagy within a cell. p62 is degraded itself after recruiting proteins to be degraded into the autophagosome, and can therefore be used to measure autophagic flux i.e. the dynamic process of autophagy and the turnover of amino acids during autophagy. In support of the increase in the expression of genes involved in autophagy, p62 levels also indicated an increase in autophagy following halofuginone treatment (see Figure 4.9). Therefore, it appears that the activation of the AAR pathway with halofuginone

treatment increases autophagy at several different steps in cardiomyocytes. This could be due to the mechanisms discussed above, as eIF2alpha activation appears to induce changes in gene expression and this is supported by downstream readout of autophagic flux.

5.12 p38 activation in inflammation and halofuginone

As previously discussed in section 1.6.7, p38 plays a key role in inducing inflammation and its pharmacological inhibition is beneficial in the context of heart failure. It has been previously reported that halofuginone inhibits TGF-β (343), an important immunomodulator that is downstream of p38. Halofuginone treated T cells exhibit a dose-dependent decrease in NFκB besides an inhibited secretion of TNF-α, interferon γ (IFN-γ), IL-4, IL-13 and TGF-β (225). More importantly, halofuginone treatment inhibits the phosphorylation of p38. In addition, in human corneal fibroblasts, halofuginone treatment reduced protein expression of Smad3 (344), a signal transducer and transcriptional modulator activated by TGF-β and involved in several signalling pathways. p38 inhibitors can prevent the activation of Smad3 and attenuate its TGF-β-induced expression (345). Besides the halofuginone-mediated inhibition of cytokines and inflammatory agents as well as the similarities between the effects of p38 inhibitors and halofuginone, inhibition of p38 phosphorylation would be expected upon halofuginone treatment. However, the effect of halofuginone on the activity of p38 in cardiomyocytes has not been previously investigated. Therefore, as I am exploring the potential cardioprotective effects of the AAR pathway using halofuginone as a tool, considering that halofuginone has anti-inflammatory effects and p38 activity and inflammation aggravates heart failure; I have hypothesised that halofuginone treatment in cardiomyocytes would be anti-inflammatory. To our surprise, halofuginone activates p38 in a dose-dependent fashion (see Figure 4.11). In addition, using the dose of

halofuginone that activates the AAR pathway and is not toxic in cardiomyocytes; p38 activity, measured by the phosphorylation of its substrate MK2, is increased by halofuginone and appears to be SB-sensitive (see Figure 4.15).

The gene expression of one of the main inflammation-associated substrates of p38, COX-2, was increased in a SB-sensitive manner in response to halofuginone (see Figure 4.17). COX-2 mediates the production of prostacyclins, a family of prostaglandins that induce platelet activation and vasodilatation and thromboxane A2, which has prothrombic effects. While prostacyclins prevent cardiac arrhythmias and platelet aggregation and have been reported as cardioprotective (346, 347), thromboxane, promotes platelet aggregation, acts as a vasoconstrictor and induces ventricular arrhythmias (348). This explains why COX-2 inhibitors can potentially lead to thrombotic cardiovascular events (349). Therefore, the halofuginone-mediated increase in COX-2 gene expression, could play a protective role and must be analysed beside the other cardioprotective effects of halofuginone.

Constitutively active form of MKK6 induces IL-6 transcription and IL-6 release in a p38-dependent manner in cardiac myocytes (116). IL-6 appears to protect cardiac cells against apoptosis in an autocrine/paracrine manner to increase cell survival during stresses known to activate p38. In contrast, there is evidence for the involvement of IL-6 in the pathophysiology of the failing heart (350). Elevated levels of IL-6 in plasma and in the heart of patients with congestive heart failure (351, 352) and the correlation with left ventricular function and cardiac injury with these levels suggests an important role for IL-6 in the cardiac context. However, despite the evidence of involvement in the progression of cardiovascular diseases, it is yet to be determined whether the increase in IL-6 levels is causative or a consequence of the pathophysiology. Halofuginone treatment in Th17 cells inhibit cell differentiation and increase levels of IFN-γ, TNF-α, and IL-6 leading to a reduction in disease severity in the context of graft versus host

disease (353). It appears that IL-6 levels increase in a SB-sensitive manner with halofuginone treatment in cardiomyocytes (see Figure 4.17). Taken together with the protective role of COX-2, this could be an adaptive mechanism in the cardiac context. Increased levels of IL-1β have been reported in atherosclerotic plaques (354) and a reduction in the expression of activity of this cytokine has been associated with a reduction in plaque size (355, 356). A recent phase 3 clinical trial Canakinumab Anti-inflammatory Thrombosis Outcomes Study (CANTOS; NCT01327846) aims to reduce cardiovascular events in patients with a recent myocardial infarction and increased C-reactive protein (CRP) levels using an antibody against IL1β (357) after the promising results of the phase 2b trial which reported reduced inflammation and fibrinogen (358). A study on IL1R1$^{-/-}$apolipoprotein E$^{-/-}$ (ApoE$^{-/-}$) mice reported decreased plaques, though plaque stability and vascular remodeling was reduced in areas where haemorrhage occurred in these animals (359). The evidence suggests that although blocking IL1β pathway appears to be protective, there is potential that this pathway plays a dual role in advanced atherosclerosis by facilitating plaque stability. Though the results were not significant, halofuginone appears to reduce the mRNA levels of the IL1R1 and its antagonist IL1RN, with a trend in this reduction being SB-sensitive (see Figure 4.17). The reduction in the gene expression of the receptor suggests that halofuginone mediates the reduction in the response to the inflammatory signal, which correlates with a reduction in levels of IL1RN, which is possibly no longer required to attenuate the signal as the reduction in receptors provides this feedback.

5.13 Use of lentiviral vectors to study gene function

Though gene therapy emerged as a tool to rectify the resulting hereditary diseases due to a missing or dysfunctional protein, it is currently a well-established method to study the function of genes of interest within cells and tissues of living organisms. Exploring the

function of genes could involve the insertion of a modified form of the gene at a specific location in the host genome, in order to replace the existing gene. This could enable researchers to elucidate the importance of certain regions of a specific gene, such as the interaction points of TAB1 identified to be important in p38 binding. Organisms without the functional regions of TAB1 would have reduced TAB1 binding to p38, potentially having a lower risk of injury upon ischaemia as this appears to be TAB1-mediated (see section 1.2.3). This is further discussed in section 8.

A second method of exploring gene function through gene therapy is by genetic engineering of knock-out animals, where the gene of interest is switched off. This could lead to embryonic or neonatal lethality which would highlight the importance of the gene in development, such as in the case of p38 (57) and TAB1 (360).

A similar approach to knock-out animals, in the cell-based system is knocking the gene down using RNA interference (RNAi). There are two types of RNA molecules that naturally exist within cells, microRNA and small interfering RNA (siRNA), which are products of genes and play the role of binding to mRNA of certain genes to alter their activity. A small hairpin RNA (shRNA) is an artificial RNA molecule with a hairpin turn that is used to silence the target gene through RNAi. An enzyme called Dicer forms siRNA from shRNA, which then binds to mRNA and cleaves it, leading to the inhibition of protein synthesis from that particular mRNA. shRNA is a more advantageous tool for RNAi as it has a relatively low rate of degradation and turnover compared to siRNA.

Exploring the AAR pathway induction by halofuginone is a feasible way to explore the potential impacts of the activation of this pathway. However, in order to confirm the effects that are observed are mediated by GCN2 and not by an off-target effect of halofuginone upstream, GCN2 was knocked-down by the use of shRNA-packed

lentiviruses and some of the readouts that were previously altered upon halofuginone treatment were observed, once again.

Following the confirmation of the knock-down of GCN2 at mRNA (see Figure 4.19) and protein level (see Figure 4.20), the phosphorylation of eIF2alpha was observed. To our surprise, eIF2alpha is still phosphorylated despite knocking down GCN2 (see Figure 4.20). In addition, the downstream effects of activated eIF2alpha, such as the increase in DDIT3 mRNA (see Figure 4.21), still persist despite knockdown of the upstream GCN2. As previously discussed in section 1.8.5, there are three other kinases upstream of eIF2alpha. Though these kinases are activated in response to different stresses, there is potential of functional redundancy between them. In a study in $PERK^{-/-}$ fibroblasts, phosphorylation of eIF2alpha is attenuated, though not completely lost in comparison to wild-type cells. This suggests another kinase fulfils, at least at low levels, the role of PERK in phosphorylating eIF2alpha. In $PERK^{-/-}$ $GCN2^{-/-}$ double knock out cells, the downstream effects of eIF2alpha, in this case cyclin D1 loss, is attenuated inferring that it is GCN2 which functions as the redundant kinase (361). For our experiments, there are two explanations for the presence of eIF2alpha phosphorylation, despite knocking down GCN2 successfully. One mechanism could be due to the redundancy of upstream kinases due to their cooperation as discussed. Another explanation is that the knockdown of the GCN2 gene was not complete, so the low level of GCN2 present might still have the ability to induce the phosphorylation of eIF2alpha as without the knock-down.

In addition, the overexpression of the wild-type GCN2 and the constitutively active GCN2 (F855L) increases the protein levels of GCN2, yet the effect on eIF2alpha phosphorylation was similar independent of the presence of overexpression vectors. Nonetheless, eIF2alpha is phosphorylated basally with the constitutively active GCN2 mutant, as expected. This could be due to the fact that eIF2alpha is already maximally

phosphorylated by the basal levels of GCN2 and there is no excess eIF2alpha which could be phosphorylated to correlate with the overexpressed levels of GCN2. Nonetheless, effects of halofuginone and the specificity of the AAR pathway as the mediator of these effects require further investigation to confirm findings. This is further discussed in section 8.

6 LIMITATIONS

Despite the importance and additions of the findings and results in this thesis to the cardiology research field, there are a few limitations to the study, which should be addressed. Quantification is the conversion of a concept to numbers, which would represent the property linked to this quantity. It is an important aspect of data analysis and aids to visualise the results easily, as well as providing a platform on which statistical tests could be performed, allowing scientists to derive the significance of the acquired results. Though most of the results are quantified in this thesis, all of the results should be quantified in order to boost the strength of the results, their reproducibility and statistical significance. Data acquired from this point on should be quantified for the above reasons.

An essential part of an experiment consists of tests referred to as controls which establishes the baseline that the experimental samples are compared to, as well as testing that the system being used works as it should. In addition, controls also allow scientists to discover potential errors in the case that the result is different from expected in the controls. Though having the correct controls for each experiment in this thesis has been given substantial consideration, certain controls are missing from the displayed results. An example of this missing control is the localisation of p38, TAB1 and MKK3b transfected alone in Figure 3.19. This would help to establish the differences the presence of the binding partner makes more clearly, even though the main difference looking examined for in this particular experiment is the difference the presence of TAB1 makes to the binding between MKK3b and p38. In future experiments, this should be paid further consideration in order to have the correct controls for the comparison of the experimental results.

In addition, just like the experimental control samples, loading controls are essential for proper interpretation of Western blots. They are used to normalise the levels of phosphorylated and total protein, confirming that the observed differences are true and not due to loading errors during the Western blotting process. Housekeeping genes with high-level and constitutive expression in the tested system are used as loading controls. Although in most experiments analysed in this thesis, either a housekeeping gene or the total protein of interest, in the analysis of phosphorylation levels, has been used, it would have been preferable to use expression of a housekeeping protein as a loading control for all performed experiments, in the event of the total protein also being altered by the treatment in question.

In the light of above limitations, future research questions should be addressed in an appropriate manner with reference to controls and quantification. These would enable the data analysis and observation in a more reproducible, reliable and clear manner.

7 CONCLUSION

To summarise TAB1 induces p38 autophosphorylation without the activation of the canonical pathway confirming there is a TAB1-mediated p38 activation pathway independent of the canonical activation mechanism. TAB1-mediated p38 autophosphorylation is sensitive to SB203580, and the key residue in this inhibitor-kinase interaction is Thr106, which when mutated renders p38 resistant to SB203580. In this study, I have found TAB1 residues Val390 and Tyr392 (mutated to Gly and Ala respectively in the CM TAB1 mutant) and Val408 and Met409 (mutated to Gly and Ala respectively in the NCM TAB1 mutant) are important in TAB1-p38 interaction and mutations of these residues lead to a reduced binding of TAB1 to p38.

This is found to consequently and independently affect p38 autophosphorylation and TAB1 substrate presentation. Furthermore, though TAB1 appears to have an effect on p38 interaction with MKK3b in in vitro assays, no competition between MKK3b and TAB1 are observed in experiments in the mammalian cell system. This appears to be due to a difference in the in-cell location of MKK3b and TAB1, with MKK3b able to attract p38 to its location despite the presence of overexpressed TAB1. This suggests that the in-cell location of p38 along with its binding partners and inducing stimuli potentially determines the differential downstream function. In addition, TAB1 phosphorylation state did not affect phosphorylation of TAK1, despite previous findings that TAK1 activity is modulated negatively by TAB1. Though preliminary, our findings motivate to encourage further investigation into p38 and TAB1 interaction mechanism, especially in the in vivo setting in order to elucidate the role of TAB1-p38 interaction in the context of cardiac ischaemia.

Moreover, the AAR pathway has not been examined previously in cardiomyocytes. Our study provides evidence for the presence of this pathway in different lines of cardiac

cells along with the induction of established downstream substrates of the pathway. It appears that halofuginone is able to induce this pathway in a specific, reversible way. In addition to previously identified substrates of this pathway such as ASNS, DDIT3 and TRIB3, our experiments provide evidence for further novel potential mechanisms mediated by p38 i.e. the potential regulation of the AAR pathway initiated by halofuginone-mediated activation of p38. Though the protective potential of halofuginone has been previously examined in the DMD setting, the data generated in this thesis provides promising evidence that halofuginone or the activation of the AAR pathway via other means could potentially alleviate the features observed in the pathophysiology of heart failure. These include changes in inflammation, autophagy, hypertrophy and MAPK activation.

8 FUTURE WORK

In order to verify that the effects of TAB1 mutations on p38 autophosphorylation observed in vitro and in bacteria are reflected in systems of higher organisms, a mammalian cell line has also been tested. The next step to obtain stronger evidence verifying the interaction points of TAB1 and p38α would be using a cell line in which the canonical pathway of p38α activation is disabled. TAK1-deficient MEFs could be used to remove the effect of the canonical pathway almost completely and attribute any resulting p38α phosphorylation to the TAB1-mediated mechanism providing a deeper understanding of the impact of this pathway.

TAB1 has recently been found to be modified by O-GlcNAcylation on Ser395 (4) and this modification has been found to play a role in the TAK1 cascade. O-GlcNAcylation may alter substrate specificity on adjacent regions by steric hindrance. Therefore, since this single site modification appears to play a role in the canonical pathway, it might be enlightening to further investigate whether this has an impact on p38 autophosphorylation. A potential way this could be done is by using an O-GlcNAcylated form of TAB1 to do IVK assays to see its effect on p38 autophosphorylation. A potential problem I could observe is that the full-length TAB1 is not soluble and the modification on Ser395 could make it even more insoluble. Nonetheless, current evidence shows that these experiments would provide valuable information into understanding TAB1-mediated activation of p38α.

Another regulation of TAB1 protein is via an E3 ubiquitin ligase called Itch. As discussed earlier, Itch binds TAB1 directly and inhibits the activation of p38. It appears that p38-mediated inflammation is suppressed by the direct interaction of Itch with TAB1 inducing its ubiquitylation and degradation (33). This mechanism could be manipulated when targeting TAB1-mediated activation of p38 to perturb the system

using different pathways. Nonetheless, caution must be exercised when approaching TAB1 from this pathway as Itch is also involved in the proteasomal degradation of TAK1. Therefore, this could have nonspecific effects on the p38 pathway and block its other crucial activities and it is important that manipulations are targeted if they are to provide meaningful results.

In addition, the function of this pathway in vivo can be studied using proteomic methods. The stable-isotope labelling of amino acids in cell culture (SILAC) proteomics methodology could be used to identify the consequences of different TAB1 mutations. The transactivator of transcription (TAT) peptide (GRKKRRQRRRPQ) is a cell penetrating peptide from human immunodeficiency virus and is a useful tool for translocating molecules across cell membranes efficiently. This peptide has been used to transfect cells with the TAB1 peptides. We have recently found the TAT peptide on the TAB1 peptide to be a stressor on cells and this could be used as a control to understand pathologic and adaptive changes in the heart associated with pressure overload and exercise leading to discovery of critical kinases and identify their function.

Furthermore, current ongoing work in our laboratory involves TAB1 knock-in mice, which harbour the mutations I have examined in this thesis, which affect the interaction between p38 and TAB1. Langendorff experiments of isolated hearts subjected to ischaemia could provide valuable information about the importance of TAB1-p38 interaction and its involvement in ischaemia. In the case that infarct size is reduced in mutant mice, it would be extremely promising to pursue this further by investigating compounds to target these interaction points to minimise ischaemic injury in high-risk patients.

Regarding the potential of the protective effects of activating the AAR pathway to minimise features of heart failure, the data in this thesis is preliminary and on its own is not sufficient to determine whether this protective role exists or not in whole hearts.

However, in house data at GSK treating heart failure models of mice with halofuginone as well as proteomics and transcriptomics studies (unpublished data) support the protective role that is provided by halofugione in these studies. Therefore, taking into account all published and unpublished evidence besides the data in this thesis, there are promising indications to investigate this pathway further. As halofuginone acts relatively upstream in the pathway, it might be more feasible to approach the pathway in a more direct and specific manner. A method to investigate this could be by looking at compounds, which would activate GCN2 directly, preventing potential upstream effects of amino acid starvation within cells, which is a complex mechanism known to cross-link different pathways including the mTOR system.

Furthermore, though the effect of halofuginone on p38 activity and downstream effectors has been investigated, this is a mechanism that should be investigated further. The potential negative feedback system provided by p38 on the AAR pathway activation could play an important role in the dampening of the effects of the activation of this stress pathway. This could have a protective effect on the cell, by keeping the activation under regulation and alter it according to the stress and the adaptive mechanisms required for cell survival. p38 activation is usually detrimental in the cardiac context and contributes to injury. Nonetheless, due to its role in a wide range of cell processes, its specific downstream effects depend on the activation mechanism and might therefore be protective depending on the stimuli. Therefore, despite being active, it could trigger cardio-protective mechanisms such as through the dampening of the AAR pathway, which perhaps should only be activated at low levels to achieve the prevention of features of heart failure. This would be akin to p38's known protective role in ischaemic preconditioning.

In addition, due to time limitations at GSK, as well as technical complication in the production of viruses targeting GCN2, the lentiviral studies in this thesis are preliminary

and need to be replicated. The issues with the downstream effects of GCN2 still being present upon its knockdown could be an artefact of the experiment and must be repeated to ensure veracity. Nonetheless, another way to investigate this would be using compounds to inhibit GCN2 to determine that the effects of halofuginone are through this kinase. It must be considered that finding specific, potent compounds is a complicated and challenging process and this might not be easily done. However, previous evidence suggests that it is a pathway worth investigating further and could provide valuable results relevant to the pharmaceutical industry and human health, since millions of people suffer from heart failure.

9 REFERENCES

1. Pearson G, Robinson F, Beers Gibson T, Xu BE, Karandikar M, Berman K, et al. Mitogen-activated protein (MAP) kinase pathways: regulation and physiological functions. Endocr Rev. 2001;22(2):153-83.
2. Lee J, Mira-Arbibe L, Ulevitch RJ. TAK1 regulates multiple protein kinase cascades activated by bacterial lipopolysaccharide. J Leukoc Biol. 2000;68(6):909-15.
3. Conner SH, Kular G, Peggie M, Shepherd S, Schuttelkopf AW, Cohen P, et al. TAK1-binding protein 1 is a pseudophosphatase. Biochem J. 2006;399(3):427-34.
4. Pathak S, Borodkin VS, Albarbarawi O, Campbell DG, Ibrahim A, van Aalten DM. O-GlcNAcylation of TAB1 modulates TAK1-mediated cytokine release. The EMBO journal. 2012;31(6):1394-404.
5. Han J, Lee JD, Bibbs L, Ulevitch RJ. A MAP kinase targeted by endotoxin and hyperosmolarity in mammalian cells. Science. 1994;265(5173):808-11.
6. Freshney NW, Rawlinson L, Guesdon F, Jones E, Cowley S, Hsuan J, et al. Interleukin-1 activates a novel protein kinase cascade that results in the phosphorylation of Hsp27. Cell. 1994;78(6):1039-49.
7. Rouse J, Cohen P, Trigon S, Morange M, Alonso-Llamazares A, Zamanillo D, et al. A novel kinase cascade triggered by stress and heat shock that stimulates MAPKAP kinase-2 and phosphorylation of the small heat shock proteins. Cell. 1994;78(6):1027-37.
8. Brewster JL, de Valoir T, Dwyer ND, Winter E, Gustin MC. An osmosensing signal transduction pathway in yeast. Science. 1993;259(5102):1760-3.
9. Jiang Y, Gram H, Zhao M, New L, Gu J, Feng L, et al. Characterization of the structure and function of the fourth member of p38 group mitogen-activated protein kinases, p38delta. The Journal of biological chemistry. 1997;272(48):30122-8.
10. Hommes DW, Peppelenbosch MP, van Deventer SJ. Mitogen activated protein (MAP) kinase signal transduction pathways and novel anti-inflammatory targets. Gut. 2003;52(1):144-51.
11. Ono K, Han J. The p38 signal transduction pathway: activation and function. Cellular signalling. 2000;12(1):1-13.
12. Sanz-Moreno V, Casar B, Crespo P. p38alpha isoform Mxi2 binds to extracellular signal-regulated kinase 1 and 2 mitogen-activated protein kinase and regulates its nuclear activity by sustaining its phosphorylation levels. Molecular and cellular biology. 2003;23(9):3079-90.
13. Yagasaki Y, Sudo T, Osada H. Exip, a splicing variant of p38alpha, participates in interleukin-1 receptor proximal complex and downregulates NF-kappaB pathway. FEBS letters. 2004;575(1-3):136-40.
14. Ninomiya-Tsuji J, Kishimoto K, Hiyama A, Inoue J, Cao Z, Matsumoto K. The kinase TAK1 can activate the NIK-I kappaB as well as the MAP kinase cascade in the IL-1 signalling pathway. Nature. 1999;398(6724):252-6.
15. Kanayama A, Seth RB, Sun L, Ea CK, Hong M, Shaito A, et al. TAB2 and TAB3 activate the NF-kappaB pathway through binding to polyubiquitin chains. Molecular cell. 2004;15(4):535-48.
16. Wang C, Deng L, Hong M, Akkaraju GR, Inoue J, Chen ZJ. TAK1 is a ubiquitin-dependent kinase of MKK and IKK. Nature. 2001;412(6844):346-51.
17. Inagaki M, Omori E, Kim JY, Komatsu Y, Scott G, Ray MK, et al. TAK1-binding protein 1, TAB1, mediates osmotic stress-induced TAK1 activation but is

dispensable for TAK1-mediated cytokine signaling. The Journal of biological chemistry. 2008;283(48):33080-6.
18. Cuadrado A, Nebreda AR. Mechanisms and functions of p38 MAPK signalling. Biochem J. 2010;429(3):403-17.
19. Denise Martin E, Felice De Nicola G, Marber MS. New Therapeutic Targets in Cardiology: p38 Alpha Mitogen-Activated Protein Kinase for Ischemic Heart Disease. Circulation. 2012;126(3):357-68.
20. Cohen P. The search for physiological substrates of MAP and SAP kinases in mammalian cells. Trends Cell Biol. 1997;7(9):353-61.
21. Cuenda A, Rousseau S. p38 MAP-kinases pathway regulation, function and role in human diseases. Biochim Biophys Acta. 2007;1773(8):1358-75.
22. Kishimoto K, Matsumoto K, Ninomiya-Tsuji J. TAK1 mitogen-activated protein kinase kinase kinase is activated by autophosphorylation within its activation loop. The Journal of biological chemistry. 2000;275(10):7359-64.
23. Derynck R, Zhang YE. Smad-dependent and Smad-independent pathways in TGF-beta family signalling. Nature. 2003;425(6958):577-84.
24. Sorrentino A, Thakur N, Grimsby S, Marcusson A, von Bulow V, Schuster N, et al. The type I TGF-beta receptor engages TRAF6 to activate TAK1 in a receptor kinase-independent manner. Nat Cell Biol. 2008;10(10):1199-207.
25. Ben-Levy R, Hooper S, Wilson R, Paterson HF, Marshall CJ. Nuclear export of the stress-activated protein kinase p38 mediated by its substrate MAPKAP kinase-2. Curr Biol. 1998;8(19):1049-57.
26. Wood CD, Thornton TM, Sabio G, Davis RA, Rincon M. Nuclear localization of p38 MAPK in response to DNA damage. International journal of biological sciences. 2009;5(5):428-37.
27. Salvador JM, Mittelstadt PR, Guszczynski T, Copeland TD, Yamaguchi H, Appella E, et al. Alternative p38 activation pathway mediated by T cell receptor-proximal tyrosine kinases. Nat Immunol. 2005;6(4):390-5.
28. Li J, Miller EJ, Ninomiya-Tsuji J, Russell RR, 3rd, Young LH. AMP-activated protein kinase activates p38 mitogen-activated protein kinase by increasing recruitment of p38 MAPK to TAB1 in the ischemic heart. Circulation research. 2005;97(9):872-9.
29. Tanno M, Bassi R, Gorog DA, Saurin AT, Jiang J, Heads RJ, et al. Diverse mechanisms of myocardial p38 mitogen-activated protein kinase activation: evidence for MKK-independent activation by a TAB1-associated mechanism contributing to injury during myocardial ischemia. Circulation research. 2003;93(3):254-61.
30. Ge B, Gram H, Di Padova F, Huang B, New L, Ulevitch RJ, et al. MAPKK-independent activation of p38alpha mediated by TAB1-dependent autophosphorylation of p38alpha. Science. 2002;295(5558):1291-4.
31. Wolf A, Beuerlein K, Eckart C, Weiser H, Dickkopf B, Muller H, et al. Identification and functional characterization of novel phosphorylation sites in TAK1-binding protein (TAB) 1. PloS one. 2011;6(12):e29256.
32. Lu G, Kang YJ, Han J, Herschman HR, Stefani E, Wang Y. TAB-1 modulates intracellular localization of p38 MAP kinase and downstream signaling. The Journal of biological chemistry. 2006;281(9):6087-95.
33. Theivanthiran B, Kathania M, Zeng M, Anguiano E, Basrur V, Vandergriff T, et al. The E3 ubiquitin ligase Itch inhibits p38alpha signaling and skin inflammation through the ubiquitylation of Tab1. Science signaling. 2015;8(365):ra22.
34. De Nicola GF, Martin ED, Chaikuad A, Bassi R, Clark J, Martino L, et al. Mechanism and consequence of the autoactivation of p38alpha mitogen-activated protein kinase promoted by TAB1. Nature structural & molecular biology. 2013;20(10):1182-90.

35. Ge B, Xiong X, Jing Q, Mosley JL, Filose A, Bian D, et al. TAB1beta (transforming growth factor-beta-activated protein kinase 1-binding protein 1beta), a novel splicing variant of TAB1 that interacts with p38alpha but not TAK1. The Journal of biological chemistry. 2003;278(4):2286-93.
36. Tanoue T, Nishida E. Molecular recognitions in the MAP kinase cascades. Cellular signalling. 2003;15(5):455-62.
37. Tanoue T, Adachi M, Moriguchi T, Nishida E. A conserved docking motif in MAP kinases common to substrates, activators and regulators. Nat Cell Biol. 2000;2(2):110-6.
38. Enslen H, Davis RJ. Regulation of MAP kinases by docking domains. Biol Cell. 2001;93(1-2):5-14.
39. Lorenz K, Schmitt JP, Schmitteckert EM, Lohse MJ. A new type of ERK1/2 autophosphorylation causes cardiac hypertrophy. Nature medicine. 2009;15(1):75-83.
40. Jacquet S, Nishino Y, Kumphune S, Sicard P, Clark JE, Kobayashi KS, et al. The role of RIP2 in p38 MAPK activation in the stressed heart. The Journal of biological chemistry. 2008;283(18):11964-71.
41. Eyers PA, van den IP, Quinlan RA, Goedert M, Cohen P. Use of a drug-resistant mutant of stress-activated protein kinase 2a/p38 to validate the in vivo specificity of SB 203580. FEBS Lett. 1999;451(2):191-6.
42. Martin JL, Avkiran M, Quinlan RA, Cohen P, Marber MS. Antiischemic effects of SB203580 are mediated through the inhibition of p38alpha mitogen-activated protein kinase: Evidence from ectopic expression of an inhibition-resistant kinase. Circ Res. 2001;89(9):750-2.
43. Clark JE, Sarafraz N, Marber MS. Potential of p38-MAPK inhibitors in the treatment of ischaemic heart disease. Pharmacol Ther. 2007;116(2):192-206.
44. Huang YM, Chen W, Potter MJ, Chang CE. Insights from free-energy calculations: protein conformational equilibrium, driving forces, and ligand-binding modes. Biophys J. 2012;103(2):342-51.
45. Pargellis C, Tong L, Churchill L, Cirillo PF, Gilmore T, Graham AG, et al. Inhibition of p38 MAP kinase by utilizing a novel allosteric binding site. Nat Struct Biol. 2002;9(4):268-72.
46. Kuma Y, Sabio G, Bain J, Shpiro N, Marquez R, Cuenda A. BIRB796 inhibits all p38 MAPK isoforms in vitro and in vivo. The Journal of biological chemistry. 2005;280(20):19472-9.
47. Hardy JA, Wells JA. Searching for new allosteric sites in enzymes. Curr Opin Struct Biol. 2004;14(6):706-15.
48. Raingeaud J, Gupta S, Rogers JS, Dickens M, Han J, Ulevitch RJ, et al. Pro-inflammatory cytokines and environmental stress cause p38 mitogen-activated protein kinase activation by dual phosphorylation on tyrosine and threonine. The Journal of biological chemistry. 1995;270(13):7420-6.
49. Karin M. Inflammation-activated protein kinases as targets for drug development. Proc Am Thorac Soc. 2005;2(4):386-90; discussion 94-5.
50. Nebreda AR, Porras A. p38 MAP kinases: beyond the stress response. Trends in biochemical sciences. 2000;25(6):257-60.
51. Wagner EF, Nebreda AR. Signal integration by JNK and p38 MAPK pathways in cancer development. Nat Rev Cancer. 2009;9(8):537-49.
52. Zhuang S, Demirs JT, Kochevar IE. p38 mitogen-activated protein kinase mediates bid cleavage, mitochondrial dysfunction, and caspase-3 activation during apoptosis induced by singlet oxygen but not by hydrogen peroxide. The Journal of biological chemistry. 2000;275(34):25939-48.

53. Puri PL, Wu Z, Zhang P, Wood LD, Bhakta KS, Han J, et al. Induction of terminal differentiation by constitutive activation of p38 MAP kinase in human rhabdomyosarcoma cells. Genes & development. 2000;14(5):574-84.
54. Bulavin DV, Saito S, Hollander MC, Sakaguchi K, Anderson CW, Appella E, et al. Phosphorylation of human p53 by p38 kinase coordinates N-terminal phosphorylation and apoptosis in response to UV radiation. The EMBO journal. 1999;18(23):6845-54.
55. Huang Y, Yuan ZM, Ishiko T, Nakada S, Utsugisawa T, Kato T, et al. Pro-apoptotic effect of the c-Abl tyrosine kinase in the cellular response to 1-beta-D-arabinofuranosylcytosine. Oncogene. 1997;15(16):1947-52.
56. Sanchez-Prieto R, Rojas JM, Taya Y, Gutkind JS. A role for the p38 mitogen-acitvated protein kinase pathway in the transcriptional activation of p53 on genotoxic stress by chemotherapeutic agents. Cancer research. 2000;60(9):2464-72.
57. Adams RH, Porras A, Alonso G, Jones M, Vintersten K, Panelli S, et al. Essential role of p38alpha MAP kinase in placental but not embryonic cardiovascular development. Molecular cell. 2000;6(1):109-16.
58. Mudgett JS, Ding J, Guh-Siesel L, Chartrain NA, Yang L, Gopal S, et al. Essential role for p38alpha mitogen-activated protein kinase in placental angiogenesis. Proceedings of the National Academy of Sciences of the United States of America. 2000;97(19):10454-9.
59. Tamura K, Sudo T, Senftleben U, Dadak AM, Johnson R, Karin M. Requirement for p38alpha in erythropoietin expression: a role for stress kinases in erythropoiesis. Cell. 2000;102(2):221-31.
60. Pombo CM, Bonventre JV, Avruch J, Woodgett JR, Kyriakis JM, Force T. The stress-activated protein kinases are major c-Jun amino-terminal kinases activated by ischemia and reperfusion. The Journal of biological chemistry. 1994;269(42):26546-51.
61. Nagarkatti DS, Sha'afi RI. Role of p38 MAP kinase in myocardial stress. J Mol Cell Cardiol. 1998;30(8):1651-64.
62. Barancik M, Htun P, Strohm C, Kilian S, Schaper W. Inhibition of the cardiac p38-MAPK pathway by SB203580 delays ischemic cell death. J Cardiovasc Pharmacol. 2000;35(3):474-83.
63. Mackay K, Mochly-Rosen D. An inhibitor of p38 mitogen-activated protein kinase protects neonatal cardiac myocytes from ischemia. The Journal of biological chemistry. 1999;274(10):6272-9.
64. Ma XL, Kumar S, Gao F, Louden CS, Lopez BL, Christopher TA, et al. Inhibition of p38 mitogen-activated protein kinase decreases cardiomyocyte apoptosis and improves cardiac function after myocardial ischemia and reperfusion. Circulation. 1999;99(13):1685-91.
65. Saurin AT, Martin JL, Heads RJ, Foley C, Mockridge JW, Wright MJ, et al. The role of differential activation of p38-mitogen-activated protein kinase in preconditioned ventricular myocytes. FASEB journal : official publication of the Federation of American Societies for Experimental Biology. 2000;14(14):2237-46.
66. Maulik N, Yoshida T, Zu YL, Sato M, Banerjee A, Das DK. Ischemic preconditioning triggers tyrosine kinase signaling: a potential role for MAPKAP kinase 2. Am J Physiol. 1998;275(5 Pt 2):H1857-64.
67. Alkhulaifi AM. Preconditioning the human heart. Ann R Coll Surg Engl. 1997;79(1):49-54.
68. Mocanu MM, Baxter GF, Yue Y, Critz SD, Yellon DM. The p38 MAPK inhibitor, SB203580, abrogates ischaemic preconditioning in rat heart but timing of administration is critical. Basic Res Cardiol. 2000;95(6):472-8.

69. Weinbrenner C, Liu GS, Cohen MV, Downey JM. Phosphorylation of tyrosine 182 of p38 mitogen-activated protein kinase correlates with the protection of preconditioning in the rabbit heart. J Mol Cell Cardiol. 1997;29(9):2383-91.
70. Winter UJ, Gitt AK, Blaum M, Fritsch J, Berge PG, Pothoff G, et al. [Cardiopulmonary capacity in patients with coronary heart disease]. Z Kardiol. 1994;83 Suppl 3:73-82.
71. Kumphune S, Bassi R, Jacquet S, Sicard P, Clark JE, Verma S, et al. A chemical genetic approach reveals that p38alpha MAPK activation by diphosphorylation aggravates myocardial infarction and is prevented by the direct binding of SB203580. The Journal of biological chemistry. 2010;285(5):2968-75.
72. Fang ZY, Marwick TH. Vascular dysfunction and heart failure: epiphenomenon or etiologic agent? Am Heart J. 2002;143(3):383-90.
73. Paulus WJ. Cytokines and heart failure. Heart Fail Monit. 2000;1(2):50-6.
74. Konstam MA, Kramer DG, Patel AR, Maron MS, Udelson JE. Left Ventricular Remodeling in Heart Failure Current Concepts in Clinical Significance and Assessment. Jacc-Cardiovascular Imaging. 2011;4(1):98-108.
75. Marks AR. Calcium cycling proteins and heart failure: mechanisms and therapeutics. The Journal of clinical investigation. 2013;123(1):46-52.
76. Ng DC, Court NW, dos Remedios CG, Bogoyevitch MA. Activation of signal transducer and activator of transcription (STAT) pathways in failing human hearts. Cardiovascular research. 2003;57(2):333-46.
77. Bellahcene M, Jacquet S, Cao XB, Tanno M, Haworth RS, Layland J, et al. Activation of p38 mitogen-activated protein kinase contributes to the early cardiodepressant action of tumor necrosis factor. Journal of the American College of Cardiology. 2006;48(3):545-55.
78. Takeishi Y, Huang Q, Abe J, Che W, Lee JD, Kawakatsu H, et al. Activation of mitogen-activated protein kinases and p90 ribosomal S6 kinase in failing human hearts with dilated cardiomyopathy. Cardiovascular research. 2002;53(1):131-7.
79. Nemoto S, Sheng Z, Lin A. Opposing effects of Jun kinase and p38 mitogen-activated protein kinases on cardiomyocyte hypertrophy. Molecular and cellular biology. 1998;18(6):3518-26.
80. Liao P, Wang SQ, Wang S, Zheng M, Zheng M, Zhang SJ, et al. p38 Mitogen-activated protein kinase mediates a negative inotropic effect in cardiac myocytes. Circulation research. 2002;90(2):190-6.
81. Martin ED, Bassi R, Marber MS. p38 MAPK in cardioprotection - are we there yet? British journal of pharmacology. 2015;172(8):2101-13.
82. Lips DJ, deWindt LJ, van Kraaij DJ, Doevendans PA. Molecular determinants of myocardial hypertrophy and failure: alternative pathways for beneficial and maladaptive hypertrophy. Eur Heart J. 2003;24(10):883-96.
83. Peterson KL. Pressure overload hypertrophy and congestive heart failure. Where is the "Achilles' heel"? Journal of the American College of Cardiology. 2002;39(4):672-5.
84. Kerkela R, Force T. p38 mitogen-activated protein kinase: a future target for heart failure therapy? Journal of the American College of Cardiology. 2006;48(3):556-8.
85. Vahebi S, Ota A, Li M, Warren CM, de Tombe PP, Wang Y, et al. p38-MAPK induced dephosphorylation of alpha-tropomyosin is associated with depression of myocardial sarcomeric tension and ATPase activity. Circulation research. 2007;100(3):408-15.
86. Andrews C, Ho PD, Dillmann WH, Glembotski CC, McDonough PM. The MKK6-p38 MAPK pathway prolongs the cardiac contractile calcium transient,

downregulates SERCA2, and activates NF-AT. Cardiovascular research. 2003;59(1):46-56.
87. Kaikkonen L, Magga J, Ronkainen VP, Koivisto E, Perjes A, Chuprun JK, et al. p38alpha regulates SERCA2a function. J Mol Cell Cardiol. 2014;67:86-93.
88. Kan H, Xie Z, Finkel MS. p38 MAP kinase-mediated negative inotropic effect of HIV gp120 on cardiac myocytes. Am J Physiol Cell Physiol. 2004;286(1):C1-7.
89. Kyriakis JM, Avruch J. Mammalian mitogen-activated protein kinase signal transduction pathways activated by stress and inflammation. Physiological reviews. 2001;81(2):807-69.
90. Hoefer J, Azam MA, Kroetsch JT, Leong-Poi H, Momen MA, Voigtlaender-Bolz J, et al. Sphingosine-1-phosphate-dependent activation of p38 MAPK maintains elevated peripheral resistance in heart failure through increased myogenic vasoconstriction. Circulation research. 2010;107(7):923-33.
91. Kumar R, Singh VP, Baker KM. The intracellular renin-angiotensin system: implications in cardiovascular remodeling. Curr Opin Nephrol Hypertens. 2008;17(2):168-73.
92. Vijayan K, Szotek EL, Martin JL, Samarel AM. Protein kinase C-alpha-induced hypertrophy of neonatal rat ventricular myocytes. American journal of physiology Heart and circulatory physiology. 2004;287(6):H2777-89.
93. Bao W, Behm DJ, Nerurkar SS, Ao Z, Bentley R, Mirabile RC, et al. Effects of p38 MAPK Inhibitor on angiotensin II-dependent hypertension, organ damage, and superoxide anion production. J Cardiovasc Pharmacol. 2007;49(6):362-8.
94. See F, Thomas W, Way K, Tzanidis A, Kompa A, Lewis D, et al. p38 mitogen-activated protein kinase inhibition improves cardiac function and attenuates left ventricular remodeling following myocardial infarction in the rat. Journal of the American College of Cardiology. 2004;44(8):1679-89.
95. Widder J, Behr T, Fraccarollo D, Hu K, Galuppo P, Tas P, et al. Vascular endothelial dysfunction and superoxide anion production in heart failure are p38 MAP kinase-dependent. Cardiovascular research. 2004;63(1):161-7.
96. Hayashi M, Kim SW, Imanaka-Yoshida K, Yoshida T, Abel ED, Eliceiri B, et al. Targeted deletion of BMK1/ERK5 in adult mice perturbs vascular integrity and leads to endothelial failure. The Journal of clinical investigation. 2004;113(8):1138-48.
97. Olson EN. Undermining the endothelium by ablation of MAPK-MEF2 signaling. The Journal of clinical investigation. 2004;113(8):1110-2.
98. Wang LJ, Fan C, Topol SE, Topol EJ, Wang Q. Mutation of MEF2A in an inherited disorder with features of coronary artery disease. Science. 2003;302(5650):1578-81.
99. Li Z, Tran TT, Ma JY, O'Young G, Kapoun AM, Chakravarty S, et al. p38 alpha mitogen-activated protein kinase inhibition improves cardiac function and reduces myocardial damage in isoproterenol-induced acute myocardial injury in rats. J Cardiovasc Pharmacol. 2004;44(4):486-92.
100. Ushio-Fukai M, Alexander RW, Akers M, Griendling KK. p38 Mitogen-activated protein kinase is a critical component of the redox-sensitive signaling pathways activated by angiotensin II. Role in vascular smooth muscle cell hypertrophy. The Journal of biological chemistry. 1998;273(24):15022-9.
101. Haq SE, Clerk A, Sugden PH. Activation of mitogen-activated protein kinases (p38-MAPKs, SAPKs/JNKs and ERKs) by adenosine in the perfused rat heart. FEBS letters. 1998;434(3):305-8.
102. Nishida K, Yamaguchi O, Hirotani S, Hikoso S, Higuchi Y, Watanabe T, et al. p38alpha mitogen-activated protein kinase plays a critical role in cardiomyocyte

survival but not in cardiac hypertrophic growth in response to pressure overload. Molecular and cellular biology. 2004;24(24):10611-20.
103. Chahine MN, Mioulane M, Sikkel MB, O'Gara P, Dos Remedios CG, Pierce GN, et al. Nuclear pore rearrangements and nuclear trafficking in cardiomyocytes from rat and human failing hearts. Cardiovascular research. 2015;105(1):31-43.
104. Wang Y, Huang S, Sah VP, Ross J, Jr., Brown JH, Han J, et al. Cardiac muscle cell hypertrophy and apoptosis induced by distinct members of the p38 mitogen-activated protein kinase family. The Journal of biological chemistry. 1998;273(4):2161-8.
105. Braz JC, Bueno OF, Liang Q, Wilkins BJ, Dai YS, Parsons S, et al. Targeted inhibition of p38 MAPK promotes hypertrophic cardiomyopathy through upregulation of calcineurin-NFAT signaling. The Journal of clinical investigation. 2003;111(10):1475-86.
106. Klein G, Schaefer A, Hilfiker-Kleiner D, Oppermann D, Shukla P, Quint A, et al. Increased collagen deposition and diastolic dysfunction but preserved myocardial hypertrophy after pressure overload in mice lacking PKCepsilon. Circulation research. 2005;96(7):748-55.
107. Liang Q, Molkentin JD. Redefining the roles of p38 and JNK signaling in cardiac hypertrophy: dichotomy between cultured myocytes and animal models. J Mol Cell Cardiol. 2003;35(12):1385-94.
108. Diwan A, Wansapura J, Syed FM, Matkovich SJ, Lorenz JN, Dorn GW, 2nd. Nix-mediated apoptosis links myocardial fibrosis, cardiac remodeling, and hypertrophy decompensation. Circulation. 2008;117(3):396-404.
109. Kilpatrick LE, Sun S, Mackie D, Baik F, Li H, Korchak HM. Regulation of TNF mediated antiapoptotic signaling in human neutrophils: role of delta-PKC and ERK1/2. J Leukoc Biol. 2006;80(6):1512-21.
110. Chuang SM, Wang IC, Yang JL. Roles of JNK, p38 and ERK mitogen-activated protein kinases in the growth inhibition and apoptosis induced by cadmium. Carcinogenesis. 2000;21(7):1423-32.
111. Okamoto S, Krainc D, Sherman K, Lipton SA. Antiapoptotic role of the p38 mitogen-activated protein kinase-myocyte enhancer factor 2 transcription factor pathway during neuronal differentiation. Proceedings of the National Academy of Sciences of the United States of America. 2000;97(13):7561-6.
112. Kaiser RA, Bueno OF, Lips DJ, Doevendans PA, Jones F, Kimball TF, et al. Targeted inhibition of p38 mitogen-activated protein kinase antagonizes cardiac injury and cell death following ischemia-reperfusion in vivo. The Journal of biological chemistry. 2004;279(15):15524-30.
113. Zechner D, Craig R, Hanford DS, McDonough PM, Sabbadini RA, Glembotski CC. MKK6 activates myocardial cell NF-kappaB and inhibits apoptosis in a p38 mitogen-activated protein kinase-dependent manner. The Journal of biological chemistry. 1998;273(14):8232-9.
114. Communal C, Colucci WS, Singh K. p38 mitogen-activated protein kinase pathway protects adult rat ventricular myocytes against beta -adrenergic receptor-stimulated apoptosis. Evidence for Gi-dependent activation. The Journal of biological chemistry. 2000;275(25):19395-400.
115. Hoover HE, Thuerauf DJ, Martindale JJ, Glembotski CC. alpha B-crystallin gene induction and phosphorylation by MKK6-activated p38. A potential role for alpha B-crystallin as a target of the p38 branch of the cardiac stress response. The Journal of biological chemistry. 2000;275(31):23825-33.
116. Craig R, Larkin A, Mingo AM, Thuerauf DJ, Andrews C, McDonough PM, et al. p38 MAPK and NF-kappa B collaborate to induce interleukin-6 gene expression and

release. Evidence for a cytoprotective autocrine signaling pathway in a cardiac myocyte model system. The Journal of biological chemistry. 2000;275(31):23814-24.
117. Zhao Y, Tan Y, Xi S, Li Y, Li C, Cui J, et al. A novel mechanism by which SDF-1beta protects cardiac cells from palmitate-induced endoplasmic reticulum stress and apoptosis via CXCR7 and AMPK/p38 MAPK-mediated interleukin-6 generation. Diabetes. 2013;62(7):2545-58.
118. Thandavarayan RA, Watanabe K, Ma M, Gurusamy N, Veeraveedu PT, Konishi T, et al. Dominant-negative p38alpha mitogen-activated protein kinase prevents cardiac apoptosis and remodeling after streptozotocin-induced diabetes mellitus. American journal of physiology Heart and circulatory physiology. 2009;297(3):H911-9.
119. Kyoi S, Otani H, Matsuhisa S, Akita Y, Tatsumi K, Enoki C, et al. Opposing effect of p38 MAP kinase and JNK inhibitors on the development of heart failure in the cardiomyopathic hamster. Cardiovascular research. 2006;69(4):888-98.
120. Zhu W, Zou Y, Aikawa R, Harada K, Kudoh S, Uozumi H, et al. MAPK superfamily plays an important role in daunomycin-induced apoptosis of cardiac myocytes. Circulation. 1999;100(20):2100-7.
121. Kang YJ, Zhou ZX, Wang GW, Buridi A, Klein JB. Suppression by metallothionein of doxorubicin-induced cardiomyocyte apoptosis through inhibition of p38 mitogen-activated protein kinases. The Journal of biological chemistry. 2000;275(18):13690-8.
122. Mackay K, Mochly-Rosen D. Involvement of a p38 mitogen-activated protein kinase phosphatase in protecting neonatal rat cardiac myocytes from ischemia. J Mol Cell Cardiol. 2000;32(8):1585-8.
123. Sharov VG, Todor A, Suzuki G, Morita H, Tanhehco EJ, Sabbah HN. Hypoxia, angiotensin-II, and norepinephrine mediated apoptosis is stimulus specific in canine failed cardiomyocytes: a role for p38 MAPK, Fas-L and cyclin D1. Eur J Heart Fail. 2003;5(2):121-9.
124. Meldrum DR, Dinarello CA, Cleveland JC, Jr., Cain BS, Shames BD, Meng X, et al. Hydrogen peroxide induces tumor necrosis factor alpha-mediated cardiac injury by a P38 mitogen-activated protein kinase-dependent mechanism. Surgery. 1998;124(2):291-6; discussion 7.
125. Iaccarino G, Ciccarelli M, Sorriento D, Galasso G, Campanile A, Santulli G, et al. Ischemic neoangiogenesis enhanced by beta2-adrenergic receptor overexpression: a novel role for the endothelial adrenergic system. Circulation research. 2005;97(11):1182-9.
126. Yamaguchi O, Watanabe T, Nishida K, Kashiwase K, Higuchi Y, Takeda T, et al. Cardiac-specific disruption of the c-raf-1 gene induces cardiac dysfunction and apoptosis. The Journal of clinical investigation. 2004;114(7):937-43.
127. Zhang D, Gaussin V, Taffet GE, Belaguli NS, Yamada M, Schwartz RJ, et al. TAK1 is activated in the myocardium after pressure overload and is sufficient to provoke heart failure in transgenic mice. Nature medicine. 2000;6(5):556-63.
128. Liao P, Georgakopoulos D, Kovacs A, Zheng M, Lerner D, Pu H, et al. The in vivo role of p38 MAP kinases in cardiac remodeling and restrictive cardiomyopathy. Proceedings of the National Academy of Sciences of the United States of America. 2001;98(21):12283-8.
129. Biesemann N, Mendler L, Kostin S, Wietelmann A, Borchardt T, Braun T. Myostatin induces interstitial fibrosis in the heart via TAK1 and p38. Cell Tissue Res. 2015.
130. Zhang S, Weinheimer C, Courtois M, Kovacs A, Zhang CE, Cheng AM, et al. The role of the Grb2-p38 MAPK signaling pathway in cardiac hypertrophy and fibrosis. The Journal of clinical investigation. 2003;111(6):833-41.

131. Streicher JM, Ren S, Herschman H, Wang Y. MAPK-activated protein kinase-2 in cardiac hypertrophy and cyclooxygenase-2 regulation in heart. Circulation research. 2010;106(8):1434-43.
132. Scharf M, Neef S, Freund R, Geers-Knorr C, Franz-Wachtel M, Brandis A, et al. Mitogen-activated protein kinase-activated protein kinases 2 and 3 regulate SERCA2a expression and fiber type composition to modulate skeletal muscle and cardiomyocyte function. Molecular and cellular biology. 2013;33(13):2586-602.
133. Vigliano CA, Cabeza Meckert PM, Diez M, Favaloro LE, Cortes C, Fazzi L, et al. Cardiomyocyte hypertrophy, oncosis, and autophagic vacuolization predict mortality in idiopathic dilated cardiomyopathy with advanced heart failure. Journal of the American College of Cardiology. 2011;57(14):1523-31.
134. Hein S, Arnon E, Kostin S, Schonburg M, Elsasser A, Polyakova V, et al. Progression from compensated hypertrophy to failure in the pressure-overloaded human heart: structural deterioration and compensatory mechanisms. Circulation. 2003;107(7):984-91.
135. Tannous P, Zhu H, Johnstone JL, Shelton JM, Rajasekaran NS, Benjamin IJ, et al. Autophagy is an adaptive response in desmin-related cardiomyopathy. Proceedings of the National Academy of Sciences of the United States of America. 2008;105(28):9745-50.
136. Ceylan-Isik AF, Dong M, Zhang Y, Dong F, Turdi S, Nair S, et al. Cardiomyocyte-specific deletion of endothelin receptor A rescues aging-associated cardiac hypertrophy and contractile dysfunction: role of autophagy. Basic Res Cardiol. 2013;108(2):335.
137. Nakai A, Yamaguchi O, Takeda T, Higuchi Y, Hikoso S, Taniike M, et al. The role of autophagy in cardiomyocytes in the basal state and in response to hemodynamic stress. Nature medicine. 2007;13(5):619-24.
138. Kassiotis C, Ballal K, Wellnitz K, Vela D, Gong M, Salazar R, et al. Markers of autophagy are downregulated in failing human heart after mechanical unloading. Circulation. 2009;120(11 Suppl):S191-7.
139. McClung JM, Judge AR, Powers SK, Yan Z. p38 MAPK links oxidative stress to autophagy-related gene expression in cachectic muscle wasting. Am J Physiol Cell Physiol. 2010;298(3):C542-9.
140. Henson SM, Lanna A, Riddell NE, Franzese O, Macaulay R, Griffiths SJ, et al. p38 signaling inhibits mTORC1-independent autophagy in senescent human CD8(+) T cells. The Journal of clinical investigation. 2014;124(9):4004-16.
141. Lin L, Tang C, Xu J, Ye Y, Weng L, Wei W, et al. Mechanical stress triggers cardiomyocyte autophagy through angiotensin II type 1 receptor-mediated p38MAP kinase independently of angiotensin II. PloS one. 2014;9(2):e89629.
142. Levine B, Kalman J, Mayer L, Fillit HM, Packer M. Elevated circulating levels of tumor necrosis factor in severe chronic heart failure. N Engl J Med. 1990;323(4):236-41.
143. Feldman AM, Combes A, Wagner D, Kadakomi T, Kubota T, Li YY, et al. The role of tumor necrosis factor in the pathophysiology of heart failure. Journal of the American College of Cardiology. 2000;35(3):537-44.
144. Behnam SM, Behnam SE, Koo JY. TNF-alpha inhibitors and congestive heart failure. Skinmed. 2005;4(6):363-8.
145. Gong KZ, Song G, Spiers JP, Kelso EJ, Zhang ZG. Activation of immune and inflammatory systems in chronic heart failure: novel therapeutic approaches. International journal of clinical practice. 2007;61(4):611-21.

146. Torre-Amione G, Kapadia S, Lee J, Durand JB, Bies RD, Young JB, et al. Tumor necrosis factor-alpha and tumor necrosis factor receptors in the failing human heart. Circulation. 1996;93(4):704-11.
147. McTiernan CF, Lemster BH, Frye C, Brooks S, Combes A, Feldman AM. Interleukin-1 beta inhibits phospholamban gene expression in cultured cardiomyocytes. Circulation research. 1997;81(4):493-503.
148. Sivasubramanian N, Coker ML, Kurrelmeyer KM, MacLellan WR, DeMayo FJ, Spinale FG, et al. Left ventricular remodeling in transgenic mice with cardiac restricted overexpression of tumor necrosis factor. Circulation. 2001;104(7):826-31.
149. Yokoyama T, Nakano M, Bednarczyk JL, McIntyre BW, Entman M, Mann DL. Tumor necrosis factor-alpha provokes a hypertrophic growth response in adult cardiac myocytes. Circulation. 1997;95(5):1247-52.
150. Marber MS, Rose B, Wang Y. The p38 mitogen-activated protein kinase pathway--a potential target for intervention in infarction, hypertrophy, and heart failure. J Mol Cell Cardiol. 2011;51(4):485-90.
151. Denise Martin E, De Nicola GF, Marber MS. New therapeutic targets in cardiology: p38 alpha mitogen-activated protein kinase for ischemic heart disease. Circulation. 2012;126(3):357-68.
152. Behr TM, Nerurkar SS, Nelson AH, Coatney RW, Woods TN, Sulpizio A, et al. Hypertensive end-organ damage and premature mortality are p38 mitogen-activated protein kinase-dependent in a rat model of cardiac hypertrophy and dysfunction. Circulation. 2001;104(11):1292-8.
153. Li M, Georgakopoulos D, Lu G, Hester L, Kass DA, Hasday J, et al. p38 MAP kinase mediates inflammatory cytokine induction in cardiomyocytes and extracellular matrix remodeling in heart. Circulation. 2005;111(19):2494-502.
154. Aukrust P, Sandberg WJ, Otterdal K, Vinge LE, Gullestad L, Yndestad A, et al. Tumor necrosis factor superfamily molecules in acute coronary syndromes. Ann Med. 2011;43(2):90-103.
155. Elkhawad M, Rudd JH, Sarov-Blat L, Cai G, Wells R, Davies LC, et al. Effects of p38 mitogen-activated protein kinase inhibition on vascular and systemic inflammation in patients with atherosclerosis. JACC Cardiovasc Imaging. 2012;5(9):911-22.
156. Hoefen RJ, Berk BC. The role of MAP kinases in endothelial activation. Vascul Pharmacol. 2002;38(5):271-3.
157. Goettsch C, Goettsch W, Muller G, Seebach J, Schnittler HJ, Morawietz H. Nox4 overexpression activates reactive oxygen species and p38 MAPK in human endothelial cells. Biochem Biophys Res Commun. 2009;380(2):355-60.
158. Mann DL. Targeted anticytokine therapy and the failing heart. Am J Cardiol. 2005;95(11A):9C-16C; discussion 38C-40C.
159. Kilberg MS, Pan YX, Chen H, Leung-Pineda V. Nutritional control of gene expression: how mammalian cells respond to amino acid limitation. Annual review of nutrition. 2005;25:59-85.
160. Eriani G, Cavarelli J, Martin F, Ador L, Rees B, Thierry JC, et al. The class II aminoacyl-tRNA synthetases and their active site: evolutionary conservation of an ATP binding site. Journal of molecular evolution. 1995;40(5):499-508.
161. Kerjan P, Triconnet M, Waller JP. Mammalian prolyl-tRNA synthetase corresponds to the approximately 150 kDa subunit of the high-M(r) aminoacyl-tRNA synthetase complex. Biochimie. 1992;74(2):195-205.
162. Ting SM, Bogner P, Dignam JD. Isolation of prolyl-tRNA synthetase as a free form and as a form associated with glutamyl-tRNA synthetase. The Journal of biological chemistry. 1992;267(25):17701-9.

163. Pain VM. Initiation of protein synthesis in eukaryotic cells. European journal of biochemistry / FEBS. 1996;236(3):747-71.
164. Kozak M. Initiation of translation in prokaryotes and eukaryotes. Gene. 1999;234(2):187-208.
165. Algire MA, Lorsch JR. Where to begin? The mechanism of translation initiation codon selection in eukaryotes. Current opinion in chemical biology. 2006;10(5):480-6.
166. Pestova TV, Kolupaeva VG, Lomakin IB, Pilipenko EV, Shatsky IN, Agol VI, et al. Molecular mechanisms of translation initiation in eukaryotes. Proceedings of the National Academy of Sciences of the United States of America. 2001;98(13):7029-36.
167. Wek RC, Jackson BM, Hinnebusch AG. Juxtaposition of domains homologous to protein kinases and histidyl-tRNA synthetases in GCN2 protein suggests a mechanism for coupling GCN4 expression to amino acid availability. Proceedings of the National Academy of Sciences of the United States of America. 1989;86(12):4579-83.
168. Zhu S, Sobolev AY, Wek RC. Histidyl-tRNA synthetase-related sequences in GCN2 protein kinase regulate in vitro phosphorylation of eIF-2. The Journal of biological chemistry. 1996;271(40):24989-94.
169. Lageix S, Zhang J, Rothenburg S, Hinnebusch AG. Interaction between the tRNA-binding and C-terminal domains of Yeast Gcn2 regulates kinase activity in vivo. PLoS genetics. 2015;11(2):e1004991.
170. Dong J, Qiu H, Garcia-Barrio M, Anderson J, Hinnebusch AG. Uncharged tRNA activates GCN2 by displacing the protein kinase moiety from a bipartite tRNA-binding domain. Molecular cell. 2000;6(2):269-79.
171. Qiu H, Hu C, Dong J, Hinnebusch AG. Mutations that bypass tRNA binding activate the intrinsically defective kinase domain in GCN2. Genes & development. 2002;16(10):1271-80.
172. Padyana AK, Qiu H, Roll-Mecak A, Hinnebusch AG, Burley SK. Structural basis for autoinhibition and mutational activation of eukaryotic initiation factor 2alpha protein kinase GCN2. The Journal of biological chemistry. 2005;280(32):29289-99.
173. Garcia-Barrio M, Dong J, Cherkasova VA, Zhang X, Zhang F, Ufano S, et al. Serine 577 is phosphorylated and negatively affects the tRNA binding and eIF2alpha kinase activities of GCN2. The Journal of biological chemistry. 2002;277(34):30675-83.
174. Johnson LN, Noble ME, Owen DJ. Active and inactive protein kinases: structural basis for regulation. Cell. 1996;85(2):149-58.
175. Pavitt GD, Ramaiah KV, Kimball SR, Hinnebusch AG. eIF2 independently binds two distinct eIF2B subcomplexes that catalyze and regulate guanine-nucleotide exchange. Genes & development. 1998;12(4):514-26.
176. Novoa I, Zeng H, Harding HP, Ron D. Feedback inhibition of the unfolded protein response by GADD34-mediated dephosphorylation of eIF2alpha. The Journal of cell biology. 2001;153(5):1011-22.
177. Novoa I, Zhang Y, Zeng H, Jungreis R, Harding HP, Ron D. Stress-induced gene expression requires programmed recovery from translational repression. The EMBO journal. 2003;22(5):1180-7.
178. Brush MH, Weiser DC, Shenolikar S. Growth arrest and DNA damage-inducible protein GADD34 targets protein phosphatase 1 alpha to the endoplasmic reticulum and promotes dephosphorylation of the alpha subunit of eukaryotic translation initiation factor 2. Molecular and cellular biology. 2003;23(4):1292-303.
179. Esposito V, Grosjean F, Tan J, Huang L, Zhu L, Chen J, et al. CHOP deficiency results in elevated lipopolysaccharide-induced inflammation and kidney injury. American journal of physiology Renal physiology. 2013;304(4):F440-50.

180. Yamaguchi H, Wang HG. CHOP is involved in endoplasmic reticulum stress-induced apoptosis by enhancing DR5 expression in human carcinoma cells. The Journal of biological chemistry. 2004;279(44):45495-502.
181. Endo M, Mori M, Akira S, Gotoh T. C/EBP homologous protein (CHOP) is crucial for the induction of caspase-11 and the pathogenesis of lipopolysaccharide-induced inflammation. J Immunol. 2006;176(10):6245-53.
182. Bruhat A, Jousse C, Wang XZ, Ron D, Ferrara M, Fafournoux P. Amino acid limitation induces expression of CHOP, a CCAAT/enhancer binding protein-related gene, at both transcriptional and post-transcriptional levels. The Journal of biological chemistry. 1997;272(28):17588-93.
183. Carraro V, Maurin AC, Lambert-Langlais S, Averous J, Chaveroux C, Parry L, et al. Amino acid availability controls TRB3 transcription in liver through the GCN2/eIF2alpha/ATF4 pathway. PloS one. 2010;5(12):e15716.
184. Nicoletti-Carvalho JE, Nogueira TC, Gorjao R, Bromati CR, Yamanaka TS, Boschero AC, et al. UPR-mediated TRIB3 expression correlates with reduced AKT phosphorylation and inability of interleukin 6 to overcome palmitate-induced apoptosis in RINm5F cells. The Journal of endocrinology. 2010;206(2):183-93.
185. Barbosa-Tessmann IP, Chen C, Zhong C, Siu F, Schuster SM, Nick HS, et al. Activation of the human asparagine synthetase gene by the amino acid response and the endoplasmic reticulum stress response pathways occurs by common genomic elements. The Journal of biological chemistry. 2000;275(35):26976-85.
186. Bruhat A, Jousse C, Carraro V, Reimold AM, Ferrara M, Fafournoux P. Amino acids control mammalian gene transcription: activating transcription factor 2 is essential for the amino acid responsiveness of the CHOP promoter. Molecular and cellular biology. 2000;20(19):7192-204.
187. Averous J, Bruhat A, Jousse C, Carraro V, Thiel G, Fafournoux P. Induction of CHOP expression by amino acid limitation requires both ATF4 expression and ATF2 phosphorylation. The Journal of biological chemistry. 2004;279(7):5288-97.
188. Su N, Kilberg MS. C/EBP homology protein (CHOP) interacts with activating transcription factor 4 (ATF4) and negatively regulates the stress-dependent induction of the asparagine synthetase gene. The Journal of biological chemistry. 2008;283(50):35106-17.
189. Guo L, Li X, Tang QQ. Transcriptional regulation of adipocyte differentiation: a central role for CCAAT/enhancer-binding protein (C/EBP) beta. The Journal of biological chemistry. 2015;290(2):755-61.
190. Tominaga H, Maeda S, Hayashi M, Takeda S, Akira S, Komiya S, et al. CCAAT/enhancer-binding protein beta promotes osteoblast differentiation by enhancing Runx2 activity with ATF4. Molecular biology of the cell. 2008;19(12):5373-86.
191. Yu X, Si J, Zhang Y, Dewille JW. CCAAT/Enhancer Binding Protein-delta (C/EBP-delta) regulates cell growth, migration and differentiation. Cancer cell international. 2010;10:48.
192. Ron D, Habener JF. CHOP, a novel developmentally regulated nuclear protein that dimerizes with transcription factors C/EBP and LAP and functions as a dominant-negative inhibitor of gene transcription. Genes & development. 1992;6(3):439-53.
193. Landschulz WH, Johnson PF, McKnight SL. The DNA binding domain of the rat liver nuclear protein C/EBP is bipartite. Science. 1989;243(4899):1681-8.
194. Wang XZ, Kuroda M, Sok J, Batchvarova N, Kimmel R, Chung P, et al. Identification of novel stress-induced genes downstream of chop. The EMBO journal. 1998;17(13):3619-30.

195. Ohoka N, Yoshii S, Hattori T, Onozaki K, Hayashi H. TRB3, a novel ER stress-inducible gene, is induced via ATF4-CHOP pathway and is involved in cell death. The EMBO journal. 2005;24(6):1243-55.
196. Ord D, Ord T. Mouse NIPK interacts with ATF4 and affects its transcriptional activity. Experimental cell research. 2003;286(2):308-20.
197. Bezy O, Vernochet C, Gesta S, Farmer SR, Kahn CR. TRB3 blocks adipocyte differentiation through the inhibition of C/EBPbeta transcriptional activity. Molecular and cellular biology. 2007;27(19):6818-31.
198. Jousse C, Deval C, Maurin AC, Parry L, Cherasse Y, Chaveroux C, et al. TRB3 inhibits the transcriptional activation of stress-regulated genes by a negative feedback on the ATF4 pathway. The Journal of biological chemistry. 2007;282(21):15851-61.
199. Prudente S, Hribal ML, Flex E, Turchi F, Morini E, De Cosmo S, et al. The functional Q84R polymorphism of mammalian Tribbles homolog TRB3 is associated with insulin resistance and related cardiovascular risk in Caucasians from Italy. Diabetes. 2005;54(9):2807-11.
200. Bussolati O, Belletti S, Uggeri J, Gatti R, Orlandini G, Dall'Asta V, et al. Characterization of apoptotic phenomena induced by treatment with L-asparaginase in NIH3T3 cells. Experimental cell research. 1995;220(2):283-91.
201. Story MD, Voehringer DW, Stephens LC, Meyn RE. L-asparaginase kills lymphoma cells by apoptosis. Cancer chemotherapy and pharmacology. 1993;32(2):129-33.
202. Kaufman RJ. Stress signaling from the lumen of the endoplasmic reticulum: coordination of gene transcriptional and translational controls. Genes & development. 1999;13(10):1211-33.
203. Koepfli JB, Mead JF, Brockman JA, Jr. An alkaloid with high antimalarial activity from Dichroa febrifuga. Journal of the American Chemical Society. 1947;69(7):1837.
204. Keller TL, Zocco D, Sundrud MS, Hendrick M, Edenius M, Yum J, et al. Halofuginone and other febrifugine derivatives inhibit prolyl-tRNA synthetase. Nature chemical biology. 2012;8(3):311-7.
205. Pines M, Snyder D, Yarkoni S, Nagler A. Halofuginone to treat fibrosis in chronic graft-versus-host disease and scleroderma. Biology of blood and marrow transplantation : journal of the American Society for Blood and Marrow Transplantation. 2003;9(7):417-25.
206. Pines M, Nagler A. Halofuginone: a novel antifibrotic therapy. General pharmacology. 1998;30(4):445-50.
207. Elkin M, Ariel I, Miao HQ, Nagler A, Pines M, de-Groot N, et al. Inhibition of bladder carcinoma angiogenesis, stromal support, and tumor growth by halofuginone. Cancer research. 1999;59(16):4111-8.
208. Koon HB, Fingleton B, Lee JY, Geyer JT, Cesarman E, Parise RA, et al. Phase II AIDS Malignancy Consortium trial of topical halofuginone in AIDS-related Kaposi sarcoma. J Acquir Immune Defic Syndr. 2011;56(1):64-8.
209. Sundrud MS, Koralov SB, Feuerer M, Calado DP, Kozhaya AE, Rhule-Smith A, et al. Halofuginone inhibits TH17 cell differentiation by activating the amino acid starvation response. Science. 2009;324(5932):1334-8.
210. Zhou H, Sun L, Yang XL, Schimmel P. ATP-directed capture of bioactive herbal-based medicine on human tRNA synthetase. Nature. 2013;494(7435):121-4.
211. Cox TR, Erler JT. Remodeling and homeostasis of the extracellular matrix: implications for fibrotic diseases and cancer. Disease models & mechanisms. 2011;4(2):165-78.

212. Ra HJ, Parks WC. Control of matrix metalloproteinase catalytic activity. Matrix biology : journal of the International Society for Matrix Biology. 2007;26(8):587-96.
213. Nagler A, Firman N, Feferman R, Cotev S, Pines M, Shoshan S. Reduction in pulmonary fibrosis in vivo by halofuginone. American journal of respiratory and critical care medicine. 1996;154(4 Pt 1):1082-6.
214. Nagler A, Gofrit O, Ohana M, Pode D, Genina O, Pines M. The effect of halofuginone, an inhibitor of collagen type i synthesis, on urethral stricture formation: in vivo and in vitro study in a rat model. The Journal of urology. 2000;164(5):1776-80.
215. Levi-Schaffer F, Nagler A, Slavin S, Knopov V, Pines M. Inhibition of collagen synthesis and changes in skin morphology in murine graft-versus-host disease and tight skin mice: effect of halofuginone. The Journal of investigative dermatology. 1996;106(1):84-8.
216. Bruck R, Genina O, Aeed H, Alexiev R, Nagler A, Avni Y, et al. Halofuginone to prevent and treat thioacetamide-induced liver fibrosis in rats. Hepatology. 2001;33(2):379-86.
217. Nagler A, Rivkind AI, Raphael J, Levi-Schaffer F, Genina O, Lavelin I, et al. Halofuginone--an inhibitor of collagen type I synthesis--prevents postoperative formation of abdominal adhesions. Annals of surgery. 1998;227(4):575-82.
218. Karakoyun B, Yuksel M, Ercan F, Salva E, Isik I, Yegen BC. Halofuginone, a specific inhibitor of collagen type 1 synthesis, ameliorates oxidant colonic damage in rats with experimental colitis. Digestive diseases and sciences. 2010;55(3):607-16.
219. Blake DJ, Weir A, Newey SE, Davies KE. Function and genetics of dystrophin and dystrophin-related proteins in muscle. Physiological reviews. 2002;82(2):291-329.
220. Cox GF, Kunkel LM. Dystrophies and heart disease. Current opinion in cardiology. 1997;12(3):329-43.
221. Nigro G, Comi LI, Politano L, Bain RJ. The incidence and evolution of cardiomyopathy in Duchenne muscular dystrophy. International journal of cardiology. 1990;26(3):271-7.
222. Huebner KD, Jassal DS, Halevy O, Pines M, Anderson JE. Functional resolution of fibrosis in mdx mouse dystrophic heart and skeletal muscle by halofuginone. Am J Physiol Heart Circ Physiol. 2008;294(4):H1550-61.
223. Roffe S, Hagai Y, Pines M, Halevy O. Halofuginone inhibits Smad3 phosphorylation via the PI3K/Akt and MAPK/ERK pathways in muscle cells: effect on myotube fusion. Experimental cell research. 2010;316(6):1061-9.
224. Schieven GL. The biology of p38 kinase: a central role in inflammation. Current topics in medicinal chemistry. 2005;5(10):921-8.
225. Leiba M, Cahalon L, Shimoni A, Lider O, Zanin-Zhorov A, Hecht I, et al. Halofuginone inhibits NF-kappaB and p38 MAPK in activated T cells. Journal of leukocyte biology. 2006;80(2):399-406.
226. Popov Y, Patsenker E, Bauer M, Niedobitek E, Schulze-Krebs A, Schuppan D. Halofuginone induces matrix metalloproteinases in rat hepatic stellate cells via activation of p38 and NFkappaB. The Journal of biological chemistry. 2006;281(22):15090-8.
227. Yanagisawa M, Kurihara H, Kimura S, Tomobe Y, Kobayashi M, Mitsui Y, et al. A novel potent vasoconstrictor peptide produced by vascular endothelial cells. Nature. 1988;332(6163):411-5.
228. Inoue A, Yanagisawa M, Kimura S, Kasuya Y, Miyauchi T, Goto K, et al. The human endothelin family: three structurally and pharmacologically distinct isopeptides predicted by three separate genes. Proceedings of the National Academy of Sciences of the United States of America. 1989;86(8):2863-7.

229. Seo B, Oemar BS, Siebenmann R, von Segesser L, Luscher TF. Both ETA and ETB receptors mediate contraction to endothelin-1 in human blood vessels. Circulation. 1994;89(3):1203-8.
230. Bacon CR, Cary NR, Davenport AP. Endothelin peptide and receptors in human atherosclerotic coronary artery and aorta. Circulation research. 1996;79(4):794-801.
231. Masaki T. Possible role of endothelin in endothelial regulation of vascular tone. Annual review of pharmacology and toxicology. 1995;35:235-55.
232. Olson KR, Duff DW, Farrell AP, Keen J, Kellogg MD, Kullman D, et al. Cardiovascular effects of endothelin in trout. The American journal of physiology. 1991;260(4 Pt 2):H1214-23.
233. Yanagisawa M, Masaki T. Endothelin, a novel endothelium-derived peptide. Pharmacological activities, regulation and possible roles in cardiovascular control. Biochemical pharmacology. 1989;38(12):1877-83.
234. Cozza EN, Chiou S, Gomez-Sanchez CE. Endothelin-1 potentiation of angiotensin II stimulation of aldosterone production. The American journal of physiology. 1992;262(1 Pt 2):R85-9.
235. Ahlborg G, Weitzberg E, Lundberg JM. Circulating endothelin-1 reduces splanchnic and renal blood flow and splanchnic glucose production in humans. Journal of applied physiology. 1995;79(1):141-5.
236. Uusimaa PA, Hassinen IE, Vuolteenaho O, Ruskoaho H. Endothelin-induced atrial natriuretic peptide release from cultured neonatal cardiac myocytes: the role of extracellular calcium and protein kinase-C. Endocrinology. 1992;130(5):2455-64.
237. Wu-Wong JR, Chiou WJ, Dixon DB, Opgenorth TJ. Dissociation characteristics of endothelin ETA receptor agonists and antagonists. Journal of cardiovascular pharmacology. 1995;26 Suppl 3:S380-4.
238. Wang J, Chiou WJ, Gagne GD, Wu-Wong JR. Internalization of type-A endothelin receptor. Journal of cardiovascular pharmacology. 2000;36(5 Suppl 1):S61-5.
239. Bremnes T, Paasche JD, Mehlum A, Sandberg C, Bremnes B, Attramadal H. Regulation and intracellular trafficking pathways of the endothelin receptors. The Journal of biological chemistry. 2000;275(23):17596-604.
240. Rao VR, Krishnamoorthy RR, Yorio T. Endothelin-1, endothelin A and B receptor expression and their pharmacological properties in GFAP negative human lamina cribrosa cells. Experimental eye research. 2007;84(6):1115-24.
241. Parker JD, Thiessen JJ. Increased endothelin-1 production in patients with chronic heart failure. American journal of physiology Heart and circulatory physiology. 2004;286(3):H1141-5.
242. Schiffrin EL. Role of endothelin-1 in hypertension and vascular disease. American journal of hypertension. 2001;14(6 Pt 2):83S-9S.
243. Agapitov AV, Haynes WG. Role of endothelin in cardiovascular disease. Journal of the renin-angiotensin-aldosterone system : JRAAS. 2002;3(1):1-15.
244. Miyauchi T, Masaki T. Pathophysiology of endothelin in the cardiovascular system. Annual review of physiology. 1999;61:391-415.
245. Sakai S, Yorikane R, Miyauchi T, Sakurai T, Kasuya Y, Yamaguchi I, et al. Altered production of endothelin-1 in the hypertrophied rat heart. Journal of cardiovascular pharmacology. 1995;26 Suppl 3:S452-5.
246. Tonnessen T, Christensen G, Oie E, Holt E, Kjekshus H, Smiseth OA, et al. Increased cardiac expression of endothelin-1 mRNA in ischemic heart failure in rats. Cardiovascular research. 1997;33(3):601-10.

247. Cody RJ, Haas GJ, Binkley PF, Capers Q, Kelley R. Plasma endothelin correlates with the extent of pulmonary hypertension in patients with chronic congestive heart failure. Circulation. 1992;85(2):504-9.
248. Kinugawa T, Kato M, Ogino K, Osaki S, Igawa O, Hisatome I, et al. Plasma endothelin-1 levels and clinical correlates in patients with chronic heart failure. Journal of cardiac failure. 2003;9(4):318-24.
249. Roskoski R, Jr. Assays of protein kinase. Methods in enzymology. 1983;99:3-6.
250. Mullis K, Faloona F, Scharf S, Saiki R, Horn G, Erlich H. Specific enzymatic amplification of DNA in vitro: the polymerase chain reaction. Cold Spring Harbor symposia on quantitative biology. 1986;51 Pt 1:263-73.
251. Mullis KB. Target amplification for DNA analysis by the polymerase chain reaction. Annales de biologie clinique. 1990;48(8):579-82.
252. Hanahan D. Studies on transformation of Escherichia coli with plasmids. Journal of molecular biology. 1983;166(4):557-80.
253. Graham FL, Smiley J, Russell WC, Nairn R. Characteristics of a human cell line transformed by DNA from human adenovirus type 5. The Journal of general virology. 1977;36(1):59-74.
254. Louis N, Evelegh C, Graham FL. Cloning and sequencing of the cellular-viral junctions from the human adenovirus type 5 transformed 293 cell line. Virology. 1997;233(2):423-9.
255. Shaw G, Morse S, Ararat M, Graham FL. Preferential transformation of human neuronal cells by human adenoviruses and the origin of HEK 293 cells. FASEB journal : official publication of the Federation of American Societies for Experimental Biology. 2002;16(8):869-71.
256. Thomas P, Smart TG. HEK293 cell line: a vehicle for the expression of recombinant proteins. Journal of pharmacological and toxicological methods. 2005;51(3):187-200.
257. Kimes BW, Brandt BL. Properties of a clonal muscle cell line from rat heart. Experimental cell research. 1976;98(2):367-81.
258. Wu ML, Tsai KL, Wang SM, Wu JC, Wang BS, Lee YT. Mechanism of hydrogen peroxide and hydroxyl free radical-induced intracellular acidification in cultured rat cardiac myoblasts. Circulation research. 1996;78(4):564-72.
259. Mestril R, Chi SH, Sayen MR, O'Reilly K, Dillmann WH. Expression of inducible stress protein 70 in rat heart myogenic cells confers protection against simulated ischemia-induced injury. The Journal of clinical investigation. 1994;93(2):759-67.
260. Levy JA. The multifaceted retrovirus. Cancer research. 1986;46(11):5457-68.
261. Freeman WM, Walker SJ, Vrana KE. Quantitative RT-PCR: pitfalls and potential. BioTechniques. 1999;26(1):112-22, 24-5.
262. Garcia-Calvo M, Peterson EP, Rasper DM, Vaillancourt JP, Zamboni R, Nicholson DW, et al. Purification and catalytic properties of human caspase family members. Cell death and differentiation. 1999;6(4):362-9.
263. Nicholson DW, Thornberry NA. Caspases: killer proteases. Trends in biochemical sciences. 1997;22(8):299-306.
264. Spirin PV, Vil'gelm AE, Prasolov VS. [Lentiviral vectors]. Molekuliarnaia biologiia. 2008;42(5):913-26.
265. Li M, Husic N, Lin Y, Snider BJ. Production of lentiviral vectors for transducing cells from the central nervous system. Journal of visualized experiments : JoVE. 2012(63):e4031.

266. Naldini L, Blomer U, Gallay P, Ory D, Mulligan R, Gage FH, et al. In vivo gene delivery and stable transduction of nondividing cells by a lentiviral vector. Science. 1996;272(5259):263-7.
267. Zufferey R, Dull T, Mandel RJ, Bukovsky A, Quiroz D, Naldini L, et al. Self-inactivating lentivirus vector for safe and efficient in vivo gene delivery. Journal of virology. 1998;72(12):9873-80.
268. Davidson BL, Breakefield XO. Viral vectors for gene delivery to the nervous system. Nature reviews Neuroscience. 2003;4(5):353-64.
269. Segura MM, Garnier A, Durocher Y, Coelho H, Kamen A. Production of lentiviral vectors by large-scale transient transfection of suspension cultures and affinity chromatography purification. Biotechnology and bioengineering. 2007;98(4):789-99.
270. Gama-Norton L, Botezatu L, Herrmann S, Schweizer M, Alves PM, Hauser H, et al. Lentivirus production is influenced by SV40 large T-antigen and chromosomal integration of the vector in HEK293 cells. Human gene therapy. 2011;22(10):1269-79.
271. Liang Y. Applications of isothermal titration calorimetry in protein science. Acta biochimica et biophysica Sinica. 2008;40(7):565-76.
272. Ladbury JE, Chowdhry BZ. Sensing the heat: the application of isothermal titration calorimetry to thermodynamic studies of biomolecular interactions. Chemistry & biology. 1996;3(10):791-801.
273. Masters SC. Co-immunoprecipitation from transfected cells. Methods Mol Biol. 2004;261:337-50.
274. Bachelard HS, Cox DW, Morris PG. Nuclear magnetic resonance as a tool to study brain metabolism. Gerontology. 1987;33(3-4):235-46.
275. Park JB, Fan CL, Hoffman BM, Adams MW. Potentiometric and electron nuclear double resonance properties of the two spin forms of the [4Fe-4S]+ cluster in the novel ferredoxin from the hyperthermophilic archaebacterium Pyrococcus furiosus. The Journal of biological chemistry. 1991;266(29):19351-6.
276. Yasuda J, Whitmarsh AJ, Cavanagh J, Sharma M, Davis RJ. The JIP group of mitogen-activated protein kinase scaffold proteins. Molecular and cellular biology. 1999;19(10):7245-54.
277. Sharrocks AD, Yang SH, Galanis A. Docking domains and substrate-specificity determination for MAP kinases. Trends in biochemical sciences. 2000;25(9):448-53.
278. Chang CI, Xu BE, Akella R, Cobb MH, Goldsmith EJ. Crystal structures of MAP kinase p38 complexed to the docking sites on its nuclear substrate MEF2A and activator MKK3b. Molecular cell. 2002;9(6):1241-9.
279. Cheung PC, Campbell DG, Nebreda AR, Cohen P. Feedback control of the protein kinase TAK1 by SAPK2a/p38alpha. The EMBO journal. 2003;22(21):5793-805.
280. Everett AW, Sinha AM, Umeda PK, Jakovcic S, Rabinowitz M, Zak R. Regulation of myosin synthesis by thyroid hormone: relative change in the alpha- and beta-myosin heavy chain mRNA levels in rabbit heart. Biochemistry. 1984;23(8):1596-9.
281. Allen DL, Leinwand LA. Postnatal myosin heavy chain isoform expression in normal mice and mice null for IIb or IId myosin heavy chains. Developmental biology. 2001;229(2):383-95.
282. Harada K, Sugaya T, Murakami K, Yazaki Y, Komuro I. Angiotensin II type 1A receptor knockout mice display less left ventricular remodeling and improved survival after myocardial infarction. Circulation. 1999;100(20):2093-9.
283. Herron TJ, McDonald KS. Small amounts of alpha-myosin heavy chain isoform expression significantly increase power output of rat cardiac myocyte fragments. Circulation research. 2002;90(11):1150-2.

284. Sugiura S, Kobayakawa N, Fujita H, Yamashita H, Momomura S, Chaen S, et al. Comparison of unitary displacements and forces between 2 cardiac myosin isoforms by the optical trap technique: molecular basis for cardiac adaptation. Circulation research. 1998;82(10):1029-34.
285. Abraham WT, Gilbert EM, Lowes BD, Minobe WA, Larrabee P, Roden RL, et al. Coordinate changes in Myosin heavy chain isoform gene expression are selectively associated with alterations in dilated cardiomyopathy phenotype. Molecular medicine. 2002;8(11):750-60.
286. Razeghi P, Young ME, Alcorn JL, Moravec CS, Frazier OH, Taegtmeyer H. Metabolic gene expression in fetal and failing human heart. Circulation. 2001;104(24):2923-31.
287. Horio T, Nishikimi T, Yoshihara F, Matsuo H, Takishita S, Kangawa K. Inhibitory regulation of hypertrophy by endogenous atrial natriuretic peptide in cultured cardiac myocytes. Hypertension. 2000;35(1 Pt 1):19-24.
288. Lu Z, Xu X, Fassett J, Kwak D, Liu X, Hu X, et al. Loss of the eukaryotic initiation factor 2alpha kinase general control nonderepressible 2 protects mice from pressure overload-induced congestive heart failure without affecting ventricular hypertrophy. Hypertension. 2014;63(1):128-35.
289. Pankiv S, Clausen TH, Lamark T, Brech A, Bruun JA, Outzen H, et al. p62/SQSTM1 binds directly to Atg8/LC3 to facilitate degradation of ubiquitinated protein aggregates by autophagy. The Journal of biological chemistry. 2007;282(33):24131-45.
290. Komatsu M, Waguri S, Koike M, Sou YS, Ueno T, Hara T, et al. Homeostatic levels of p62 control cytoplasmic inclusion body formation in autophagy-deficient mice. Cell. 2007;131(6):1149-63.
291. Chan TO, Zhang J, Rodeck U, Pascal JM, Armen RS, Spring M, et al. Resistance of Akt kinases to dephosphorylation through ATP-dependent conformational plasticity. Proceedings of the National Academy of Sciences of the United States of America. 2011;108(46):E1120-7.
292. Okuzumi T, Fiedler D, Zhang C, Gray DC, Aizenstein B, Hoffman R, et al. Inhibitor hijacking of Akt activation. Nature chemical biology. 2009;5(7):484-93.
293. Deval C, Chaveroux C, Maurin AC, Cherasse Y, Parry L, Carraro V, et al. Amino acid limitation regulates the expression of genes involved in several specific biological processes through GCN2-dependent and GCN2-independent pathways. FEBS J. 2009;276(3):707-18.
294. Wang XZ, Ron D. Stress-induced phosphorylation and activation of the transcription factor CHOP (GADD153) by p38 MAP Kinase. Science. 1996;272(5266):1347-9.
295. Marciniak SJ, Yun CY, Oyadomari S, Novoa I, Zhang Y, Jungreis R, et al. CHOP induces death by promoting protein synthesis and oxidation in the stressed endoplasmic reticulum. Genes & development. 2004;18(24):3066-77.
296. Oh-Hashi K, Maruyama W, Isobe K. Peroxynitrite induces GADD34, 45, and 153 VIA p38 MAPK in human neuroblastoma SH-SY5Y cells. Free Radic Biol Med. 2001;30(2):213-21.
297. Young PR, McLaughlin MM, Kumar S, Kassis S, Doyle ML, McNulty D, et al. Pyridinyl imidazole inhibitors of p38 mitogen-activated protein kinase bind in the ATP site. The Journal of biological chemistry. 1997;272(18):12116-21.
298. Morel C, Ibarz G, Oiry C, Carnazzi E, Berge G, Gagne D, et al. Cross-interactions of two p38 mitogen-activated protein (MAP) kinase inhibitors and two cholecystokinin (CCK) receptor antagonists with the CCK1 receptor and p38 MAP kinase. The Journal of biological chemistry. 2005;280(22):21384-93.

299. Kumar S, Jiang MS, Adams JL, Lee JC. Pyridinylimidazole compound SB 203580 inhibits the activity but not the activation of p38 mitogen-activated protein kinase. Biochem Biophys Res Commun. 1999;263(3):825-31.
300. Eyers PA, Craxton M, Morrice N, Cohen P, Goedert M. Conversion of SB 203580-insensitive MAP kinase family members to drug-sensitive forms by a single amino-acid substitution. Chemistry & biology. 1998;5(6):321-8.
301. Gum RJ, McLaughlin MM, Kumar S, Wang Z, Bower MJ, Lee JC, et al. Acquisition of sensitivity of stress-activated protein kinases to the p38 inhibitor, SB 203580, by alteration of one or more amino acids within the ATP binding pocket. The Journal of biological chemistry. 1998;273(25):15605-10.
302. Zhou H, Zheng M, Chen J, Xie C, Kolatkar AR, Zarubin T, et al. Determinants that control the specific interactions between TAB1 and p38alpha. Molecular and cellular biology. 2006;26(10):3824-34.
303. Shibuya H, Yamaguchi K, Shirakabe K, Tonegawa A, Gotoh Y, Ueno N, et al. TAB1: an activator of the TAK1 MAPKKK in TGF-beta signal transduction. Science. 1996;272(5265):1179-82.
304. Sakurai H, Miyoshi H, Mizukami J, Sugita T. Phosphorylation-dependent activation of TAK1 mitogen-activated protein kinase kinase kinase by TAB1. FEBS letters. 2000;474(2-3):141-5.
305. Mann DL. Stress-activated cytokines and the heart: from adaptation to maladaptation. Annual review of physiology. 2003;65:81-101.
306. Dinarello CA, Pomerantz BJ. Proinflammatory cytokines in heart disease. Blood purification. 2001;19(3):314-21.
307. Force T, Hajjar R, Del Monte F, Rosenzweig A, Choukroun G. Signaling pathways mediating the response to hypertrophic stress in the heart. Gene expression. 1999;7(4-6):337-48.
308. Bogoyevitch MA. Signalling via stress-activated mitogen-activated protein kinases in the cardiovascular system. Cardiovascular research. 2000;45(4):826-42.
309. Stewart DJ, Kubac G, Costello KB, Cernacek P. Increased plasma endothelin-1 in the early hours of acute myocardial infarction. Journal of the American College of Cardiology. 1991;18(1):38-43.
310. Neunteufl T, Berger R, Pacher R. Endothelin receptor antagonists in cardiology clinical trials. Expert opinion on investigational drugs. 2002;11(3):431-43.
311. Neuhold S, Huelsmann M, Strunk G, Struck J, Adlbrecht C, Gouya G, et al. Prognostic value of emerging neurohormones in chronic heart failure during optimization of heart failure-specific therapy. Clinical chemistry. 2010;56(1):121-6.
312. Murphy GA, Fiuzat M, Bristow MR. Targeting heart failure therapeutics: a historical perspective. Heart failure clinics. 2010;6(1):11-23.
313. Clozel M, Breu V, Burri K, Cassal JM, Fischli W, Gray GA, et al. Pathophysiological role of endothelin revealed by the first orally active endothelin receptor antagonist. Nature. 1993;365(6448):759-61.
314. Suzuki T, Hoshi H, Mitsui Y. Endothelin stimulates hypertrophy and contractility of neonatal rat cardiac myocytes in a serum-free medium. FEBS letters. 1990;268(1):149-51.
315. Irukayama-Tomobe Y, Miyauchi T, Sakai S, Kasuya Y, Ogata T, Takanashi M, et al. Endothelin-1-induced cardiac hypertrophy is inhibited by activation of peroxisome proliferator-activated receptor-alpha partly via blockade of c-Jun NH2-terminal kinase pathway. Circulation. 2004;109(7):904-10.
316. Bruneau BG, de Bold AJ. Selective changes in natriuretic peptide and early response gene expression in isolated rat atria following stimulation by stretch or endothelin-1. Cardiovascular research. 1994;28(10):1519-25.

317. Sakai S, Miyauchi T, Yamaguchi I. Long-term endothelin receptor antagonist administration improves alterations in expression of various cardiac genes in failing myocardium of rats with heart failure. Circulation. 2000;101(24):2849-53.
318. Shimoyama H, Sabbah HN, Borzak S, Tanimura M, Shevlyagin S, Scicli G, et al. Short-term hemodynamic effects of endothelin receptor blockade in dogs with chronic heart failure. Circulation. 1996;94(4):779-84.
319. Kiowski W, Sutsch G, Hunziker P, Muller P, Kim J, Oechslin E, et al. Evidence for endothelin-1-mediated vasoconstriction in severe chronic heart failure. Lancet. 1995;346(8977):732-6.
320. Mulder P, Richard V, Derumeaux G, Hogie M, Henry JP, Lallemand F, et al. Role of endogenous endothelin in chronic heart failure: effect of long-term treatment with an endothelin antagonist on survival, hemodynamics, and cardiac remodeling. Circulation. 1997;96(6):1976-82.
321. Cowburn PJ, Cleland JG, McArthur JD, MacLean MR, McMurray JJ, Dargie HJ. Short-term haemodynamic effects of BQ-123, a selective endothelin ET(A)-receptor antagonist, in chronic heart failure. Lancet. 1998;352(9123):201-2.
322. Kalra PR, Moon JC, Coats AJ. Do results of the ENABLE (Endothelin Antagonist Bosentan for Lowering Cardiac Events in Heart Failure) study spell the end for non-selective endothelin antagonism in heart failure? International journal of cardiology. 2002;85(2-3):195-7.
323. McMurray JJ, Ray SG, Abdullah I, Dargie HJ, Morton JJ. Plasma endothelin in chronic heart failure. Circulation. 1992;85(4):1374-9.
324. Sagnella GA. Measurement and significance of circulating natriuretic peptides in cardiovascular disease. Clinical science. 1998;95(5):519-29.
325. Nishikimi T, Maeda N, Matsuoka H. The role of natriuretic peptides in cardioprotection. Cardiovascular research. 2006;69(2):318-28.
326. Yoshimura M, Yasue H, Morita E, Sakaino N, Jougasaki M, Kurose M, et al. Hemodynamic, renal, and hormonal responses to brain natriuretic peptide infusion in patients with congestive heart failure. Circulation. 1991;84(4):1581-8.
327. Clarkson PB, Wheeldon NM, MacFadyen RJ, Pringle SD, MacDonald TM. Effects of brain natriuretic peptide on exercise hemodynamics and neurohormones in isolated diastolic heart failure. Circulation. 1996;93(11):2037-42.
328. Sakai S, Miyauchi T, Kobayashi T, Yamaguchi I, Goto K, Sugishita Y. Altered expression of isoforms of myosin heavy chain mRNA in the failing rat heart is ameliorated by chronic treatment with an endothelin receptor antagonist. Journal of cardiovascular pharmacology. 1998;31 Suppl 1:S302-5.
329. Shimomura H, Terasaki F, Hayashi T, Kitaura Y, Isomura T, Suma H. Autophagic degeneration as a possible mechanism of myocardial cell death in dilated cardiomyopathy. Japanese circulation journal. 2001;65(11):965-8.
330. Nakaoka M, Iwai-Kanai E, Katamura M, Okawa Y, Mita Y, Matoba S. An alpha-adrenergic agonist protects hearts by inducing Akt1-mediated autophagy. Biochemical and biophysical research communications. 2015;456(1):250-6.
331. Zhu H, Tannous P, Johnstone JL, Kong Y, Shelton JM, Richardson JA, et al. Cardiac autophagy is a maladaptive response to hemodynamic stress. The Journal of clinical investigation. 2007;117(7):1782-93.
332. Kim J, Kundu M, Viollet B, Guan KL. AMPK and mTOR regulate autophagy through direct phosphorylation of Ulk1. Nature cell biology. 2011;13(2):132-41.
333. Ogata M, Hino S, Saito A, Morikawa K, Kondo S, Kanemoto S, et al. Autophagy is activated for cell survival after endoplasmic reticulum stress. Molecular and cellular biology. 2006;26(24):9220-31.

334. Kroemer G, Marino G, Levine B. Autophagy and the integrated stress response. Molecular cell. 2010;40(2):280-93.
335. Rzymski T, Milani M, Pike L, Buffa F, Mellor HR, Winchester L, et al. Regulation of autophagy by ATF4 in response to severe hypoxia. Oncogene. 2010;29(31):4424-35.
336. Talloczy Z, Jiang W, Virgin HWt, Leib DA, Scheuner D, Kaufman RJ, et al. Regulation of starvation- and virus-induced autophagy by the eIF2alpha kinase signaling pathway. Proceedings of the National Academy of Sciences of the United States of America. 2002;99(1):190-5.
337. Ye J, Kumanova M, Hart LS, Sloane K, Zhang H, De Panis DN, et al. The GCN2-ATF4 pathway is critical for tumour cell survival and proliferation in response to nutrient deprivation. The EMBO journal. 2010;29(12):2082-96.
338. Milani M, Rzymski T, Mellor HR, Pike L, Bottini A, Generali D, et al. The role of ATF4 stabilization and autophagy in resistance of breast cancer cells treated with Bortezomib. Cancer research. 2009;69(10):4415-23.
339. Behrends C, Sowa ME, Gygi SP, Harper JW. Network organization of the human autophagy system. Nature. 2010;466(7302):68-76.
340. De Duve C, Wattiaux R. Functions of lysosomes. Annual review of physiology. 1966;28:435-92.
341. Wolfe DM, Lee JH, Kumar A, Lee S, Orenstein SJ, Nixon RA. Autophagy failure in Alzheimer's disease and the role of defective lysosomal acidification. The European journal of neuroscience. 2013;37(12):1949-61.
342. Shintani T, Klionsky DJ. Autophagy in health and disease: a double-edged sword. Science. 2004;306(5698):990-5.
343. Xavier S, Piek E, Fujii M, Javelaud D, Mauviel A, Flanders KC, et al. Amelioration of radiation-induced fibrosis: inhibition of transforming growth factor-beta signaling by halofuginone. The Journal of biological chemistry. 2004;279(15):15167-76.
344. Nelson EF, Huang CW, Ewel JM, Chang AA, Yuan C. Halofuginone down-regulates Smad3 expression and inhibits the TGFbeta-induced expression of fibrotic markers in human corneal fibroblasts. Molecular vision. 2012;18:479-87.
345. Tsukada S, Westwick JK, Ikejima K, Sato N, Rippe RA. SMAD and p38 MAPK signaling pathways independently regulate alpha1(I) collagen gene expression in unstimulated and transforming growth factor-beta-stimulated hepatic stellate cells. The Journal of biological chemistry. 2005;280(11):10055-64.
346. Kormoczy PS, Vertesi C, Mikus E, Tardos L, Kovacs G. Cardioprotective effect of prostacyclin and 7-oxo-PGI2 in rats against chronic isoproterenol damage. Prostaglandins. 1987;33(4):505-16.
347. Fetalvero KM, Martin KA, Hwa J. Cardioprotective prostacyclin signaling in vascular smooth muscle. Prostaglandins & other lipid mediators. 2007;82(1-4):109-18.
348. Bing RJ, Yamamoto T, Yamamoto M, Kakar R, Cohen A. New look at myocardial infarction: toward a better aspirin. Cardiovascular research. 1999;43(1):25-31.
349. Bing RJ, Lomnicka M. Why do cyclo-oxygenase-2 inhibitors cause cardiovascular events? Journal of the American College of Cardiology. 2002;39(3):521-2.
350. Wollert KC, Drexler H. The role of interleukin-6 in the failing heart. Heart failure reviews. 2001;6(2):95-103.
351. MacGowan GA, Mann DL, Kormos RL, Feldman AM, Murali S. Circulating interleukin-6 in severe heart failure. The American journal of cardiology. 1997;79(8):1128-31.

352. Tsutamoto T, Hisanaga T, Wada A, Maeda K, Ohnishi M, Fukai D, et al. Interleukin-6 spillover in the peripheral circulation increases with the severity of heart failure, and the high plasma level of interleukin-6 is an important prognostic predictor in patients with congestive heart failure. Journal of the American College of Cardiology. 1998;31(2):391-8.
353. Cheng H, Tian J, Zeng L, Pan B, Li Z, Song G, et al. Halofugine prevents cutaneous graft versus host disease by suppression of Th17 differentiation. Hematology. 2012;17(5):261-7.
354. Galea J, Armstrong J, Gadsdon P, Holden H, Francis SE, Holt CM. Interleukin-1 beta in coronary arteries of patients with ischemic heart disease. Arteriosclerosis, thrombosis, and vascular biology. 1996;16(8):1000-6.
355. Chi H, Messas E, Levine RA, Graves DT, Amar S. Interleukin-1 receptor signaling mediates atherosclerosis associated with bacterial exposure and/or a high-fat diet in a murine apolipoprotein E heterozygote model: pharmacotherapeutic implications. Circulation. 2004;110(12):1678-85.
356. Bhaskar V, Yin J, Mirza AM, Phan D, Vanegas S, Issafras H, et al. Monoclonal antibodies targeting IL-1 beta reduce biomarkers of atherosclerosis in vitro and inhibit atherosclerotic plaque formation in Apolipoprotein E-deficient mice. Atherosclerosis. 2011;216(2):313-20.
357. Ridker PM, Thuren T, Zalewski A, Libby P. Interleukin-1beta inhibition and the prevention of recurrent cardiovascular events: rationale and design of the Canakinumab Anti-inflammatory Thrombosis Outcomes Study (CANTOS). American heart journal. 2011;162(4):597-605.
358. Ridker PM, Howard CP, Walter V, Everett B, Libby P, Hensen J, et al. Effects of interleukin-1beta inhibition with canakinumab on hemoglobin A1c, lipids, C-reactive protein, interleukin-6, and fibrinogen: a phase IIb randomized, placebo-controlled trial. Circulation. 2012;126(23):2739-48.
359. Alexander MR, Moehle CW, Johnson JL, Yang Z, Lee JK, Jackson CL, et al. Genetic inactivation of IL-1 signaling enhances atherosclerotic plaque instability and reduces outward vessel remodeling in advanced atherosclerosis in mice. The Journal of clinical investigation. 2012;122(1):70-9.
360. Komatsu Y, Shibuya H, Takeda N, Ninomiya-Tsuji J, Yasui T, Miyado K, et al. Targeted disruption of the Tab1 gene causes embryonic lethality and defects in cardiovascular and lung morphogenesis. Mechanisms of development. 2002;119(2):239-49.
361. Hamanaka RB, Bennett BS, Cullinan SB, Diehl JA. PERK and GCN2 contribute to eIF2alpha phosphorylation and cell cycle arrest after activation of the unfolded protein response pathway. Molecular biology of the cell. 2005;16(12):5493-501.